Infection and Transmission Dynamics of *Plasmodium vivax* in Papua New Guinea

INAUGURALDISSERTATION

zur

Erlangung der Würde eines Doktors der Philosophie

vorgelegt der

Philosophisch-Naturwissenschaftlichen Fakultät

der Universität Basel

von

Rahel Wampfler geb. Amstutz

aus

Lenk im Simental (BE) und Sigriswil (BE)

Basel, 2017

Genehmigt von der Philosophisch-Naturwissenschaftlichen Fakultät auf Antrag von

Prof. Dr. Ingrid Felger und Dr. Ian Hastings

Basel, den 24. März 2015

Prof. Dr. Jörg Schibler

Dekan

For my dear husband Simon,
our lovely daughter Johanna
and our precious baby to come

Table of Contents

Summary

Background

Plasmodium vivax mainly affects Asia, Central and South America and is responsible for 350-450 millions cases per year, hence 25-40% of annual infections of malaria worldwide. In Papua New Guinea (PNG) *P. vivax* prevalence is among the highest worldwide. The biggest challenge for the control of *P. vivax* infections is the formation of dormant liver stages, which have the ability to relapse and cause disease even after successful clearance of asexual stages in the blood circulation. *P. vivax* strains in PNG relapse frequently and fast, and one of the highest doses of Primaquine is necessary to reduce the relapse rate in this region.

Aims and objectives

The overall aim of this thesis was to deepen our understanding of *P. vivax* molecular epidemiology, infections, transmission and its contribution to the infectious reservoir of *P. vivax* malaria in PNG. The specific objectives pursued can be summarized as follows. First, to assess *P. vivax* infection dynamics and transmission dynamics in semi-immune children and to contribute to the understanding of the biology of relapses by comparing two treatment arms. Second, to identify the best RNA sampling strategy for field surveys and improve molecular detection and quantification of *P. falciparum* and *P. vivax* gametocytes in field samples. Third, to develop genotyping tools to better study the dynamics of gametocyte production in multi-clone infections in consecutive samples.

Methods

For the above objectives, the laboratory work of this thesis was split into three parts.

P. vivax PCR-positive blood samples from a treatment-to-reinfection survey were genotyped by the marker *msp1*F3 and analyzed for gametocyte carriage by *pvs25* qRT-PCR. These samples were collected from 524 children aged 5-10 years and actively and passively followed-up over 8 months in PNG. The children were randomly attributed to two treatment arms consisting of blood-

stage clearing drugs and either PQ or placebo. Genotyping data and gametocyte positivity were used to investigate the contribution of relapses to the infectious reservoir of *P. vivax* malaria. The molecular epidemiology of relapses was assessed by comparing the investment in gametocytogenesis, the molecular force of blood-stage infections ($_{mol}$FOB, number of distinct blood-stage infections per child and year) and the duration of infections in both trial arms using a Bayesian approach that allows for imperfect detection of blood-stage infections.

In a cross-sectional survey in 315 5-10 years old children from Papua New Guinea, the optimal strategy for gametocyte detection in field studies was assessed. Gametocytes need to be detected by amplification of stage-specific transcripts, which requires RNA-preserving blood sampling. The efficiency of sampling and storage on filter paper versus in solution were compared.

111 archived DNA samples from PNG were genotyped by capillary electrophoresis for 6 length-polymorphic and gametocyte-specific markers and their diversity was determined. Serial dilution of gametocyte enriched culture of *P. falciparum* 3D7 strain permitted to establish the detection limit of each marker *in vitro*. The two most promising markers, *pfg377 and pfs230,* were then tested to simultaneously genotype paired RNA and DNA samples from 46 individuals from Burkina Faso.

Results

In the randomized treatment-to-reinfection trial, children who received PQ showed 82% lower risk of experiencing at least one *P. vivax* infection. The estimated duration of infection, the parasite density and the probability of detection of individual infecting clone (detectability) was similar in both arms of the trial. Gametocyte densities and carriage in positive samples also did not differ between trial arms. Durations increased by age, whereas parasite density and detectability decreased by age. Over the 8 months follow-up, $_{mol}$FOB in placebo arm was 9.9 infections per child and year and almost three times as high as $_{mol}$FOB in PQ arm with 3.5. About 2 relapses were observed per each new infection at all villages. The increasing individual exposure of participants, as measured by $_{mol}$FOB, translated proportionally into an increased relapse burden.

In the cross-sectional survey in PNG, RNAprotect resulted in the highest proportion of gametocyte positive samples and gametocyte-specific transcript yields. The RNA-based detection resulted in a *P. falciparum* positivity of 24.1%; of these 40.8% carried gametocytes. *P. vivax* positivity was 38.4% with 38.0% carrying gametocytes. Most of the gametocyte carriers were also positive by DNA-based detection.

Analysis of genotyping markers of *P. falciparum* gametocytes revealed highest discrimination power for *pfs230* with 18 alleles, followed by *pfg377* with 15 alleles. When assays were performed in parallel on RNA and DNA, only 85% *pfs230* samples and 60% *pfg377* samples contained at least one matching genotype in DNA and RNA.

Conclusion

This thesis was the first attempt to fill the gaps in the knowledge of infection dynamics of relapses and new infections in semi-immune children. By comparing two trial arms results demonstrated how relapses and new infections have similar duration, parasite density, detectability and investment in gametocytogenesis. The mathematical model applied to genotyping data from the two treatment arms proved very useful to evaluate the infection dynamics of *P. vivax*. This was achieved despite a major complication of *P. vivax* molecular epidemiology, namely the unknown history of infections in our participants giving rise to relapses.

Data generated during the course of this thesis was used to highlight that relapses are the major contributors to *P. vivax* infections and transmission in PNG.

The molecular genotyping tools developed to study *P. falciparum* gametocyte transmission dynamics will open up new investigations of clone interaction, within-host competition, and clonal fitness. So far, very little is known on gametocyte dynamics in natural infections, where concurrent clonal infections might contribute to transmission equally or in competition with each other. This determines parasite recombination in mosquitoes, which in turn has major consequences for development of multi-locus drug resistance phenotypes or antigenic diversity.

Acknowledgements

This piece of work would not have been possible without the precious support and inputs of Ingrid Felger, who gave me the chance to do my PhD under her supervision at the Swiss Tropical and Public Health Institute. I very much appreciated to always find an open door. Despite being extremely busy with assessments of all kind, she always took time to discuss ideas and results with me, to review my numerous drafts and to give me feedback. She constantly encouraged me to attend conferences and to present my work. Ingrid, your endurance inspired me many times throughout my thesis. Thank you!

Thanks to Ian Hastings for being my external co-referee and giving great support through these years. Though I was always very nervous before the committee meetings, I always enjoyed to discuss the progress of my thesis with you and to hear your comments and suggestions. I'm also very thankful to Thomas Smith and Ivo Mueller, the experts of my thesis committee, for their invaluable inputs and feedbacks.

My time as a student has been very joyful thanks to all the precious colleagues in MolPar and GR units: Peter, Sebi, Esther, Serej, Adi, Oli, Alex, Bea, Till, Niggi, Nicole, Hai, Michael, Tereza and to the entertaining master students and Zivis. I always enjoyed the coffee breaks, the conversations and your support. I greatly appreciated the tasty and very hot Chefilaus dinners of Ingrid and Peter in their welcoming home. We had great conversations that I will remember for the rest of my life.

A special thank goes to Natalie with her contagious enthusiasm. She has been an inspiration for many R-scripts and for different concepts of thinking and has been a very delightful friend to work with. She never got tired to answer my translational questions, i.e: "Wie sagt man umgangsprachlich 'nüchtern'?" "Sober." "Ist das nur für ein Alkohol-nüchtern oder auch für ein allgemeines Nüchtern?" "ich denke für beides. *Smile"*.

Thanks goes also to Françoise for her clemency concerning my lab-ordering manners and for all the diverting lunch times with her. It was always a big pleasure to speak some French in the lab and she was one of the corner stones, who encouraged me to do so with my daughter. Thank you.

Further, I would like to thank all my friends and colleagues from the 2nd floor: Matthias, Sergio, Noemi, Gordana, Beni, Wendelin (please stop smoking even if you're more productive than I :D), Christoph S., Therese, Daniel, Felista, Michelle, Chris, Roberto, Kirsten, Mireia and Sonia and many others. My colleagues from the ground floor and cellar: Joelle, Julia, Ursi, Scheuri, Monica, Pascale and Michael and many others. Thanks also to my precious friends from the 3rd floor: Mohamad, Yingsi, Alex, Frédérique and all others.

I also enjoyed being part of the Support Group of Swiss TPH. It was great to talk about sustainable projects and prepare the different fundraising Bazaars. Thanks to all the "Managing board": Peter O, Peter S, Daniel T, Valérie, Susi, Françoise, Dagmar, Michael K, Helen and Marco. I really enjoyed meeting you and share time with you discussing all these exciting projects. This helped me to get the feeling to really make a difference in the life of children and people.

I'm grateful to the Human Resources, who supported me with all the logistics and paperwork during my pregnancies and other special enquiries. Thanks to the library staff for looking up so many historical papers for me, to the secretary and the medical center for welcoming me with all my requests (quiet room, withdrawal of whole blood for research, numerous forgotten badges, etc).

I also want to thank Amanda, Leanne, Cristian & Anita, Stephan, Andrea K, Wang and many others at Swiss TPH, WEHI, Manaus and Mahidol University for their great support, help with statistics, encouragements, invaluable exchanges and always useful comments and recommendations. I'm grateful to Mariabeth Silkey for her hard work on the database, helping out with the statistics and not getting tired of running the triplet model all over again.

For the project on gametocyte detection strategies, I'm thankful to Sarah Javati and all the field teams and participants in PNG. Sarah well smoothed the way to complete this work. Thanks also to Felista Mwingira and Dania Mueller for their precious support.

The study on the gametocyte genotyping markers would not have been possible without the great support of Peter Beck in getting access to these high quality samples from Burkina Faso. I'm thankful to all the field workers and the study participants. I really enjoyed to be part of the study team.

An unforgettable part of my thesis has been the trip to Acre in the Amazon region in Brazil that became possible in the frame of the precious collaboration with Marcelo Ferreira and his field team. Thank you for this trip, the so warm welcome in your family and the kind people in your lab. This trip was a success in many regards, personally and scientifically. Thanks to Bruna and Roberta to withdraw numerous samples of blood for me, for teaching me how to do so, too, and how to talk with the patients and take care of them, and for the innumerable good conversations in the evening and the trips to a good churrasco (barbecue party). I also enjoyed the friendship with the microscopists, who always called me when a patient was diagnosed with malaria at the health

center and who always welcomed me in their office during a malaria-free day. I'm grateful to Pablo for his advises and enthusiasm. I'll never forget when I once was with him on the way to visit a secluded farm in this wild region. Out of scare of being bitten by a mosquito, I put so much repellent that Pablo suddenly exclaimed: "Isto mata a gente também!" (This also kills people!) and immediately opened the window of the car. Thanks to Cristian for his dear skype-coaching during this period and to Camilla for spending so much time with me back in São Paulo to prepare the samples.

I also really enjoyed the collaboration with the GR unit and the side project on the Heterochromatin Protein 1 inducible-knockout strain, and I learnt so much during this time. Thank you for this opportunity.

For the "dynamics" projects, I'm very thankful to Leanne for conducting the fieldwork and to all the participants and field teams. Thank you for not giving up with the cleaning of the data set. Thank you Tom for writing an essential part of the methods…a part that I still try to fully understand: the triplet model. This was a very interesting project, never ending and probably much richer than I ever thought. I'm grateful to all those, who encouraged me and helped me with inputs and suggestions throughout these two years.

Great thanks go to my family, Simon and my daughter Johanna for their patience and compassion, backing me up in all situations and bringing so much joy to my life. You were cooking when I didn't have time, bringing me to and picking me up from the office when I didn't feel to go by bike and you sacrificed so much time to give me the opportunity to finish this work. I thank also my friend Brigitte for her ground-standing advices and having always an open ear when I got lost between work and family. Last but not least, I want to thank God for giving me the faith and the trust to go on every day. He's my core scientist. I learnt not to give up, knowing that He had plans full of love. He helped me not to lose hearts when I knew how great He was.

Abbreviations

ACT	Artemisinin-Combination Therapy
AL	Artemether-Lumefantrine
AQ	Amodiaquine
CE	Capillary Electrophoresis
CQ	Chloroquine
DALY	Disability Adjusted Life-Years
DOT	Directly Observed Treatment
DNA	Desoxyribonucleic Acid
DTT	Dithiothreitol
G6PD	Glucose-6-Phosphate-Dehydrogenase
H_E	Expected heterozygosity
LM	Light Microscopy
MDA	Mass Drug Administration
MOI	Multiplicity of Infection
FOB	molecular Force of Blood-Stage Infection
FOI	molecular Force of Infection
MDA	Mass Drug Administration
MS	Microsatellite
MSAT	Mass Screen and Treatment
Msp1F3	Merozoite Surface Protein 1, F3 region
PCR	Polymerase Chain Reaction
Pf	*Plasmodium falciparum*
Pfs25	*P. falciparum* 25kDa Ookinete Surface Antigen Precursor
PL	Placebo
PNG	Papua New Guinea
PQ	Primaquine
Pv	*Plasmodium vivax*
Pvs25	*P. vivax* 25kDa Ookinete Surface Antigen Precursor
qRT-PCR	Quantitative Reverse Transcriptase-PCR

QT-NASBA	Quantitative Nucleic Acid Sequence Based Amplification
RDT	Rapid Diagnostic Test
RNA	Ribonucleic Acid
rRNA	ribosomal RNA
SP	Sulphadoxine-Pyrimethamine
Swiss TPH	Swiss Tropical and Public Health Institute
WB	Whole Blood
WHO	World Health Organization

Chapter 1: Introduction

Malaria: a short overview

Malaria is a life threatening disease and was responsible for 198 million cases and estimated 584'000 deaths in 2013 (WHO, 2014). 3.2 billion people are estimated to be at risk of malaria. The majority of the cases (90%) were reported in the African continent and the majority of the victims (78%) are children under 5 years of age (WHO, 2014). In schools, the presence and active participation of children is repeatedly hindered due to malaria episodes.

Malaria is caused by five species of parasite of the genus *Plasmodium* that affects humans – *P. falciparum*, *P. vivax*, *P. malariae*, *P. ovale* and *P. knowlesi*. *P. falciparum* is responsible for most mortality and morbidity and predominates in Sub-Saharan Africa, where it accounts for up to 10% of all DALYs (Jamison et al., 2006). The diversity found in this parasite shows a joint origin with its host, the humans. It is suggested to have migrated out of Africa together with humans for over 50’000 to 60’000 years (Tanabe et al., 2010). *P. vivax* was recently suggested to be also of African origin (Liu et al., 2014). *P. vivax* infections generally cause less morbidity, but this parasite is more widespread and predominates malaria areas outside of Africa (Guerra et al., 2010). The other three species are found less frequently and occur sympatric with *P. falciparum* and/or *P. vivax*. *P. knowlesi* is a zoonotic malaria parasite and transmission is observed from Macaca monkeys to humans of Southeast Asia (Cox-Singh et al., 2008). *P. knowlesi* probably did not emerge only recently, but it likely was confounded with *P. malariae* in human infections until molecular methods became available (Singh et al., 2004).

Gametocytes and specific aspects of transmission of malaria

The transmission of malaria depends on the presence of mature sexual stages, called gametocytes, in the human peripheral blood. *P. falciparum* gametocyte maturation in the human host is classified into five stages (I-V), with stage V being the infectious transmission-stage (Sinden and Smalley, 1979). Apart from morphological changes during gametocytogenesis, the parasite undergoes alterations on molecular level in preparation for rapid adaptation to the mosquito midgut. In *P. falciparum*, this involves 150 to 300 genes found to be up regulated (Lasonder et al., 2002; Silvestrini et al., 2005; Young et al., 2005). The microscopic detection limit of gametocytes (or parasites) in blood smears is dependent on the number of fields examined and requires a density for reliable detection of at least 10 gametocytes/µl whole blood (WB) (Bejon et al., 2006). To detect lower gametocytaemia, molecular tools are necessary (Babiker and Schneider, 2008; Ouédraogo et al., 2009). The worldwide used marker for the detection of mature gametocyte is the *25 kDa ookinete surface antigen precursor* (*pfs25*), which is highly expressed in female stage V *P. falciparum* gametocytes (Babiker et al., 1999; Schneider et al., 2004; Tao et al., 2014; Young et al., 2005). Quantitative nucleic acid sequence based amplification (QT-NASBA) assays and quantitative reverse transcriptase-PCR (qRT-PCR) techniques based on *pfs25* enhance the detection and quantification of gametocytes to the order of 0.02-0.1 gametocyte/µl WB (Babiker and Schneider, 2008; Schneider et al., 2004).

Studies on *P. falciparum* gametocytes showed their little sensitivity to many antimalarials (Baird, 2009). Mature *P. falciparum* gametocytes were insensitive to common antimalarial drugs like Chloroquine (CQ) or non-Artemisinin-combination therapy drugs (non-ACT), whereas immature *P. falciparum* gametocytes are partially susceptible to these treatments (reviewed in (Bousema and Drakeley, 2011; White, 2008)). Artemisinin-combination therapy (ACT), e.g. Artemether-Lumefantrine (AL), is highly active against immature gametocytes and generally lowers the rate of post-treatment gametocytaemia and malaria transmission. The 8-aminoquinoles, e.g. Primaquine (PQ), occupy a unique position, as they effectively kill mature sexual stages of *P. falciparum* and shorten post-treatment gametocytaemia (Eziefula et al., 2014; Pukrittayakamee et al., 2004; Shekalaghe et al., 2007a). Based on QT-NASBA as detection method, the mean circulation time of gametocytes after non-ACT treatment was around 55 days, ACT treatment reduced the duration fourfold to 13.4 days and PQ-ACT treatment reduced to another twofold to 6.3 days (Bousema et al., 2010). Despite good tolerability and safety of PQ in children (Betuela et al., 2012a), clinical use of PQ remains limited due to its hematotoxic effects in glucose-6-phosphate dehydrogenase (G6PD)-deficient patients (Alving et al., 1956). Recent studies are thus focusing in reducing the PQ dose for gametocyte clearance in *P. falciparum* malaria. They found that 0.4 mg/kg PQ had similar gametocidal efficacy compared to the reference 0.75 mg/kg (Eziefula et al., 2014). Since 2012, WHO guidelines recommend a single dose of 0.25 mg/kg for blocking transmission (WHO, 2012).

Submicroscopic gametocyte carriers are important for malaria transmission (Babiker et al., 1999; Ouédraogo et al., 2009). Schneider and co-workers reported that carriers with submicroscopic gametocyte densities efficiently infected mosquitoes in Kenya. They concluded that submicroscopic carriers constitute a reservoir of human malaria (Schneider et al., 2007). In an area of seasonal *falciparum* malaria from Burkina Faso, Ouédraogo and co-workers calculated the contribution of submicroscopic gametocyte carriage in asymptomatic children to the infectious reservoir to be 24% (Ouédraogo et al., 2009). The same study showed that mosquitoes were infected when fed on parasite positive blood with a *P. falciparum* gametocyte density below 1 gametocyte/µl WB. Ouédragodo and co-workers concluded that the relative contribution of submicroscopic gametocyte carriers to transmission might be low, but their relative abundance in a population may counterbalance this. Submicroscopic gametocyte carriers are thus important contributors to malaria transmission (Ouédraogo et al., 2009).

P. vivax gametocytes were observed within 3 days after the first asexual parasites were observed in the peripheral blood (McKenzie et al., 2007). In contrast to *P. falciparum*, all gametocyte stages of *P. vivax* circulated in the peripheral blood (Graves et al., 1988). Also gametocytes were more commonly observed by microscopy in *P. vivax* infections (57% of infections) than in *P. falciparum* infections (9% of infections)(Mckenzie et al., 2006). Gametocytes often comprise <15% of *P. vivax* and <5% of *P. falciparum* asexual parasites (Bousema and Drakeley, 2011; Huh et al., 2011). Nevertheless, gametocytes circulated for a maximum of 3 days in *P. vivax* infections, whereas the mean circulation time of *P. falciparum* gametocytes was over 6 days (Bousema et al., 2010; Carter and Graves, 1988). In natural infections, 67% of *P. vivax 18S rRNA* positive samples contained gametocytes as determined by *pvs25* QT-NASBA (Beurskens et al., 2009). However, most data available to date on *P. vivax* gametocytaemia are based on light microscopy, which is missing multiple submicroscopic gametocyte densities. Additional molecular studies on gametocyte dynamics in natural *P. vivax* infections, on contribution of relapses to gametocyte prevalence and on gametocyte drug sensitivity are needed to better understand the effects of interventions on transmission of *P. vivax*.

Plasmodium vivax: a challenge in research and epidemiology

P. vivax sporozoites can develop at lower temperatures than *P. falciparum*. This fact results in higher *P. vivax* prevalence in temperate zones compared to *P. falciaprum*. In contrast to *P. falciparum*, *P. vivax* parasites can persist over long periods as dormant liver stages called hypnozoites, the causative agents of relapses and thus a reservoir of infection (Imwong et al., 2007). *P. vivax* merozoites show a preferential invasion of reticulocytes (Russell et al., 2011), which is thought to account for generally lower parasitaemia in *P. vivax* compared to *P. falciparum* infections. *P. vivax* invasion also depends mainly on the Duffy binding receptor (Hans et al., 2005). But repeatedly Duffy-negativity was recently found to not completely protect against *vivax* malaria

(Mendes et al., 2011; Ngassa Mbenda and Das, 2014). *P. vivax* asexual blood stages are thought to not sequester, but limited microvascular cytoadherence of *P. vivax* to lungs and spleen corresponding to 10% of the cytoadherence found in *P. falciparum* was reported (Anstey et al., 2007; Carvalho et al., 2010). Less than 15% of blood stages develop into sexual gametocytes as detected by light microscopy (Huh et al., 2011). By a further mosquito bite, mature gametocytes are taken up with a blood meal. In the mosquito midgut sexual reproduction and recombination takes place.

It was not yet possible to establish stable *Plasmodium vivax* erythrocyte cycle in continuous *in vitro* cultures (Galinski et al., 2013; Golenda et al., 1997). The limited material gained from patient samples constitute a major limitation for cell biology studies (reviewed in (Galinski et al., 2013)). Transcriptome data of stages of the asexual cycle of *P. vivax* was published in 2008 (Bozdech et al., 2008), 5 years later than the transcriptome data of *P. falciparum* (Bozdech et al., 2003). The biology of the two species, *P. falciparum* and *P. vivax*, differs extremely and observations on protein function made on *P. falciparum* can often not be applied for *P. vivax* (Bozdech et al., 2008). The transcriptome of sexual stage has not yet been published, but this will immensely facilitate studies on *P. vivax* gametocyte. Furthermore, studies on the cell biology of *P. vivax* and on drug development, e.g. targeting the dormant liver stages, are limited to non-human primate models (Galinski et al., 2013), experimental infections in human volunteers (McCarthy et al., 2013) and cohort studies in endemic settings. The latter being the most widely used in the last decade.

P. vivax is mainly affecting Asia, Central and South America and is thought to be responsible for 25-40% of annual infections of malaria worldwide (Hay et al., 2004; Mendis et al., 2001; Price et al., 2007). Guerra and co-workers mapped the global distribution of *P. vivax* (Guerra et al., 2010). According to their findings, up to 2.85 billion people are at risk of *P. vivax* infections. The total number of cases per year is estimated between 350-450 millions (Baird, 2007a; Price et al., 2007). The geographical distribution of endemic *P. vivax* malaria is wider than *P. falciparum*, while both species are co-endemic in most areas (Guerra et al., 2010). Only in sub-Saharan zones, where Duffy negativity is prevalent, *P. vivax* is rare compared to *P. falciparum* (Miller et al., 1976; WHO, 2014). *P. vivax* prevalence in co-endemic areas was frequently reported to be lower than that of *P. falciparum*. The lower observed prevalence might be explained by the tendency of *P. vivax* to maintain low-density parasitaemia compromising diagnostic sensitivity of light microscopy (Mueller et al., 2009). Higher and more precise prevalence data of *P. vivax* are obtained with PCR based detection methods (Rosanas-Urgell et al., 2010).

High malaria burden in Papua New Guinea

Malaria prevalence in PNG ranges from very low endemic regions in highlands to highly endemic regions in the lowlands. WHO recently classified PNG among the countries controlling malaria; long-lasting insecticide-treated bed nets were delivered to 68% of the population living at high-risk of malaria (WHO, 2014). Despite the increased attempts to control malaria, it is still a major public health problem in PNG and is responsible for 10% of all deaths in children under 5 years, thus being the fifth cause of death in young children (premature child delivery being the leading cause with 18%) (WHO, 2011).

Four out of five *Plasmodium spp*. that infect humans are found in both lowland and highland areas of PNG (Genton et al., 2008; Mehlotra et al., 2000; Mueller et al., 2002). The predominant *Plasmodium* species of malaria in PNG are *P. falciparum* and *P. vivax* (Figure 1). *P. malariae* is unequally distributed among the major endemic areas of PNG (Mueller et al., 2003). Madang Province is the most highly malaria endemic region in PNG. A study conducted in 206 school children from Megiar and Mugil in Madang Province in 2004 showed that 83.7% of all *Plasmodium* infections were due to *P. falciparum* (41.2% *Pf* single-species infection), *P. vivax* was present in 42.1% of infections (12.1% *Pv* single-species infection), *P. malariae* in 8.4% (1% *Pm* single-species infection) and *P. ovale* was present in 1.2% of infections (no *Po* single-species infection) (Michon et al., 2007). A more recent study reported the prevalence of *Plasmodium* species in 1-4 years old children from the East Sepik province, the second most highly malaria endemic region in PNG. Parasite detection by Ligase detection reaction-Fluorescent microsphere assay (post-PCR LDR-FMA) indicated that in these young children *P. vivax* was the most prevalent species accounting for 53.0% of infections, followed by *P. falciparum* (49.6% of infections) *P. malariae* and *P. ovale* (9.9% and 2.7% of infections, respectively) (Lin et al., 2010). More than 20% of all infections harbored mixed *Plasmodia* species (Lin et al., 2010; Mehlotra et al., 2000; Michon et al., 2007).

A recent study in severe malaria cases from PNG showed that co-infections of *P. falciparum* and *P. vivax* (50 out of 340 severe malaria cases) were associated with more severe symptoms and more deaths than single infection of either species (Manning et al., 2011). *Plasmodium* species co-infections and their association with clinical outcomes highlight the importance of understanding the dynamics of co-infection and their possible relevance for transmission.

The distribution of *Plasmodium* spp. in PNG today is highly related to the history of control and eradication attempts (Mueller et al., 2003). Prior to vector control programs, mostly based on DDT spraying (1957), *P. vivax* generally has been the predominant parasite, followed by *P. falciparum* and *P. malariae* (Hairston et al., 1947). After abandoning the spraying program in 1970, a shift to *P. falciparum* predominance was observed (Mehlotra et al., 2000). Changes in patterns of drug use and the spread of drug resistance against CQ and Amodiaquine (AQ) might also have contributed to this shift (Desowitz and Spark, 1987; Mueller et al., 2003). The first cases of CQ resistant

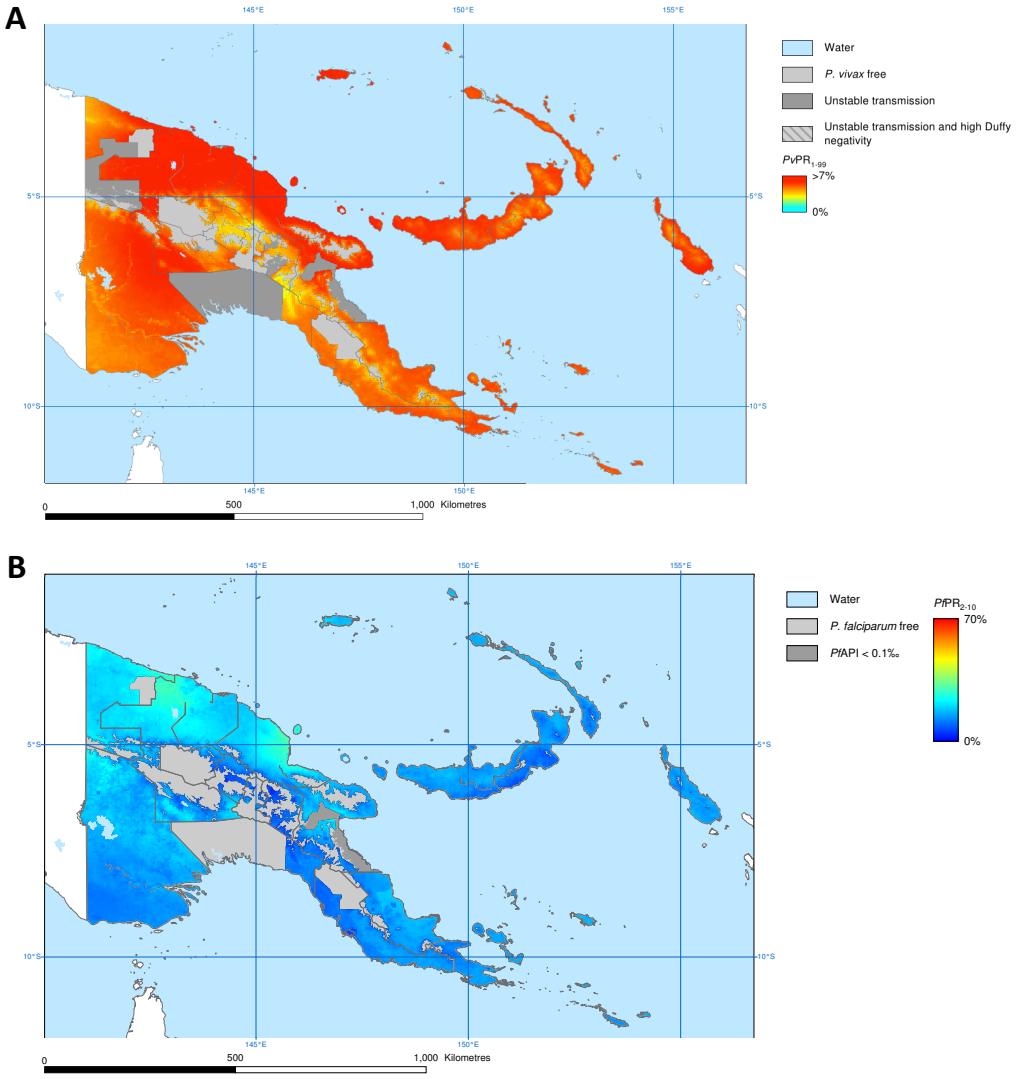

Figure 1. Distribution of *P. vivax* (**A**) and *P. falciparum* (**B**) prevalence rates by LM in 2010, modified from (Gething et al., 2012).

P. falciparum and *P. vivax* parasites were observed in 1976 and in 1989, respectively, leading to the introduction of combination therapy of CQ or AQ plus Sulfadoxine-Pyrimethamine (SP) in 2000 (Mueller et al., 2003; Rieckmann et al., 1989). Six years later WHO recommended the use of ACT with Artemether-Lumefrantrine (AL) as first line treatment. At that time increasing numbers of treatment failures with non-ACT were reported (Marfurt et al., 2007). Although the effectiveness of AL under ideal trial conditions was very promising, some treatment failures against AL were observed in young PNG children in a non-clinical-trial setting (Schoepflin et al., 2010). Sub-optimal adherence to the recommended treatment and insufficient fat supplementation best explained the suboptimal effectiveness and highlighted potential problems with unsupervised usage of AL in routine treatment at the field site (Schoepflin et al., 2010). ACTs are highly effective against blood stages of *P. vivax* (Karunajeewa et al., 2008), but no combination is active against latent liver stages

causing relapses (Sinclair et al., 2009). To achieve radical cure from *P. vivax*, ACT treatment should be complemented with the standard PQ treatment (0.5mg/kg daily for 14 days)(WHO, 2010). In PNG, PQ treatment was not formally implemented as part of treatment guidelines until 2010 (Betuela et al., 2012b). PQ is the only effective drug against *P. vivax* hypnozoites, the dormant liver stages. In samples from treatment-to-reinfection surveys relapses cannot be differentiated by genotyping from new infections, nor from treatment failures, because relapses can be homologous and heterologous to the initial infection. Thus, the contribution of reactivated dormant liver stages to recurrent *P. vivax* infections cannot be directly quantified (Baird, 2009).

Betuela and co-workers estimated the proportion of relapses in a study design, where relapses were prevented in one of the treatment arms by adding PQ to the regimen (Betuela et al., 2012b). Relapses were responsible for about 50% of recurrent infections and for 60% of clinical illness within the first 3 months after treatment in children aged 1-5 years. Although the follow-up period lasted for over 9 months, no effect of PQ treatment was observed after the initial 3 months. This suggested a high prevalence of rapidly relapsing strains similar to the well-studied Chesson strain (Craige and Alving, 1947; White, 2011). Interestingly, PQ treatment did not prevent high-density clinical *vivax* infections during these first 3 months of follow-up. The authors argued that relapsing strains are genetically related to clones that caused the primary infections, due to sexual recombination between co-transmitted clones in the mosquito midgut. Following a primary infection, children would develop partial immunity against genetically related clones relapsing at a later stage and reaching only low parasite densities (Betuela et al., 2012b; Collins et al., 2004). The equal number of high-density clinical *vivax* infections observed in both treatment arms were therefore explained by new infections of none-related parasite clones, which could not be prevented by Primaquine treatment.

In summary, PNG is one of the countries suffering most from the burden of *P. vivax* malaria (WHO, 2014). *P. vivax* prevalence is among the highest worldwide and is co-endemic with other three major *Plasmodium* species: *P. falciparum*, *P. ovale* and *P. malariae* (WHO, 2014). Mixed-species infections are common and species interactions and within host competition can thus be studied. *P. vivax* strains in PNG relapse frequently and fast, hence one of the highest doses of PQ is necessary to reduce the relapse rate in this region (Baird, 2007b; Goller et al., 2007). Though the different aspects mentioned above make malaria research in PNG indeed attractive, they are a great challenge for malaria control in PNG.

Context of this PhD thesis

Study site and Albinama cohort design

This thesis is part of a larger study conducted by an international group of collaborators under the leadership of Papua New Guinea Institute of Medical Research (PNG IMR). The DNA and RNA samples analyzed in this thesis derive from a prospective longitudinal cohort study, which was conducted from September 2009 to June 2010 in the Albinama area, Maprik district, PNG. The aim of this study is to obtain a profound understanding of the effect of liver and blood-stage clearance on the incidence of malaria infections and disease in semi-immune children. The cohort included 504 children aged 5-10 years at enrolment, which were randomized to two treatment arms (Figure 2A):

- 257 children receiving a treatment of Chloroquine (CQ), Artemether-Lumefantrine (AL), Primaquine (PQ arm)
- 247 children receiving a treatment of Chloroquine (CQ), Artemether-Lumefantrine (AL), Placebo (placebo arm)

For enrolment, children were screened for eligibility and underwent clinical examination to assess health status and medical history after written informed consent was obtained from parents or a legal guardian, and a unique identification number was assigned to each child. Treatment commenced two weeks after enrolment and consisted of a 3-day course of CQ (days 1-3), a 4-week course of PQ or Placebo (days 1-5, 8-12, 15-19 and 22-26) and a 3-day course of AL (days 15-17)(Figure 2A). Effect of these drugs on the parasite stages are shown in Table 1.

Succeeding treatment, the children were followed-up for 8 months (Figure 2B). They were clinically examined and a baseline 10ml venous blood sample was collected at three days after final DOT. Subsequent regular finger-prick blood samples were taken in two-week intervals for the first three months and monthly thereafter. Active follow-up included two-weekly morbidity control for febrile symptoms. Passive follow-up was performed continuously at Albinama health center. Upon febrile symptoms accompanied from malaria positive blood smear or positive rapid diagnostic test, children were treated according to national treatment guidelines using AL medication if available.

DNA of each sample taken from regular bleeds, active and passive follow-up was extracted from 100-150µl blood pellet at PNG IMR. RNA was extracted from 50µl whole blood spotted on Whatman 3MM filter paper, stored for 2-4 weeks at room temperature, then transferred into TRIzol solution and stored long term at -80°C.

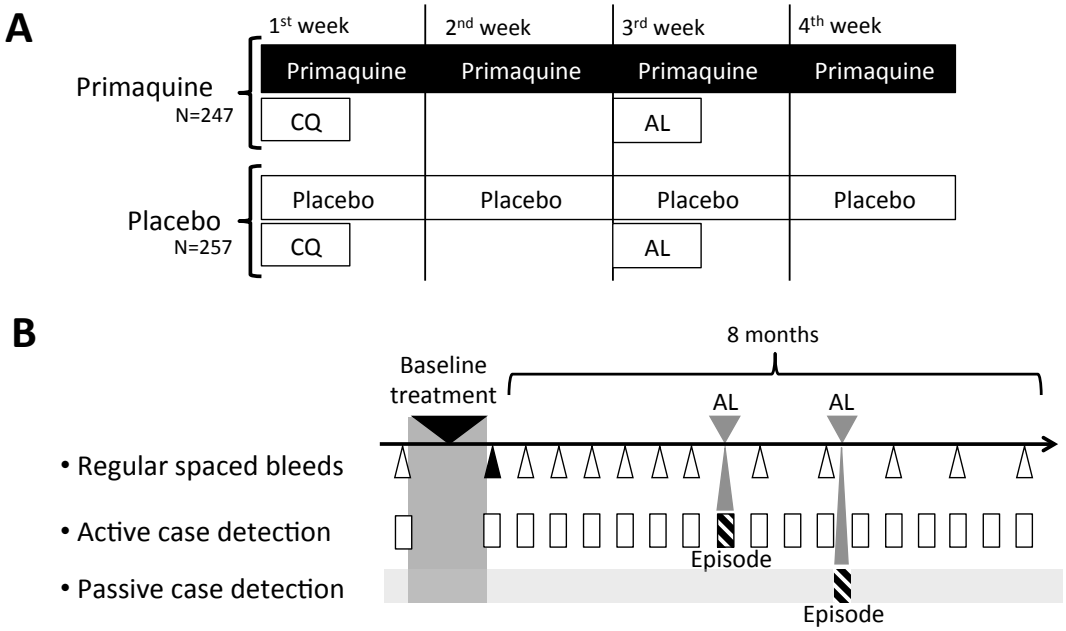

Figure 2. Schematic study design of the Albinama cohort. **A**. Baseline treatment of the two study arms. 0.5mg/kg/daily Primaquine dose was administered over 20 days. CQ: 25mg/kg/total dose of Chloroquine. AL: 3 days regimen of Artemether-Lumefantrine. **B**. Schematic design of the follow-up period. A finger prick blood sample was taken at enrolment (white triangle) and a venous blood sample was taken after baseline treatment (black triangle). Two-weekly and later monthly finger prick blood samples were taken during the follow-up period (white triangle). Active case detection was two-weekly over the whole study period (white rectangle). Passive case detection at Albinama health centers was available over the whole study period (light grey rectangle). Symptomatic (fever >37.5°C) and LM or RDT positive children (episode) were treated with AL or similar antimalarial if available (dashed rectangle).

Table 1. Drugs used in the present study and their effects on *P. falciparum* and *P. vivax* parasitic stages. The combination of all three drugs in the PQ arm is thought to lead to a radical cure.

Drug	Effect on				References
	Asexual blood-stages	Gametocytes immature	Gametocytes mature	*vivax* Hypnozoites	
CQ	+	(+)	-	-	(Smalley and Sinden, 1977; White, 2008)
AL	+	+	-	-	(Bousema et al., 2006; Okell et al., 2008; White, 2008)
PQ	-	-	+	+	(Pukrittayakamee et al., 2004; Shekalaghe et al., 2007b)

CQ: Chloroquine; PQ: Primaquine; AL: Artemether-Lumefantrine

Gametocyte detection and genotyping

Gametocytes are the parasite stage that is transmitted from humans to mosquito. RNA-based detection of gametocytes was shown to be over 100x more sensitive than the routine light microscopy (Schneider et al., 2007). Extraction of parasite mRNA permits to amplify gametocyte-specific transcripts by NASBA method, RT-PCR or qRT-PCR (Beurskens et al., 2009; Kuamsab et al., 2012; Lima et al., 2012; Mlambo et al., 2008). However, RNA collection in epidemiological studies is a challenge, as adherence to storage time and temperature are often logistically demanding (Jones et al., 2012). RNA-stabilizing reagents considerably facilitate the handling of RNA in field settings. The target genes for gametocyte detection are the *P. falciparum pfs25* and the *P. vivax pvs25* gene. *Pfs25* was highly expressed in female gametocytes (Tao et al., 2014; Young et al., 2005) and similar high expression is expected for *P. vivax*. During the course of this thesis a quantitative real-time PCR (qRT-PCR) was developed to precisely amplify gametocyte-specific mRNA of the *P. vivax pvs25* genes. This gene was observed to show little sequence polymorphism among isolates all over the world (Kang et al., 2013; Prajapati et al., 2011; Sattabongkot et al., 2003; Zakeri et al., 2009). No male gametocyte specific qRT-PCR has yet been described nor been used in field studies (White et al., 2014).

Genotyping of gametocytes is of a great interest to identify gametocyte-producing clones within multiple clone infections and to analyze transmission dynamics over time (Nakazawa et al., 2011; Nwakanma et al., 2008). *Pfs230* and *pfg377* are both polymorphic *P. falciparum* gametocyte-specific genes. *Pfg377* is involved in osmiophilic body formation and egression of female gametes (de Koning-Ward et al., 2008). *Pfs230* was shown to be involved to mediate cell-to-cell adherence in the mosquito midgut (Rupp et al., 2011). Genotyping studies have shown that some gametocytes were detectable several months during the dry season and were the most possible source of the next outbreak during the rainy season (Abdel-Wahab et al., 2002).

Blood-stage genotyping

Genotyping based on size polymorphic markers and capillary electrophoresis-based sizing of PCR products (PCR-CE) has become the method of choice for many epidemiological studies which need to differentiate co-infecting clones (Falk et al., 2006; Koepfli et al., 2011; Schoepflin et al., 2009). PCR-CE can precisely discriminate alleles differing in size by few base pairs only. Accuracy of sizing is the major advantage of CE over earlier genotyping methods such as PCR-restriction fragment length polymorphism (PCR-RFLP). Although genotyping does not permit the differentiation between treatment failures, new infections and relapses in endemic areas (Bruce et al., 2000), genotyping of recurrent *P. vivax* infections after AL administration showed that the drug was more effective than estimated by microscopy-based positivity (Barnadas et al., 2011).

Koepfli and co-workers evaluated and optimized CE-based genotyping assays for large field studies (Koepfli et al., 2011, 2009). The polymorphic fragment 3 of the gene encoding merozoite surface protein 1 (*msp1F3*) showed high diversity and robust PCR amplification.

High diversity of a marker is likely maintained in a population by chance if a marker is neutral, e.g. non-coding microsatellites. Alternatively, density dependent selection can drive diversity of coding markers, e.g. surface antigens such as Pv*msp1,* as they favor rare alleles. No trend of diversifying selection was observed for Pv*msp1* in PNG (Koepfli et al., 2009). However, Pv*msp1* is a potential vaccine candidate (reviewed in (Galinski and Barnwell, 2008)), thus shifts in the allelic diversity of Pv*msp1* might reflect rising antigen-immunity against specific alleles of *msp1*.

Multiplicity of infection and molecular force of infection

The two parameters Multiplicity of Infection (MOI) and molecular Force of Infection ($_{mol}$FOI) can be determined at high-resolution by genotyping using capillary electrophoresis for sizing of PCR fragments (Koepfli et al., 2011; Mueller et al., 2012; Schoepflin et al., 2009). MOI is defined as the number of parasite clones concurrently infecting one individual. MOI has been used as one of several parameters to monitor the impact of interventions (Kyabayinze et al., 2008). MOI in natural infections varies with malaria endemicity and age (Arnot, 1998; Mueller et al., 2012). MOI in *P. falciparum* has been found to increase during early childhood until the age of 10 and decrease thereafter (Falk et al., 2006; Mueller et al., 2012; Smith et al., 1999). MOI in *P. vivax* infections increased in young children up to 2 years and remained stable thereafter until the age of 4.5 years (Koepfli et al., 2011). MOI data of children aged 5 to 10 are still missing for *P. vivax* infections.

$_{mol}$FOI describes the number of new clones acquired per person per year. Genotyping permits to distinguish new parasite clones from co-infecting clones and thus calculate $_{mol}$FOI. Mueller and co-workers showed that $_{mol}$FOI was highly associated with the incidence of clinical malaria (defined as >2500 parasites/µl) in *P. falciparum* infected 1-4 year old children from PNG (Mueller et al., 2012). $_{mol}$FOI increased significantly with age, showed strong seasonality and was reduced by half in children using insecticide treated bed-nets. In consideration of relapses, estimates of $_{mol}$FOI for *P. vivax* comprise two sources of blood-stage infections: newly acquired infections (analogous to *P. falciparum*) and relapses from dormant liver stages. The term molecular force of blood-stage infections ($_{mol}$FOB) was therefore introduced for *P. vivax* (Koepfli et al., 2013). $_{mol}$FOB for *P. vivax* was also determined for the same cohort of 1-4 year old children (Koepfli et al., 2013). *P. vivax* $_{mol}$FOB was also significantly associated with clinical episodes (defined as >500 *P. vivax* parasites/µl) and showed high seasonality, but in contrast to *P. falciparum* $_{mol}$FOB of *P. vivax* was not age-dependent in this age group (Koepfli et al., 2013).

The average $_{mol}$FOB in young children was shown to be 14.6 clones/child/year, more than twice as high as *P. falciparum* $_{mol}$FOI (5.9 clones/child/year) (Koepfli et al., 2013; Mueller et al., 2012). The incidence of clinical *P. vivax* illness was highest in very youngest children (<2 years). It was speculated that the high $_{mol}$FOB was driving the fast acquisition of *P. vivax* immunity in young children from PNG (Koepfli et al., 2013).

Aims and objectives of this Thesis

The aims of this thesis were threefold: (i) assess *P. vivax* infection dynamics and transmission dynamics in semi-immune children and contribute to the understanding of the biology of relapses by comparing two treatment arms, (ii) identify the best RNA sampling strategy for field surveys and improve molecular detection and quantification of *P. falciparum* and *P. vivax* gametocytes in field samples, (iii) develop genotyping tools to better study the number of co-infecting clones simultaneously producing gametocytes and contributing to transmission, and the dynamics of gametocyte production in multi-clone infections in consecutive samples.

The following objectives were accomplished:

Objective I: RNA sampling method in the field

- To determine the optimal strategy for gametocyte detection in field surveys.
- To quantitatively evaluate the sensitivity of DNA-based and RNA-based detection of blood-stages of the *Plasmodium spp*.
- To test the stability of RNA in stored blood samples and that of extracted RNA over a two-year interval.
- To establish a *P. falciparum* gametocyte trend line *in vitro* cultures for quantification of *P. falciparum* gametocytes in field samples.

Objective II: Novel molecular tools to study transmission dynamics of *P. falciparum*

- To compile a list with the most polymorphic and highly expressed *P. falciparum* gametocyte genotyping markers from available transcriptome data and literature.
- To improve the discriminatory power of known gametocyte-specific genotyping markers: *pfg377* and *pfs230.*
- To test the detection limit and sensitivity of gametocyte genotyping markers *in vitro* reared *P. falciparum* gametocytes.
- To evaluate the diversity and thus the discriminatory power of each marker in field samples from PNG.
- To investigate gametocyte-producing clones in paired DNA and RNA field samples from Burkina Faso.

Objective III. The contribution of relapses to the burden of *P. vivax* malaria

- To determine the individual co-infecting clones in over 1000 *P. vivax*-positive blood samples for the highly polymorphic marker *msp1*F3 in the Albinama cohort.
- To estimate the contribution of relapses to the number of infections per child.
- To identify the *P. vivax* gametocyte carriers by molecular methods and assess the contribution of relapses to transmission.

Objective IV. Infection dynamics of *P. vivax*

- To estimate the detectability, the probability to detect a clone in a given sample, by applying a mathematical Bayesian approach to the genotyping data of the Albinama cohort.
- To describe *P. vivax* duration of infection of new infections and relapses.
- To evaluate the contribution of relapses to infections in areas of different transmission intensity by comparing *P. vivax* $_{mol}$FOB in two treatment arms.
- To investigate age trends in *P. vivax* infection dynamics.

Objective V. *P. falciparum* and *P. vivax* transmission-stage dynamics

- To describe the submicroscopic reservoir and the number of asymptomatic infections contributing to transmission of *P. vivax* and *P. falciparum* malaria.
- To compare the gametocytogenesis of *P. falciparum* and *P. vivax* in semi-immune children of the Albinama cohort.
- To assess the differences in gametocytogenesis of *P. vivax* new infection and relapses by comparing two treatment arms.
- To evaluate the contribution to transmission of *P. vivax* new infection and relapses by comparing the gametocyte densities in two treatment arms.
- To investigate a long-term effect of PQ on the transmission dynamics of *P. falciparum*.

Additional contributions to related research projects

In the course of this thesis, I had the possibility to contribute to a wide range of projects. In one already published project, I contributed by:

- Development of over 30 qPCR assays for the evaluation of the up-regulation in the early stage of commitment to *P. falciparum* gametocytogenesis. RNAs of an inducible *P. falciparum* Heterochromatin Protein 1 knockdown of *P. falciparum* 3D7 strain were extracted, reverse transcribed and tested for this project (Brancucci et al., 2014 , see Appendixe A).

In other projects that are currently in press or in preparation, I contributed by:

- Collection of over 30 *P. vivax* field samples in the Amazon region of Brazil and subsequent on-field purification and enrichment of gametocytes. A part of these samples were used for the development of a dilution trend line of gametocytes to establish a reliable quantification of *pvs25* transcripts (Koepfli et al., – in press).
- Another part of these gametocyte samples is currently being analyzed in an international collaboration aiming at the first description of the transcriptome of sexual stages of *P. vivax* (in preparation).

References

Abdel-Wahab, A., Abdel-Muhsin, A.-M.A., Ali, E., Suleiman, S., Ahmed, S., Walliker, D., Babiker, H.A., 2002. Dynamics of gametocytes among Plasmodium falciparum clones in natural infections in an area of highly seasonal transmission. J. Infect. Dis. 185, 1838–1842.

Alving, A.S., Carson, P.E., Flanagan, C.L., Ickes, C.E., 1956. Enzymatic deficiency in primaquine-sensitive erythrocytes. Science 124, 484–485.

Anstey, N.M., Handojo, T., Pain, M.C.F., Kenangalem, E., Tjitra, E., Price, R.N., Maguire, G.P., 2007. Lung injury in vivax malaria: pathophysiological evidence for pulmonary vascular sequestration and posttreatment alveolar-capillary inflammation. J. Infect. Dis. 195, 589–596.

Arnot, D., 1998. Unstable malaria in Sudan: the influence of the dry season. Clone multiplicity of Plasmodium falciparum infections in individuals exposed to variable levels of disease transmission. Trans. R. Soc. Trop. Med. Hyg. 92, 580–585.

Babiker, H.A., Abdel-Wahab, A., Ahmed, S., Suleiman, S., Ranford-Cartwright, L., Carter, R., Walliker, D., 1999. Detection of low level Plasmodium falciparum gametocytes using reverse transcriptase polymerase chain reaction. Mol. Biochem. Parasitol. 99, 143–148.

Babiker, H.A., Schneider, P., 2008. Application of molecular methods for monitoring transmission stages of malaria parasites. Biomed. Mater. Bristol Engl. 3, 034007.

Baird, J.K., 2007a. Neglect of Plasmodium vivax malaria. Trends Parasitol. 23, 533–539.

Baird, J.K., 2007b. A rare glimpse at the efficacy of primaquine. Am. J. Trop. Med. Hyg. 76, 201–202.

Baird, J.K., 2009. Resistance to Therapies for Infection by Plasmodium vivax. Clin. Microbiol. Rev. 22, 508–534.

Barnadas, C., Koepfli, C., Karunajeewa, H.A., Siba, P.M., Davis, T.M.E., Mueller, I., 2011. Characterization of Treatment Failure in Efficacy Trials of Drugs against Plasmodium vivax by Genotyping Neutral and Drug Resistance-Associated Markers▿. Antimicrob. Agents Chemother. 55, 4479–4481.

Bejon, P., Andrews, L., Hunt-Cooke, A., Sanderson, F., Gilbert, S.C., Hill, A.V., 2006. Thick blood film examination for Plasmodium falciparum malaria has reduced sensitivity and underestimates parasite density. Malar. J. 5, 104.

Betuela, I., Bassat, Q., Kiniboro, B., Robinson, L.J., Rosanas-Urgell, A., Stanisic, D., Siba, P.M., Alonso, P.L., Mueller, I., 2012a. Tolerability and safety of primaquine in Papua New Guinean children 1 to 10 years of age. Antimicrob. Agents Chemother. 56, 2146–2149.

Betuela, I., Rosanas-Urgell, A., Kiniboro, B., Stanisic, D.I., Samol, L., de Lazzari, E., Del Portillo, H.A., Siba, P., Alonso, P.L., Bassat, Q., Mueller, I., 2012b. Relapses contribute significantly to the risk of Plasmodium vivax infection and disease in Papua New Guinean children 1-5 years of age. J. Infect. Dis. 206, 1771–1780.

Beurskens, M., Mens, P., Schallig, H., Syafruddin, D., Asih, P.B.S., Hermsen, R., Sauerwein, R., 2009. Quantitative determination of Plasmodium vivax gametocytes by real-time quantitative nucleic acid sequence-based amplification in clinical samples. Am. J. Trop. Med. Hyg. 81, 366–369.

Bousema, J.T., Schneider, P., Gouagna, L.C., Drakeley, C.J., Tostmann, A., Houben, R., Githure, J.I., Ord, R., Sutherland, C.J., Omar, S.A., Sauerwein, R.W., 2006. Moderate effect of artemisinin-based combination therapy on transmission of Plasmodium falciparum. J. Infect. Dis. 193, 1151–1159.

Bousema, T., Drakeley, C., 2011. Epidemiology and infectivity of Plasmodium falciparum and Plasmodium vivax gametocytes in relation to malaria control and elimination. Clin. Microbiol. Rev. 24, 377–410.

Bousema, T., Okell, L., Shekalaghe, S., Griffin, J.T., Omar, S., Sawa, P., Sutherland, C., Sauerwein, R., Ghani, A.C., Drakeley, C., 2010. Revisiting the circulation time of Plasmodium falciparum gametocytes: molecular detection methods to estimate the duration of gametocyte carriage and the effect of gametocytocidal drugs. Malar. J. 9, 136.

Bozdech, Z., Llinás, M., Pulliam, B.L., Wong, E.D., Zhu, J., DeRisi, J.L., 2003. The transcriptome of the intraerythrocytic developmental cycle of Plasmodium falciparum. PLoS Biol. 1, E5.

Bozdech, Z., Mok, S., Hu, G., Imwong, M., Jaidee, A., Russell, B., Ginsburg, H., Nosten, F., Day, N.P.J., White, N.J., Carlton, J.M., Preiser, P.R., 2008. The transcriptome of Plasmodium vivax reveals divergence and diversity of transcriptional regulation in malaria parasites. Proc. Natl. Acad. Sci. U. S. A. 105, 16290–16295.

Brancucci, N.M.B., Bertschi, N.L., Zhu, L., Niederwieser, I., Chin, W.H., Wampfler, R., Freymond, C., Rottmann, M., Felger, I., Bozdech, Z., Voss, T.S., 2014. Heterochromatin protein 1 secures survival

and transmission of malaria parasites. Cell Host Microbe 16, 165–176.

Bruce, M.C., Galinski, M.R., Barnwell, J.W., Donnelly, C.A., Walmsley, M., Alpers, M.P., Walliker, D., Day, K.P., 2000. Genetic diversity and dynamics of plasmodium falciparum and P. vivax populations in multiply infected children with asymptomatic malaria infections in Papua New Guinea. Parasitology 121 (Pt 3), 257–272.

Carter, R., Graves, P.M., 1988. Gametocytes Carter R, Graves PM. Gametocytes. In: Wernsdorfer WH, McGregor I, editors. Malaria. Churchill Livingstone; Edinburgh, U.K.: 1988. pp. 253–306. In: Malaria. Churchill Livingstone; Edinburgh, U.K., pp. pp. 253–306.

Carvalho, B.O., Lopes, S.C.P., Nogueira, P.A., Orlandi, P.P., Bargieri, D.Y., Blanco, Y.C., Mamoni, R., Leite, J.A., Rodrigues, M.M., Soares, I.S., Oliveira, T.R., Wunderlich, G., Lacerda, M.V.G., del Portillo, H.A., Araújo, M.O.G., Russell, B., Suwanarusk, R., Snounou, G., Rénia, L., Costa, F.T.M., 2010. On the cytoadhesion of Plasmodium vivax-infected erythrocytes. J. Infect. Dis. 202, 638–647.

Collins, W.E., Jeffery, G.M., Roberts, J.M., 2004. A retrospective examination of reinfection of humans with Plasmodium vivax. Am. J. Trop. Med. Hyg. 70, 642–644.

Cox-Singh, J., Davis, T.M.E., Lee, K.-S., Shamsul, S.S.G., Matusop, A., Ratnam, S., Rahman, H.A., Conway, D.J., Singh, B., 2008. Plasmodium knowlesi malaria in humans is widely distributed and potentially life threatening. Clin. Infect. Dis. Off. Publ. Infect. Dis. Soc. Am. 46, 165–171.

Craige, B., Alving, A.S., 1947. The Chesson strain of Plasmodium vivax malaria; relationship between prepatent period, latent period and relapse rate. J. Infect. Dis. 80, 228–236.

De Koning-Ward, T.F., Olivieri, A., Bertuccini, L., Hood, A., Silvestrini, F., Charvalias, K., Berzosa Díaz, P., Camarda, G., McElwain, T.F., Papenfuss, T., Healer, J., Baldassarri, L., Crabb, B.S., Alano, P., Ranford-Cartwright, L.C., 2008. The role of osmiophilic bodies and Pfg377 expression in female gametocyte emergence and mosquito infectivity in the human malaria parasite Plasmodium falciparum. Mol. Microbiol. 67, 278–290.

Desowitz, R.S., Spark, R.A., 1987. Malaria in the Maprik area of the Sepik region, Papua New Guinea: 1957-1984. Trans. R. Soc. Trop. Med. Hyg. 81, 175–176.

Eziefula, A.C., Bousema, T., Yeung, S., Kamya, M., Owaraganise, A., Gabagaya, G., Bradley, J., Grignard, L., Lanke, K.H.W., Wanzira, H., Mpimbaza, A., Nsobya, S., White, N.J., Webb, E.L., Staedke, S.G., Drakeley, C., 2014. Single dose primaquine for clearance of Plasmodium falciparum gametocytes in children with uncomplicated malaria in Uganda: a randomised, controlled, double-blind, dose-ranging trial. Lancet Infect. Dis. 14, 130–139.

Falk, N., Maire, N., Sama, W., Owusu-Agyei, S., Smith, T., Beck, H.-P., Felger, I., 2006. Comparison of PCR-RFLP and Genescan-based genotyping for analyzing infection dynamics of Plasmodium falciparum. Am. J. Trop. Med. Hyg. 74, 944–950.

Galinski, M.R., Barnwell, J.W., 2008. Plasmodium vivax: who cares? Malar. J. 7, S9.

Galinski, M.R., Meyer, E.V.S., Barnwell, J.W., 2013. Plasmodium vivax: modern strategies to study a persistent parasite's life cycle. Adv. Parasitol. 81, 1–26.

Genton, B., D'Acremont, V., Rare, L., Baea, K., Reeder, J.C., Alpers, M.P., Müller, I., 2008. Plasmodium vivax and mixed infections are associated with severe malaria in children: a prospective cohort study from Papua New Guinea. PLoS Med. 5, e127.

Gething, P.W., Elyazar, I.R.F., Moyes, C.L., Smith, D.L., Battle, K.E., Guerra, C.A., Patil, A.P., Tatem, A.J., Howes, R.E., Myers, M.F., George, D.B., Horby, P., Wertheim, H.F.L., Price, R.N., Müeller, I., Baird, J.K., Hay, S.I., 2012. A long neglected world malaria map: Plasmodium vivax endemicity in 2010. PLoS Negl. Trop. Dis. 6, e1814.

Golenda, C.F., Li, J., Rosenberg, R., 1997. Continuous in vitro propagation of the malaria parasite Plasmodium vivax. Proc. Natl. Acad. Sci. U. S. A. 94, 6786–6791.

Goller, J.L., Jolley, D., Ringwald, P., Biggs, B.-A., 2007. Regional differences in the response of Plasmodium vivax malaria to primaquine as anti-relapse therapy. Am. J. Trop. Med. Hyg. 76, 203–207.

Graves, P.M., Burkot, T.R., Carter, R., Cattani, J.A., Lagog, M., Parker, J., Brabin, B.J., Gibson, F.D., Bradley, D.J., Alpers, M.P., 1988. Measurement of malarial infectivity of human populations to mosquitoes in the Madang area, Papua, New Guinea. Parasitology 96 (Pt 2), 251–263.

Guerra, C.A., Howes, R.E., Patil, A.P., Gething, P.W., Van Boeckel, T.P., Temperley, W.H., Kabaria, C.W., Tatem, A.J., Manh, B.H., Elyazar, I.R.F., Baird, J.K., Snow, R.W., Hay, S.I., 2010. The international limits and population at risk of Plasmodium vivax transmission in 2009. PLoS Negl. Trop. Dis. 4, e774.

Hairston, N.G., Bang, F.B., Maier, J., 1947. Malaria in the natives of New Guinea. Trans. R. Soc. Trop. Med. Hyg. 40, 795–807.

Hans, D., Pattnaik, P., Bhattacharyya, A., Shakri, A.R., Yazdani, S.S., Sharma, M., Choe, H., Farzan, M., Chitnis, C.E., 2005. Mapping binding residues in the Plasmodium vivax domain that binds Duffy antigen during red cell invasion. Mol. Microbiol. 55, 1423–1434.

Hay, S.I., Guerra, C.A., Tatem, A.J., Noor, A.M., Snow, R.W., 2004. The global distribution and population at risk of malaria: past, present, and future. Lancet Infect. Dis. 4, 327–336.

Huh, A.-J., Kwak, Y.G., Kim, E.S., Lee, K.S., Yeom, J.-S., Cho, Y.-K., Kim, C.-S., Park, J.-W., 2011. Parasitemia Characteristics of Plasmodium vivax Malaria Patients in the Republic of Korea. J. Korean Med. Sci. 26, 42.

Imwong, M., Snounou, G., Pukrittayakamee, S., Tanomsing, N., Kim, J.R., Nandy, A., Guthmann, J.-P., Nosten, F., Carlton, J., Looareesuwan, S., Nair, S., Sudimack, D., Day, N.P.J., Anderson, T.J.C., White, N.J., 2007. Relapses of Plasmodium vivax infection usually result from activation of heterologous hypnozoites. J. Infect. Dis. 195, 927–933.

Jamison, D.T.D.T., Breman, J.G.J.G., Measham, A.R.A.R., Alleyne, G.G., Claeson, M.M., Evans, D.B.D.B., Jha, P.P., Mills, A.A., Musgrove, P.P. (Eds.), 2006. Disease Control Priorities in Developing Countries, 2nd ed. World Bank, Washington (DC).

Jones, S., Sutherland, C.J., Hermsen, C., Arens, T., Teelen, K., Hallett, R., Corran, P., van der Vegte-Bolmer, M., Sauerwein, R., Drakeley, C.J., Bousema, T., 2012. Filter paper collection of Plasmodium falciparum mRNA for detecting low-density gametocytes. Malar. J. 11, 266.

Kang, J.-M., Ju, H.-L., Moon, S.-U., Cho, P.-Y., Bahk, Y.-Y., Sohn, W.-M., Park, Y.-K., Cha, S.H., Kim, T.-S., Na, B.-K., 2013. Limited sequence polymorphisms of four transmission-blocking vaccine candidate antigens in Plasmodium vivax Korean isolates. Malar. J. 12, 144.

Karunajeewa, H.A., Mueller, I., Senn, M., Lin, E., Law, I., Gomorrai, P.S., Oa, O., Griffin, S., Kotab, K., Suano, P., Tarongka, N., Ura, A., Lautu, D., Page-Sharp, M., Wong, R., Salman, S., Siba, P., Ilett, K.F., Davis, T.M.E., 2008. A trial of combination antimalarial therapies in children from Papua New Guinea. N. Engl. J. Med. 359, 2545–2557.

Koepfli, C., Colborn, K.L., Kiniboro, B., Lin, E., Speed, T.P., Siba, P.M., Felger, I., Mueller, I., 2013. A high force of plasmodium vivax blood-stage infection drives the rapid acquisition of immunity in papua new guinean children. PLoS Negl. Trop. Dis. 7, e2403.

Koepfli, C., Mueller, I., Marfurt, J., Goroti, M., Sie, A., Oa, O., Genton, B., Beck, H.-P., Felger, I., 2009. Evaluation of Plasmodium vivax genotyping markers for molecular monitoring in clinical trials. J. Infect. Dis. 199, 1074–1080.

Koepfli, C., Robinson, L., Rarau, P., Salib, M., Sambale, N., Betuela, I., Nuitragool, W., Barry, A.E., Siba, P., Felger, I., Mueller, I., – in press. Blood-stage parasitaemia and age determine Plasmodium falciparum and P. vivax gametocytaemia in Papua New Guinea. PLoS One.

Koepfli, C., Ross, A., Kiniboro, B., Smith, T.A., Zimmerman, P.A., Siba, P., Mueller, I., Felger, I., 2011. Multiplicity and diversity of Plasmodium vivax infections in a highly endemic region in Papua New Guinea. PLoS Negl. Trop. Dis. 5, e1424.

Kuamsab, N., Putaporntip, C., Pattanawong, U., Jongwutiwes, S., 2012. Simultaneous detection of Plasmodium vivax and Plasmodium falciparum gametocytes in clinical isolates by multiplex-nested RT-PCR. Malar. J. 11, 190.

Kyabayinze, D.J., Karamagi, C., Kiggundu, M., Kamya, M.R., Wabwire-Mangen, F., Kironde, F., Talisuna, A., 2008. Multiplicity of Plasmodium falciparum infection predicts antimalarial treatment outcome in Ugandan children. Afr. Health Sci. 8, 200–205.

Lasonder, E., Ishihama, Y., Andersen, J.S., Vermunt, A.M.W., Pain, A., Sauerwein, R.W., Eling, W.M.C., Hall, N., Waters, A.P., Stunnenberg, H.G., Mann, M., 2002. Analysis of the Plasmodium falciparum proteome by high-accuracy mass spectrometry. Nature 419, 537–542.

Lima, N.F., Bastos, M.S., Ferreira, M.U., 2012. Plasmodium vivax: reverse transcriptase real-time PCR for gametocyte detection and quantitation in clinical samples. Exp. Parasitol. 132, 348–354.

Lin, E., Kiniboro, B., Gray, L., Dobbie, S., Robinson, L., Laumaea, A., Schöpflin, S., Stanisic, D., Betuela, I., Blood-Zikursh, M., Siba, P., Felger, I., Schofield, L., Zimmerman, P., Mueller, I., 2010. Differential patterns of infection and disease with P. falciparum and P. vivax in young Papua New Guinean children. PloS One 5, e9047.

Liu, W., Li, Y., Shaw, K.S., Learn, G.H., Plenderleith, L.J., Malenke, J.A., Sundararaman, S.A., Ramirez, M.A., Crystal, P.A., Smith, A.G., Bibollet-Ruche, F., Ayouba, A., Locatelli, S., Esteban, A., Mouacha, F., Guichet, E., Butel, C., Ahuka-Mundeke, S., Inogwabini, B.-I., Ndjango, J.-B.N., Speede, S., Sanz, C.M., Morgan, D.B., Gonder, M.K., Kranzusch, P.J., Walsh, P.D., Georgiev, A.V., Muller, M.N., Piel,

A.K., Stewart, F.A., Wilson, M.L., Pusey, A.E., Cui, L., Wang, Z., Färnert, A., Sutherland, C.J., Nolder, D., Hart, J.A., Hart, T.B., Bertolani, P., Gillis, A., LeBreton, M., Tafon, B., Kiyang, J., Djoko, C.F., Schneider, B.S., Wolfe, N.D., Mpoudi-Ngole, E., Delaporte, E., Carter, R., Culleton, R.L., Shaw, G.M., Rayner, J.C., Peeters, M., Hahn, B.H., Sharp, P.M., 2014. African origin of the malaria parasite Plasmodium vivax. Nat. Commun. 5, 3346.

Manning, L., Laman, M., Law, I., Bona, C., Aipit, S., Teine, D., Warrell, J., Rosanas-Urgell, A., Lin, E., Kiniboro, B., Vince, J., Hwaiwhanje, I., Karunajeewa, H., Michon, P., Siba, P., Mueller, I., Davis, T.M.E., 2011. Features and prognosis of severe malaria caused by Plasmodium falciparum, Plasmodium vivax and mixed Plasmodium species in Papua New Guinean children. PloS One 6, e29203.

Marfurt, J., Müeller, I., Sie, A., Maku, P., Goroti, M., Reeder, J.C., Beck, H.-P., Genton, B., 2007. Low efficacy of amodiaquine or chloroquine plus sulfadoxine-pyrimethamine against Plasmodium falciparum and P. vivax malaria in Papua New Guinea. Am. J. Trop. Med. Hyg. 77, 947–954.

McCarthy, J.S., Griffin, P.M., Sekuloski, S., Bright, A.T., Rockett, R., Looke, D., Elliott, S., Whiley, D., Sloots, T., Winzeler, E.A., Trenholme, K.R., 2013. Experimentally induced blood-stage Plasmodium vivax infection in healthy volunteers. J. Infect. Dis. 208, 1688–1694.

McKenzie, F.E., Jeffery, G.M., Collins, W.E., 2007. Gametocytemia and fever in human malaria infections. J. Parasitol. 93, 627–633.

Mckenzie, F.E., Wongsrichanalai, C., Magill, A.J., Forney, J.R., Permpanich, B., Lucas, C., Erhart, L.M., O'Meara, W.P., Smith, D.L., Sirichaisinthop, J., Gasser, R.A., Jr, 2006. Gametocytemia in Plasmodium vivax and Plasmodium falciparum infections. J. Parasitol. 92, 1281–1285.

Mehlotra, R.K., Lorry, K., Kastens, W., Miller, S.M., Alpers, M.P., Bockarie, M., Kazura, J.W., Zimmerman, P.A., 2000. Random distribution of mixed species malaria infections in Papua New Guinea. Am. J. Trop. Med. Hyg. 62, 225–231.

Mendes, C., Dias, F., Figueiredo, J., Mora, V.G., Cano, J., de Sousa, B., do Rosário, V.E., Benito, A., Berzosa, P., Arez, A.P., 2011. Duffy negative antigen is no longer a barrier to Plasmodium vivax--molecular evidences from the African West Coast (Angola and Equatorial Guinea). PLoS Negl. Trop. Dis. 5, e1192.

Mendis, K., Sina, B.J., Marchesini, P., Carter, R., 2001. The neglected burden of Plasmodium vivax malaria. Am. J. Trop. Med. Hyg. 64, 97–106.

Michon, P., Cole-Tobian, J.L., Dabod, E., Schoepflin, S., Igu, J., Susapu, M., Tarongka, N., Zimmerman, P.A., Reeder, J.C., Beeson, J.G., Schofield, L., King, C.L., Mueller, I., 2007. The risk of malarial infections and disease in Papua New Guinean children. Am. J. Trop. Med. Hyg. 76, 997–1008.

Miller, L.H., Mason, S.J., Clyde, D.F., McGinniss, M.H., 1976. The resistance factor to Plasmodium vivax in blacks. The Duffy-blood-group genotype, FyFy. N. Engl. J. Med. 295, 302–304.

Mlambo, G., Vasquez, Y., LeBlanc, R., Sullivan, D., Kumar, N., 2008. A filter paper method for the detection of Plasmodium falciparum gametocytes by reverse transcription polymerase chain reaction. Am. J. Trop. Med. Hyg. 78, 114–116.

Mueller, I., Schoepflin, S., Smith, T.A., Benton, K.L., Bretscher, M.T., Lin, E., Kiniboro, B., Zimmerman, P.A., Speed, T.P., Siba, P., Felger, I., 2012. Force of infection is key to understanding the epidemiology of Plasmodium falciparum malaria in Papua New Guinean children. Proc. Natl. Acad. Sci. U. S. A. 109, 10030–10035.

Mueller, I., Taime, J., Ibam, E., Kundi, J., Lagog, M., Bockarie, M., Reeder, J.C., 2002. Complex patterns of malaria epidemiology in the highlands region of Papua New Guinea. P. N. G. Med. J. 45, 200–205.

Mueller, I., Taime, J., Ivivi, R., Yala, S., Bjorge, S., Riley, I.D., Reeder, J.C., 2003. The epidemiology of malaria in the Papua New Guinea highlands: 1. Western Highlands Province. P. N. G. Med. J. 46, 16–31.

Mueller, I., Widmer, S., Michel, D., Maraga, S., McNamara, D.T., Kiniboro, B., Sie, A., Smith, T.A., Zimmerman, P.A., 2009. High sensitivity detection of Plasmodium species reveals positive correlations between infections of different species, shifts in age distribution and reduced local variation in Papua New Guinea. Malar. J. 8, 41.

Nakazawa, S., Culleton, R., Maeno, Y., 2011. In vivo and in vitro gametocyte production of Plasmodium falciparum isolates from Northern Thailand. Int. J. Parasitol. 41, 317–323.

Ngassa Mbenda, H.G., Das, A., 2014. Molecular evidence of Plasmodium vivax mono and mixed malaria parasite infections in Duffy-negative native Cameroonians. PloS One 9, e103262.

Nwakanma, D., Kheir, A., Sowa, M., Dunyo, S., Jawara, M., Pinder, M., Milligan, P., Walliker, D., Babiker, H.A., 2008. High gametocyte complexity and mosquito infectivity of Plasmodium falciparum in the Gambia. Int. J. Parasitol. 38, 219–227.

Okell, L.C., Drakeley, C.J., Ghani, A.C., Bousema, T., Sutherland, C.J., 2008. Reduction of transmission from malaria patients by artemisinin combination therapies: a pooled analysis of six randomized trials. Malar. J. 7, 125.

Ouédraogo, A.L., Bousema, T., Schneider, P., de Vlas, S.J., Ilboudo-Sanogo, E., Cuzin-Ouattara, N., Nébié, I., Roeffen, W., Verhave, J.P., Luty, A.J.F., Sauerwein, R., 2009. Substantial contribution of submicroscopical Plasmodium falciparum gametocyte carriage to the infectious reservoir in an area of seasonal transmission. PloS One 4, e8410.

Prajapati, S.K., Joshi, H., Dua, V.K., 2011. Antigenic repertoire of Plasmodium vivax transmission-blocking vaccine candidates from the Indian subcontinent. Malar. J. 10, 111.

Price, R.N., Tjitra, E., Guerra, C.A., Yeung, S., White, N.J., Anstey, N.M., 2007. Vivax malaria: neglected and not benign. Am. J. Trop. Med. Hyg. 77, 79–87.

Pukrittayakamee, S., Chotivanich, K., Chantra, A., Clemens, R., Looareesuwan, S., White, N.J., 2004. Activities of artesunate and primaquine against asexual- and sexual-stage parasites in falciparum malaria. Antimicrob. Agents Chemother. 48, 1329–1334.

Rieckmann, K.H., Davis, D.R., Hutton, D.C., 1989. Plasmodium vivax resistance to chloroquine? Lancet 2, 1183–1184.

Rosanas-Urgell, A., Mueller, D., Betuela, I., Barnadas, C., Iga, J., Zimmerman, P.A., del Portillo, H.A., Siba, P., Mueller, I., Felger, I., 2010. Comparison of diagnostic methods for the detection and quantification of the four sympatric Plasmodium species in field samples from Papua New Guinea. Malar. J. 9, 361.

Rupp, I., Sologub, L., Williamson, K.C., Scheuermayer, M., Reininger, L., Doerig, C., Eksi, S., Kombila, D.U., Frank, M., Pradel, G., 2011. Malaria parasites form filamentous cell-to-cell connections during reproduction in the mosquito midgut. Cell Res. 21, 683–696.

Russell, B., Suwanarusk, R., Borlon, C., Costa, F.T.M., Chu, C.S., Rijken, M.J., Sriprawat, K., Warter, L., Koh, E.G.L., Malleret, B., Colin, Y., Bertrand, O., Adams, J.H., D'Alessandro, U., Snounou, G., Nosten, F., Rénia, L., 2011. A reliable ex vivo invasion assay of human reticulocytes by Plasmodium vivax. Blood 118, e74–81.

Sattabongkot, J., Tsuboi, T., Hisaeda, H., Tachibana, M., Suwanabun, N., Rungruang, T., Cao, Y.-M., Stowers, A.W., Sirichaisinthop, J., Coleman, R.E., Torii, M., 2003. Blocking of transmission to mosquitoes by antibody to Plasmodium vivax malaria vaccine candidates Pvs25 and Pvs28 despite antigenic polymorphism in field isolates. Am. J. Trop. Med. Hyg. 69, 536–541.

Schneider, P., Bousema, J.T., Gouagna, L.C., Otieno, S., van de Vegte-Bolmer, M., Omar, S.A., Sauerwein, R.W., 2007. Submicroscopic Plasmodium falciparum gametocyte densities frequently result in mosquito infection. Am. J. Trop. Med. Hyg. 76, 470–474.

Schneider, P., Schoone, G., Schallig, H., Verhage, D., Telgt, D., Eling, W., Sauerwein, R., 2004. Quantification of Plasmodium falciparum gametocytes in differential stages of development by quantitative nucleic acid sequence-based amplification. Mol. Biochem. Parasitol. 137, 35–41.

Schoepflin, S., Lin, E., Kiniboro, B., DaRe, J.T., Mehlotra, R.K., Zimmerman, P.A., Mueller, I., Felger, I., 2010. Treatment with Coartem (Artemether-Lumefantrine) in Papua New Guinea. Am. J. Trop. Med. Hyg. 82, 529–534.

Schoepflin, S., Valsangiacomo, F., Lin, E., Kiniboro, B., Mueller, I., Felger, I., 2009. Comparison of Plasmodium falciparum allelic frequency distribution in different endemic settings by high-resolution genotyping. Malar. J. 8, 250.

Shekalaghe, S.A., Bousema, J.T., Kunei, K.K., Lushino, P., Masokoto, A., Wolters, L.R., Mwakalinga, S., Mosha, F.W., Sauerwein, R.W., Drakeley, C.J., 2007a. Submicroscopic Plasmodium falciparum gametocyte carriage is common in an area of low and seasonal transmission in Tanzania. Trop. Med. Int. Health TM IH 12, 547–553.

Shekalaghe, S.A., Drakeley, C., Gosling, R., Ndaro, A., van Meegeren, M., Enevold, A., Alifrangis, M., Mosha, F., Sauerwein, R., Bousema, T., 2007b. Primaquine clears submicroscopic Plasmodium falciparum gametocytes that persist after treatment with sulphadoxine-pyrimethamine and artesunate. PloS One 2, e1023.

Silvestrini, F., Bozdech, Z., Lanfrancotti, A., Di Giulio, E., Bultrini, E., Picci, L., Derisi, J.L., Pizzi, E., Alano, P., 2005. Genome-wide identification of genes upregulated at the onset of gametocytogenesis in Plasmodium falciparum. Mol. Biochem. Parasitol. 143, 100–110.

Sinclair, D., Zani, B., Donegan, S., Olliaro, P., Garner, P., 2009. Artemisinin-based combination therapy for treating uncomplicated malaria. Cochrane Database Syst. Rev. CD007483.

Sinden, R.E., Smalley, M.E., 1979. Gametocytogenesis of Plasmodium falciparum in vitro: the cell-cycle.

Parasitology 79, 277–296.
Singh, B., Kim Sung, L., Matusop, A., Radhakrishnan, A., Shamsul, S.S.G., Cox-Singh, J., Thomas, A., Conway, D.J., 2004. A large focus of naturally acquired Plasmodium knowlesi infections in human beings. Lancet 363, 1017–1024.
Smalley, M.E., Sinden, R.E., 1977. Plasmodium falciparum gametocytes: their longevity and infectivity. Parasitology 74, 1–8.
Smith, T., Felger, I., Tanner, M., Beck, H.P., 1999. Premunition in Plasmodium falciparum infection: insights from the epidemiology of multiple infections. Trans. R. Soc. Trop. Med. Hyg. 93 Suppl 1, 59–64.
Tanabe, K., Mita, T., Jombart, T., Eriksson, A., Horibe, S., Palacpac, N., Ranford-Cartwright, L., Sawai, H., Sakihama, N., Ohmae, H., Nakamura, M., Ferreira, M.U., Escalante, A.A., Prugnolle, F., Björkman, A., Färnert, A., Kaneko, A., Horii, T., Manica, A., Kishino, H., Balloux, F., 2010. Plasmodium falciparum accompanied the human expansion out of Africa. Curr. Biol. CB 20, 1283–1289.
Tao, D., Ubaida-Mohien, C., Mathias, D.K., King, J.G., Pastrana-Mena, R., Tripathi, A., Goldowitz, I., Graham, D.R., Moss, E., Marti, M., Dinglasan, R.R., 2014. Sex-partitioning of the Plasmodium falciparum stage V gametocyte proteome provides insight into falciparum-specific cell biology. Mol. Cell. Proteomics MCP 13, 2705–2724.
White, N.J., 2008. The role of anti-malarial drugs in eliminating malaria. Malar. J. 7 Suppl 1, S8.
White, N.J., 2011. Determinants of relapse periodicity in Plasmodium vivax malaria. Malar. J. 10, 297.
White, N.J., Ashley, E.A., Recht, J., Delves, M.J., Ruecker, A., Smithuis, F.M., Eziefula, A.C., Bousema, T., Drakeley, C., Chotivanich, K., Imwong, M., Pukrittayakamee, S., Prachumsri, J., Chu, C., Andolina, C., Bancone, G., Hien, T.T., Mayxay, M., Taylor, W.R., von Seidlein, L., Price, R.N., Barnes, K.I., Djimdé, A., Ter Kuile, F., Gosling, R., Chen, I., Dhorda, M.J., Stepniewska, K., Guérin, P., Woodrow, C.J., Dondorp, A.M., Day, N.P., Nosten, F.H., 2014. Assessment of therapeutic responses to gametocytocidal drugs in Plasmodium falciparum malaria. Malar. J. 13, 483.
WHO, 2010. Guidelines for the Treatment of Malaria, 2nd ed, WHO Guidelines Approved by the Guidelines Review Committee. World Health Organization, Geneva.
WHO, 2011. WHO | World Malaria Report 2011 [WWW Document]. WHO. URL http://www.who.int/malaria/world_malaria_report_2011/en/ (accessed 9.20.12).
WHO, 2012. Malaria Policy Advisory Committee to the WHO: conclusions and recommendations of September 2012 meeting. Malar. J. 11, 424.
WHO, 2014. WHO | World Malaria Report 2014 [WWW Document]. WHO. URL http://www.who.int/malaria/publications/world_malaria_report_2014/report/en/ (accessed 2.9.15).
Young, J.A., Fivelman, Q.L., Blair, P.L., de la Vega, P., Le Roch, K.G., Zhou, Y., Carucci, D.J., Baker, D.A., Winzeler, E.A., 2005. The Plasmodium falciparum sexual development transcriptome: A microarray analysis using ontology-based pattern identification. Mol. Biochem. Parasitol. 143, 67–79.
Zakeri, S., Razavi, S., Djadid, N.D., 2009. Genetic diversity of transmission blocking vaccine candidate (Pvs25 and Pvs28) antigen in Plasmodium vivax clinical isolates from Iran. Acta Trop. 109, 176–180.

Chapter 2: Strategies for Detection of *Plasmodium species* Gametocytes

OPEN ACCESS Freely available online

PLOS ONE

Strategies for Detection of *Plasmodium species* Gametocytes

Rahel Wampfler[1,2☯], Felistas Mwingira[1,2☯], Sarah Javati[1,2,3], Leanne Robinson[3], Inoni Betuela[3], Peter Siba[3], Hans-Peter Beck[1,2], Ivo Mueller[3,4], Ingrid Felger[1,2*]

1 Swiss Tropical and Public Health Institute, Basel, Switzerland, **2** University of Basel, Basel, Switzerland, **3** Papua New Guinea Institute of Medical Research, Goroka, Papua New Guinea, **4** Infection and Immunity Division, Walter and Eliza Hall Institute, Parkville, Victoria, Australia

Abstract

Carriage and density of gametocytes, the transmission stages of malaria parasites, are determined for predicting the infectiousness of humans to mosquitoes. This measure is used for evaluating interventions that aim at reducing malaria transmission. Gametocytes need to be detected by amplification of stage-specific transcripts, which requires RNA-preserving blood sampling. For simultaneous, highly sensitive quantification of both, blood stages and gametocytes, we have compared and optimized different strategies for field and laboratory procedures in a cross sectional survey in 315 5-9 yr old children from Papua New Guinea. qRT-PCR was performed for gametocyte markers pfs25 and pvs25, *Plasmodium* species prevalence was determined by targeting both, 18S rRNA genes and transcripts. RNA-based parasite detection resulted in a *P. falciparum* positivity of 24.1%; of these 40.8% carried gametocytes. *P. vivax* positivity was 38.4%, with 38.0% of these carrying gametocytes. Sensitivity of DNA-based parasite detection was substantially lower with 14.1% for *P. falciparum* and 19.6% for *P. vivax*. Using the lower DNA-based prevalence of asexual stages as a denominator increased the percentage of gametocyte-positive infections to 59.1% for *P. falciparum* and 52.4% for *P. vivax*. For studies requiring highly sensitive and simultaneous quantification of sexual and asexual parasite stages, 18S rRNA transcript-based detection saves efforts and costs. RNA-based positivity is considerably higher than other methods. On the other hand, DNA-based parasite quantification is robust and permits comparison with other globally generated molecular prevalence data. Molecular monitoring of low density asexual and sexual parasitaemia will support the evaluation of effects of up-scaled antimalarial intervention programs and can also inform about small scale spatial variability in transmission intensity.

Citation: Wampfler R, Mwingira F, Javati S, Robinson L, Betuela I, et al. (2013) Strategies for Detection of *Plasmodium species* Gametocytes. PLoS ONE 8(9): e76316. doi:10.1371/journal.pone.0076316

Editor: Rick Edward Paul, Institut Pasteur, France

Received April 24, 2013; **Accepted** August 23, 2013; **Published** September 27, 2013

Funding: This work was supported by the Swiss National Science Foundation (grant no. 310030_134889), the International Centers of Excellence in Malaria Research (grant no. U19 AI089686-03) and the Brazilian Swiss Joint Research Programme (grant no. BJRP 0112-07). L. Robinson was supported by an Australian National Health and Medical Research Council Early Career Fellowship #1016443. The funders had no role in study design, data collection and analysis, decision to publish, or preparation of the manuscript.

Competing interests: The authors have declared that no competing interests exist.

* E-mail: ingrid.felger@unibas.ch

☯ These authors contributed equally to this work.

Introduction

The importance of molecular monitoring of gametocytes of *Plasmodium* parasites is increasingly acknowledged, because it provides fast and sensitive quantification of the parasite stage required for transmission from humans to mosquito vectors. Molecular techniques detect particularly very low gametocyte densities that escape detection by light microscopy (LM). Gametocyte densities are an important measure for evaluating effects of interventions that aim at reducing transmission, such as specific drugs, vaccines or bednets [1–3]. Monitoring gametocytes in population studies can inform about the human infective reservoir and provides relevant data for transmission models.

Mature stage V gametocytes circulate in the peripheral blood of infected humans for a mean period of 6.4 days or a maximum of 3 weeks, but often at sub-microscopic levels [2,4]. The proportion of gametocytes among total parasites per host ranged from 0.2% in young children to 5.7% in adults [5]. By molecular techniques gametocytes are differentiated from concurrent asexual forms by targeting RNA transcripts of gametocyte-specifically expressed genes. In the past, detection of submicroscopic gametocytaemia of *P. falciparum* and *P. vivax* was achieved by two non-quantitative methods, reverse transcription-PCR (RT-PCR) and nucleic acid sequence based amplification techniques (NASBA) [4,6–9]. Currently quantitative NASBA techniques are applied increasingly for gametocyte detection of both, *P. falciparum* [10] and *P. vivax*

[11]. For this work we have developed and validated quantitative qRT-PCR TaqMan probe-based assays for *P. falciparum* and *P. vivax* gametocytes.

In view of large field studies planned to monitor effects of antimalarial interventions, robust sampling strategies and laboratory assays are needed. For the detection of gametocytes of malaria parasites, we have evaluated and compared several approaches adapted specifically to those meso- to highly endemic settings where several *Plasmodium* species occur together. Diagnosis of multiple species incurs substantial costs for cross sectional surveys or surveillance, when mostly uninfected individuals or asymptomatic parasite carriers require testing. This issue was addressed by introducing a generic screening assay to determine initially in a single experiment all those samples positive for any *Plasmodium* species. Only samples positive in the generic test were carried forward to species-specific and gametocyte assays. Our aim was to devise a parsimonious but sensitive diagnostic approach, generating robust information on asexual stage and gametocyte densities. These strategies should be useful for investigating transmission dynamics in longitudinal studies.

Prompted by previous reports of successful usage of finger prick blood collected on various filter paper brands in the field [6,7], we have compared the efficiency of sampling and storage on filter paper versus in solution. Three different sampling strategies were applied in the field: (i) whole blood stored in RNAprotect® cell reagent, (ii) whole blood spotted onto Whatman® 3MM filter paper, air dried and stored in TRIzol® reagent thereafter, and (iii) Whatman FTA classic cards. The focus of this study was on the practical field work in the endemic settings with realistic time periods and limited access to freezers. This adds to some recent comparisons of laboratory cultured gametocytes under a variety of controlled conditions and stored for a maximum period of 3 months until processing of samples [8,12]. Both these studies provided a good overview on various brands of filter papers. However, under the specific conditions of malaria surveillance or intervention programs, time intervals from sample collection to processing in the molecular laboratory will likely extend beyond 3 months. Therefore we have investigated the stability of RNA in stored blood samples and that of extracted RNA over a two year interval.

High throughput of samples requiring RNA extraction for gametocyte detection becomes a technical challenge in the context of intensified malaria surveillance. RNA extraction from filter papers is more tedious and contamination prone than handling liquid samples in 96-well format. We have therefore investigated the field applicability of RNAprotect solution (Qiagen) which stabilizes RNA for short term storage and transport at ambient temperature and permits RNA extraction in 96 well plates. We made use of the availability of DNA and RNA of each sample for evaluating the diagnostic sensitivity of DNA-based versus RNA-based parasite detection in field samples. Due to the high abundance of transcripts of our molecular marker 18S rRNA we expected detection of very low density infections, even below the detection limit of standard PCR.

In Papua New Guinea (PNG) all four major *Plasmodium* spp. infecting humans co-occur, whereby *P. falciparum* and *P. vivax* are the predominant *Plasmodium* species with similar frequency [13]. Malaria endemicity is geographically variable throughout PNG with variations not only along broad environmental gradients, but also between villages only a few kilometers apart [14] and even between different clusters of houses within the same villages [15,16]. In this work we have compared several sampling methods and molecular diagnostic approaches, the summary of which lead us to propose a parsimonious strategy for high throughput molecular monitoring in endemic areas with several sympatric *Plasmodium* species.

Materials and Methods

Study population and ethics

Samples were collected from February to March 2010 from 315 mostly asymptomatic children aged 5 to 9 years. This cross-sectional survey formed part of a major cohort study conducted in the Albinama region of Maprik District, East Sepik Province, a malaria endemic area in PNG. Written informed consent was obtained from parents or guardians of each child. Ethical clearance for all molecular analyses was obtained from the Medical Research Advisory Committee of the PNG Ministry of Health (MRAC no. 1206) and from the Ethics Committee of Basel (no. 237/11).

Blood collection and sample storage and transport

From each study participant approximately 250µl of blood was collected in the village by finger prick into a BD microtainer™ containing EDTA. Samples were stored by three different methods: (i) 50 µl whole blood spotted on Whatman® 3MM filter paper directly after bleeding, air dried and stored for 2-4 weeks at +4 °C. Then each blood spot was cut into multiple pieces, transferred into a microfuge tube containing 300 µl TRIzol® reagent (Life Technologies, Zug, Switzerland) and stored at -80°C until shipment on wet ice packs to the molecular laboratory; upon arrival filter papers again were stored at -80°C until RNA extraction. When handling filter papers, RNase was eliminated by RNase away™ Reagent (Ambion) (ii). 50 µl whole blood spotted on FTA classic cards (Whatman, cat. number: WB120205) directly after bleeding, air-dried completely, stored at +4°C and shipped with desiccant at ambient temperature, then again stored at -20°C until RNA extraction (iii). After transport to the field laboratory and within a maximum of 4 hours following blood collection, 50 µl whole blood was transferred from the microtainer into 250 µl RNAprotect® cell reagent (Qiagen). The mixture was stored at -20°C until transported with wet ice pack cooling to the molecular laboratory. RNAprotect and FTA card samples were stored for 5-8 months before nucleic acids were extracted. Filter papers in TRIzol were stored for up to 1 year.

The sampling methods described should not be considered optimized procedures, but rather reflect the best possible option under the specific field conditions. Clearly, the shorter the storage at ambient temperature and the time span to RNA extraction, the better. But stricter protocols are often only

realizable under trial conditions or when working with in vitro cultured parasites or blood from travel clinics.

Extraction of nucleic acids

RNA extraction. All three blood samples collected from 315 study participants were subject to different RNA extraction protocols that had been optimized with *P. falciparum* 3D7 in vitro culture.

(i) Whatman 3MM filter paper: RNA was extracted from whole blood spotted on Whatman 3MM filter paper (corresponding to 25µl whole blood) and stored in TRIzol. Filter papers were transferred from TRIzol into 600 µl RLT lysis buffer containing β-mercaptoethanol (Qiagen RNeasy® plus mini kit) and incubated for 15 min at 30°C on a shaker at 1000 rpm. After centrifugation for 30 sec at 13000g the aqueous phase was transferred to a gDNA eliminator column, a kit component. From this step onwards, the instructions of the kit supplier (Qiagen) were followed closely. The now following procedure included an on-column DNase digest performed after the first washing step with buffer RW1. 10 µl RNase-free DNase (Qiagen) was mixed with 70 µl RDD buffer and added to the membrane. DNA digestion was allowed to proceed for 15 min at room temperature and then terminated by a wash step with buffer RW1 and the supplier's protocol was continued. Finally RNA was eluted in 50 µl RNase-free dH2O and stored for short term at -20°C, for long term at -80°C.

(ii) Whatman® FTA classic cards: RNA was extracted from FTA cards using the Qiagen RNeasy® plus mini kit protocol to 5 filter discs punched out from FTA cards impregnated with whole blood using a Harris Micro-Punch (tip diameter 3.0 mm). Discs were vortexed in buffer RLT Plus for 1 minute and the incubated for 30 min at room temperature (24-27°C) followed by a gDNA eliminator column and an on-column DNase digestion (all Qiagen) according to the manufacturer's protocols. Yields at room temperature were higher than those at incubation temperature of 50°C. We also tested an alternative strategy for RNA extraction from FTA cards following the Whatman FTA Protocol BR01 (http://www.whatman.com/UserFiles/File/Protocols/Bioscience/BR01). Substantial costs for the recommended RNA processing buffer and our RNA yields severely compromised by the necessity for DNase digestion of extracted RNA prompted us to discontinue this approach.

(iii) RNAprotect® cell reagent: RNA was extracted from 300 µl total volume (50µl whole blood plus 250µl RNAprotect reagent) using the RNeasy® plus mini kit protocol for spin column followed by on-column DNase digestion (all from Qiagen). All procedures followed those described in (i) with exception of the first step. This protocol starts with centrifugation for 15 min at 14'000 g. If a pellet was visible, all supernatant was removed and stored at -80°C for subsequent RNA extractions. If no pellet was visible, the centrifugation was repeated. If still no pellet was visible, 250 µl supernatant were removed and to the remaining 50 µl left in the tube RLT lysis buffer was added and RNA was extracted as described above in procedure (i).

The outcome in common of all our attempts to optimize RNA extraction points towards the use of on-column DNase digestion for minimizing loss of RNA.

DNA extraction. Parasite genomic DNA was extracted from all 311 blood samples, from 4 study participants these samples were missing. After removal of plasma and storage of blood pellets at -20°C for a maximum of two years, 50-150 µl blood pellet was used for DNA extraction (individual volumes were recorded) using FavorPrep™ 96-well genomic DNA extraction kit (Favorgen, Taiwan). DNA was eluted in 200 µl elution buffer and stored at -20°C.

Molecular detection of *Plasmodium* parasites

The workflow in Figure **1** depicts the series of consecutive assays performed with both RNA and DNA samples. The infecting Plasmodium species was determined by quantitative PCR (qPCR) using a gDNA template extracted from blood pellets and in parallel also by quantitative reverse-transcription PCR (qRT-PCR) using RNA obtained from the 3 different sampling methods.

RNA-based *Plasmodium species* diagnosis. After extraction all RNA samples were tested by qPCR targeting genes encoding 18S rRNA to confirm complete digestion of gDNA in a StepOne Plus® Real-Time PCR system (Applied Biosystems). This was followed by a generic qRT-PCR using the same generic primers and probe but on RNA in a one-tube reaction combining the reverse transcription and amplification reaction. Primers and probes are listed in Table **S1**, reaction mixes and PCR profiles are listed in Table **S2**. The RNA-based *P. falciparum* assay targeted A-type 18S rRNA transcripts expressed in asexual stages [17], whereas the generic assay targeting conserved regions would amplify all 5 copies of 18S rRNA genes in the genomes of *P. falciparum* and *P. vivax* [18]. All samples positive by the generic *Plasmodium* sp. assay were further analyzed by species–specific qRT-PCR reactions in a simplex reaction for *P. falciparum* and *P. ovale*, and as a duplex reaction for *P. vivax* and *P. malariae*. Primers and probes are listed in Table **S1**. Due to the generally higher parasitaemia in *P. falciparum* than in *P. vivax* infections, 18S rRNA transcripts in *P. falciparum* samples were highly abundant compared to 18S rRNA of for *P. vivax*. During extensive test evaluation we have observed a low level of aerosol-derived contamination when introducing negative controls, i.e. extraction of water. This low level of air-bourne contamination found in some, but not all negative samples, was corrected for by introducing a cut-off of 10 copies/µl extracted RNA for *P. falciparum* 18S rRNA qRT-PCR; for *P. vivax* no cut off was required. The cut off was identified in a plot of all measured transcript copy numbers by the point from which copy numbers rose above a steady baseline. By introducing a cut-off for *P. falciparum*, 51 previously *Pf* qRT-PCR positive samples were considered false positive. All except one sample had been *P. falciparum* negative by qPCR. This finding gave support to the choice of 10 copies/µl extracted RNA as our cut off.

Each plate carried a dilution series of assay-specific control plasmids with the respective template inserted at concentrations of 10^6,10^4 and 10^2 copies of template/reaction in

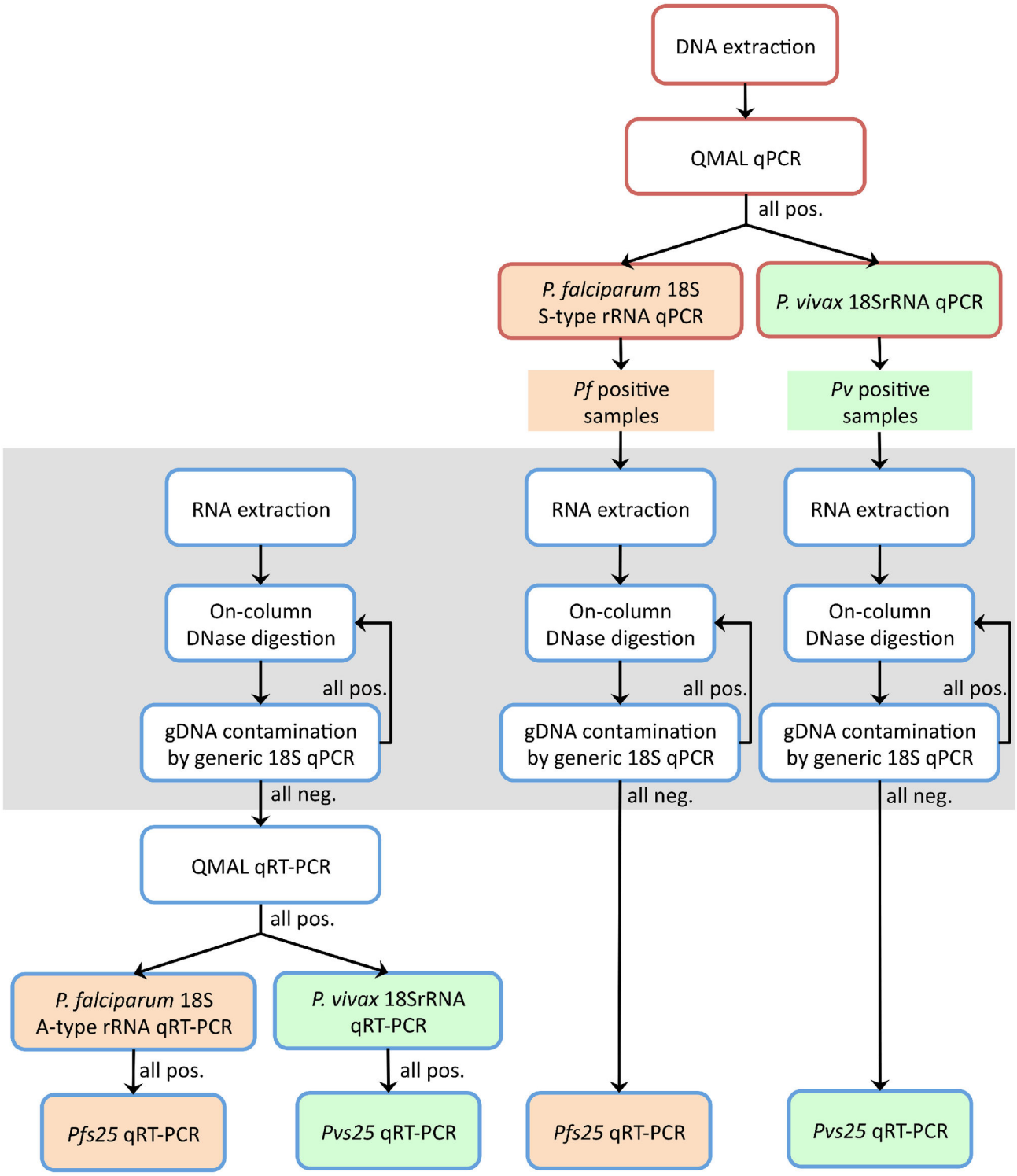

Figure 1. Flow diagram of molecular analyses performed for detection of asexual and sexual parasite stages of *P. vivax* and *P. falciparum* in field samples from PNG. Red and blue frames indicate assays done on DNA and on RNA, respectively. Orange and green boxes are *P. falciparum* and *P. vivax*-specific assays, respectively. *P. malariae* and *P. ovale* assays are not included in the diagram.

doi: 10.1371/journal.pone.0076316.g001

duplicates. For each plate standard curves were generated from these values for quantification of copy numbers in test samples.

DNA-based species diagnosis. As depicted in Figure **1**, all DNA samples were first tested for positivity for any *Plasmodium* parasite species by a generic assay. All samples positive by generic assay were quantified by simplex qPCRs for *P. falciparum* and *P. vivax. P. malariae* and *P. ovale* assays were not performed on DNA level, only on RNA level.

Gametocyte-specific assays

For detection and quantification of *P. falciparum* and *P. vivax* gametocytes qRT-PCRs targeting the two orthologues *pfs25* and *pvs25* transcripts (GenBank accession no: AF193769.1 and GU256271.1, respectively) were developed and validated. These genes are the most frequently used markers for gametocyte detection in NASBA. *Pfs25* is highly expressed in mature gametocytes [4]. Sequences of oligonucleotides are given in Table **S1**, the composition of reaction mixes and thermo profiles are shown in Table **S2**. *Pfs25 and pvs25* primers as well as the *pfs25* HEX-BHQ1-labeled and *pvs25* FAM-BHQ1-labeled probes were selected within non-polymorphic positions identified by alignment of all publicly available nucleotide sequences. Of 138 *P. vivax pvs25* sequences, none showed polymorphism at sequences targeted by our assay, with the exception of a SNP observed in a single isolate, however, this DNA was no more available from the authors for confirmation of sequencing [19]. The region of *pfs25* targeted by our qRT-PCR assay is similar to that of the *pfs25* qNASBA assay of Schneider and coworkers [10], whose molecular beacon overlaps with the forward primer of our qRT-PCR assay. *Pvs25* primers and probe target the gene region also chosen by Beurskens and coworkers [11], whose molecular beacon is identical with our probe.

Gametocyte trend line used for conversion of *pfs25* transcript copy numbers into gametocyte counts

A synchronized (5% sorbitol) 3D7 ring culture of 8% parasitaemia was induced to undergo gametocytogenesis at day -2 by reducing the hematocrit and doubling the Albumax concentration in the medium. At day -1, induced trophozoites were diluted to 2% and a second stress medium was added. At day 0, regular medium was added to the gametocytes (modified after [20]). At day 1 and until day 9, 50mM N-acetylglucosamine was added to the gametocytes to reduce surviving of asexual stages [21]. At day 12, gametocytes were purified by a percoll gradient [22] and counted in a Neubauer Cell Count Chamber at 3 different concentrations. The purified gametocytes were diluted in full medium to concentrations of 10'000, 1'000, 100, 50, 10, 5, 1, 0.5, 0.1, 0.05, 0.01, 0.005 gametocytes/µl in triplicates. 50 µl of gametocyte dilution was added to 250 µl RNAprotect cell reagent (Qiagen) and frozen at -20°C. RNA was extracted using the RNeasy plus 96well Kit (Qiagen) with an additional on column DNase digestion step and amplified on *pfs25* qRT-PCR and QMAL qPCR. A linear regression was applied on the $\log_{10}$ transformed copy numbers of the gametocyte trend line by R version 2.14.0 [23]. The regression coefficient (r^2) was 0.95 ($p<0.0001$). The conversion from transcript copy numbers to gametocytes was as follows: gametocyte counts/µl whole blood = $10^{-1.6225}$ * (copy number pfs25 transcripts/µl whole blood) $^{0.8518}$.

Light microscopy (LM)

Blood slides with thick and thin smears were collected in duplicate for each patient and examined microscopically for *Plasmodium* parasite density (asexual stages and gametocytes) and species identification. Three reads were done and densities counted over 200 white blood cells, which were then converted into parasite s/µl by assuming 8000 white blood cells/µl whole blood.

Statistical analysis

Parasite counts by LM were multiplied by 40 (200WBC ◊ 8000WBC/µl blood) and $\log_{10}$ transformed. Template copy number/µl whole blood obtained from qPCR and qRT-PCR were $\log_{10}$ transformed. Only samples with positive cell counts in both tests were considered. For comparing molecular and microscopic parasite quantification methods, linear regression was applied to the log-transformed densities and DNA or transcript copy numbers. Correlation coefficients were calculated with R [23]. F-statistic was applied to test whether regressions (e.g., LM versus molecular detection) were significant.

Results

Validation of assays and Limit of Detection (LOD) for amplification of gDNA and cDNA

For each assay the respective PCR fragment was inserted into a plasmid as described previously [24]. Serial dilutions of these control plasmids were made in quintuplicates. LOD was defined as the lowest concentration of control plasmid (in copy number/µl) yielding positive results in >50% of parallel samples tested. LOD and amplification efficiencies (calculated as Efficiency = $10^{(-1/Slope)}$ -1) of each assay is listed in Table **S3**.

Prevalence of *Plasmodium sp.* in study population by RNA-based versus DNA-based detection

Detection of any Plasmodium species (generic assay) as well as specific detection of *P. falciparum* or *P. vivax* was performed in parallel on DNA and RNA for all samples. DNA-based detection followed our previously described protocol [24]. For RNA-based detection by qRT-PCR the same primers and probes were utilized, except for the *P. falciparum* assay, which on RNA level targets the A-type 18S rRNA instead of the S-type gene as in qPCR [17]. The generic assays on RNA and DNA level were carried out on all samples, whereas the species-specific assays were only performed in samples previously positive by the generic assay according to Figure **1**. Due to the low local prevalence of *P. malariae* and *P. ovale*, both these species were only detected by RNA-based assays, DNA-based assays were omitted. To reduce complexity in Figure **1**, the performed *P. malariae* and *P. ovale* assays were not included.

Table 1. Prevalence of asexual and sexual stages of *P. falciparum* and *P. vivax* detected by microscopy, qPCR or qRT-PCR in samples from 315 children from PNG.

	Detection method of asexual *Plasmodium* stages		
	Light microscopy	DNA-based approach	RNA-based approach
Sample size (N)	301	311	315
P. falciparum prevalence	20/301 (6.6%)	44/311 (14.1%)	76/315 (24.1%)
Pf gametocyte carriers in *Pf* pos.	7/20 (35.0%)	26/44 (59.1%)	31/76 (40.8%)
P. vivax prevalence	40/301 (13.3%)	61/311 (19.6%)	121/315 (38.4%)
Pv gametocyte carriers in *Pv* pos.	23/40 (57.5%)	32/61 (52.4%)	46/121 (38.0%)

doi: 10.1371/journal.pone.0076316.t001

The initial analysis, carried out to screen for the presence of any malaria parasite, detected 112/311 parasite positive DNA samples, whereas RNA-based 169/315 samples were positive. Such discrepancy in positivity mirrors the high sensitivity of detection when targeting highly abundant 18S rRNA transcripts (probably >10^6 per cell), as opposed to only 5 copies of the 18S rRNA gene per genome [18].

All DNA or RNA samples positive by the generic assays were further analyzed by species specific qPCR or qRT-PCR assays, which also targeted 18S rRNA sequences, yet not the conserved part, but stretches instead that differed between *Plasmodium* species. We have compared parasite positivity obtained by both qPCR and qRT-PCR and by light microscopy in our samples (Table **1**). *P. falciparum* prevalence was 14.1% in DNA samples, but 24.1% in RNA samples. The discrepancy was even larger for *P. vivax*, with 19.6% DNA-based and twice as high RNA-based positivity (38.4%). As expected light microscopy provided the lowest prevalence rate (6.6% for *P. falciparum* and 13.3% for *P. vivax*). Because most parasite carriers were asymptomatic, many of these infections likely harbored low parasite densities around the detection limit of microscopy.

Quantification of parasites

For most research questions quantitative parasitological data is desirable. When introducing molecular measures for parasite quantification, their performance with respect to the classical techniques needs to be evaluated. We therefore compared parasite counts by the different methods. Quantification of *P. vivax* was expected to be particularly difficult for two reasons: firstly, in our study area *P. vivax* densities are about 10 fold lower than *P. falciparum* densities [25], thus detection by PCR is more likely affected by the so called “Monte Carlo effect”, i.e., the random presence or absence of template in a tested DNA aliquot deriving from a blood sample of very low parasitaemia. The additional detection of a large number of scanty parasitaemias by the molecular assay of high sensitivity will lower the median parasite density compared to microscopy. Secondly, due to the presence of *P. vivax* schizont stages in the peripheral blood, a single parasite is not equivalent to one genome, but could account for a per parasite >20 fold higher copy number of the target gene.

To permit parasite quantification based on target gene or transcript copy numbers detected by our 18S rRNA assays, we have plotted densities by light microscopy (LM) versus DNA- or RNA-based quantification (Figure **2**). Only samples positive by both compared tests were considered. For *P. falciparum* 17 LM/DNA, 20 LM/RNA and 42 DNA/RNA positive pairs were available, for *P. vivax* these were 29 LM/DNA, 37 LM/RNA and 58 DNA/RNA pairs. For *P. falciparum* (upper panel Figure **2**), parasite quantification by LM and qPCR correlated well (r^2=0.81), when assuming presence of mainly ring/early trophozoite stage parasites in peripheral blood samples (equal to1 genome/parasite).

For *P. vivax* (lower panel Figure **2**) LM parasite counts and DNA copy numbers correlated less well (r^2=0.35). Confidence intervals wider than those for *P. falciparum* denote a less robust quantification for *P. vivax*, likely due to the presence of schizonts or the overall lower densities. For both parasite species the correlation between the measurements for RNA transcripts versus gene copies was around 50% (Figure **2**, panels on the right). In Figure **2** all regressions on the log-transformed data were significant to a p-value less than 0.001.

Due to the lower sensitivity of LM compared to both molecular methods, only a very limited number of samples was available with data from all quantification methods, which does not represent a robust basis for conversion of molecular data. Nevertheless, we have explored this possibility for conversion and calculated the median parasite densities quantified by qPCR or qRT-PCR (Table **S4**) by using the algorithm determined in the regression analyses (shown in Figure **2**). As expected, mean parasite densities by DNA based quantification were lower than by LM, reflecting the contribution of the additional samples sub-patent by LM and with presumably lower parasite densities. RNA-based quantification was not consistent between *P. falciparum* and *P vivax*.

Our efforts to generate molecularly determined parasite counts provided preliminary evidence for a good predictive relationship between DNA copy numbers and microscopic parasite density, especially for *P. falciparum*. Yet, this approach needs further validation by a larger sample set to provide a solid mathematical function for this relationship.

Co-infections with multiple *Plasmodium species*

To determine the overall prevalence of any *Plasmodium species* or of each specific species, we took into account all positive test results from DNA- and RNA-based assays (Table **S5**). Overall malaria parasite prevalence in the 315 children was 54.3%. Of these, almost a quarter had P. falciparum/P. vivax mixed infections (21.1%). Triple infections of *P. falciparum, P. vivax* and either *P. malariae* or *P. ovale* were seen in very few cases (0.6% and 3.5%). P. malariae single infections were less than 1%; no *P. ovale* single infection was observed.

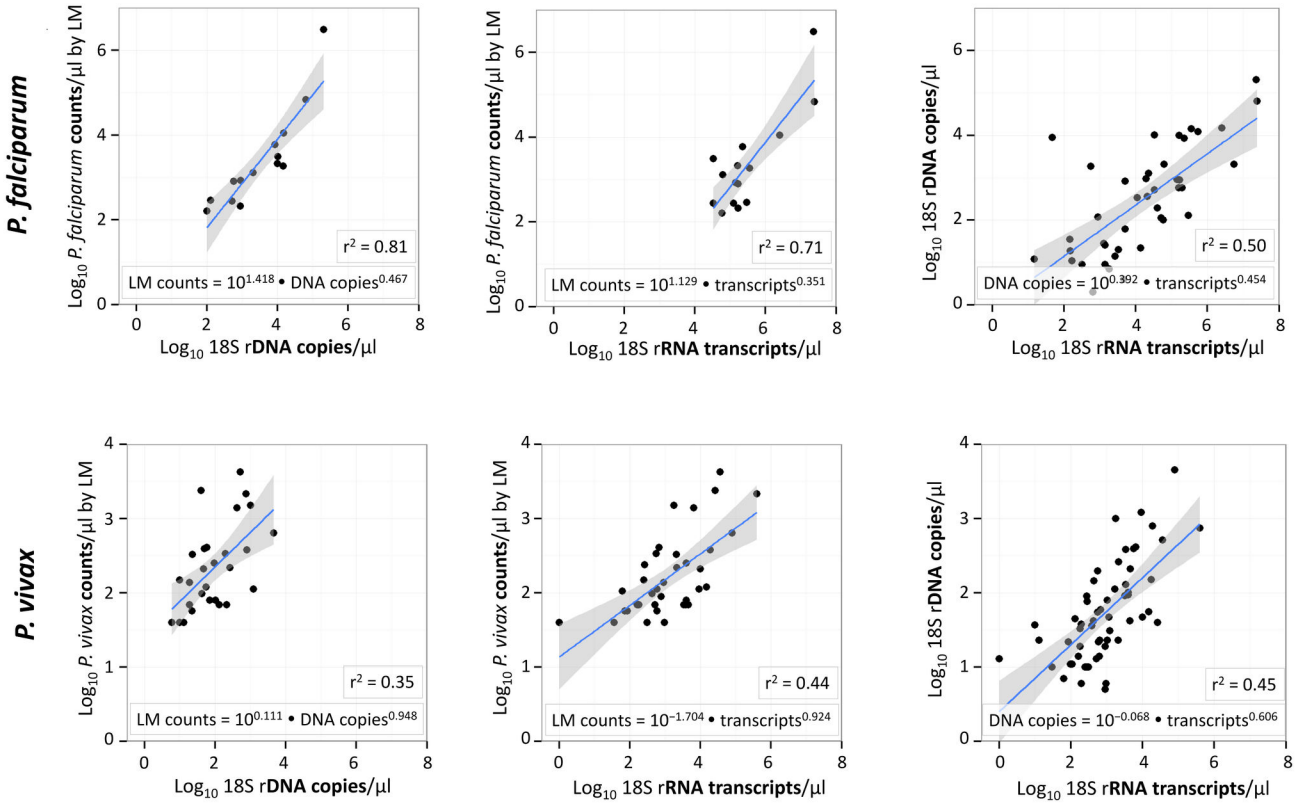

Figure 2. DNA- versus RNA-based quantification of *Plasmodium* parasites by qPCR and qRT-PCR of 18S rRNA genes or transcripts in comparison to light microscopy (LM). *P. falciparum* (upper panel) and *P. vivax* (lower panel). Boxed values indicate the correlation coefficient (r^2) and the conversion functions extracted from these data. All correlation coefficients (r^2) were significant (p-value < 0.001).

doi: 10.1371/journal.pone.0076316.g002

Gametocyte prevalence rates for *P. falciparum* and *P. vivax*

In our hands RNA extraction from FTA classic cards did not yield satisfactory results, despite efforts in optimizing the extraction protocol with the Qiagen RNeasy Plus mini kit. In contrast, gDNA could be extracted from these cards, but positivity in the *Plasmodium* species assays was reduced compared to results from the two alternative sampling methods (data not shown). Storage time >3 months or another, by us unnoticed problem during sampling, shipment or storage, all could have compromised RNA integrity on FTA cards. Our failure to detect gametocyte-specific RNA is in line with a similar work on field samples from Brazil [26].

RNA was extracted successfully from all blood samples collected by both strategies, RNAprotect® and filterpaper/TRIzol®. Of 315 children tested by any sampling method, 32 and 46 carried *P. falciparum* and *P. vivax* gametocytes, respectively (Table **1**). To evaluate the differential performance of the two sampling approaches, we have compared the gametocyte positivity and transcripts numbers by either method for *P. falciparum* and *P. vivax* (Figure **3**). RNAprotect® sampling yielded more *P. falciparum* positive samples than filterpaper/TRIzol®. In samples positive by both methods, transcript copy numbers were higher for RNAprotect® sampling as shown in a comparison of paired results (Figure **3**, bar chart). For *P. vivax*, each of the methods missed about one third of gametocyte positive samples as compared to the summary result. The great fluctuation in *P. vivax* positivity and quantification is likely due to the overall lower density of *P. vivax* asexual stages and gametocytes. By LM no *P. falciparum* or *P. vivax* gametocytes were observed, thus confirming the well established superiority of molecular gametocytes detection. We have assessed how far gametocyte prevalence is associated with asexual densities (Figure **S1**). A positive association of high 18S rRNA transcripts and gametocyte prevalence was observed for *P. vivax* and *P. falciparum*. This association was also seen for 18S rDNA copy numbers of *P. vivax*, but not *P. falciparum*. The data available was rather limited; a more robust investigation of these relationships would require a larger sample set.

Evaluation of *P. falciparum* and *P. vivax* gametocyte quantification assays

For quantification of gametocytes in a blood sample, the number of detected transcripts per sample is not meaningful without a standard curve that permits transforming copy

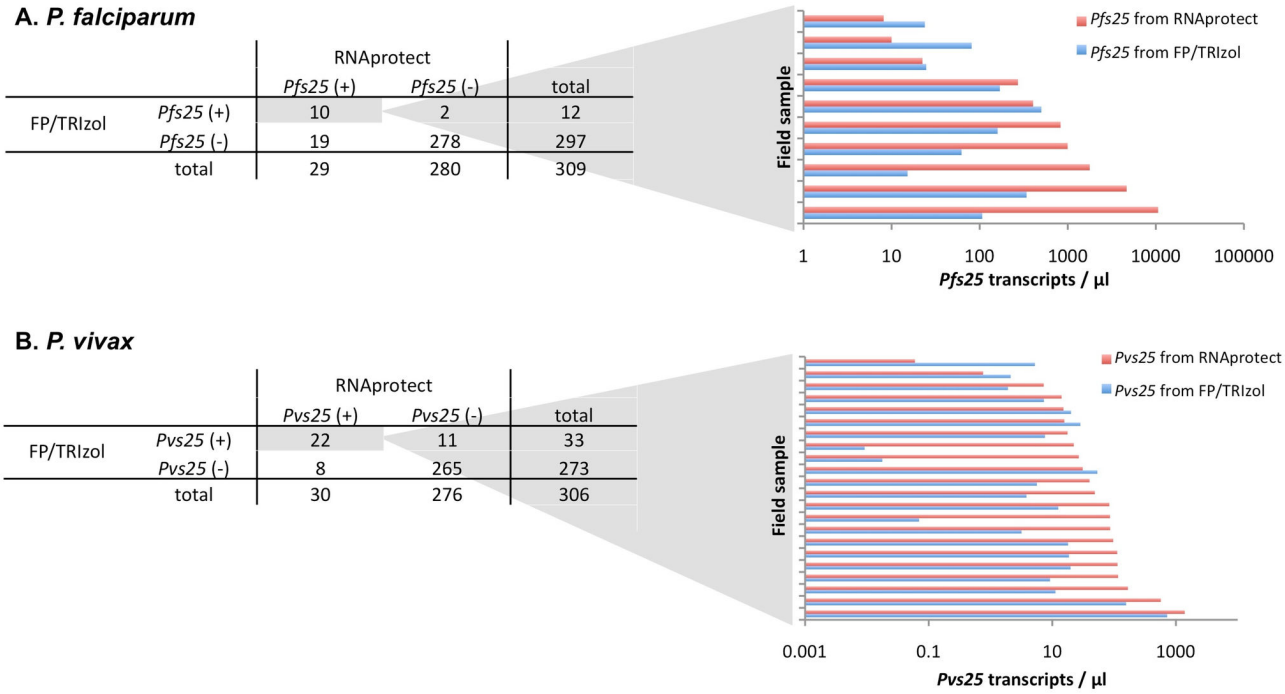

Figure 3. Comparison of two blood sampling strategies for measuring gametocyte prevalence rates. (A) *P. falciparum*, (B) *P. vivax*. Gametocyte positivity (left panel) and transcript copy numbers (right panel) are shown for RNAprotect solution versus filter paper soaked in TRIzol. Only samples were compared for which both measurements were available.

doi: 10.1371/journal.pone.0076316.g003

numbers into gametocyte counts. Therefore a gametocyte trend line was generated from 3D7 in vitro culture by counting gametocytes prior to harvesting RNA. Figure **4** presents the standard curve used for estimating gametocyte loads in our samples and for establishing the detection limit of our qRT-PCR assays. According to the conversion factor obtained from regression analysis (see method section), one *P. falciparum* gametocyte corresponds to 87.05 *pfs25* transcript copies (95% CI: 65.55-115.60). This translates into a limit of detection (LOD) of 0.02-0.05 gametocyte / µl blood when 50 µl blood or parasite culture was subject to RNA extraction. If volumes larger than 50 µl of blood would be sampled, our *pfs25* qRT-PCR would even permit an almost 2-fold greater sensitivity (1 gametocyte / 100 µl blood). This example indicates that LOD based on transcript copy numbers rather than gametocytes only describes detection potential, whereas presence or absence of gametocytes determines the effective sensitivity. Our LOD compares to that published for qNASBA-based gametocyte detection [27]. Due to the lack of *P. vivax in vitro* culture, we had to use the *P. falciparum* based conversion factor for calculating *P. vivax* gametocyte loads. Median gametocyte numbers per µl blood were 0.99 (1st quartile, 3rd quartile: 0.27, 4.95) for *P. falciparum* and 0.34 (1st quartile, 3rd quartile: 0.11, 0.68) for *P. vivax*. So far we failed to establish gametocyte assays for *P. malariae* and *P. ovale* due to yet little success to find *pfs25* orthologues in these species.

Effect of storage duration on stability of *pfs25* transcripts

Two years after extraction of RNA from both types of samples, RNAprotect® and filter paper/TRIzol®, we have repeated *pfs25* qRT-PCR of a subset of all samples representing the full range of transcript copy numbers. Sample pairs plotted side by side did not indicate compromised RNA stability after 2 years of storage at -80°C (Figure **5**). Other protein coding transcripts were not tested and the stability of *pfs25* RNA may represent an exception rather than the rule.

Discussion

The difference in DNA- versus RNA-based *Plasmodium* species determination derives from the dramatic difference in the number of templates per parasite. Each *Plasmodium* parasite harbors only 5 copies of the *18S rRNA* gene, 3 S-type (detected by our qPCR assay) and 2 A-type genes [18], whereas many thousands or even some million copies of *18S rRNA* transcripts can be expected per cell. The use of these extremely abundant transcripts for parasite detection warrants great care during RNA extraction, a large number of negative controls and precise definition of a cut-off to avoid false positives through potential aerosols (low level of signal caused by airborne templates). Depending on the research question, outermost sensitivity may be desired, e.g. when searching for very rare infections in a close to elimination setting. When

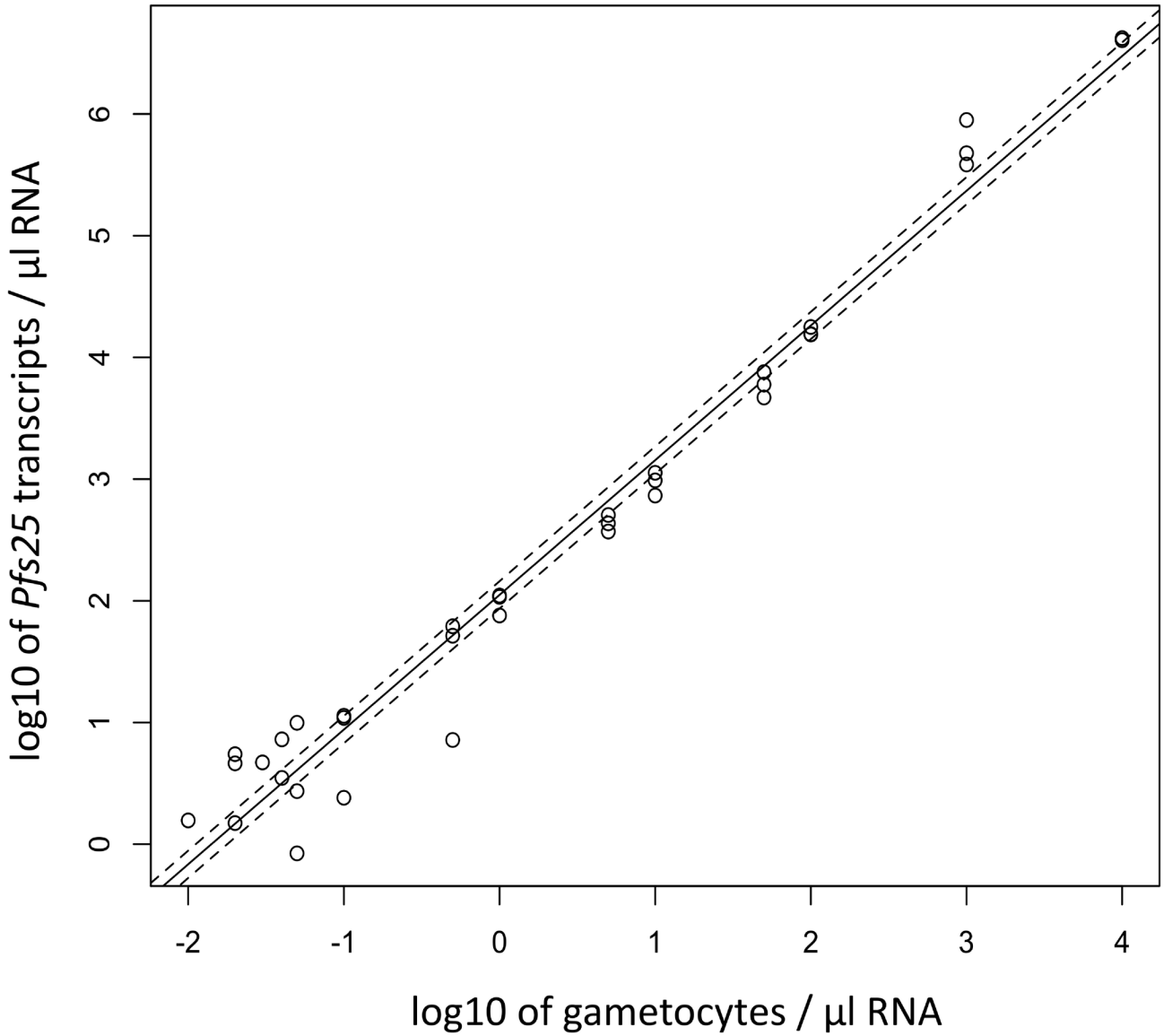

Figure 4. Gametocyte trend line generated with 3D7 *P. falciparum* in vitro culture for converting *pfs25* transcript copy numbers into gametocyte counts. Dashed lines indicate 95% confidence interval of intercept.

doi: 10.1371/journal.pone.0076316.g004

pooling samples for massive parasitological screening, such high sensitivity is a prerequisite. These issues might attract further attention in the eliminations context when sensitive diagnosis is required for detection of asymptomatic parasite carriers with low density, as well as for tracking both asexual and sexual stages in parallel [26].

Sensitivity of detection of blood-borne parasites is defined in a major way by the volume of blood analyzed, which for very low parasitaemias may or may not contain a parasite by chance. In asymptomatic infections the probability of detection of malaria parasites is hampered by generally low densities. Accordingly, the chances of gametocyte detection are even more limited. Our gametocyte assay was found to be sufficiently sensitive to reproducibly detect a single gametocyte in 50 µl whole blood. Because 1 gametocyte corresponded on average to 87 *pfs25* transcript copies, it seems likely that extracting RNA from 100 µl whole blood could have improved detection of scarce gametocytaemia. Generally the blood volume collected in population studies is limited, as up to 250 µl of whole blood can be obtained by finger prick, the usual sampling method for large-scale field surveys and cohort studies. After setting aside aliquots for blood films, serology and DNA extraction, starting material for gametocyte detection is restricted, but should be maximized according to the above results.

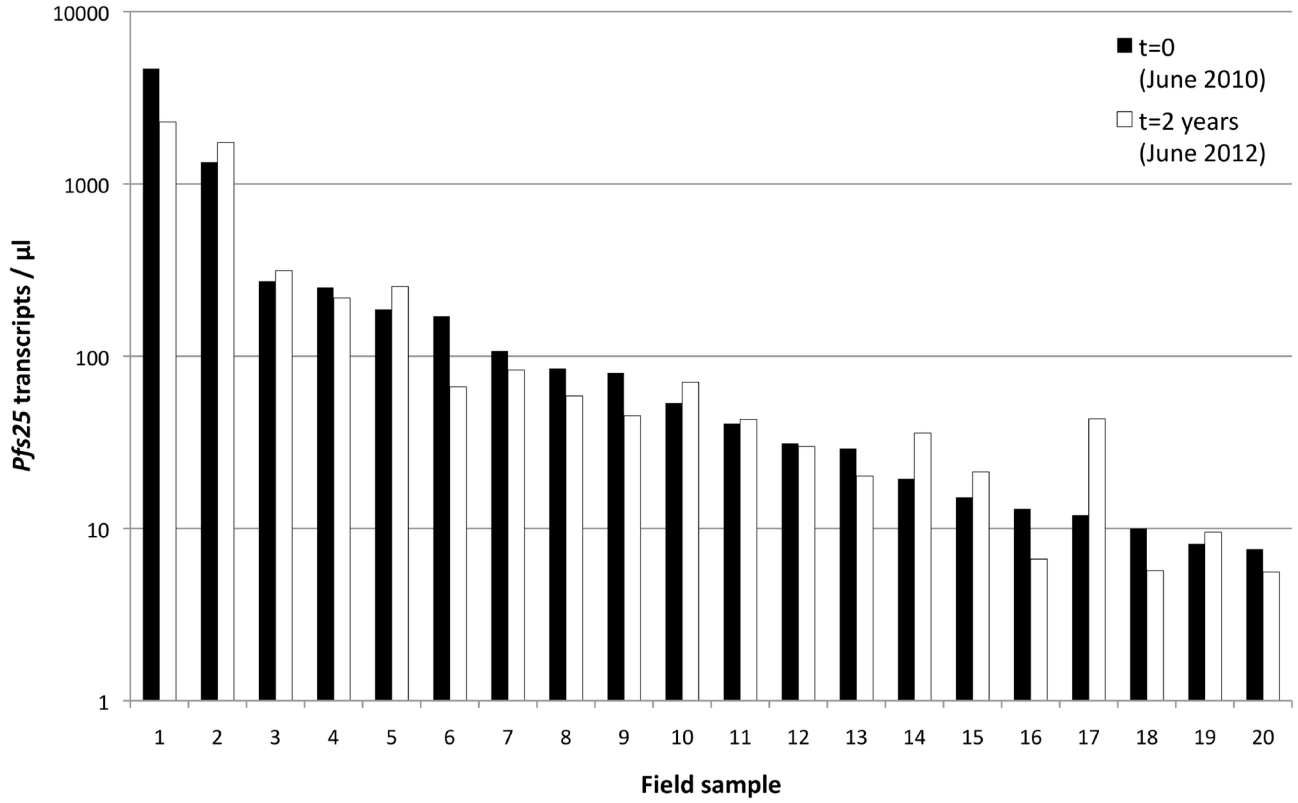

Figure 5. Effect of extended storage time on *pfs25* transcripts. 20 samples were chosen to represent a wide range of transcript copy numbers at start of the 2 yr storage period. The initial copy numbers (black bars) are shown next to copy number detected 2 yrs later in the same RNA sample (white bars).

doi: 10.1371/journal.pone.0076316.g005

When describing DNA- or RNA-based diagnostic assays, the sensitivity of parasite detection is generally presented on the basis of experiments with *in vitro* cultured parasites under optimal laboratory conditions [28]. Yet, for *P. vixax in vitro* culture is not available. The approach used in our study takes into account the conditions under which field samples were collected and shipped, mirroring the setting of routine malariological surveillance. To permit direct comparison of *P. falciparum* and *P. vivax* densities, parasites of both species ideally should be quantified in the same way by extracting an algorithm for converting template copy numbers detected in each sample into parasite s/µl whole blood. We have determined this relationship (Figure **2**) and quantified the median parasite densities for *P. falciparum* and *P. vivax* based on the correlations observed (Table **S4**). For both species DNA based quantification produced mean parasite densities lower that those by LM, because the increased molecular detection contributed primarily samples with parasite densities below the detection limit of LM. RNA-based parasite densities revealed a much greater variance than DNA-based quantification and thus provided less precise estimates of parasite density. This likely reflects small variations in sampling or processing, or could derive from longer delays in reaching the molecular laboratory for some of the samples. The generally adverse and variable field conditions could differentially impair the RNA quality in certain samples. Our data suggests that quantification based on RNA needs further validation.

Our study aimed at improving blood-sampling techniques in the field at remote sites. For this we have optimized gametocyte detection and quantification and compared RNA stability achieved by three sampling methods. We were only able to extract RNA reliably from samples stored in TRIzol and RNAprotect. Samples stored on FTA cards did not give satisfactory results. In contrast, Pritsch and co-workers [12] reported successful RNA extraction from Whatman FTA classic cards. The comparability of these sampling procedures with our results is limited, because our starting material consisted of low density asymptomatic field samples that had been stored for 6 months, whereas storage time was not specified in the earlier publication [12]. In a comprehensive comparison of several filter papers for collecting low density gametocytes, Jones and coworkers [8] reported a much lower amplification success of pfs25 transcripts from FTA classic cards compared to Whatman 3MM untreated filter paper. This is in line with our observations. But also in that study filter papers were stored only for up to 3 months. In our experience, samples from major field surveys very often are stored for periods longer than 3 months and longer than originally anticipated. Storage periods

of 4 weeks of 3 months, which is normally evaluated in comparative analysis of sampling materials, is very brief given the average duration of large scale field studies. Particularly cohort studies may well last over a year, e.g. to capture seasonal changes. We therefore reported the sensitivity of asexual stage and gametocyte detection after extended storage periods of up to 1 year and confirmed the stability of *pfs25* transcripts even after long term storage of 2 years.

Whatman 3MM non-impregnated filter paper has been used successfully in several recent studies [7,12,29], all reporting good RNA yields from blood spotted on filter paper without addition of any RNA-stabilizing reagent such as RNAprotect or TRIzol, but storage duration in these studies was up to 3 months only. We have shown that even long term storage of the blood impregnated 3MM filter paper in TRIzol is possible.

RNAprotect sampling showed best results, despite a delay of several hours until whole blood samples were transferred from EDTA microtainer into RNAprotect reagent. This contrasts with conclusions of a previous study that suggested compromised RNA stability after a 6 hrs delay prior to addition of RNAprotect [7]. The optimal sampling of whole blood in a RNA stabilizing agent would involve blood collection directly into tubes containing RNAprotect. But skin contact to RNAprotect, an irritant substance, should be avoided; thus finger prick blood is first collected in microtainers prior to transferring a 50 µl or larger aliquot into a tube pre-filled with 5 volumes RNAprotect solution. In this field survey we attempted to limit the delay until transfer in stabilizing agent to a maximum of 4 hours. A recent major field study conducted in Burkina Faso has demonstrated the feasibility of mixing whole blood with RNAprotect reagent directly at the site of blood collection without any delay [30]. In conclusion, for field settings far away from laboratory facilities, the latter approach of transferring whole blood directly into RNAprotect immediately after blood collection represents the optimal strategy, which, however, requires thorough training of field staff, e.g. on contamination-free pipetting of an aliquot whole blood from a microtainer into the prepared RNAprotect tube.

By detecting transcripts from late stage V gametocytes, we targeted specifically the parasite population in the human host most relevant for transmission. This depicts the impact of transmission-reducing interventions more closely than markers of earlier gametocyte stages, as not all committed rings might successfully develop into mature gametocytes. The presence of gametocytes is no evidence for subsequent transmission success of gametocytes to the vector. The relationship of gametocyte densities and successful infection of mosquitoes is of great relevance for molecular monitoring of interventions, but only recently first results were published on the prediction of mosquito infection from gametocyte densities [3]. It remains to be shown how molecular gametocyte counts in the host compare to the classical measure of transmission, the entomological inoculation rate [31]. We have evaluated procedures for gametocyte detection and quantification. Sampling strategy and molecular assays can be considered robust tools for molecular epidemiological studies and might prove valuable for estimating the impact of transmission-reducing interventions, such as drugs, vaccines, or vector control.

Supporting Information

Figure S1. Proportion of gametocyte carriers (gray) among *P. falciparum* (upper panel) and *P. vivax* (lower panel) infections separated into three copy number categories for 18S rDNA detected by qPCR or 18S rRNA transcripts detected by qRT-PCR. Sample size of both groups within a category is indicated by numbers within the bars.
(EPS)

Table S1. Primer and probe sequences.
(DOC)

Table S2. PCR profiles and reaction mixes.
(DOC)

Table S3. Limit of detection and amplification efficiencies of all molecular markers determined with control plasmids.
(DOC)

Table S4. Median density of *P. falciparum* and *P. vivax* parasite s/µl detected by microscopy, qPCR or qRT-PCR in samples from 315 children from PNG.
(DOC)

Table S5. Overall parasite prevalence derived from combined results of DNA- and RNA-based detection methods in study population (n=315) and distribution of mixed species co-infections in parasite positive samples.
(DOC)

Author Contributions

Analyzed the data: RW IF. Wrote the manuscript: IF. Conceived the field study: IM. Designed molecular work: IF. Extracted nucleic acids from various blood sampling strategies: RW FM SJ. Developed and validated quantification of parasite stages: RW. Conducted and supervised sample collection in the field: IB LR PS. Supported test development and provided materials for assay validation: HPB.

References

1. Carter R, Mendis KN, Miller LH, Molineaux L, Saul A (2000) Malaria transmission-blocking vaccines - how can their development be supported? Nat Med 6: 241-244. doi:10.1038/73062. PubMed: 10700212.
2. Ouédraogo AL, Bousema T, Schneider P, de Vlas SJ, Ilboudo-Sanogo E et al. (2009) Substantial contribution of submicroscopical *Plasmodium falciparum* gametocyte carriage to the infectious reservoir in an area of seasonal transmission. PLOS ONE 4: e8410. doi:10.1371/journal.pone.0008410. PubMed: 20027314.
3. Churcher TS, Bousema T, Walker M, Drakeley C, Schneider P et al. (2013) Predicting mosquito infection from *Plasmodium falciparum* gametocyte density and estimating the reservoir of infection. Elife 2: e00626. doi:10.7554/eLife.00626. PubMed: 23705071.
4. Babiker HA, Abdel-Wahab A, Ahmed S, Suleiman S, Ranford-Cartwright L et al. (1999) Detection of low level *Plasmodium falciparum* gametocytes using reverse transcriptase polymerase chain reaction. Mol Biochem Parasitol 99: 143-148. doi:10.1016/S0166-6851(98)00175-3. PubMed: 10215031.
5. Ouédraogo AL, Bousema T, de Vlas SJ, Cuzin-Ouattara N, Verhave JP et al. (2010) The plasticity of *Plasmodium falciparum* gametocytaemia in relation to age in Burkina Faso. Malar J 9: 281. doi:10.1186/1475-2875-9-281. PubMed: 20939916.
6. Maeno Y, Nakazawa S, Dao ID, Yamamoto N, Giang ND et al. (2008) A dried blood sample on filter paper is suitable for detecting Plasmodium falciparum gametocytes by reverse transcription polymerase chain reaction. Acta Trop 107: 121-127.
7. Mlambo G, Vasquez Y, LeBlanc R, Sullivan D, Kumar N (2008) A filter paper method for the detection of *Plasmodium falciparum* gametocytes by reverse transcription polymerase chain reaction. Am J Trop Med Hyg 78: 114-116. PubMed: 18187793.
8. Jones S, Sutherland CJ, Hermsen C, Arens T, Teelen K et al. (2012) Filter paper collection of *Plasmodium falciparum* mRNA for detecting low-density gametocytes. Malar J 11: 266. doi:10.1186/1475-2875-11-266. PubMed: 22873569.
9. Kuamsab N, Putaporntip C, Pattanawong U, Jongwutiwes S (2012) Simultaneous detection of *Plasmodium vivax* and *Plasmodium falciparum* gametocytes in clinical isolates by multiplex-nested RT-PCR. Malar J 11: 190. doi:10.1186/1475-2875-11-190. PubMed: 22682065.
10. Schneider P, Schoone G, Schallig H, Verhage D, Telgt D et al. (2004) Quantification of *Plasmodium falciparum* gametocytes in differential stages of development by quantitative nucleic acid sequence-based amplification. Mol Biochem Parasitol 137: 35-41. doi:10.1016/j.molbiopara.2004.03.018. PubMed: 15279949.
11. Beurskens M, Mens P, Schallig H, Syafruddin D, Asih PB et al. (2009) Quantitative determination of *Plasmodium vivax* gametocytes by real-time quantitative nucleic acid sequence-based amplification in clinical samples. Am J Trop Med Hyg 81: 366-369. PubMed: 19635900.
12. Pritsch M, Wieser A, Soederstroem V, Poluda D, Eshetu T et al. (2012) Stability of gametocyte-specific Pfs25-mRNA in dried blood spots on filter paper subjected to different storage conditions. Malar J 11: 138. doi:10.1186/1475-2875-11-138. PubMed: 22545954.
13. Müller I, Bockarie M, Alpers MP, Smith T (2003) The epidemiology of malaria in Papua New Guinea. Trends Parasitol 19: 253-259. doi:10.1016/S1471-4922(03)00091-6. PubMed: 12798082.
14. Genton B, Al-Yaman F, Beck HP, Hii J, Mellor S et al. (1995) The epidemiology of malaria in the Wosera area, East Sepik Province, Papua New Guinea, in preparation for vaccine trials. II. Mortality and morbidity. Ann Trop Med Parasitol 89: 377-390. PubMed: 7487224.
15. Cattani JA, Moir JS, Gibson FD, Ginny M, Paino J et al. (1986) Small-area variations in the epidemiology of malaria in Madang Province. PNG Med J 29: 11-17. PubMed: 3529703.
16. Hii JL, Smith T, Mai A, Mellor S, Lewis D et al. (1997) Spatial and temporal variation in abundance of Anopheles (*Diptera*:*Culicidae*) in a malaria endemic area in Papua New Guinea. J Med Entomol 34: 193-205. PubMed: 9103763.
17. Li J, Gutell RR, Damberger SH, Wirtz RA, Kissinger JC et al. (1997) Regulation and trafficking of three distinct 18 S ribosomal RNAs during development of the malaria parasite. J Mol Biol 269: 203-213. doi:10.1006/jmbi.1997.1038. PubMed: 9191065.
18. Nishimoto Y, Arisue N, Kawai S, Escalante AA, Horii T et al. (2008) Evolution and phylogeny of the heterogeneous cytosolic SSU rRNA genes in the genus Plasmodium. Mol Phylogenet Evol 47: 45-53. doi:10.1016/j.ympev.2008.01.031. PubMed: 18334303.
19. Prajapati SK, Joshi H, Dua VK (2011) Antigenic repertoire of *Plasmodium vivax* transmission-blocking vaccine candidates from the Indian subcontinent. Malar J 10: 111. doi:10.1186/1475-2875-10-111. PubMed: 21535892.
20. Fivelman QL, McRobert L, Sharp S, Taylor CJ, Saeed M et al. (2007) Improved synchronous production of *Plasmodium falciparum* gametocytes in vitro. Mol Biochem Parasitol 154: 119-123. doi:10.1016/j.molbiopara.2007.04.008. PubMed: 17521751.
21. Ponnudurai T, Lensen AH, Leeuwenberg AD, Meuwissen JH (1982) Cultivation of fertile *Plasmodium falciparum* gametocytes in semi-automated systems. 1. Static cultures. Trans R Soc Trop Med Hyg 76: 812-818. doi:10.1016/0035-9203(82)90116-X. PubMed: 6761910.
22. Kariuki MM, Kiaira JK, Mulaa FK, Mwangi JK, Wasunna MK et al. (1998) *Plasmodium falciparum*: purification of the various gametocyte developmental stages from in vitro-cultivated parasites. Am J Trop Med Hyg 59: 505-508. PubMed: 9790418.
23. R Development Core Team (2011) R: A language and environment for statistical computing, Vienna, Austria ISBN 3-900051-07-0. Available: http://www.R-project.org/. Vienna, Austria: R Foundation for Statistical Computing.
24. Rosanas-Urgell A, Mueller D, Betuela I, Barnadas C, Iga J et al. (2010) Comparison of diagnostic methods for the detection and quantification of the four sympatric *Plasmodium species* in field samples from Papua New Guinea. Malar J 9: 361: 1475-2875-9-361. PubMed: 21156052. doi:10.1186/1475-2875-9-361 PubMed: 21156052
25. Genton B, Al-Yaman F, Beck HP, Hii J, Mellor S et al. (1995) The epidemiology of malaria in the Wosera area, East Sepik Province, Papua New Guinea, in preparation for vaccine trials. I. Malariometric indices and immunity. Ann Trop Med Parasitol 89: 359-376. PubMed: 7487223.
26. Lima NF, Bastos MS, Ferreira MU (2012) *Plasmodium vivax*: reverse transcriptase real-time PCR for gametocyte detection and quantitation in clinical samples. Exp Parasitol 132: 348-354. doi:10.1016/j.exppara.2012.08.010. PubMed: 22940017.
27. Schneider P, Bousema T, Omar S, Gouagna L, Sawa P et al. (2006) (Sub)microscopic *Plasmodium falciparum* gametocytaemia in Kenyan children after treatment with sulphadoxine-pyrimethamine monotherapy or in combination with artesunate. Int J Parasitol 36: 403-408. doi:10.1016/j.ijpara.2006.01.002. PubMed: 16500657.
28. Murphy SC, Prentice JL, Williamson K, Wallis CK, Fang FC et al. (2012) Real-time quantitative reverse transcription PCR for monitoring of blood-stage *Plasmodium falciparum* infections in malaria human challenge trials. Am J Trop Med Hyg 86: 383-394. doi:10.4269/ajtmh.2012.10-0658. PubMed: 22403305.
29. Baird JK, Purnomo, Basri H, Bangs MJ, Andersen EM et al. (1993) Age-specific prevalence of *Plasmodium falciparum* among six populations with limited histories of exposure to endemic malaria. Am J Trop Med Hyg 49: 707-719. PubMed: 8279639.
30. Tiono AB, Ouédraogo A, Ogutu B, Diarra A, Coulibaly S et al. (2013) A controlled, parallel, cluster-randomized trial of community-wide screening and treatment of asymptomatic carriers of *Plasmodium falciparum* in Burkina Faso. Malar J 12: 79. doi:10.1186/1475-2875-12-79. PubMed: 23442748.
31. Sinden RE, Blagborough AM, Churcher T, Ramakrishnan C, Biswas S et al. (2012) The design and interpretation of laboratory assays measuring mosquito transmission of Plasmodium. Trends Parasitol 28: 457-465. doi:10.1016/j.pt.2012.07.005. PubMed: 22980759.

Supplementary Figure S1

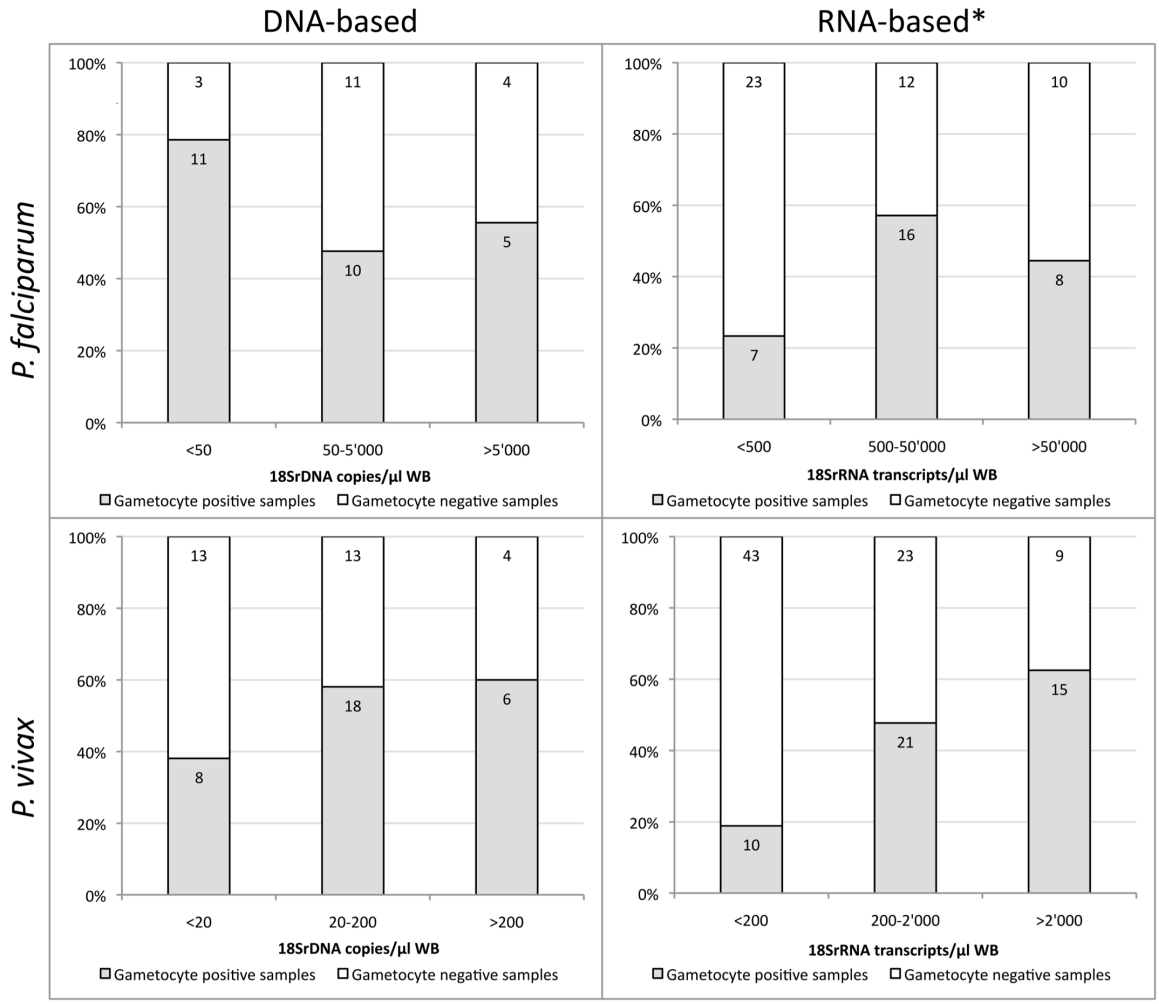

* Significant difference between groups (X^2 contingency table, p-value < 0.05)

Figure S1. Number of gametocyte carriers by *Plasmodium species* and detection method

Supplementary Table S1.

Table S1. Primer and probe sequences.

A. Generic qPCR and qRT-PCR assays (target: conserved regions in 18S rRNA)		
Species	Primer	Sequence (5′ -> 3′)
Plasmodium sp.	QMAL_fw	TTA GAT TGC TTC CTT CAG TRC CTT ATG*
	QMAL_rev	TGT TGA GTC AAA TTA AGC CGC AA
	QMAL_probe	FAM-TCA ATT CTT TTA ACT TTC TCG CTT GCG CGA –BHQ
B. Species-specific qPCRs and qRT-PCR assays		
Species	Primer	Sequence (5′ -> 3′)
P. falciparum (DNA)	Pf_S18S_fw	TAT TGC TTT TGA GAG GTT TTG TTA CTT TG
	Pf_S18S_rev	ACC TCT GAC ATC TGA ATA CGA ATG C
	Pf_S18S_probe	FAM-ACG GGT AGT CAT GAT TGA GTT-MGB-BHQ
P. falciparum (RNA)	Pf_A18S_fw	TCC GAT AAC GAA CGA GAT CTT AAC
	Pf_A18S_rev	ATG TAT AGT TAC CTA TGT TCA ATT TCA
	PF_A18S_probe	FAM-TAG CGG CGA GTA CAC TAT A-MGB-BHQ
P. vivax (DNA & RNA)	Pv_18S_fw	GCT TTG TAA TTG GAA TGA TGG GAA T
	Pv_18S_rev	ATG CGC ACA AAG TCG ATA CGA AG
	Pv_18S_probe	HEX-AGC AAC GCT TCT AGC TTA -MGB-NFQ
P. malariae (DNA & RNA)	same primers and probe as in ref. 24	
P. ovale (DNA & RNA)	same primers and probe as in ref. 24	
C. Gametocyte-specific *pfs25* and *pvs25* qRT-PCR		
Species	Primer	Sequence (5′>3′)
P. falciparum	pfs25_fw	GAA ATC CCG TTT CAT ACG CTT G
	pfs25_rev	AGT TTT AAC AGG ATT GCT TGT ATC TAA
	pfs25_probe	HEX-TGT AAG AAT GTA ACT TGT GGT AAC GGT-BHQ1
P. vivax	pvs25_fw	ACA CTT GTG TGC TTG ATG TAT GTC
	pvs25_rev	ACT TTG CCA ATA GCA CAT GAG CAA
	pvs25_probe	FAM-TGC ATT GTT GAG TAC CTC TCG GAA-BHQ1

* wobble R = A/G

Supplementary Table S2.

Table S2. PCR profiles and reaction mixes.

A. qPCR			
qPCR Reaction mix[1]			
Total volume 12 µL	1X gene expression master mix[2] 800 nM primer mix 200 nM probe[2] 2µl of RNA		
qPCR Thermo profile[3]			
Stage	Step	Temperature	Time
Holding	UDG	50°C	2 minutes
Holding	Activation of AmpliTaq polymerase	95°C	10 minutes
Cycling (45x)	Denature	95°C	15 seconds
	Anneal/Extend	58°C	1 minute

B. qRT-PCR: one-tube protocol using the TaqMan® RNA-to-C_T™ *1-Step* Kit[2]			
qRT-PCR Reaction mix [1]			
Total volume 12.5 µL	1X RT-to-CT master mix[2] 800 nM primer mix 200 nM probe[2] 2µl of RNA 0.3 µl of Taqman RT enzyme mix (ArrayScript™ UP Reverse Transcriptase and RNase Inhibitor)		
qRT-PCR Thermo profile[3]			
Stage	Step	Temperature	Time
Holding	Reverse transcription	48°C	15 minutes
Holding	Activation of AmpliTaq polymerase	95°C	10 minutes
Cycling (45x)	Denature	95°C	15 seconds
	Anneal/Extend	58°C	1 minute

[1] Reaction mix was prepared on a template-free bench wiped with 2.5M hypochlorite solution. Prepared master mix was added to the reaction plate before transfer to PCR cabinet for template addition. Applied Biosystem's MicroAmp® 0.1ml Fast Optical 96-Well Reaction Plate was used for both qPCR and qRT-PCR.

[2] Life Technologies Applied Biosystems, Zug, Switzerland

[3]The GENEX standard thermo profile of StepOnePlus Real-Time PCR system (Applied Biosystems) was modified for both qPCR and qRT-PCR. A maximum of 45 cycles of amplification was set. And all samples with Ct value ≤45 were considered positive.

Supplementary Table S3.

Table S3. Limit of detection and amplification efficiencies of all molecular markers determined with control plasmids.

Assay	**Limit of detection copy number /µl***	**Amplification efficiencies**
Generic 18S rRNA	1	96.5
P. falciparum 18S rRNA (S-type)	1	82.5
P. vivax 18S rRNA	3	82.2
P. malariae 18S rRNA	1	99.9
P.ovale 18S rRNA	1	92.8
pfs25	1	95.2
pvs25	0.5	92.0

*determined by serial dilution in quintuplicate of control plasmids (PCR template = insert of control plasmid).

Supplementary Table S4.

Table S4. Median density of *P. falciparum* and *P. vivax* parasites/µl detected by microscopy, qPCR or qRT-PCR in samples from 315 children from PNG.

	Quantification method of asexual *Plasmodium* stages		
	Light microscopy	DNA-based approach	RNA-based approach
P. falciparum quantification median [1st quartile, 3rd quartile	1071 [285, 3839]	350 [24, 1898]	1297 [164, 36904]
P. vivax quantification median [1st quartile, 3rd quartile]	106 [69, 330]	8 [6, 13]	98 [66, 160]

Supplementary Table S5.

Table S5. Overall parasite prevalence derived from combined results of DNA- and RNA-based detection methods in study population (n=315) and distribution of mixed species co-infections in parasite positive samples.

Assay / marker gene	**Positivity**[1]
Plasmodium generic assay	171/315 (54.3%)
Pf single infection	32/171 (18.7%)
Pv single infection	79/171 (46.2%)
Pm single infection	1/171 (0.6%)
Po single infection	0/171 (0%)
Pf + *Pv* infection	36/171 (21.1%)
Pf + *Pm* infection	3/171 (1.8%)
Pf + *Po* infection	0/171 (0%)
Pv + *Pm* infection	2/171 (1.2%)
Pv + *Po* infection	0/171 (0%)
Pf + *Pv* + *Pm* infection	1/171 (0.6%)
Pf + *Pv* + *Po* infection	6/171 (3.5%)
Pf + *Pv* + *Pm* + *Po* infection	0/171 (0%)
missed species typing[2]	11/171 (6.4%)
any *Pf*	78/171 (45.6%)
any *Pv*	124/171 (72.5%)
any *Pm*	7/171 (4.1%)
any *Po*	6/171 (3.5%)

[1]The slight discrepancy to those prevalence rates given in Table 1 derives from very few samples positive by DNA-based detection, but negative by RNA-based detection. Accordingly, the summary result given here shows a slightly higher positivity.

[2]Eleven samples were positive for the *Plasmodium* genus-specific assay, but were negative in all species-specific assays. All but one of these 11 samples derived from RNA-based detection and were characterized by very low copy number (<10 transcripts). These samples must be considered false positive. Due to highly abundant 18S rRNA transcripts in each cell, a low level of aerosol-derived contamination is possible. In principle, this issue can be addressed by introducing a cut-off (e.g. for *P. falciparum* 18S rRNA qRT-PCR we in fact applied a cut-off of 10 copies/µl extracted RNA). But our use of the generic assay for screening for all parasite species did not permit application of a stringent cut-off, which according to the occurrence of very high parasite densities would be oriented at *P. falciparum*. Cut off application to *P. vivax* would lead to exclusion of some very low-density infections. In consequence, the true parasite prevalence by our generic assay most probably is slightly lower, i.e. excluding the 11 potentially false positive samples and thus amounting to 160/315 (50.8%).

Chapter 3: Genotyping *Plasmodium falciparum* Gametocytes

MAJOR ARTICLE

Novel Genotyping Tools for Investigating Transmission Dynamics of *Plasmodium falciparum*

Rahel Wampfler,[1,2] Lincoln Timinao,[1,2,3] Hans-Peter Beck,[1,2] Issiaka Soulama,[4] Alfred B. Tiono,[4] Peter Siba,[3] Ivo Mueller,[5,6] and Ingrid Felger[1,2]

[1]Medical Parasitology and Infection Biology, Swiss Tropical and Public Health Institute, [2]University of Basel, Switzerland; [3]Papua New Guinea Institute of Medical Research, Goroka, Eastern Highland Province; [4]Centre National de Recherche et de Formation sur le Paludisme, Ouagadougou, Burkina Faso; [5]Walter and Eliza Hall Institute, Parkville, Victoria, Australia; and [6]Barcelona Centre for International Health Research (CRESIB), Spain

Background. Differentiation between gametocyte-producing *Plasmodium falciparum* clones depends on both high levels of stage-specific transcripts and high genetic diversity of the selected genotyping marker obtained by a high-resolution typing method. By analyzing consecutive samples of one host, the contribution of each infecting clone to transmission and the dynamics of gametocyte production in multiclone infections can be studied.

Methods. We have evaluated capillary electrophoresis based differentiation of 6 length-polymorphic gametocyte genes. RNA and DNA of 25 μL whole blood from 46 individuals from Burkina Faso were simultaneously genotyped.

Results. Highest discrimination power was achieved by *pfs230* with 18 alleles, followed by *pfg377* with 15 alleles. When assays were performed in parallel on RNA and DNA, 85.7% of all *pfs230* samples and 59.5% of all *pfg377* samples contained at least one matching genotype in DNA and RNA.

Conclusions. The imperfect detection in both, DNA and RNA, was identified as major limitation for investigating transmission dynamics, owing primarily to the volume of blood processed and the incomplete representation of all clones in the sample tested. Abundant low-density gametocyte carriers impede clone detectability, which may be improved by analyzing larger volumes and detecting initially sequestered gametocyte clones in follow-up samples.

Keywords. *Plasmodium falciparum*; transmission dynamics; gametocytes; genotyping; capillary electrophoresis; pfg377; pfs230.

Malaria infection and transmission dynamics both describe the appearance, loss or persistence of genotypes of *Plasmodium* parasites in a given host. Although infection dynamics describe longitudinal changes among asexual parasite clones, the focus of transmission dynamics lies on the sexual stages, gametocytes. To answer gaps in our knowledge on parasite reproduction and transmission, both the sexual and asexual stages, concurrently present in a host, need to be analyzed by genotyping. Examples of specific research questions are: Do all concurrent *P. falciparum* clones contribute to gametocyte production? Do drug-resistant clones contribute more to transmission? Does within-host competition between clones or other environmental factors affect the start and duration of gametocyte production?

Superinfections of already infected hosts and a high number of concurrent infections are common in areas of high malaria transmission. Polymorphic molecular markers are amplified to differentiate concurrent clones. The number of clones per blood sample (multiplicity) varies according to the transmission intensity; mean multiplicity of infection (MOI) was 2 in Papua New Guinea (PNG) and almost twice as much in Tanzania [1]. MOI is age-dependent and peaks in highly endemic settings in the age range of 5–9 year-olds [2].

Received 4 January 2014; accepted 28 March 2014; electronically published 25 April 2014.

Information presented in part as a poster: BioMed Central's 2nd Malaria Conference Challenges in Malaria Research: Progress Towards Elimination", Basel, Switzerland, 10–12 October 2012.

Correspondence: Ingrid Felger, PhD, Swiss Tropical and Public Health Institute, Socinstrasse 57, CH-4002 Basel, Switzerland (ingrid.felger@unibas.ch).

The Journal of Infectious Diseases 2014;210:1188–97

DOI: 10.1093/infdis/jiu236

Human and rodent models suggested that clone multiplicity affects transmission stages [3–5]. Antimalarials also were found to affect transmission. Residual submicroscopic parasitemia after ACT treatment was associated with a higher transmission in Kenyan children [4], but the individual clones within the infection were not differentiated in this study. A further determinant of transmission is the quantity and duration of gametocyte production. Asexual *P. falciparum* clones can persist in a host for many months as asymptomatic infections [6]. From this observation the question arises whether gametocytes are produced continuously by each clone, and whether gametocyte production is up-regulated or suppressed by concurrent clones of the same or other *Plasmodium* species.

Genotyping of gametocytes depends on high stage-specific expression and high genetic diversity of the chosen genotyping marker in the study area. Classical length-polymorphic markers for differentiation of gametocytes are *pfs230* and *pfg377. Pfs230* was first observed as a potential transmission-blocking antigen in 1988 and thereafter characterized by several immunological studies [7–10]. Williamson and co-workers first described 2 polymorphic repeat regions in *pfs230* by comparing 5 cultured parasite lines [11]. A separate polymorphic, glutamate-rich region within *pfs230* was described, but diversity was limited [12].

Another frequently used genotyping marker, *pfg377,* is specifically expressed in female gametocytes. Transcripts are detectable from gametocyte stage III onward [13]. Menegon and co-workers developed 4 *pfg377* gametocyte genotyping assays [14]. The first longitudinal monitoring of gametocyte-producing clones was conducted in samples from Sudan. Results indicated that gametocytes were present for up to 8 months of dry season and thus were considered the most probable source of malaria outbreaks in the following rainy season [5, 15]. Gametocytes from multiclone *P. falciparum* infections persisted 3 times longer than those from single-clone infections; thus multiplicity of infection may promote either longer persistence or continuous production of gametocytes [5]. Feeding experiments in the Gambia confirmed that gametocytes from coinfecting clones were simultaneously transmitted to mosquitoes [16]. Despite a lower multiplicity of gametocyte clones compared to asexual MOI, it was found that clones not detected on RNA level still produced gametocytes and nevertheless contributed to transmission [16]. Of all asexual clones detected in Thai patients, 25% had no corresponding *pfg377* transcript and thus no molecularly detectable level of gametocytes [17].

These previous studies have provided relevant information on malaria epidemiology and transmission dynamics but were hampered by the limited resolution of the available gametocyte-genotyping methods. Size-polymorphic diversity of molecular markers used in these earlier studies was maximal 7 for *pfg377* and 4 for *pfs230* [12, 16]. To improve the discriminatory power of markers *pfg377* and *pfs230*, we created amplicons spanning several polymorphic domains of these genes and increased accuracy of fragment sizing by replacing gel-based sizing by capillary electrophoresis (CE). In addition, we screened the gametocyte transcriptome [18] for tandem repeat-containing genes expressed only in gametocytes and evaluated these in search for novel high-resolution markers. Our assays were applied to asexual parasites by targeting genomic DNA (gDNA) from field samples and in parallel to gametocytes from the same blood samples by targeting RNA. Our aim was to employ high-resolution typing to gain a clearer picture on how many coinfecting asexual clones simultaneously produce gametocytes.

METHODS

Study Population and Ethics

The diversity of genotyping markers was determined in 111 archived anonymized DNA samples collected in Madang province, PNG, from April 2004 to February 2005 [19]. Scientific approval and ethical clearance was obtained from the Medical Research and Advisory Committee of the Ministry of Health in PNG (MRAC no. 09.24). Informed consent was obtained from parents or legal guardians prior to sampling. In addition, 46 archived anonymous RNA samples collected in the course of a cluster-randomized trial in Saponé, Burkina Faso [NCT01256658] [20] were used for evaluation of gametocyte detection assays. Ethical clearance was obtained from the National Ethical Committee for Health Research of Burkina Faso (no. 2013-3-019).

Nucleic Acid Extraction

DNA samples from PNG, stored at −20°C, had been extracted previously using QIAamp DNA Blood Kit (Qiagen) [19]. Total RNA of Burkina Faso samples was extracted from 25 µL whole blood stored with 125 µL RNAprotect Cell reagent (Qiagen). RNeasy Plus 96 kit (Qiagen) was used as previously described [21]. RNA was eluted in 50 µL water. The gDNA was eluted simultaneously from the gDNA elimination column (provided by the kit) using the QIAamp 96 Blood DNA Kit (Qiagen) protocol from the column washing step onwards. The gDNA was eluted twice in 50 µL of 40°C prewarmed AE elution buffer (Qiagen) following 30 minutes incubation. RNA and gDNA samples were stored at −20°C.

Validation of Genotyping Assays and Determination of Allelic Diversity of Markers

Diversity of 6 genotyping markers was determined in 111 gDNA samples from PNG. Primer sequences for *pfg377* (PF3D7_1250100), *pfs230* (PF3D7_0209000), *pf11.1* (PF3D7_1038400), *PF11_0214* (PF3D7_1120700), *PFI1210w* (PF3D7_0924600), and *PFL0545w* (PF3D7_1211000) are given in Table 1. Composition of reaction mixes and thermo profiles are shown in Supplementary Table 1. For CE sizing the

Table 1. Primary and Nested Primer Sequences for Gametocyte Genotyping Markers

Marker	Primer	Sequences (5′->3′)
Pfs230		
Primary	Pfs230_PF	AAG ACA TGT CGC CCA GGG ATA
	Pfs230_PR	TTC TTC TTC ATC ACC AAA TGG ATA T
Nested	Pfs230_NF	**VIC** - CAG GGA TAA TTT TGT AAT RGA TGA TG[a]
	Pfs230_NR	ACC TTG CCT TTC TTT TTC ATC TAC A - tail
Pfg377		
Primary	Pfg377_PF	CAC AAC GAA GGT TAT ATA CCT CAT AC
	Pfg377_PR	TCC ATT CTT CTT TAA GGT TCG CTT C
Nested	Pfg377_NF	**6FAM** - GAA GAT GAC GAA GGG GAT GAA G
	Pfg377_NR	CTG TAA GAA TTG GTT ATT ACT TTT GTG G - tail
PF11.1		
Primary	Pf11.1_PF1[b]	GAT ATA TTC TAA TAA T|TG TTC CAA TGG
	Pf11.1_PF2	AAG TGC AGG GGA TAG TGC AG
	Pf11.1_PR	CGG TAA TAC CAT AAG CTC CTC CT
Nested	Pf11.1_NF	**6FAM** - GGA ATA AGG ATG ATG ATG ACG AA
	Pf11.1_NR	AAC CTT CAA ATT CTT TGT CTC TTT C - tail
PF11_0214		
Primary	PF11_0214_PF	TCG AGA CAA ATT GAA AAG TTA TGG
	PF11_0214_PR	TTA GTG GAT AAA TGA ATA TCT ACC G
Nested	PF11_0214_NF	**6FAM** - AAT GAT ACA GAT TGT GAA GAA TGG T
	PF11_0214_NR	TGA GGA ATA TCG TTT TGT ATA AAT GTT - tail
PFI1210w		
Primary	PFI1210w_PF	TTG ATA AGG GAT ATA TAC ACA ACC ATA
	PFI1210w_PR	TTC CCG TTG TGT ATT TAA GTA GAA T
Nested	PFI1210w_NF	**6FAM** - TGT TTC AAT TTA CCA TCT TTC TTT TC
	PFI1210w_NR	GTT TTT CAA TTT TTA TGT TGT TCT CCA - tail
PFL0545w		
Primary	PFL0545w_PF	GGA AGG AAA CGA AGA AGA AAC A
	PFL0545w_PR	AAA GAT TGA AAT GGA GAT TCA CCT
Nested	PFL0545w_NF	**VIC** - TGA CAA AGG GCA CTT TAT TAT TT
	PFL0545w_NR	TTT CTT CAA CAG CAT TTT GCA T – tail

[a] Primer sequence contains a wobble: R = A/G.

[b] Pf11.1_PF1 is spanning an intron boundary indicated by "|".

products were diluted in water according to their agarose gel band intensity. Samples were analyzed by ABI3130*xl* using GS500LIZ as size standard. Electropherograms were analyzed using GeneMapper Software version 3.7. A cutoff set at 250 fluorescence units (FU) defined the minimal required peak height. In samples containing dominant peaks of >10 000 FU, the cutoff was increased to 500 FU. Stutter peaks (defined by accompanying peaks with a regular pattern of >6 bp and heights <20% of the main peak) were censored. A bin width of 3 bp was defined for each allele to accommodate small variations in fragment sizing. To test whether a size standard containing larger fragments would provide more accurate CE sizing, a subset of 13 *pfg377* fragments were simultaneously sized by CE using GS1200LIZ (Applied Biosystems). The expected heterozygosity (H_E) was calculated as published elsewhere [22].

Sequencing of PCR Fragments of Single Clone Infections for Evaluating Fragment Sizing

Nucleotide sequences of 12 *pfg377* and 10 *pfs230* nested polymerase chain reaction (nPCR) fragments from single clone infections were determined in both directions for *pfg377* and in one direction for *pfs230* by direct Sanger sequencing. Sequences were analyzed with BioEdit version 7.3.2, and alignments were performed with T-Coffee multiple alignment server and BoxShade server version 3.21. Sequences were submitted to GenBank [KJ566743-KJ566764].

Evaluation of Sensitivity of Reverse Transcription (RT)-PCR

The detection limits of all nested RT-PCR assays were evaluated on a trendline of stage IV/V gametocyte in vitro culture of *P. falciparum* 3D7 as previously described [21]. RT of

gene-specific complementary DNA (cDNA) was performed in a multiplex reaction using *pfg377* and *pfs230* primary reverse primers, 15 µL RNA and Superscript II (Invitrogen) according to the manufacturer's protocol. In a second multiplex RT reaction cDNA was reverse transcribed for *pf11.1, PF10_0214, PFI1210w,* and *PFL0545w* using the primary reverse primers (Table 1). In total, 4 µL of cDNA were added to the primary PCR (pPCR) mix and 2 µL of primary product to nPCR. The composition of reaction mixes and thermo profiles are shown in Supplementary Table 1. The nPCR products were run on a 2% agarose gel. The detection limit of each marker was compared to that of *pfs25* qRT-PCR, which is highly sensitive and widely used [21].

Effects of DNase Treatment on RNA Quality

For marker *pf11.1* an additional forward PCR primer was designed to span an exon-intron boundary (Table 1). Including this primer-binding site into an amplicon covering the polymorphic region of *pf11.1* resulted in a 680 bp longer fragment. The sensitivity of both *pf11.1* assays was assessed with 2 gametocyte trendlines that differed by omitting the DNase digest for the intron-spanning assay [21]. Assay conditions were identical except for a higher annealing temperature (58°C) for pPCR with the intron-spanning primer.

Evaluation of Gametocyte Genotyping Markers in Field Samples

The discrimination power for gametocyte clones in field samples was assessed for the 2 most diverse markers using 46 RNAs from Burkina Faso. Alleles detected on RNA level were compared to those found in gDNA of the same sample. In total, 5 µL RNA, equivalent to 2.5 µL whole blood, were reverse-transcribed and amplified for *pfs230* and *pfg377* by AffinityScript One-Step RT-PCR kit (Agilent Technologies) in simplex reactions. The nPCR was performed using 1 µL of primary product. Composition of reaction mixes and thermo profiles are shown in Supplementary Table 1. Reaction conditions were modified because the SuperScript II protocol (Invitrogen) used for work on parasite culture performed less well in field samples (data not shown).

The gDNA coextracted from the same blood samples was amplified for *pfg377* and *pfs230* as described above with the following modifications: an increased amount of 5 µL gDNA, equivalent to 1.25 µL whole blood, was added into a 30 µL reaction. Numbers of gametocytes originally present in whole blood samples were calculated by a conversion factor of $10^{-1.6225} \times (\text{copy number } pfs25 \text{ transcripts/µL whole blood})^{0.8518}$ as described elsewhere [21]. Correlation between gametocyte density (*pfs25* transcripts) and asexual density (S-type *18SrRNA* copy numbers) with DNA or RNA-derived MOI was analyzed by Kendall rank correlation τ for nonparametric data.

RESULTS

High Allelic Diversity of Gametocyte Genotyping Markers in PNG

New length polymorphic and gametocyte specifically expressed genes were selected by screening publically available gametocyte transcriptome data [18] followed by tandem repeat detection using Tandem Repeats Finder [23]. Primers were designed to maximize size variation in amplified fragments. For *pfg377* we combined polymorphic regions 2 and 3 described by Menegon into one larger amplicon [14]. Similarly, also our *pfs230* amplicon spans 2 polymorphic regions (Figure 1*A*). Diversity of both markers in 111 gDNAs from PNG was highest with 18 *pfs230* alleles ($H_E = 0.92$) and 15 *pfg377* alleles ($H_E = 0.81$). The detection limit of each assay and parameters describing the genetic diversity and resolution of each marker are listed in Table 2. Allelic frequencies of the 6 gametocyte markers showed equal distribution for most of the *pfs230* alleles, but for *pfg377* a predominant allele (39%; Figure 1*B*). Sequence alignments of 12 *pfg377* and 10 *pfs230* nPCR products (Supplementary Figure 1) served for validating CE fragment sizing. Sizing of *pfs230* fragments was more accurate than that of the larger *pfg377* fragments. Comparison of 38 amplicons sized in parallel with GS500LIZ and GS1200LIZ size standards indicated that GS1200LIZ yielded better resolution for *pfg377* with amplicon sizes >700 bp (Supplementary Figure 2). GS500LIZ worked well for *pfs230* with amplicons <600 bp.

Detection Limits of Gametocyte Assays Assessed With a Trendline of Cultured Gametocytes

The limit of detection (LOD) of our gametocyte typing assays ranged from 1 (*pfg377* and *pf11.1* without DNase digestion) to 5 (*pf11.1* with DNase digestion) and 10 gametocytes/µL culture (*pfs230,* PF11_0214, PFI1201w and PFL0545w; Table 2). These LODs were 50–500 times less sensitive than that of *pfs25*, a qRT-PCR assay able to detect 0.02 gametocytes/µL blood [21, 24]. Our *pfg377* LOD was in line with earlier reports [14].

Quantifying the Gain in Sensitivity After Bypassing DNase Digestion

Using an intron-spanning marker permits omitting DNase digestion prior to reverse transcription but also increases amplicon length. By using alternative primers for marker *pf11.1* we analyzed whether bypassing digestion would exceed the benefit of a smaller amplicon. Sensitivity was 5-fold higher for the 680 bp longer fragment not requiring DNase digestion (Table 2).

Evaluation of Gametocyte Typing Markers in Field Samples

Markers *pfs230* and *pfg377* were genotyped in parallel in paired DNA/RNA samples coextracted from 46 blood samples from Burkina Faso, all of which had been gametocyte-positive by *pfs25* qRT-PCR. RT-PCR was successful in 42/46 field samples

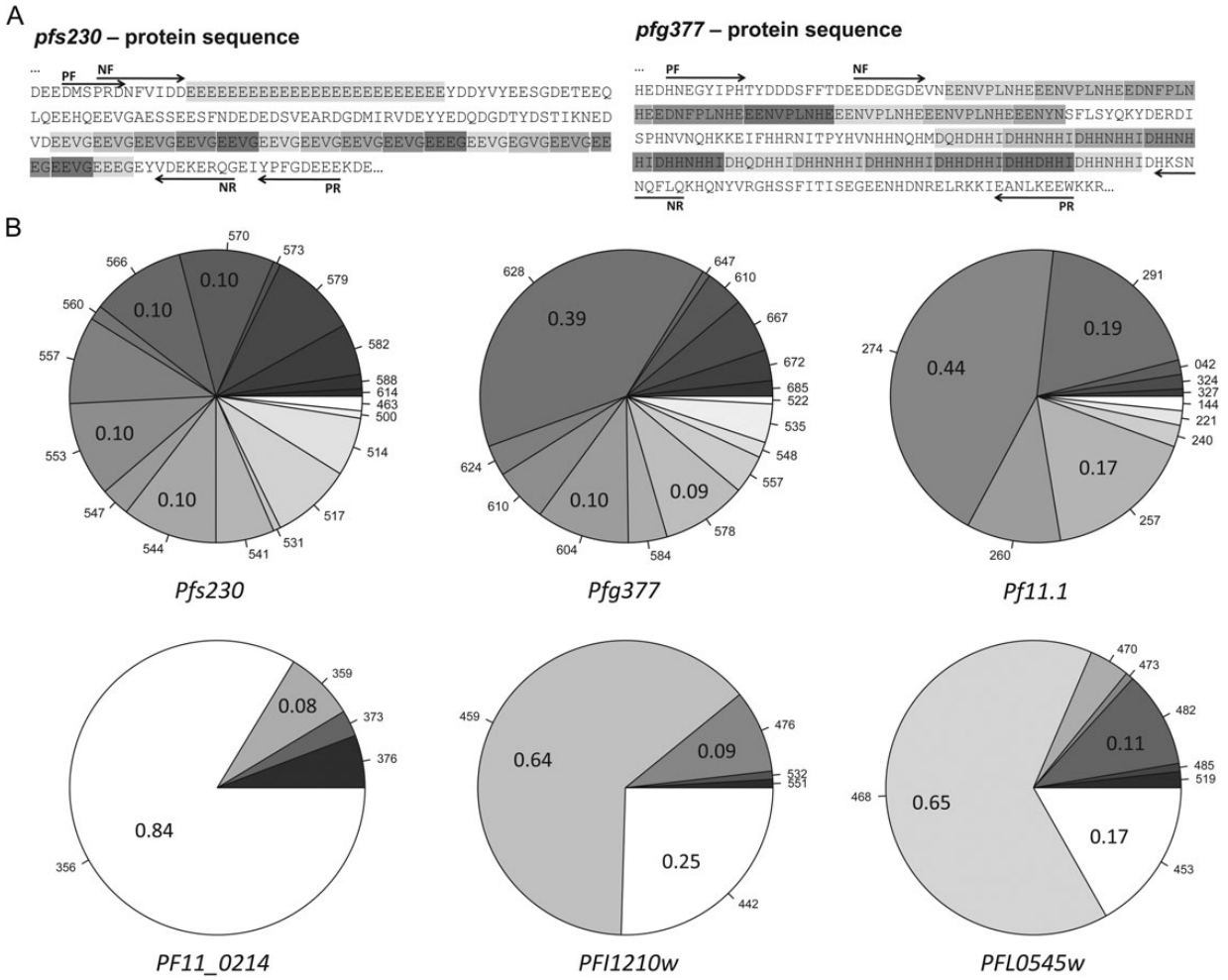

Figure 1. Location of repeat regions within *pfs230* and *pfg377* amplicons and allelic diversity of 6 gametocyte markers. *A*, Markers *pfs230* and *pfg377* both span 2 distinct repeat regions. Individual repeat units are in shades of grey. Protein sequences of *Plasmodium falciparum* strain 3D7 were derived from PlasmoDB: PF3D7_0209000 (*pfs230*) and PF3D7_1250100 (*pfg377*). *B*, Allelic frequencies of 6 molecular markers for genotyping gametocytes determined in 111 cross-sectional samples from Papua New Guinea. Highest diversity was found for *pfs230* (18 alleles) and *pfg377* (15 alleles). The rounded average allele size is indicated for each allele in addition to the frequencies of the most frequent alleles of each marker in the study population. Abbreviations: NF, nested PCR forward primer; NR, nested PCR reverse primer; PCR, polymerase chain reaction; PF, primary PCR forward primer; PR, primary PCR reverse primer.

for *pfs230* and in 37/46 samples for *pfg377*. For *pfs230* 18 alleles were detected and 19 for *pfg377*. For each blood sample, genotypes detected in gDNA were compared with genotypes amplified from gametocyte transcripts. A higher concordance between DNA- and RNA-derived genotypes was observed for *pfs230* (Figure 2). From the total of 93 *pfs230* PCR fragments amplified from all DNA samples, 41 (44.1%) were not observed in the corresponding RNA fraction. These clones either did not produce gametocytes or were below the detection limit of RT-PCR. For *pfg377* 61.5% (48/78) of fragments were missed on RNA level (Table 3). Similarly, MOI on DNA level (MOI_{DNA}) was higher for *pfs230* with a mean of 2.21 [range 1–5] infections per carrier in contrast to 2.11 [range 1–4] for *pfg377*, also arguing for *pfs230* as the more sensitive marker. When combining all DNA- and RNA-derived genotypes per sample, mean MOI of *pfs230* and *pfg377* increased to 3.14 [range 1–6] and 3.08 [range 1–5], respectively (Table 3). This combined MOI ($MOI_{combined}$) represents a more realistic, though still underestimated number of any stage of all coinfecting clones per sample. No correlation between MOI_{RNA}, MOI_{DNA}, $MOI_{combined}$, and gametocyte or asexual densities was found (Kendall rank correlation, all τ's > 0, all *P*-values > .07).

DISCUSSION

Gametocyte typing depends on detection of transcripts from genes exclusively transcribed in gametocytes. In addition, extensive length polymorphism is required to permit tracking of

Table 2. Resolution of 6 Polymorphic Gametocyte Markers in Comparison to Asexual Marker Msp2 in 111 *P. falciparum* Positive Cross-Sectional Samples From PNG

Marker	Positive Samples	No. of Clones	No. of Alleles	CE-Product Size Range	Mean MOI	H_E	In Vitro Detection Limit (Gametocyte/µL 3D7 Culture)
Msp2[a]	111/111	. . .	. . .	. . .	1.56	. . .	. . .
Pfs230	95/111	124	18	463–614	1.31	0.923	10
Pfg377	97/111	117	15	521–695	1.21	0.816	1
Pf11.1	100/111	125	10	143–327	1.25	0.734	1 if intron boundary 5 if no intron boundary
PF11_0214	100/111	104	4	355–376	1.04	0.293	10
PFI1210w	90/111	110	5	442–551	1.22	0.527	10
PFL0545w	95/111	113	7	453–519	1.19	0.546	10

Abbreviations: H_E, heterozygosity; MOI, multiplicity of infection; Msp2, merozoite surface protein 2.

[a] Results from [19].

gametocytes from multiclone infections. Multiple *P. falciparum* infections can coexist over weeks or months, but the variation in their relative densities and contribution to transmission over time has not yet been adequately quantified. The available data on gametocytes production of individual co-infecting clones were compromised by limited size-polymorphism in marker *pfg377*-R3 [5, 15–17, 25]. High-endemic settings are characterized by high MOI, where a limited marker resolution of ≥7 alleles will not adequately discriminate gametocytes of all clones present in a sample. By combining 2 repeat regions into 1 amplicon, we substantially improved the discriminatory power of both major markers. In 46 samples from Burkina Faso we detected 19 *pfg377* and 18 *pfs230* alleles by CE. A comparable diversity was observed in samples from PNG indicating that these markers may have sufficiently high diversity for genotyping in both African and non-African populations with different transmission intensity.

High MOI in the Burkina Faso study area [26] can contribute to discrepant results between RNA- and DNA-derived MOI.

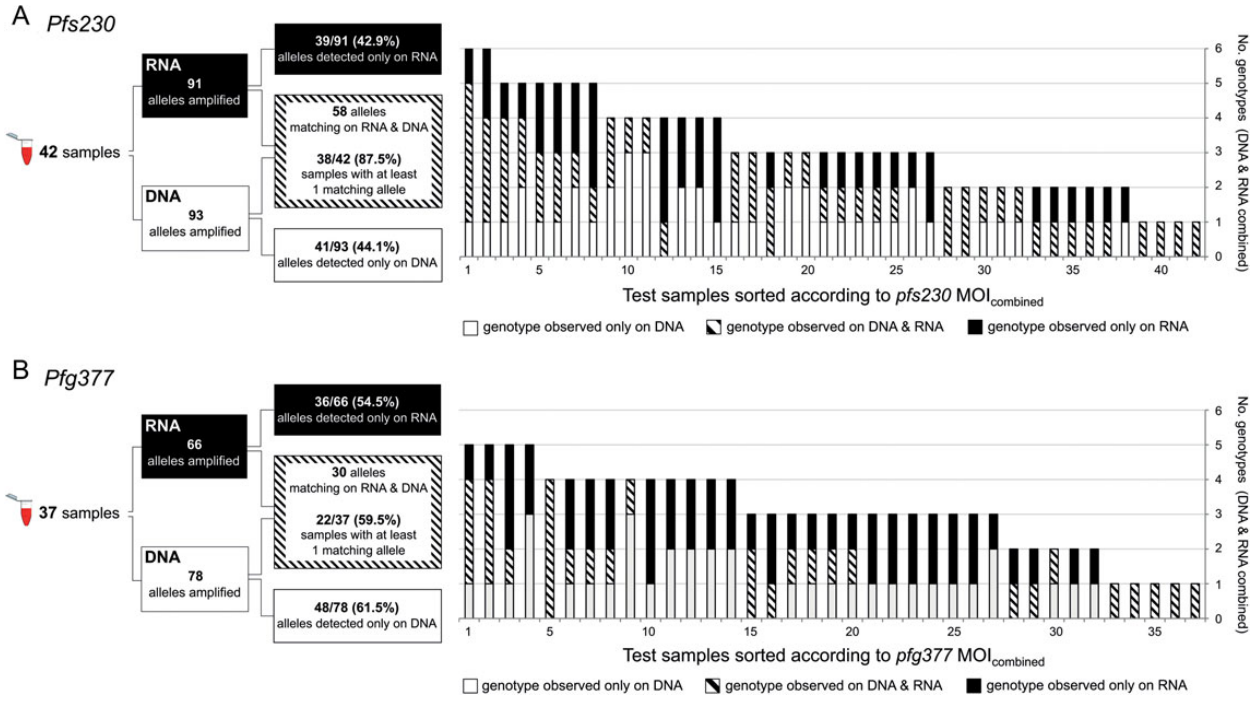

Figure 2. Schematic of analytical procedures (*right panel*) and overlap of genotypes detected simultaneously in RNA and DNA by blood sample (*left panel*). *A, Pfs230,* 42 paired RNA/DNA samples. *B, Pfg377,* 37 paired RNA/DNA samples. Abbreviation: MOI, multiplicity of infection.

Table 3. Discrimination Power and Test Sensitivity of Gametocyte Typing Markers *pfs230* and *pfg377* in 46 Blood Samples From Burkina Faso

Marker	*pfs230*	*pfg377*
No. of successful amplified samples	42/46	37/46
Detection limit in field samples[a]	2 gametocyte/µL WB	3.5 gametocyte/µL WB
Median gametocyte count[a]	17.0 gametocyte/µL WB	17.9 gametocyte/µL WB
No. of different alleles	18	19
DNA/RNA sample pairs with at least 1 matching PCR fragment	38/42 (85.7%)	22/37 (59.5%)
Total no. of PCR fragments detected (DNA and RNA combined)	132	114
Proportion of DNA fragments not found on RNA level	41/93 (44.1%)	48/78 (61.5%)
Proportion of RNA fragments not found on DNA level	39/91 (42.9%)	36/66 (54.5%)
Combined mean MOI (DNA and RNA)	3.14 [range 1–6]	3.08 [range 1–5]
Mean MOI (DNA)	2.21 [range 1–5]	2.11 [range 1–4]
Mean MOI (RNA)	2.17 [range 1–5]	1.78 [range 1–4]

Abbreviations: MOI, Multiplicity of infection; PCR, polymerase chain reaction; WB, whole blood.

[a] Determined by a conversion factor based on *pfs25* transcripts copies/µL RNA [21].

High MOI implies high clone competition in the host, resulting in turn in fluctuations in clone densities [27]. During PCR the presence of several templates of various concentrations may lead to template competition. Both effects of high MOI result in imperfect detectability [28]. This effect of competing templates, leading to lack of detection of genotypes either in DNA- or RNA-based detection, is enhanced by applying a cut-off for peak height in CE to separate background noise from real signals (Figure 3). In view of these inherent shortfalls, it seems essential to optimize sampling and preservation of both DNA and RNA to maximize the volume of template in PCR and RT-PCR in order to minimize the failures to detect all alleles present.

When comparing paired RNA- and DNA-derived fragments, 3 scenarios are expected: (I) RNA- and DNA-derived alleles match; here asexual stages and gametocytes of a clone are concurrently present in the blood sample, or DNA- and RNA- alleles both derive from gametocytes only. Yet, in multiclone infections a perfect match might be rare because the ratio of asexual vs sexual stages of each clone could differ considerably. (II) DNA-derived alleles exceed those obtained from RNA of the same sample. This is intuitively expected, because only some of the concurrent clones might produce gametocytes, as suggested by the frequent absence of gametocytes in some of the *P. falciparum*-positive blood samples despite molecular detection. (III) RNA-derived alleles are detected despite their absence on DNA level. This could occur when a gametocyte clone is still circulating while its asexual stages are already cleared by the immune system or below the detection limit. The gametocytes' nuclear DNA in this scenario remains below the detection limit of PCR or suffers from competition in multiclone infections.

In our study all 3 scenarios were seen, with scenario I predominant for *pfs230* and scenario II for *pfg377*. An explanation for this discrepancy is offered by the differential performance of our 2 markers, which differed in their ability to detect a clone on both DNA- plus RNA level: *pfs230* detected at least one matching genotype in >80% of samples, in contrast to only 60% for *pfg377*. Similarly, more RNA clones were missed by *pfg377* (60%) than by *pfs230* (45%). This argues for a higher sensitivity of *pfs230* compared to *pfg377* RT-PCR.

The imperfect detectability observed in asexual clones [6, 28] is aggravated in gametocyte detection, because gametocytes occur in densities about 100-fold lower than asexual stages [29]. Detection of gametocytes depends greatly on the blood volume processed, whereby a rare gametocyte clone might be present or absent by chance in the limited volume of blood processed. An additional limitation specific for *Pfg377* consists in its expression restricted to female gametocytes. Our RT-PCR assays amplified gametocyte-specific transcripts in field samples that contained as little as 2 gametocytes/µL whole blood, as indicated by the LOD for *pfs230* and is thus in the range of previously published assays [14, 30]. Even though this LOD permits detection of submicroscopic gametocytes, it does not reach the up to 100-fold higher sensitivity of *pfs25* qRT-PCR [21]. This difference is mainly due to a lower expression rate of *pfs230* compared to *pfs25*. Amplicon size and differential stability of the RNA may play an additional role as previously suggested [21].

We propose another strategy to address the problem of imperfect detectability of gametocyte clones: a longitudinal study design would permit to detect a particular genotype on RNA-level in a subsequent blood samples harboring higher gametocyte density. It is possible that sexual and asexual densities do not peak at the same time due to a 10 days maturation period of gametocytes. Therefore, a better match may be achieved by comparing results from consecutive bleeds. A gametocyte clone missed at an earlier sampling date might appear in the following sample. This approach parallels our strategy adapted to track asexual clones also fluctuating in their densities over time [28, 31, 32]. Nevertheless, even a longitudinal approach to gametocyte tracking will not overcome the imperfect detection of a gametocytemia that is persistently very low.

No other candidate of higher diversity and sensitivity than our CE-based *pfg377* and *pfs230* assays was found. Thus, length polymorphism of intragenic repeat regions in gametocyte-expressed genes seems to be less extensive than in genes

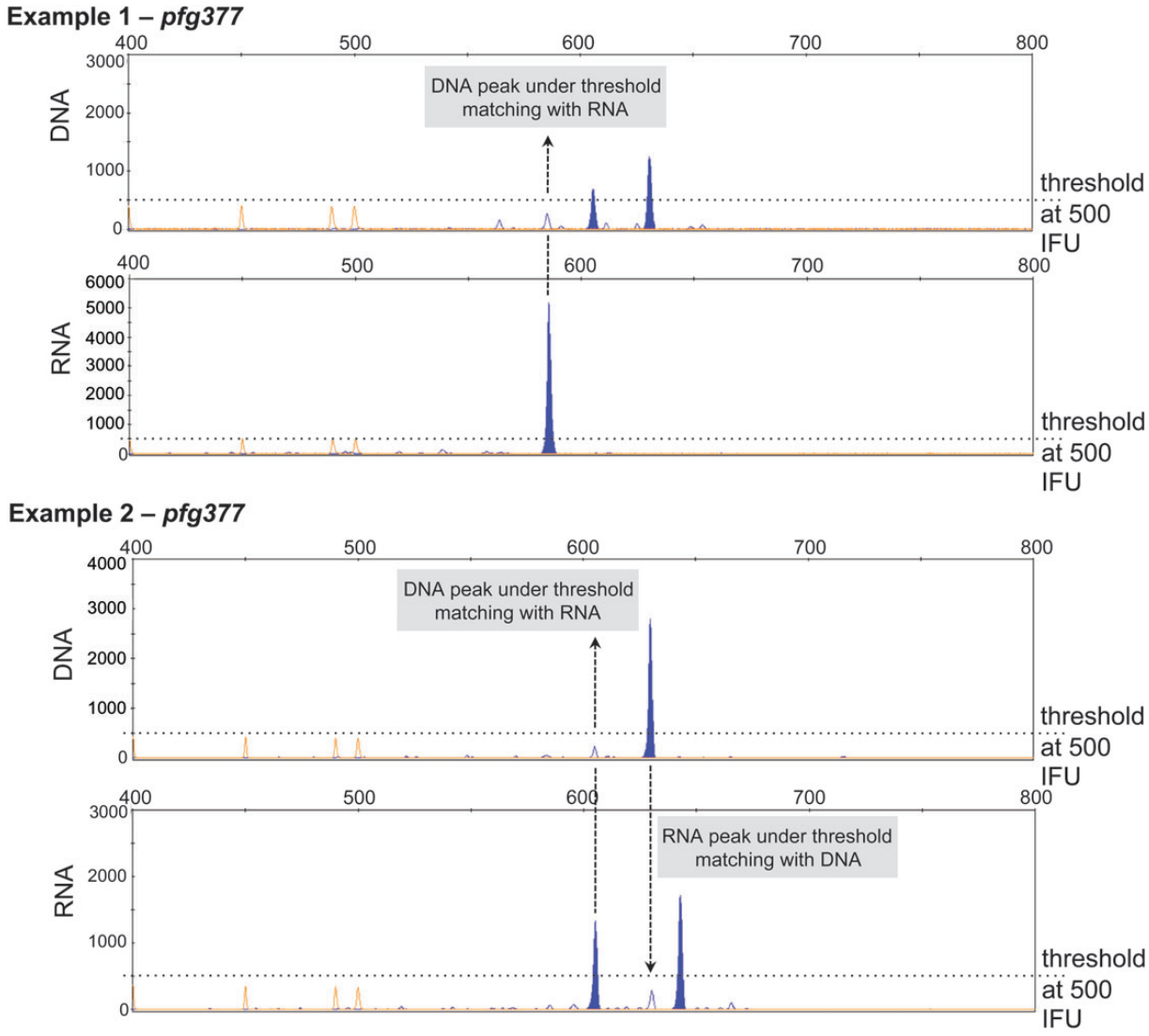

Figure 3. Electropherograms of *pfg377* fragments amplified by nested PCR from gDNA and nested RT-PCR from RNA coextracted from the same sample. Arrows indicate minority peaks, which had fallen below the cutoff, whereas matching fragments of significant peak height were present in the corresponding sample. Abbreviation: RT-PCR, reverse transcription polymerase chain reaction.

expressed in asexual stages. For improving discrimination power beyond 18 alleles by *pfs23*-CE, alternative approaches could be investigated in, for example, future detection of single nucleotide polymorphisms by targeted next generation sequencing. However, the major challenges will likely persist, e.g. imperfect clone detectability in a limited blood volume from the field, expression levels of polymorphic gametocyte-specific genes, and assay sensitivity impaired by long amplicons.

A major gap in our knowledge of *P. falciparum* transmission dynamics is the onset and duration of gametocytogenesis of each asexual clone in relation to coinfecting clones and the contribution of resistant clones to transmission. We envisage that the molecular description of clone transmission dynamics may yield molecular gametocyte-specific parameters similar to those used in the description of infection dynamics and complementing these, for example, the duration of gametocyte production or multiplicity of gametocyte clones. This will open up new investigations of clone interaction, within-host competition, and clonal fitness. So far, very little is known on gametocyte dynamics in natural infections, where concurrent clonal infections might contribute to transmission equally or in competition with each other. This determines parasite recombination in mosquitoes, which in turn has major consequences for development of multilocus drug resistance phenotypes or antigenic diversity.

In summary, we improved the resolution of existing markers for discriminating gametocyte clones, but were unable to find

alternative polymorphic markers of higher diversity. *Pfs230* emerged as the most sensitive and diverse marker. Detectability of minority clones was identified as a major problem for matching asexual clones with their gametocytes. The loss of minority clones seemed strongest in the high transmission setting with high mean MOI where about half of all clones were missed in either of the paired samples. Longitudinal analyses are needed to permit temporally staggered alignment of fragments to compensate imperfect detectability. This calls for longitudinal studies with short-term sampling intervals specifically designed for genotyping DNA and RNA targets in parallel.

Supplementary Data

Supplementary materials are available at *The Journal of Infectious Diseases* online (http://jid.oxfordjournals.org/). Supplementary materials consist of data provided by the author that are published to benefit the reader. The posted materials are not copyedited. The contents of all supplementary data are the sole responsibility of the authors. Questions or messages regarding errors should be addressed to the author.

Notes

Acknowledgments. We thank the study participants and their parents or guardians, and the field teams in PNG and Burkina Faso.

Author contribution. R. W. and I. F. designed and performed research and wrote the article; I. S., A. B. T., and P. S. contributed field samples, L. T., H. P. B., and I. M. contributed new reagents or analytical tools.

Financial support. This work was supported by Swiss National Science Foundation [grant 310030_134889], International Centers of Excellence in Malaria Research [grant U19 AI089686), National Health and Medical Research Council [grants GNT1021544 and GNT1043345] and Bill and Melinda Gates Foundation [grant OPP1034577].

Potential conflicts of interest. All authors: No reported conflicts.

All authors have submitted the ICMJE Form for Disclosure of Potential Conflicts of Interest. Conflicts that the editors consider relevant to the content of the manuscript have been disclosed.

References

1. Schoepflin S, Valsangiacomo F, Lin E, Kiniboro B, Mueller I, Felger I. Comparison of *Plasmodium falciparum* allelic frequency distribution in different endemic settings by high-resolution genotyping. Malar J **2009**; 8:250.
2. Smith T, Beck H-P, Kitua A, et al. Age dependence of the multiplicity of *Plasmodium falciparum* infections and of other malariological indices in an area of high endemicity. Trans R Soc Trop Med Hyg **1999**; 93 (suppl 1):15–20.
3. Wargo AR, Huijben S, de Roode JC, Shepherd J, Read AF. Competitive release and facilitation of drug-resistant parasites after therapeutic chemotherapy in a rodent malaria model. Proc Natl Acad Sci U S A **2007**; 104:19914–9.
4. Beshir KB, Sutherland CJ, Sawa P, et al. Residual *Plasmodium falciparum* parasitemia in Kenyan children after artemisinin-combination therapy is associated with increased transmission to mosquitoes and parasite recurrence. J Infect Dis **2013**; 208:2017–24.
5. Nassir E, Abdel-Muhsin AM, Suliaman S, et al. Impact of genetic complexity on longevity and gametocytogenesis of *Plasmodium falciparum* during the dry and transmission-free season of eastern Sudan. Int J Parasitol **2005**; 35:49–55.
6. Felger I, Maire M, Bretscher MT, et al. The dynamics of natural *Plasmodium falciparum* infections. PLoS ONE **2012**; 7:e45542.
7. Kaslow DC, Quakyi IA, Syin C, et al. A vaccine candidate from the sexual stage of human malaria that contains EGF-like domains. Nature **1988**; 333:74–6.
8. Eksi S, Czesny B, Van Gemert GJ, Sauerwein RW, Eling W, Williamson KC. Malaria transmission-blocking antigen, Pfs230, mediates human red blood cell binding to exflagellating male parasites and oocyst production. Mol Microbiol **2006**; 61:991–8.
9. Williamson KC, Keister DB, Muratova O, Kaslow DC. Recombinant Pfs230, a *Plasmodium falciparum* gametocyte protein, induces antisera that reduce the infectivity of *Plasmodium falciparum* to mosquitoes. Mol Biochem Parasitol **1995**; 75:33–42.
10. Pradel G. Proteins of the malaria parasite sexual stages: expression, function and potential for transmission blocking strategies. Parasitology **2007**; 134(Pt. 14):1911–29.
11. Williamson KC, Kaslow DC. Strain polymorphism of *Plasmodium falciparum* transmission-blocking target antigen Pfs230. Mol Biochem Parasitol **1993**; 62:125–7.
12. Niederwieser I, Felger I, Beck HP. Limited polymorphism in *Plasmodium falciparum* sexual-stage antigens. Am J Trop Med Hyg **2001**; 64:9–11.
13. Alano P, Read D, Bruce M, et al. COS cell expression cloning of Pfg377, a *Plasmodium falciparum* gametocyte antigen associated with osmiophilic bodies. Mol Biochem Parasitol **1995**; 74:143–56.
14. Menegon M, Severini C, Sannella A, et al. Genotyping of *Plasmodium falciparum* gametocytes by reverse transcriptase polymerase chain reaction. Mol Biochem Parasitol **2000**; 111:153–61.
15. Abdel-Wahab A, Abdel-Muhsin AM, Ali E, et al. Dynamics of gametocytes among *Plasmodium falciparum* clones in natural infections in an area of highly seasonal transmission. J Infect Dis **2002**; 185:1838–42.
16. Nwakanma D, Kheir A, Sowa M, et al. High gametocyte complexity and mosquito infectivity of *Plasmodium falciparum* in the Gambia. Int J Parasitol **2008**; 38:219–27.
17. Nakazawa S, Culleton R, Maeno Y. In vivo and in vitro gametocyte production of *Plasmodium falciparum* isolates from Northern Thailand. Int J Parasitol **2011**; 41:317–23.
18. Young JA, Fivelman QL, Blair PL, et al. The *Plasmodium falciparum* sexual development transcriptome: a microarray analysis using ontology-based pattern identification. Mol Biochem Parasitol **2005**; 143:67–79.
19. Marfurt J, Mueller I, Sie A, et al. Low efficacy of amodiaquine or chloroquine plus sulfadoxine-pyrimethamine against *Plasmodium falciparum* and *P. vivax* malaria in Papua New Guinea. Am J Trop Med Hyg **2007**; 77:947–54.
20. Tiono AB, Ouedraogo A, Ogutu B, et al. A controlled, parallel, cluster-randomized trial of community-wide screening and treatment of asymptomatic carriers of *Plasmodium falciparum* in Burkina Faso. Malar J **2013**; 12:79.
21. Wampfler R, Mwingira F, Javati S, et al. Strategies for detection of *Plasmodium* species gametocytes. PLoS ONE **2013**; 8:e76316.
22. Koepfli C, Ross A, Kiniboro B, et al. Multiplicity and diversity of *Plasmodium vivax* infections in a highly endemic region in Papua New Guinea. PLoS Negl Trop Dis **2011**; 5:e1424.
23. Benson G. Tandem repeats finder: a program to analyze DNA sequences. Nucleic Acids Res **1999**; 27:573–80.
24. Schneider P, Schoone G, Schallig H, et al. Quantification of *Plasmodium falciparum* gametocytes in differential stages of development by quantitative nucleic acid sequence-based amplification. Mol Biochem Parasitol **2004**; 137:35–41.
25. Gatei W, Kariuki S, Hawley W, et al. Effects of transmission reduction by insecticide-treated bed nets (ITNs) on parasite genetics population structure: I. The genetic diversity of *Plasmodium falciparum* parasites by microsatellite markers in western Kenya. Malar J **2010**; 9:353.
26. Soulama I, Nebie I, Ouedraogo A, et al. *Plasmodium falciparum* genotypes diversity in symptomatic malaria of children living in an urban and a rural setting in Burkina Faso. Malar J **2009**; 8:135.

27. Henning L, Schellenberg D, Smith T, et al. A prospective study of *Plasmodium falciparum* multiplicity of infection and morbidity in Tanzanian children. Trans R Soc Trop Med Hyg **2004**; 98:687–94.
28. Koepfli C, Schoepflin S, Bretscher M, et al. How much remains undetected? Probability of molecular detection of human *Plasmodia* in the field. PLoS ONE **2011**; 6:e19010.
29. Ouedraogo AL, Bousema T, de Vlas SJ, et al. The plasticity of *Plasmodium falciparum* gametocytaemia in relation to age in Burkina Faso. Malar J **2010**; 9:281.
30. Maeno Y, Nakazawa S, Dao LD, et al. A dried blood sample on filter paper is suitable for detecting *Plasmodium falciparum* gametocytes by reverse transcription polymerase chain reaction. Acta Trop **2008**; 107:121–7.
31. Sama W, Owusu-Agyei S, Felger I, Vounatsou P, Smith T. An immigration-death model to estimate the duration of malaria infection when detectability of the parasite is imperfect. Stat Med **2005**; 24:3269–88.
32. Bretscher MT, Valsangiacomo F, Owusu-Agyei S, Penny MA, Felger I, Smith T. Detectability of *Plasmodium falciparum* clones. Malar J **2010**; 9:234.

Supplementary File S1

A

***pfs230* – protein alignment**

```
3D7    1 RDNFVIDDEEEEEEEEEEEE-EEEEEEEEEEEEYDDYVYEESGDETEEQLQEEHQEEVG
S36    1 RDNFVIDDEEEEEEEEEEEEEEEEEEEEEEEEYDDYVYEESGDETEEQLQEEHQEEVG
S47    1 RDNFVIDDEEEEEEEEEEEE-EEEEEEEEEEEYDDYVYEESGDETEEQLQEEHQEEVG
S32    1 RDNFVIDDEEEEEEEEEEEEEEEEEEEEEEEEYDDYVYEESGDETEEQLQEEHQEEVG
S39    1 RDNFVIDDEEEEEEEEEEE---EEEEEEEEEEEYDDYVYEESGDETEEQLQEEHQEEVG
S33    1 RDNFVIDDEEEEEEEEEEE-EEEEEEEEEEEYDDYVYEESGDETEEQLQEEHQEEVG
S41    1 RDNFVIDDEEEEEEEEEEEEEEEEEEEEEEEEYDDYVYEESGDETEEQLQEEHQEEVG
S42    1 RDNFVIDDEEEEEEEEEEE-EEEEEEEEEEEYDDYVYEESGDETEEQLQEEHQEEVG
S31    1 RDNFVIDDEEEEEEEEEEEEEEEEEEEEEEEEYDDYVYEESGDETEEQLQEEHQEEVG
S44    1 RDNFVIDDEEEEEEEEEEEE-EEEEEEEEEEEYDDYVYEESGDETEEQLQEEHQEEVG
S45    1 RDNFVIDDEEEEEEEEEEEEEEEEEEEEEEEEYDDYVYEESGDETEEQLQEEHQEEVG

3D7   60 AESSEESFNDEDEDSVEARDGDMIRVDEYYEDQDGDTYDSTIKNEDVDE----EVGEEVG
S36   61 AESSEESFNDEDEDSVEARDGDMIRVDEYYEDQDGDTYDSTIKNEDVDE----EVGEEVG
S47   60 AESSEESFNDEDEDSVEARDGDMIRVDEYYEDQDGDTYDSTIKNEDVDEDADEEVGEEVG
S32   61 AESSEESFNDEDEDSVEARDGDMIRVDEYYEDQDGDTYDSTIKNEDADEDADEEVGEEVG
S39   58 AESSEESFNDEDEDSVEARDGDMIRVDEYYEDQDGDTYDSTIKNEDVDE----EVGEEVG
S33   60 AESSEESFNDEDEDSVEARDGDMIRVDEYYEDQDGDTYDSTIKNEDVDE----EVGEEVG
S41   61 AESSEESFNDEDEDSVEARDGDMIRVDEYYEDQDGDTYDSSLKNEDVDEHADAEVGEEVG
S42   60 AESSEESFNDEDEDSVEARDGDMIRVDEYYEDQDGDTYDSTIKNEDVDEDADEEVGEDAD
S31   61 AESSEESFNDEDEDSVEARDGDMIRVDEYYEDQDGDTYDSTIKNEDVDEDADEEVGEEVG
S44   60 AESSEESFNDEDEDSVEARDGDMIRVDEYYEDQDGDTYDSTIKNEDVDEDADEEVGEELG
S45   61 AESSEESFNDEDEDSVEARDGDMIRVDEYYEDQDGDTYDSTIKNEDVDEDADEEVGEEVG

3D7  116 EEVGEEVGE----EVGEEVGEEVGEEVGEEEGEEVGEGVGEEVGEEEGEEVGEEEG
S36  117 EEVGEEVGE----------------EVGEEVGEEEGEEVGEGVGEEVREEEGEEVGEEEG
S47  120 EEVGEEVGE----------EVGEEVGEEVGEEEGEEVGEGVGEEVGEEEGEEVGEEEG
S32  121 EEVGEEVGE----------EVGEEVDEEVGEEVGDEEGEGEVGEELGEEEGEEVGEEEG
S39  114 EEVGEEVGE----EVGEEVGEEVDEEVGEEVGEEEGEEVGEEGEEEGEEVGEEEG
S33  116 EEVGEEVGE----EVGEEVGEEVDEEVGEEVGEEEGEEVGEEGEEEGEEVGEEEG
S41  121 EEVGAEVGE--------EVGEEVGEEVGEEVGEEEGEEVGEGVGEELREDEGEEVGEEEG
S42  120 EEVGEEVGE----EVGEEVGEEVGEEVGEEEGEEVGEGVGEEVGEEEGEEVGEEEG
S31  121 EEVGEEVGE----EVGEEVGEEVGEEVGEEEGEEVGEGVGEEVGEEEGEEVGEEEG
S44  120 EEVGEEVGEEVGEEVGEEVGEEVGEEVGEEEGEDVGEGVGEEVGQEEGEEVGEEEG
S45  121 EEVGEEVGEEVGEEVGEEVGEEVGEEVGEEEGEEVGEGVGEEVGEEEGEEVGEEEG

3D7  172 EYVDEKERQG  282
S36  161 EYVDEKERQG  171
S47  168 EYVDEKERQG  178
S32  169 EYVDEKERQG  179
S39  170 EYVDEKERQG  180
S33  172 EYVDEKERQG  182
S41  173 EYVDEKERQG  183
S42  176 EYVDEKERQG  186
S31  177 EYVDEKERQG  187
S44  180 EYVDEKERQG  190
S45  181 EYVDEKERQG  191
```

***pfg377* – protein alignment**

```
3D7    1 EDDEGDEVNEENVPLNHEE----------------------------ENVPLNHEEDNFPL
G19    1 EDDEGDEVNEENVPLNHEE-------------------------------------ENVPL
G5     1 EDDEGDEVNEENVPLNHEE-----------------ENVPLNHEEDNFPLNHEEDNFPL
G7     1 EDDEGDEVNEENVPLNHEE-------------------------------------DNFPL
G1     1 EDDEGDEVNEENVPLNHEE--------------------------ENVPLNHEEDNFPL
G9     1 EDDEGDEVNEENVPLNHEE-----------------ENVPLNHEEENVPLNHEEDNFPL
G2     1 EDDEGDEVNEENVPLNHEE----------------------------ENVPLNHEEDNFPL
G11    1 EDDEGDEVNEENVPLNHEE-----------------ENVPLNHEEDNFPLNHEEDNFPL
G4     1 EDDEGDEVNEENVPLNHEE-----------------ENVPLNHEEDNFPLNHEEDNFPL
G14    1 EDDEGDEVNEENVPLNHEE----------ENVPLNHEEENVPLNHEEENVPLNHEEENVPL
G15    1 EDDEGDEVNEENVPLNHEE----------ENVPLNHEEENVPLNHEEENVPLNHEEENVPL
G16    1 EDDEGDEVNEENVPLNHEEENVPLNHEEENVPLNHEEDNFPLNHEEDNFPLNHEEENVPL
G17    1 EDDEGDEVNEENVPLNHEEENVPLNHEEENVPLNHEEENVPLNHEEENVPLNHEEENVPL

3D7   34 NHEEDNFPLNHEEENVPLNHEEENVPLNHEEENVPLNHEEENYNSFLSYQKYDERDISPH
G19   25 NHEEENVPLNHEEENVPLNHEEENVPLNHEEENVPLNHEEENYNSFLSYQKYDERDISPH
G5    43 NHEEDNFPLNHEEENVPLNHEEENVPLNHEEENVPLNHEEENYNSFLSYQKYDERDISPH
G7    25 NHEEDNFPLNHEEENVPLNHEEENVPLNHEEENVPLNHEEENYNSFLSYQKYDERDISPH
G1    34 NHEEDNFPLNHEEENVPLNHEEENVPLNHEEENVPLNHEEENYNSFLSYQKYDERDISPH
G9    43 NHEEDNFPLNHEEENVPLNHEEENVPLNHEEENVPLNHEEENYNSFLSYQKYDERDISPH
G2    34 NHEEDNFPLNHEEDNFPLNHEEENVPLNHEEENVPLNHEEENYNSFLSYQKYDERDISPH
G11   43 NHEEDNFPLNHEEENVPLNHEEENVPLNHEEENVPLNHEEENYNSFLSYQKYDERDISPH
G4    43 NHEEDNFPLNHEEENVPLNHEEENVPLNHEEENVPLNHEEENYNSFLSYQKYDERDISPH
G14   52 NHEEENVPLNHEEENVPLNHEEENVPLNHEEENVPLNHEEENYNSFLSYQKYDERDISPH
G15   52 NHEEENVPLNHEEENVPLNHEEENVPLNHEEENVPLNHEEENYNSFLSYQKYDERDISPH
G16   61 NHEEENVPLNHEEENVPLNHEEENVPLNHEEENVPLNHEEENYNSFLSYQKYDERDISPH
G17   61 NHEEENVPLNHEEENVPLNHEEENVPLNHEEENVPLNHEEENYNSFLSYQKYDERDISPH

3D7   94 NVNQHKKEIFHHRNITPYHVNHHNQHMDQHDHHIDHHN-------HHIDHHNHHIDHHNH
G19   85 NVNQHKKEIFHHRNITPYHVNHHNQHMDQHDHHIDHHN----------------------
G5   103 NVNQHKKEIFHHRNITPYHVNHHNQHMDQHDHHIDHHN----------------------
G7    85 NVNQHKKEIFHHRNITPYHVNHHNQHMDQHDHHIDHHN--------------HHIDHHNH
G1    94 NVNQHKKEIFHHRNITPYHVNHHNQHMDQHDHHIDHHN----------------------H
G9   103 NVNQHKKEIFHHRNITPYHVNHHNQHMDQHDHHIDHHN----------------------
G2    94 NVNQHKKEIFHHRNITPYHVNHHNQHMDQHDHHIDHHN--------------HHIDHHNH
G11  103 NVNQHKKEIFHHRNITPYHVNHHNQHMDQHDHHIDHHN----------------------H
G4   103 NVNQHKKEIFHHRNITPYHVNHHNQHMDQHDHHIDHHNQHMDQHD--------------H
G14  112 NVNQHKKEIFHHRNITPYHVNHHNQHMDQHDHHIDHHN--------------HHIDHHNH
G15  112 NVNQHKKEIFHHRNITPYHVNHHNQHMDQHDHHIDHHN-------HHIDHHNHHIDHHNH
G16  121 NVNQHKKEIFHHRNITPYHVNHHNQHMDQHDHHIDHHN--------------HHIDHHNH
G17  121 NVNQHKKEIFHHRNITPYHVNHHNQHMDQHDHHIDHHN-------HHIDHHNHHIDHHNH

3D7  147 HIDHHNHHIDHQDHHIDHHNHHIDHHNHHIDHHDHHIDHHDHHIDHHNHHIDHKSNNQFLQ  207
G19  123 ------HHIDHHNHHIDHHDHHIDHHNHHIDHHDHHIDHHDHHIDHHNHHIDHKSNNQFLQ  176
G5   141 ----------------------HHIDHHNHHIDHHDHHIDHHDHHIDHHNHHIDHKSNNQFLQ  181
G7   131 HIDHHNHHIDHQDHHIDHHNHHIDHHNHHIDHHDHHIDHHDHHIDHHNHHIDHKSNNQFLQ  190
G1   133 HIDHHNHHIDHHNHHIDHQDHHIDHHNHHIDHHDHHIDHHDHHIDHHNHHIDHKSNNQFLQ  193
G9   141 ------HHIDHHNHHIDHQDHHIDHHNHHIDHHDHHIDHHDHHIDHHNHHIDHKSNNQFLQ  194
G2   140 HIDHHNHHIDHQDHHIDHHNHHIDHHNHHIDHHDHHIDHHDHHIDHHNHHIDHKSNNQFLQ  199
G11  142 HIDHHNHHIDHHNHHIDHQDHHIDHHNHHIDHHDHHIDHHDHHIDHHNHHIDHKSNNQFLQ  201
G4   149 HIDHHNHHIDHHNHHIDHQDHHIDHHNHHIDHHNHHIDHHDHHIDHHNHHIDHKSNNQFLQ  209
G14  158 HIDHHNHHIDHHNHHIDHQDHHIDHHNHHIDHHDHHIDHHDHHIDHHNHHIDHKSNNQFLQ  217
G15  165 HIDHHNHHIDHQDHHIDHHNHHIDHHNHHIDHHDHHIDHHDHHIDHHNHHIDHKSNNQFLQ  225
G16  167 HIDHHNHHIDHQDHHIDHHNHHIDHHNHHIDHHDHHIDHHDHHIDHHNHHIDHKSNNQFLQ  227
G17  174 HIDHHNHHIDHQDHHIDHHNHHIDHHNHHIDHHDHHIDHHDHHIDHHNHHIDHKSNNQFLQ  233
```

B

***pfs230* – nucleotide sequence size**

Sample	Size by CE (bp)*	Size by Sequencing (bp)
3D7	538.5	544
S36	510.1	511
S47	528.3	532
S32	531.0	535
S39	533.2	538
S33	538.0	544
S41	541.1	547
S42	547.1	556
S31	550.0	559
S44	558.8	568
S45	559.6	571

*Using Size Standard GS500LIZ (Applied Biosystem)

***pfg377* – nucleotide sequence size**

Sample	Size by CE (bp)*	Size by Sequencing (bp)
3D7	591.2	621
G19	523.3	531
G5	534.2	543
G7	557.5	573
G1	563.4	579
G9	566.6	585
G2	576.8	600
G11	582.9	606
G4	598.8	627
G14	614.6	654
G15	629.2	675
G16	631.0	681
G17	641.3	702

*Using Size Standard GS500LIZ (Applied Biosystem)

Figure S1. Alignments of 10 *pfs230* and 12 *pfg377* protein sequences obtained by PCR amplification of the respective genes from single-clone infected PNG field isolates. Sequencing by direct Sanger sequencing in one direction with nested PCR reverse primer of *pfs230* and in both directions with nested PCR forward and reverse primers of *pfg377*. *Pfs230* nested PCR forward primer was found to be not suitable for sequencing. **A**. Protein sequence alignments of *pfs230* (left panel) and *pfg377* (right panel). Combination of two polymorphic regions resulted in increased marker diversity. 3D7 strain protein sequences derive from PlasmoDB: *pfs230*, PF3D7_0209000 and *pfg377*, PF3D7_1250100. **B**. Comparison of fragment sizes measured by capillary electrophoresis with sizes obtained by Sanger sequencing, which would be explained by the fact that the sized fragments were larger than the largest fragment (500 bp) of the GS500LIZ size standard (Applied Biosystems). The underestimation was less pronounced for *pfs230* due to smaller PCR fragments.

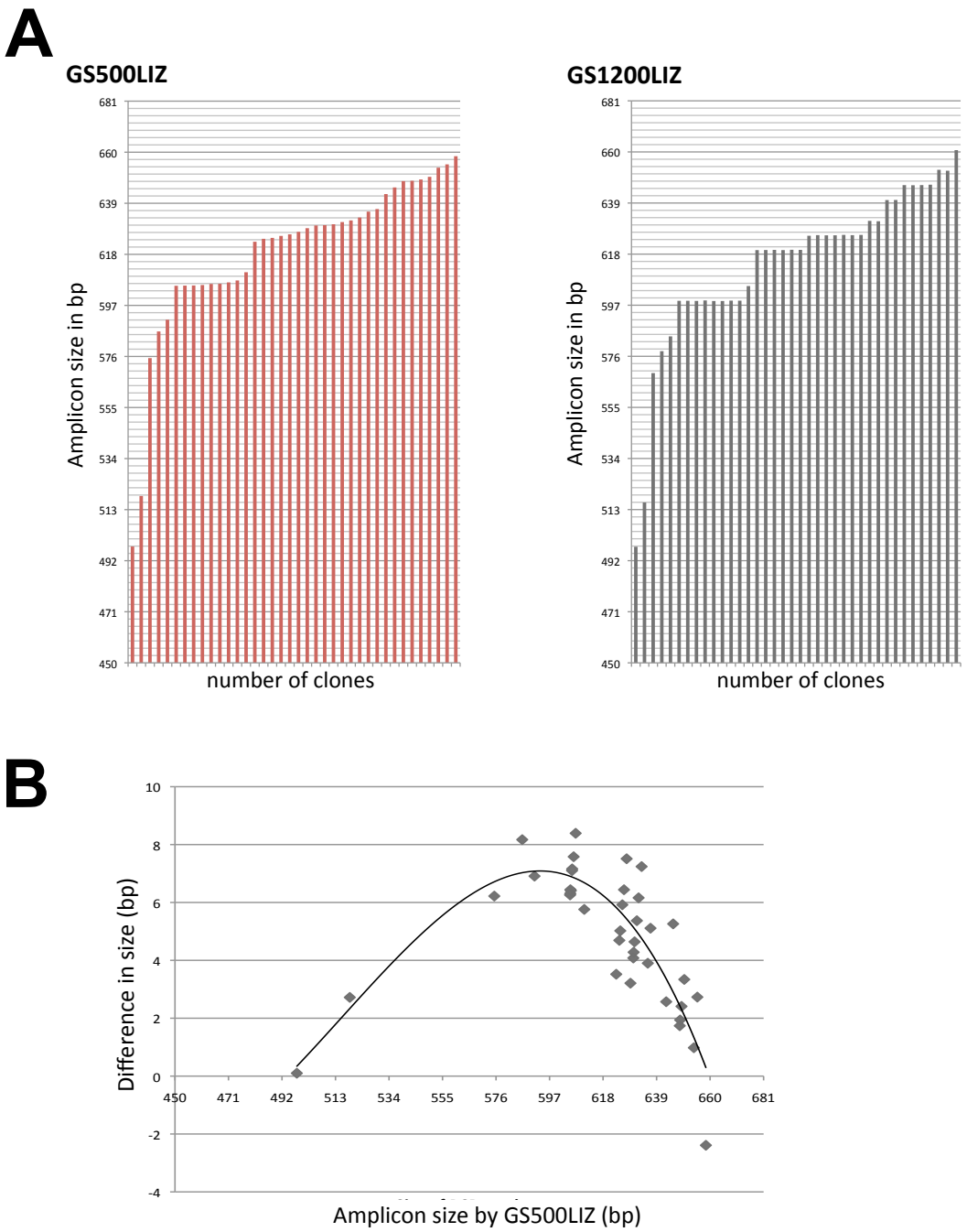

Figure S2. Comparison of fragments sizes obtained by using two different capillary electrophoresis (CE) size standards applied to 38 *pfg377* amplicons detected in 13 blood samples. To investigate whether a size standard containing fragments up to 1200 bp would provide more accurate *pfg377* fragments sizing, a subset of 13 samples was simultaneously sized by CE for *pfg377* using either the GS500LIZ or the GS1200LIZ (Applied Biosystems). **A**. Distribution of amplicon sizes by using GS500LIZ (left panel) or GS1200LIZ (right panel). Better resolution, especially in the size range over 600bp, was obtained for GS1200LIZ. **B**. Difference of sizes by GS500LIZ minus sizes by GS1200LIZ plotted over the amplicon size of GS500LIZ. Curve shows a polynomic equation: $y = -5E\text{-}06x^3 + 0.0083x^2 + 689.48$. A non-linear overestimation of size by GS500LIZ was found. This leads to the conclusion that GS500LIZ size standard is sufficient for *pfs230*, as amplicons are <600bp. For *pfg377* with amplicons >700 bp the GS1200LIZ size standard provides improved sizing.

Supplementary Table S2.

Table S2. (RT)-PCR mixes and thermo profiles.

A) PCR for genotyping DNA field samples

	Reagents	Concentration	Volume	Temperature	Time	Cycles
Primary (3 duplex reactions) reaction mix and thermo profile[a]	ddH_2O		11µl	94°C	15sec	1x
	Solis Buffer B	10x	2µl	94°C	15sec	25x
	dNTPs	2mM	2.8µl	57°C[b]	30sec	
	$MgCl_2$	25mM	1.6µl	72°C	40sec	
	Primer mix PF+PR of 1st marker	10µM each	0.5µl	72°C	5min	1x
	Primer mix PF+PR of 2nd marker	10µM each	0.5µl			
	Solis Taq Polymerase	500u/µl	0.6µl			
	DNA		1µl			
	Totat volume		20µl			
Nested (simplex) reaction mix and thermo profile	Reagents	Concentration	Volume	Temperature	Time	Cycles
	ddH_2O		12.6µl	94°C	15sec	1x
	Solis Buffer B	10x	2µl	94°C	15sec	30x
	dNTPs	2mM	2µl	58°C[c]	30sec	
	$MgCl_2$	25mM	1.6µl	72°C	40sec	
	Primer mix NF+NR -labelled	10µM each	0.5µl	72°C	5min	1x
	Solis Taq Polymerase	500u/µl	0.3µl			
	Primary PCR product		1µl			
	Totat volume		20µl			

B) SuperScript II RT-PCR for 3D7 in vitro gametocyte culture

	Reagents	Concentration	Volume	Temperature	Time	Cycles
Superscript II RT (duplex and multiplex reactions) reaction mix and thermo profile[d]	RNA		15µl	65°C	5min	1x
	ddH_2O		1.95µl	42°C	1min	1x
	dNTPs	25mM	0.75µl	42°C	50min	1x
	Riverse primer mix[d]	10µM each	0.3µl	70°C	15min	1x
	Buffer Superscript 1st Strand	5x	6µl			
	DTT	0.1 M	3µl			
	RNaseOUT	40u/µl	1.5µl			
	Superscript II RTase	200u/µl	1.5µl			
	Totat volume		30µl			
Primary (simplex) reaction mix and thermo profile	Reagents	Concentration	Volume	Temperature	Time	Cycles
	ddH_2O		14µl	94°C	15sec	1x
	Phusion Buffer HF	5x	6µl	94°C	15sec	20x
	dNTPs	2mM	4.2µl	57°C[c,f]	30sec	
	Primer mix PF+PR[e]	10µM each	0.5µl	72°C	40sec	
	Phusion High-Fidelity Polymerase	2u/µl	0.3µl	72°C	5min	1x
	Primary PCR product		1µl			
	Totat volume		20µl			

Nested (simplex) reaction mix and thermo profile	Reagents	Concentration	Volume	Temperature	Time	Cycles
	ddH_2O		11.1µl	94°C	15sec	1x
	Solis Buffer B	10x	2µl	94°C	15sec	30x
	dNTPs	2mM	2µl	58°C[c]	30sec	
	$MgCl_2$	25mM	1.6µl	72°C	40sec	
	Primer mix NF+NR:	10µM each	1µl	72°C	5min	1x
	Solis Taq Polymerase	500u/µl	0.3µl			
	Primary PCR product		2µl			
	Totat volume		20µl			

C) AffinityScript RT-PCR for genotyping field samples

cDNA Affinity One-step primary (simplex) reaction mix and thermo profile	Reagents (prepared on ice)	Concentration	Volume	Temperature	Time	Cycles
	RNase-free Water		17.5µl	45°C	30min	1x
	Hercules MasterMix	2x	25µl	92°C	2min	1x
	Primer mix PF+PR: Pfg377 or Pfs230	10µM each	1.5µl	92°C	20sec	30x
	AffinityScript RT-enzyme	500u/µl	1µl	57°C	20sec	
	RNA		5µl	68°C	45sec	
	Total volume		50µl	68°C	5min	1x
Nested (simplex) reaction mix and thermo profile	Reagents	Concentration	Volume	Temperature	Time	Cycles
	ddH_2O		11.4µl	94°C	15sec	1x
	Solis Buffer B	10x	2µl	94°C	15sec	30x
	dNTPs	2mM	2µl	58°C	30sec	
	$MgCl_2$	25mM	1.6	72°C	40sec	
	Primer mix NF+NR -labelled: Pfg377 or Pfs230	10µM each	1µl	72°C	5min	1x
	Solis Taq Polymerase	500u/µl	1µl			
	Primary PCR product		1µl			
	Totat volume		20µl			

Abbreviations: NF, nested PCR forward primer; NR, nested PCR reverse primer; PF, primary PCR forward primer; PR, primary PCR reverse primer.

[a]Duplex reactions: 1. *pfg377/pfs230*; 2. Pf11.1 (no intron boundary)/PF11_0214 and 3. PFI1205w/PFL0545w.

[b]Annealing temperature for the duplex PFI1210w/PFL0545w was 50°C.

[c]Annealing temperature for the simple reactions PFI1210w and PFL0545w was 50°C.

[d]Primers used for duplex reaction: Pfg377_PR and Pfs230_PR; for multiplex reaction: Pf11.1_PR, PF11_0214_PR, PFI1205w_PR and PFL0545w_PR.

[f]Annealing temperature of Pf11.1 assay spanning intron boundary was 58°C.

[e]Pf11.1 primary primers for intron spanning assay were: Pf11.1_PF1 + Pf11.1_PR. Primers for short fragment were: Pf11.1_PF2 + Pf11.1_PR

Chapter 4: *Plasmodium vivax* Hypnozoite Reservoir

Full title:

Strategies for Understanding and Reducing the *Plasmodium vivax* and *Plasmodium ovale* Hypnozoite Reservoir in Papua New Guinean Children: A Randomized Placebo-Controlled Trial and Mathematical Model

Leanne J. Robinson[1,2,3,], Rahel Wampfler[4,5], Inoni Betuela[1], Stephan Karl[2,3], Michael T. White[6], Connie S.N. Li Wai Suen[2,3], Natalie E. Hofmann[4,5], Benson Kinboro[1], Andreea Waltmann[2,3], Jessica Brewster[2], Lina Lorry[1], Nandao Tarongka[1], Lornah Samol[1], Mariabeth Silkey[4], Quique Bassat[8], Peter M. Siba[1,7], Louis Schofield[2,3,8], Ingrid Felger[4,5] and Ivo Mueller[2,3,9#].

[1]Vector Borne Diseases Unit, PNG Institute of Medical Research, Madang & Maprik, Papua New Guinea
[2]Population Health and Immunity Division, Walter and Eliza Hall Institute of Medical Research, Parkville, Australia
[3]Department of Medical Biology, University of Melbourne, Victoria, Australia
[4]Molecular Diagnostics Unit, Swiss Tropical & Public Health Institute, Basel, Switzerland
[5]University of Basel, Basel, Switzerland
[6]MRC Centre for Outbreak Analysis and Modelling, Imperial College London, United Kingdom
[7] School of Veterinary and Biomedical Sciences, James Cook University, Townsville, Australia
[8]Australian Institute of Tropical Health and Medicine, James Cook University, Cairns, Australia
[9]ISGlobal, Barcelona Ctr. Int. Health Res. (CRESIB), Hospital Clínic - Universitat de Barcelona, Barcelona, Spain
[#]Corresponding author

– This manuscript is submitted to PLoS Medecine –

Abstract

Background:

The undetectable hypnozoite reservoir for relapsing *Plasmodium vivax* and *ovale* malarias presents a major challenge for malaria control and elimination in endemic countries. This study aims to directly determine the contribution of relapses to the burden of *P. vivax* and *P. ovale* infection, illness and transmission in Papua New Guinean (PNG) children.

Methods and Findings:

524 children aged 5-10 years were enrolled into a randomized placebo-controlled double-blind trial of blood- plus liver-stage (chloroquine (CQ,3d), artemether-lumefantrine (AL,3d) and primaquine (PQ,20d, 10mg/kg total dose)) or blood-stage drugs only (CQ, AL plus placebo (20d)) and followed actively for 9-months. A basic stochastic transmission model was developed to estimate the potential effect of mass-drug administration (MDA) for the prevention of recurrent *P. vivax* infections. Targeting hypnozoites through PQ treatment reduced the risk of having at least one PCR-detectable *P. vivax* or *P. ovale* infection during 8-months of follow-up by 82% (95% CI [75, 86], p<0.001) and 69% (95% CI [23, 87], p=0.011) respectively, and the risk of having at least one clinical *P. vivax* episode by 75% (95% CI [39, 89], p=0.002). PQ also reduced the molecular force of blood-stage *P. vivax* infection in the first 3 months of follow-up by 79% (95% CI [72, 85], p<0.001). Children who received PQ had a 73% lower risk of carrying *P. vivax* gametocytes (95% CI [62, 81], p<0.001). PQ had a comparable effect irrespective of the presence of *P. vivax* blood-stage infections at the time of treatment (p = 0.14). Modelling revealed MSAT with highly sensitive qPCR, or MDA with blood-stage treatment alone, would have only a transient effect on *P. vivax* transmission levels, while MDA that includes liver-stage treatment is predicted to be a highly effective strategy for *P. vivax* elimination.

Conclusions:

Relapses cause ~4/5 *P. vivax* infections and at least 3/5 *P. ovale* infections in PNG children and are important in sustaining transmission. MDA campaigns combining blood- and liver-stage treatment are highly efficacious interventions for reducing *P. vivax* and *P. ovale* transmission.

Introduction

Renewed intensification of global malaria control efforts over the last 15 years have been successful in significantly reducing the global burden of malaria, with many countries in the Asia-Pacific and the Americas seeing a reduction of >90% in the number of clinical cases [1]. As a consequence 34 countries are actively attempting to eliminate malaria and many others are considering to do so in near future [2] In 2013, the political leaders of Central American and East Asian countries, representing >60% of the global population, have declared their intention to eliminate malaria for their regions by 2020 and 2030, respectively [3,4]. In parallel to this reduction in overall incidence, a pronounced shift in species composition has been observed with *P. vivax* now the predominant *Plasmodium spp.* in the vast majority of countries outside Africa [2], accounting for 90-100% of clinical cases in countries such as Guatemala, Brazil, Solomon Islands and Vanuatu [1].

Despite a significant reduction in *P. vivax* malaria in the last 20 years, *P. vivax* has several biological characteristics that enable it to evade existing control and elimination efforts, which are mainly directed against *P. falciparum* blood stages [5,6]. First and foremost is the ability of *P. vivax* to relapse weeks, months and years after a primary infection, via a poorly understood reactivation of dormant hypnozoite stages in the liver [7]. These stages cannot be detected with currently available diagnostic tools and are not cleared upon treatment with routinely administered anti-malarial drugs, unless primaquine, a drug that requires at least a 7-14 day administration and can cause severe haemolysis in people with glucose-6-phosphate dehydrogenase (G6PD) deficiency, is added to the treatment [8].

In *P. vivax* endemic regions, hypnozoites constitute a reservoir of diverse *P. vivax* strains that will cause blood stage infections at a later point in time [9,10]. They are therefore likely to not only account for a high number of *P. vivax* blood stage infections but also contribute a high number of concurrently circulating parasite clones in the blood. Despite recent advances in molecular detection and genotyping of *P. vivax* parasites [11], it is not yet possible to determine if an infection detected in the blood of an individual originated from a new sporozoite inoculation or is a relapse from a hypnozoite. *P. vivax* produces gametocytes rapidly and continuously over the course of an infection [10] and even low-density infections are thus potentially infectious. If all clones, relapse-derived or newly acquired, produce gametocytes concurrently, these infections can potentially be transmitted together and the chance for sexual recombination in the mosquito is greatly increased, thus contributing to the maintenance of a high genetic diversity even at low transmission levels [12–14].

P. vivax is thus considered one of the major challenges for elimination of malaria outside Africa [15]. Better data and tools are urgently required to estimate the *P. vivax* hypnozoite reservoir, quantify relapse burden, better understand potential relapse triggers and develop the most appropriate public health intervention strategies [15–17].

In malaria-endemic areas of Papua New Guinea (PNG), where all four human *Plasmodium* species co-exist, infection and illness from *P. vivax* predominates in young children [18,19] and is gradually replaced by *P. falciparum* as the main cause of disease in older children and adults [20], although *P. vivax* infections remain common throughout childhood and into adulthood, ranging from 13-36% in cross-sectional surveys conducted in PNG between 2005 and 2010 [21–24]. *P. ovale* and *P. malariae* are much less common, with a 2010 survey revealing a prevalence of 0.1% and 1.3% respectively (by quantitative real-time polymerase chain reaction (qPCR)), and are mostly observed in mixed-species infections [22, (Koepfli, Robinson et al., PLoS One, in revision]. PNG standard anti-malarial treatment is artemether-lumefantrine, which acts against the blood-stage of the parasite but does not eliminate hypnozoites. In the absence of a nation-wide cost-effective strategy of screening for G6PD, primaquine treatment for clearing liver stages, although recommended for G6PD normal patients, is rarely given. Consequently, relapses are expected to contribute significantly to the high burden and limited seasonality of *P. vivax* in PNG children [18,26]. A previous study in PNG children aged 1-5 years observed that presumptive artesunate (7d) and primaquine (14, partially supervised) mass-treatment to clear hypnozoites reduced the risk of *P. vivax* clinical episodes by 28% (p= 0.042) and 33% (p= 0.015) compared to only blood-stage treatment and no treatment, respectively [27]. Although the study used a sub-optimal treatment regimen, and thus substantially underestimated the hypnozoite burden, it did highlight the significant challenge relapses pose to successful control and eventual elimination of *P. vivax* malaria in PNG and provide strong rationale for conducting a more comprehensive clinical trial with an in-depth molecular diagnostics component.

Intensified national control efforts have seen the prevalence of light-microscopy detectable *P. vivax* malaria parasites in the general population decrease from 17% in 2006, to 8% in 2010 [Koepfli, Robinson et al., PLoS One, in revision], to 0.5% in 2014 [28]. Despite these gains, a large reservoir of individuals infected with submicroscopic *P. vivax* persists. In a 2010 survey, *P. vivax* prevalence by qPCR was 12.8%. Of these infections, 89.6% were asymptomatic, 53.8% submicroscopic and 48.9% carried *P. vivax* gametocytes (Koepfli, Robinson et al., submitted PLoS One). Similarly high rates of persistent asymptomatic *P. vivax* infections and gametocyte carriage were also found in surveys in Thailand [29,30] and Brazil [31] that have seen substantial recent reductions in transmission.

Mass screening and treatment (MSAT) and mass drug administration (MDA) with Artemisinin-based combination therapies (ACTs) have been advocated as important tools to reduce the asymptomatic *P. falciparum* reservoir [32,33]. These interventions are also likely to be of great importance for *P. vivax* elimination. Significant questions remain, however, none greater than how to best attack with the undetectable hypnozoite reservoir.

To address these critical questions we have conducted a randomised double-blind placebo-controlled trial of a highly efficacious primaquine treatment regimen in PNG children aged 5-10 years, using detailed molecular diagnostics to directly measure the contribution of relapses to the

burden of *P. vivax and P. ovale* infection, disease and transmission. By using this data in mathematical models, we further estimate the potential effect of MDA with treatment regimens that are part of first-line policy or regimens currently under investigation in clinical trials [34,35], for the prevention of recurrent *P. vivax* infections, providing critical evidence-based recommendations for policy makers.

Materials and methods

Study site, design and participants

The study was conducted from 17 August 2009 to 20 May 2010 in 5 village clusters (13 hamlets) of the Albinama and Balif areas of Maprik District, East Sepik Province, where both *P. falciparum* and *P. vivax* are hyperendemic and *P. vivax* is responsible for the majority of malaria infection and disease in the first 3 years of life [18,22,36]. Malaria transmission is moderately seasonal, peaking in the early wet season from December to March [26]. Health services for the area are provided by Albinama health sub-centre, Balif aid post and a system of village health volunteers operating in all study villages.

Between August and September 2009, 529 children aged 5 to 10 years, whose parents provided written informed consent to their participation were screened for inclusion into this parallel double-blind placebo-controlled trial. Children were enrolled if they fulfilled the following criteria: (i) aged 5-10 years (±3 months in children without known date of birth, (ii) enrolled at selected elementary schools and permanent residents of the area, (iii) no disability, (iv) no chronic illness, (v) no known allergy to study drugs, (vi) Hb >5 g/dL, (vii) no severe malnutrition (defined by the PNG national guidelines as weight-for-age nutritional Z score [WAZ] <60th percentile), and (viii) no G6PD deficiency. The inclusion criteria were amended during the study to allow children aged 5-6 years but who were not yet enrolled at elementary school to participate in the study. This was necessary to ensure we adequately covered the desired 5-10 year age range and reached the required sample size of 525 without expanding the geographical area. Five children were excluded on the basis of G6PD deficiency and 524 were block randomised using a 1:1 allocation ratio to receive 20 days of directly observed treatment (DOT) over 4 weeks (26 days) of either: chloroquine (CQ, $DOT_{1\text{-}3}$), artemether-lumefantrine (Coartem®) (AL, $DOT_{11\text{-}13}$) and primaquine (PQ, $DOT_{1\text{-}20}$; 0.5mg/kg); or CQ ($DOT_{1\text{-}3}$), AL ($DOT_{11\text{-}13}$) and placebo ($DOT_{1\text{-}20}$) (PL/CQ/AL) (Figure S1). This treatment regimen was deliberately chosen to maximise efficacy and the dose of each drug timed such that there would be minimal residual drug by Day 0 of the follow-up. In order to achieve this, a 4 week wash out period was required for CQ and the 20 days of PQ DOTs were scheduled Monday to Friday of these 4 weeks (Figure S1), for ease of direct supervision of every dose. AL was administered due to the fact that there is documented CQ resistance in PNG and the PNG National Treatment Guidelines for *P. vivax* are AL plus PQ. The administration of AL on DOTs 11-13 (Days 15-17) was deliberate so that it wouldn't interfere with CQ and drug levels would have

reduced to zero by baseline. The intention was not to trial this unconventional drug regimen as a treatment for implementation, but rather as a maximally effective treatment to ensure radical cure in half of the cohort and thus allow a detailed investigation of relapses. Participants, field teams and investigators were all blinded with respect to treatment allocation.

The study received ethical clearance from the PNG IMR Institutional Review Board (0908), the PNG Medical Advisory Committee (09.11), the Ethics Committee of Basel 237/11 and was conducted in full accordance with the Declaration of Helsinki. The study was retrospectively registered on ClinicalTrials.gov (NCT02143934) on 20 May 2014. All authors affirm that other trials involving primaquine they are involved in are registered on ClinicalTrials.gov (NCT01837992; NCT02364583).

Inclusion criteria, randomisation, blinding, and treatment allocation

After enrollment, children were randomly allocated to the PQ/CQ/AL or PL/CQ/AL treatment group using a pre-assigned list. Randomisation lists were prepared by independent statistician using Microsoft Excel and consisted of ID assignments in blocks of 6, each block comprising a list of the same 6 letters in random order. The independent statistician assigned 3 randomly selected letters to the PQ drug containers and the 3 other letters to the PL drug containers. The coding document was held by the statistician until completion of the trial. PQ and PL were identical in size, shape and color. The entire study team and principal investigators remained fully blinded for the entire study period.

Clinical procedures and follow-up

Clinical assessment at enrolment included screening for symptoms of febrile illness, a detailed history of bednet use and recent illness/anti-malarial treatment and collection of a finger-prick blood sample for assessment of G6PD deficiency using the visual, tube-based G6PD assay (Dojindo Laboratories, Japan), haemoglobin measurement and later immunological and molecular studies. Children who were febrile were tested using a malaria rapid diagnostic test (RDT; CareStart™ Malaria pLDH/HRP2 Combo; AccessBio, USA) and if positive treated with AL during $DOT_{1\text{-}3}$. DOT_1 was administered at the end of the enrolment visit, with the subsequent 19 DOTs administered daily from Monday-Friday over the subsequent 4 weeks (Figure S1). All DOTs were supervised by a member of the clinical field team and were co-administered with food and well tolerated [37].

Three days after final DOT (i.e., 4 weeks after enrolment), a venous sample was collected and defined as Baseline: (timepoint 'Day 0' of study). Children were then actively monitored for the presence of febrile symptoms every fortnight for 8 months, with passive surveillance measures implemented at local health centres, aid posts and via the village health worker network. In all symptomatic children, *Plasmodium spp.* infection was initially confirmed using RDT and a 250µL finger-prick blood sample was collected for confirmation of infection by light microscopy (LM) and

quantitative real-time PCR (qPCR). Only symptomatic children who tested positive by RDT and/or LM were treated with AL. PQ was not re-administered for RDT and/or LM confirmed *P. vivax* malaria episodes during follow-up. All other illness episodes detected were referred to the local health centre and treated in accordance with PNG treatment guidelines. Finger-prick blood samples were also collected from all children every 2 weeks for the first 12 weeks and every 4 weeks thereafter during the follow-up period (Figure S2). Children were considered lost to follow-up if they permanently relocated outside of the study area or withdrew from the study.

Laboratory Methods

All blood samples collected during active and passive surveillance were examined by LM and qPCR. Blood films were examined independently by two skilled microscopists, blind to allocated treatment for 200 thick-film fields (1000X magnification) before being declared *Plasmodium*-negative. Parasite density was calculated from the number of parasites per 200-500 leucocytes (depending on parasite density) and an assumed leucocyte density of 8,000/μL (WHO Malaria Microscopy Training Guide). Slides discrepant for positivity/negativity, speciation or density (>2 log difference) were adjudicated by a WHO certified Level 1 (expert) microscopist. Slides were scored as LM-positive for an individual *Plasmodium* species, if the species was detected independently by at least 2 microscopists and/or subsequent qPCR diagnosis confirmed the presence of the species. Densities were calculated as the geometric mean densities of all positive reads.

Venous blood samples were separated into plasma, peripheral blood mononuclear cells (PBMCs) and red cell pellets and stored at -80 and -20°C respectively. Finger-prick blood samples were separated into plasma and red cell pellets and stored at -80 and -20°C respectively. DNA was extracted using the FavorPrep™ 96-well genomic DNA extraction kit (Favorgen, Ping-Tung, Taiwan) from the red cell pellet fraction of all samples. *Plasmodium spp.* infections were detected using a generic qPCR to detect all four species, after which species-specific (*P. falciparum, P. vivax, P. malariae* and *P. ovale*) qPCRs were performed on *Plasmodium* positive samples [38,39]. The *P. ovale* PCR detects both *P. ovale curtisi* and *P. ovale wallikeri*. In addition, samples positive for *P. vivax* by qPCR were tested for gametocytes by *Pvs25* quantitative reverse transcription (qRT-)PCR [38] and individual *P. vivax* clones genotyped by capillary electrophoresis using the molecular marker *msp1F3* [40] to determine the number of genetically distinct *P. vivax* blood-stage clones acquired per individual per year-at-risk, i.e., the molecular force of blood-stage infections ($_{mol}$FOB) [41].

Statistical Analysis and Modelling

For analysis purposes, a clinical episode of *P. vivax* or *P. falciparum* malaria was defined as febrile illness (current or previous 48 hours) plus the presence of *P. vivax* or *P. falciparum* parasites by LM (any density). The primary trial endpoint was defined as time-to-first *P. vivax* infection by

qPCR. Secondary endpoints included time-to-first *P. vivax* infection by light microscopy, time-to-first *P. vivax* clinical episode, incidence rate of clinical *P. vivax* episodes, incidence of genetically distinct *P. vivax* infections ($_{mol}$FOB), time-to-first *P. falciparum, P. malariae and P. ovale* infection by qPCR, time-to-first *P. falciparum* clinical episode. A sample size of 250 children per arm was calculated using hazard-rate based calculations (log-rank tests) based on the effects (30% reduction in PQ group) observed in [27] with a α–error of 5% and a power of 80% and assuming a 30% increase in time-to-first infections following additional distributions of long-lasting insecticide treated nets. Sample sizes were increased by 5% to account for children receiving less than 14 doses of primaquine or placebo.

Time-to-first *Plasmodium* infection or episode and its association with treatment and covariates were modelled using Cox regression and the proportional-hazards assumption was checked using the test based on the Schoenfeld residuals. For these analyses, time at risk was censored on the last day before the first of two consecutively missed active follow-up visits. Kaplan-Meier estimates were computed for each endpoint by *Plasmodium* species and method of *Plasmodium* diagnosis. The log-rank test was used to test for differences between survival curves. In all survival analyses, children were considered 'at risk' until they reached the endpoint of interest, withdrew, were lost to follow-up, censored or completed the study. Village membership was fitted as a fixed effect in the Cox proportional hazards model using the equation: h(t)=h_0 (t) exp(β_1 x_1+ β_2 x_2+β_3 x_3+ β_4 x_4); where x_1= treatment, x_2 = age, x_3 = village, and x_4 = infection status by the same *Plasmodium* species at enrolment.

Negative binomial regression models were used to calculate incidence rate of clinical episodes, $_{mol}$FOB and *P. vivax* gametocyte positivity. In these models, time at risk was calculated for individual children based on the number of attended versus missed visits. If a child was not seen for a consecutive time period of 108 days during the follow up period, time at risk was censored at the last attended active or passive visit. In addition, for the molecular analyses, time at risk was reduced for children who were not seen for consecutive intervals of 42 days by subtracting the days of the missed intervals from the overall individual time at risk. As per PNG treatment guidelines, treatment during the follow-up period was only given if a clinical episode was detected. A potential competing risk scenario would therefore only happen is if treatment was administered for a clinical episode with one species before the first event for a heterologous species endpoint had occurred. However, since incidence rate of clinical episodes was very low, this occurred very rarely. It should also be noted that the times at risk for the analyses of different endpoints were not adjusted for the post-treatment prophylactic effects of the aforementioned treatments. Clinical malaria episode incidence rate ratios were derived from models adjusted for treatment, age and *P. vivax* positivity by PCR at enrolment, while the models for $_{mol}$FOB and *P. vivax* gametocyte positivity were further adjusted for village of residence. Differences between treatment groups at enrolment were investigated using chi-square and Fisher's exact tests for categorical characteristics and Student's *t*-test for normally-distributed continuous variables. All tests were two-tailed and the confidence level was set at 95%. All analyses were performed using R version 3.0.3. [42] and/or Stata 12 [43].

The effects of mass drug administration (MDA) and mass screen and treat (MSAT) programmes with anti-malarial drugs currently recommended as first-line treatment policy on the dynamics of *P. vivax* and *P. falciparum* transmission were investigated using mathematical models. The model simulated the impact of a 3 day course of either dihydroartemisinin-piperaquine (DHA-PIP) or chloroquine (CQ) to clear blood-stages [44], and a 14 day primaquine regimen to clear liver-stages. The model also simulated the impact of tafenoquine plus CQ treatment, a highly promising, short-course anti-relapse therapy, which is currently undergoing phase 3 clinical trials [34]. A classical Ross-Macdonald model [45,46] was used to describe the qualitative dynamics of *P. falciparum* following treatment of 'at risk' populations with drugs for clearing blood-stage infections. This model was extended to incorporate relapse infections of *P. vivax*, and the effects of primaquine treatment for the clearance of liver-stage hypnozoites [47]. In brief, individuals in a population can be susceptible to blood-stage infections with no liver-stage hypnozoites (S_0), infected with blood-stage parasites but no hypnozoites (I_0), susceptible to blood-stage infection but carrying hypnozoites (S_L), and infected with both blood-stage parasites and hypnozoites (I_L). Full details of the deterministic differential equations describing the mathematical models and parameter definitions are provided in the Supplementary Information Text 1. The model was also implemented in a stochastic framework with population size 5,000 to capture stochastic variation and the potential for the elimination of transmission.

Results

Enrolment and baseline characteristics of children

Of the 524 G6PD-normal children that were randomised to receive Primaquine(PQ)/ Chloroquine(CQ)/Artemether-lumefantrine(AL) or Placebo(PL)/CQ/AL a total of 504 children 4.8-10.5 years completed at least 14 days of DOT PQ/PL treatment and were followed actively and passively for 32 weeks post-baseline (Figure 1).

No significant differences in demographic characteristics and infection status were observed at enrolment between treatment groups (Table 1). At baseline (~ 4 weeks after enrolment and commencement of drug treatment), 4 children were *P. vivax* positive by qPCR (2 each in the PL and PQ arms), 2 children in the PL arm were *P. falciparum* positive and 1 of these was also *P. vivax* positive. These children were exempted from the respective analyses of time-to-first infection. No *Plasmodium* infections were detected by LM at baseline. During follow-up, an average of 82% (IQR [67-92]) of children were seen at each active case detection time-point. The average number of study contacts during follow-up did not differ between treatment arms (PL: 14.0, PQ: 14.4; p=0.25; Student's t-test).

Table 1. Demographic and clinical characteristics of the cohort at enrolment, classified by allocated treatment. Data are percentages or mean±SD.

	Placebo	Primaquine	P-value
N	257	247	
Male sex (%)	49.8	48.6	0.78
Age (years)	7.7 ±1.5	7.5 ±1.6	0.40
Weight (kg)	19.7±3.2	19.8±3.6	0.82
Village (%)			
Albinama	23.0	22.7	
Amahup	27.3	24.7	
Balanga	12.5	9.3	0.57
Balif	24.5	26.7	
Bolumita	12.8	16.6	
Bed net use (%)	93.4	93.1	0.91
Infection by PCR (%*)			
P. vivax	44.8	50.2	0.22
P. falciparum	23.7	23.9	0.97
P. ovale	1.9	4.9	0.07
P. malariae	13.2	15.4	0.49
Non-P. vivax	14.0	11.7	0.45
Fever (%)	15.2	14.6	0.85
Haemoglobin (g/dL)	10.9 ±1.3	10.8 ±1.3	0.78

* Prevalence includes single and mixed-species infections.

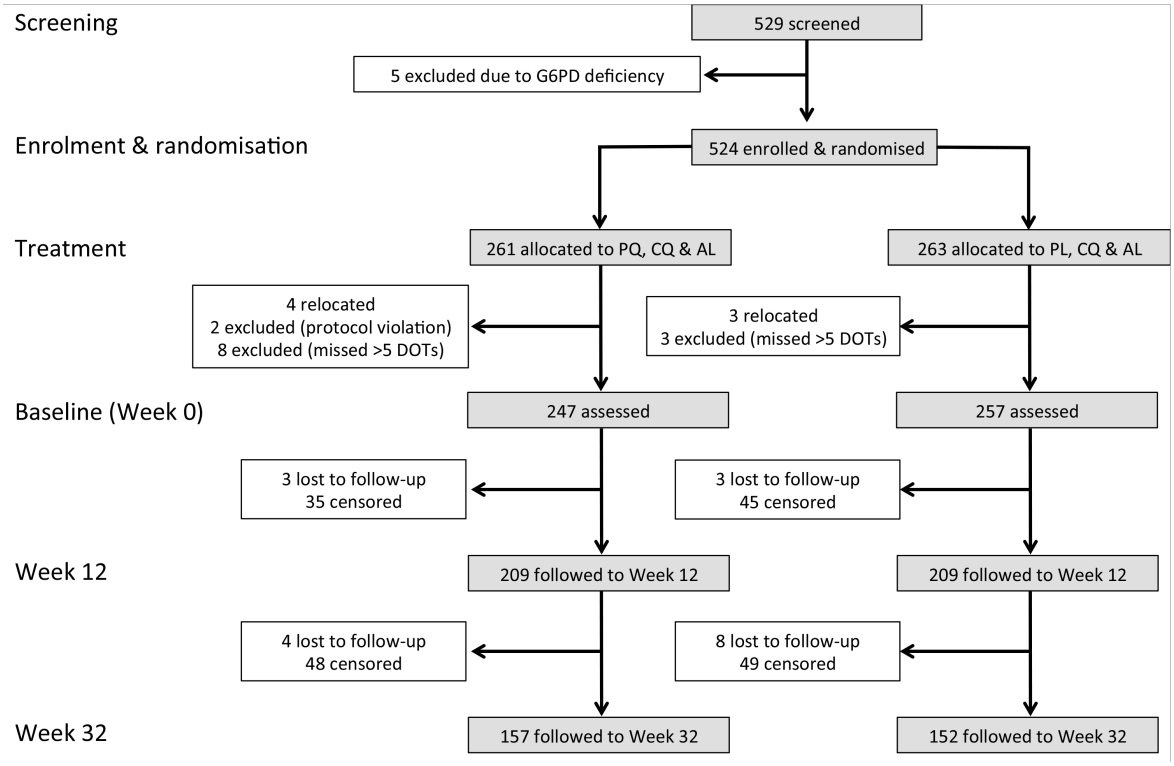

Figure 1. Consort diagram: study design, randomisation and retention of study participants during follow-up. Children were censored on the last day before the first of two consecutive missed clinical visits.

Risk of *P. vivax* infection during follow-up

The time to first or only *P. vivax* blood-stage infection (as detected by qPCR) differed significantly between the two treatment arms: only 25.5% (63/247) of children who received PQ experienced at least one new *P. vivax* infection compared to 65.0% (167/257) in the PL arm (p< 0.0001; Table 2; Fig. 2A). qPCR-positive, recurrent *P. vivax* blood-stage infections were detected rapidly in the PL arm, with 31.5% (80/254) of children infected by day 42 compared to only 8.2% (20/245) in the PQ arm (Fig. 2A). As expected, LM-positive infections were less common in both arms and were observed later during follow-up (Figure 2B).

Clearance of liver-stages through PQ treatment resulted in an 82-84% reduction in the risk of recurrent *P. vivax* blood-stage infections diagnosed by qPCR (HR=0.18, 95% CI [0.14, 0.25], p<0.001) and LM (HR=0.16, 95% CI [0.11, 0.24], p<0.001), respectively compared to PL (Table 2). This increased to an 83-88% reduction in risk when only the first 3 months of follow-up were considered (qPCR: HR=0.17, 95% CI [0.12, 0.24] p<0.001; LM: HR=0.12, 95% CI [0.07, 0.19] p<0.001; Table 2).

There is considerable heterogeneity in the prevalence and risk of *P. vivax* infection across the study villages. The risk of first *P. vivax* infection (by qPCR and LM) differed significantly among children living in different villages, with the highest risk in Bolumita (qPCR HR=4.70, 95% CI [3.14, 7.02], p<0.0001; LM HR=4.62, 95% CI [2.92, 7.30], p<0.0001) and Balanga (qPCR HR=2.33, 95% CI [1.53, 3.55], p<0.0001; LM HR=1.70, 95% CI [1.03, 2.81], p=0.04). There is however no interaction between village and treatment effect. The risk of first *P. vivax* blood-stage infection diagnosed by qPCR after treatment was not significantly associated with age (qPCR HR=0.95, 95% CI [0.87, 1.03] p=0.19), however there was a 15% reduction in risk of having at least one LM-patent *P. vivax* infection with each additional year of life (LM HR=0.85, 95% CI [0.77, 0.95], p = 0.003). As with village, there was no interaction between age and treatment effect.

When all *P. vivax* infections in a child were genotyped to identify new infections in the context of ongoing multiple clone infections, PQ treatment was associated with a 77% reduction in the incidence of genetically distinct *P. vivax* bloodstage clones ($_{mol}$FOB) (PQ arm: $_{mol}$FOB = 1.62/year; PL arm: $_{mol}$FOB = 4.74/year, IRR = 0.23, 95% CI [0.18, 0.31], p<0.001; Table 3). The effect of the PQ treatment on $_{mol}$FOB was significantly larger in the first 3 months (IRR = 0.21, 95% CI [0.15, 0.28], p<0.001) than in months 4-8 (IRR = 0.34, 95% CI [0.24, 0.48], p<0.001; Table 3).

In addition, PQ treatment was associated with a 75% reduction in the hazard of becoming positive for *P. vivax* gametocytes by *Pvs25* qRT-PCR (HR=0.25, 95% CI [0.17, 0.37], p<0.001; Table 2). The incidence rate of *P. vivax* gametocytes (defined as the number of *Pvs25* qRT-PCR positive samples during follow-up) was more strongly reduced in the first 3 months (IRR = 0.18, 95% CI [0.11,0.30]) than in the subsequent 5 months (months 4-8: IRR 0.37, 95% CI [0.24,0.57]; Table 3).

Table 2. Time to first (or only) *P. vivax*/*P. ovale* re-infection, *P. vivax* clinical malaria episode, *P. vivax* gametocyte positive sample in treatment groups during the entire 8 month follow-up period and during the first 3 months of follow-up.

	Placebo			Primaquine			Cox Model Estimate*		
	Events	PYR	Incidence Risk	Events	PYR	Incidence Risk	HR	95% CI	P-value
P. vivax infections by PCR									
0-8 months	167	63.6	2.62	63	100.6	0.63	0.18	[0.14, 0.25]	<0.001
0-3 months	152	43.4	3.50	48	54.9	0.87	0.17	[0.12, 0.24]	<0.001
P. vivax infections by LM									
0-8 months	122	83.4	1.46	40	111.7	0.36	0.16	[0.11, 0.24]	<0.001
0-3 months	104	51.3	2.03	22	58.3	0.38	0.12	[0.07, 0.19]	<0.001
P. vivax clinical malaria episode									
0-8 months	21	109.0	0.19	7	112.5	0.06	0.25	[0.11, 0.61]	0.002
0-3 months	15	61.2	0.25	4	60.2	0.07	0.19	[0.06, 0.58]	0.004
P. vivax gametocyte positivity									
0-8 months	99	93.3	1.06	35	112.9	0.31	0.25	[0.17, 0.37]	<0.001
0-3 months	70	53.9	1.30	16	58.9	0.27	0.18	[0.10, 0.30]	<0.001
P. ovale infections by PCR									
0-8 months	17	118.0	0.14	7	120.6	0.06	0.31	[0.13, 0.77]	0.011
0-3 months	10	61.7	0.16	1	60.3	0.02	0.08	[0.01, 0.67]	0.019

* *P. vivax* cox model estimates adjust for treatment, age, village and *P. vivax* infection status at enrolment. *P.ovale* cox model estimates adjust for treatment, age, village and *P.ovale* infection status at enrolment. The number of children considered to be at risk on Day 0 is 257 in the placebo arm and 247 in the primaquine arm, except for *P. vivax* infections by PCR where corresponding numbers at risk are 254 and 245 respectively since infections on Day 0 were considered treatment failures and hence excluded. HR, hazard ratio; PYR, person years at risk.

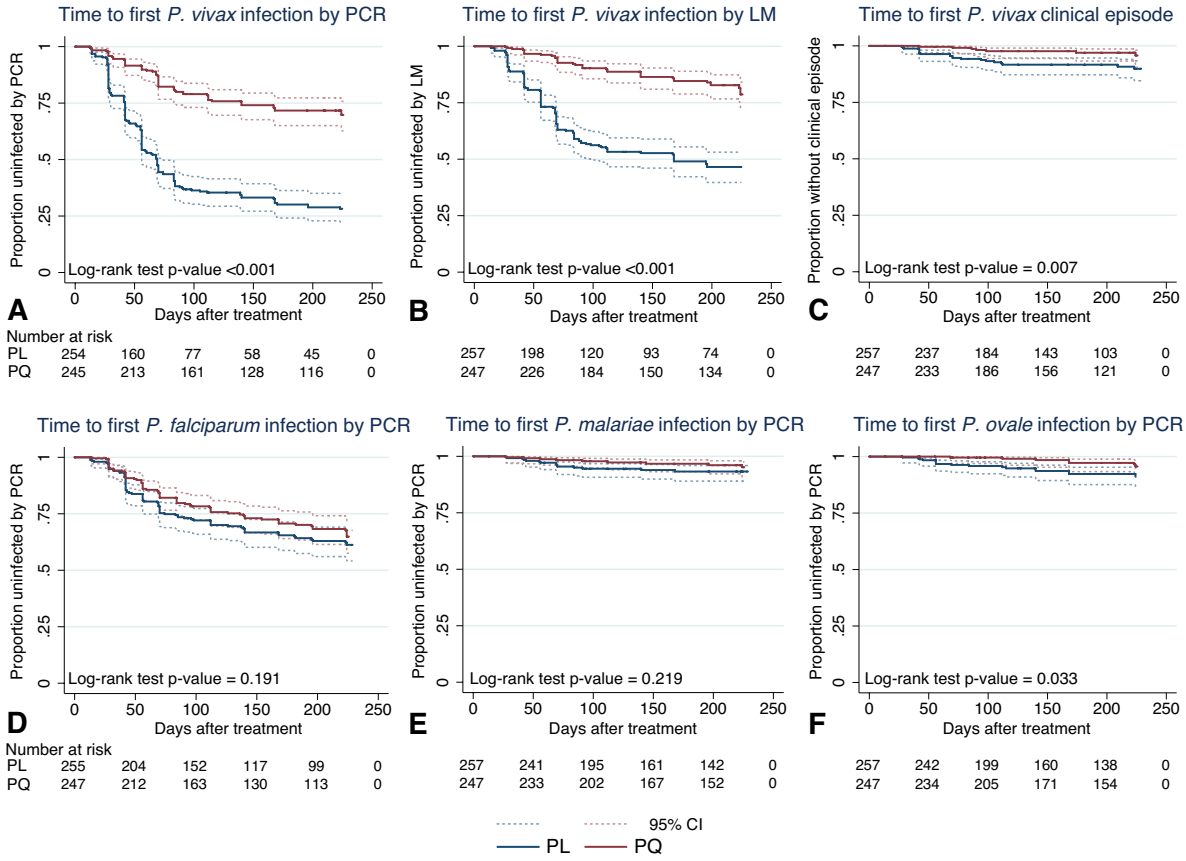

Figure 2. Kaplan-Meier plots showing the time to first (or only) **(A)** *P. vivax* infection by PCR, **(B)** *P. vivax* infection by light microscopy, **(C)** *P. vivax* clinical episode by light microscopy, **(D)** *P. falciparum* infection by PCR, **(E)** *P. malariae* infection by PCR and **(F)** *P. ovale* infection by PCR, in the two treatment arms. Dashed lines represent the respective 95% confidence intervals.

Irrespective of treatment group, clinical *P. vivax* malaria episodes were rare, with only 28 children experiencing at least 1 clinical *P. vivax* episode during the 32-week follow-up period (incidence risk: 0.19/child/year in PL and 0.06/child/year in PQ arm, Table 2). The clearance of hypnozoites by PQ treatment was associated with an 81% reduction in the hazard of experiencing a *P. vivax* clinical episode of any density in the first 3 months of follow-up (HR=0.19, 95% CI [0.06, 0.58], p=0.004; Table 2; Fig. 2C) and a 75% reduction in the entire follow-up period (HR=0.25, 95% CI [0.11, 0.61], p=0.002; Table 2).

Risk of non-*P. vivax* malaria infection during follow-up

Although the number of *P. ovale* infections diagnosed by PCR in either arm was low, PQ treatment was associated with a 92% reduction in the risk of *P. ovale* blood-stage infections diagnosed by qPCR in the first 3 months of follow-up (HR=0.08, 95% CI [0.01, 0.67], p=0.019) and a 69% reduction in the entire 8 months of follow-up (HR= 0.31, 95% CI [0.13, 0.77] p=0.011), compared to PL (Figure 2F; Table 2).

Table 3. Incidence rate of *P. vivax* clinical malaria of any density, genetically distinct *P. vivax* blood-stage clones and gametocyte positivity in treatment groups during the entire 8 month follow-up period, and separately for 0-3 and 4-8 months of follow-up.

	Placebo			Primaquine			Model Estimate*		
	Events	PYR	Incidence Rate	Events	PYR	Incidence Rate	IRR	95% CI	P-value
P. vivax clinical malaria episode – any density									
0-8 months	23	139.8	0.16	11	139.6	0.08	0.43	[0.21, 0.90]	0.026
0-3 months	15	55.9	0.30	5	54.3	0.09	0.31	[0.11, 0.86]	0.025
4-8 months	7	83.0	0.08	5	83.1	0.06	0.59	[0.17, 2.08]	0.410
Genetically distinct *P. vivax* blood-stage clones									
0-8 months	653	122.1	4.74	196	120.6	1.62	0.23	[0.18, 0.31]	<0.001
0-3 months	430	55.5	7.75	102	53.7	1.90	0.21	[0.15, 0.28]	<0.001
4-8 months	221	66.5	3.32	94	66.0	1.42	0.34	[0.24, 0.48]	<0.001
P. vivax gametocyte positivity									
0-8 months	202	122.1	1.65	63	120.6	0.52	0.27	[0.19, 0.38]	<0.001
0-3 months	101	55.5	1.82	20	53.7	0.37	0.18	[0.11, 0.30]	<0.001
4-8 months	100	66.5	1.50	42	66.0	0.64	0.37	[0.24, 0.57]	<0.001

*The time at risk is calculated independently for each subject for each time range with applicable study censoring for either active clinical or PCR detection. IRRs are derived from a negative binomial regression model adjusted for treatment, age, village and *P. vivax* positivity by PCR at enrolment. Clinical malaria episodes IRRs are derived from a negative binomial regression adjusted for treatment, age and *P. vivax* positivity by PCR at enrolment. The number of children considered at risk on Day 0 is 245 in the placebo arm and 253 in the primaquine arm. The number of children considered at risk on study day 96 is 207 in the primaquine arm and 205 in the placebo arm. IRR, incidence rate ratio; PYR, person years at risk.

Table 4. Time to first (or only) *P. falciparum/P. malariae* re-infection and *P. falciparum* clinical malaria in treatment groups in the entire follow-up period.

	Placebo			Primaquine			Cox Model Estimate*		
	Events	PYR	Incidence Risk	Events	PYR	Incidence Risk	HR	95% CI	P-value
P. falciparum infections by PCR									
0-8 months	85	96.0	0.88	72	101.0	0.71	0.77	[0.56, 1.06]	0.104
P. falciparum infections by LM									
0-8 months	52	108.8	0.48	53	107.1	0.50	0.93	[0.63, 1.37]	0.706
P. falciparum clinical malaria episode									
0-8 months	21	109.4	0.19	27	105.4	0.26	1.33	[0.75, 2.36]	0.333
P. malariae infections by PCR									
0-8 months	15	118.2	0.13	9	119.4	0.07	0.55	[0.24, 1.26]	0.157

**P. falciparum* cox model estimates adjust for treatment, age, village and *P. falciparum* infection status at enrolment. *P. malariae* cox model estimates adjust for treatment, age, village and *P. malariae* infection status at enrolment. The number of children considered to be at risk on Day 0 is 257 in the placebo arm and 247 in the primaquine arm, except for *P. falciparum* infections by PCR where corresponding numbers at risk are 255 and 247 respectively since infections on Day 0 were considered treatment failures and hence excluded. HR, hazard ratio; PYR, person years at risk.

There was no significant association between PQ treatment and time to first (or only) *P. falciparum* blood-stage infection by qPCR (p=0.104, Figure 2D; Table 4) or LM (p=0.706; Table 4), and no effect of PQ treatment on time to first (or only) *P. falciparum* clinical episode during the 8 months of follow-up (p=0.333; Table 4). Although there was no significant association between PQ treatment and time to first (or only) *P. malariae* blood-stage infection by qPCR during the entire follow-up period (HR = 0.53, 95% CI [0.23, 1.23], p = 0.139, Figure 2E; Table 4), there was a trend towards an association in the first 3 months of follow-up (HR = 0.36, 95% CI [0.13, 1.02], p=0.055.

Implications for malaria control and elimination strategies

Any MSAT intervention will only target individuals with detectable blood-stage parasitaemia. In the current cohort, 47.4% (239/504) of children had a *P. vivax* infection (single or mixed-species) at enrolment and another 12.9% (65/504) were positive with non-*P. vivax* blood-stage infections (Table 1). In the absence of PQ treatment, children with no patent infections at enrolment were significantly less rapidly re-infected with *P. vivax* (55.2% (58/105) became infected during 8 months of follow-up) than those that had patent *P. vivax* (70.5% (79/112)) and *P. falciparum/P. malariae/P. ovale* infections (81.1% (30/37), log-rank test: p < 0.001, Figure 3, Table S1). In the PQ group, children with no patent infections were also less likely to be re-infected (17.9% (17/95)) than those in the other two groups (*Pv*: 31.7% (39/123), *non-Pv*: 25.9% (7/27), log-rank test: p = 0.0412, Figure 3, Table S1), indicating that these children were more likely to live in low transmission areas. PQ treatment was therefore equally efficient in preventing recurrent *P. vivax* infections in children with *P. vivax*, non-*vivax* or no blood-stage infection at enrolment (Cox regression, adjusted for age and village of residence: LR = 3.87 df = 2, p = 0.14 for treatment-by-infection status interaction).

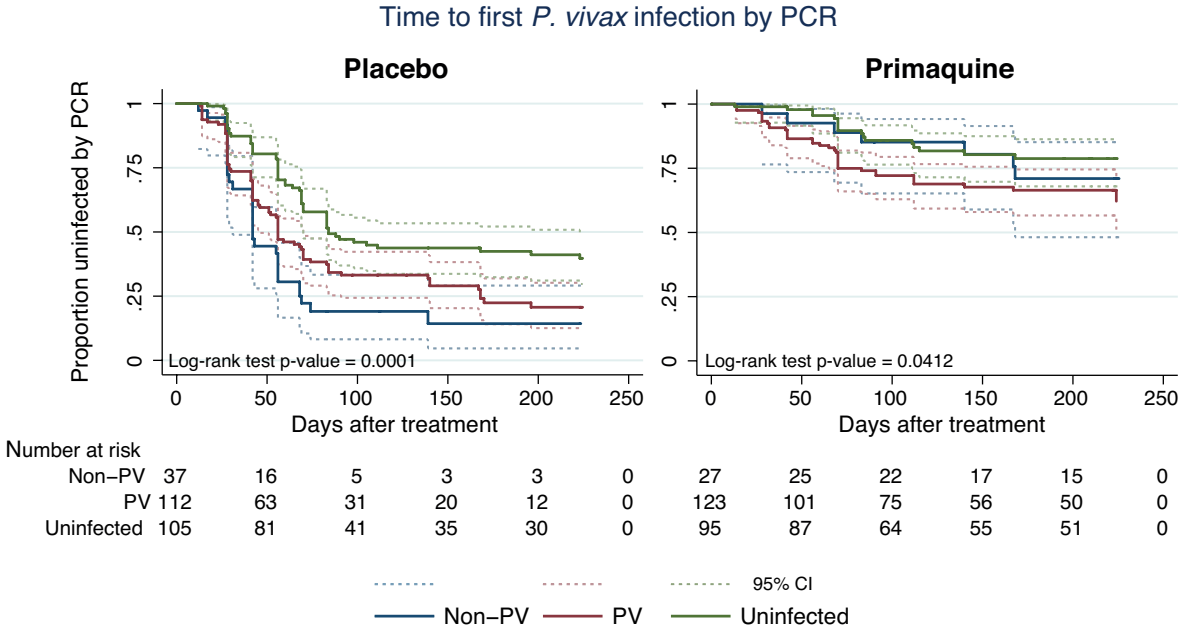

Figure 3. Kaplan-Meier plots showing the time to first (or only) *P. vivax* infection by PCR in the Placebo and Primaquine arms, stratified by *Plasmodium* infection status.

The potential effect of MDA and MSAT with either blood-stage only or blood- plus liver-stage drugs on the population prevalence of *P. vivax* and *P. falciparum* infections was further investigated using a basic stochastic transmission model. Administration of blood-stage drugs (DHA-PIP or CQ) was assumed to clear existing blood stage infections and provide a 4 week period of prophylactic protection against new infections, tafenoquine plus CQ was assumed to clear blood and liver-stage infections and provide 8 weeks of causal prophylactic protection (for full model details please refer to Supplementary Information Text 1). Figure 4 illustrates the predicted qualitative dynamics of *P. falciparum* and *P. vivax* transmission following two rounds of MDA (Panels A and B) and MSAT (Panels C and D) interventions with 80% coverage, separated by 6 months. The interventions are predicted to cause a sharp decline in prevalence, followed by a gradual return to pre-intervention levels.

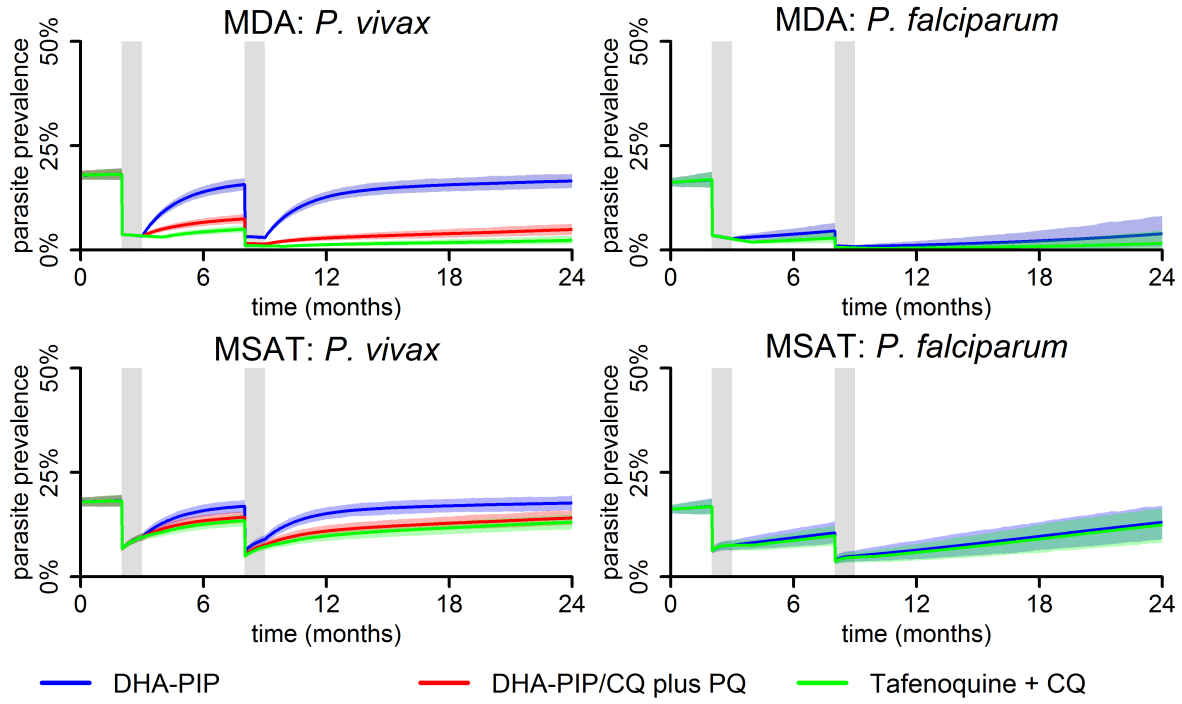

Figure 4. Comparison of two rounds of MDA (Panels A and B) and MSAT (Panels C and D) at 80% coverage 6 months apart with anti-malarial drugs on *P. vivax* (Panels A and C) and *P. falciparum* (Panels B and D) blood-stage parasite prevalence, as predicted by a stochastic model in a human population of size 5,000. The solid lines represent the mean of 1,000 repeat simulations and the shaded areas represent the envelopes containing 95% of stochastic simulations. The grey bars denote the time of each treatment round and the duration of prophylactic protection. Dihydroartemisinin-piperaquine (DHA-PIP) or chloroquine (CQ) were assumed to be administered as part of a 3 day regimen providing prophylaxis for one month. Primaquine (PQ) was assumed to be administered as part of a 14 day regimen providing prophylaxis for 15 days. Tafenoquine (TQ) was assumed to be administered via a single dose providing prophylaxis for two months.

MDA is predicted to achieve much larger prevalence reductions than MSAT, mostly due to the proportion of infections missed by the MSAT programme due to imperfect diagnostic sensitivity, but also because of the prophylactic protection in treated but uninfected individuals under the MDA programme.

The initial reductions achieved by each of the interventions against *P. falciparum* and *P. vivax* are the same, however, when only blood-stage drugs are administered, a rapid rebound in *P. vivax* prevalence is predicted due to the hypnozoite reservoir which is left unaffected by the treatment. Notably, *P. vivax* levels are predicted to return to pre-intervention levels within 6 months post intervention for both the MDA and MSAT interventions (blue curves in Panels A and C, respectively). The MDA programme is especially effective for *P. falciparum*, with prevalence predicted to remain below 20% of the pre-intervention levels for the modelled 16 months after the programme (Panel B).

Only the addition of 8-aminoquinolines to a regimen of blood-stage drugs targets the hypnozoite reservoir and prevents the rapid resurgence of *P.* vivax blood-stage infections caused by relapses. Consequently, interventions with primaquine are shown to result in a sustained reduction of the *P. vivax* burden (red curves in Panels A and C). Especially in the case of MDA (red curve, Panel A), *P. vivax* parasite prevalence is predicted to remain very low (<10%) during the modelled 16 months post intervention. Tafenoquine is estimated to be more effective than primaquine at reducing prevalence due to the higher levels of efficacy and the longer duration of causal prophylaxis [34].

Discussion

By selectively removing hypnozoites from half the children in the cohort, this study confirms that relapses from long-lasting liver-stages account for 4 out of 5 *P. vivax* infections and and 3 out of 5 *P. ovale* infections in Papua New Guinean children aged 5-10 years living in an area with hyperendemic transmission.

The risk of having at least one PCR-detectable *P. vivax* infection during 8-months of follow-up was reduced by 82% by PQ treatment. This is substantially higher than the 44% reduction observed in our earlier study [48] that used a 30% lower dose of primaquine combined with 7 days of artesunate, confirming that this earlier treatment regimen was not fully effective in preventing relapses. PQ also reduced the incidence of genetically distinct blood-stage infections ($_{mol}$FOB) [41] in the first 3 months of follow-up by a similar amount (79%), indicating that relapses accounted for ~4/5 of all *P. vivax* infections in PNG children. Although the effect of the PQ treatment decreased with time since treatment, the incidence of new infections in the PQ arm was nevertheless still reduced by more than half (66%) after 3 months of follow–up. This 'wash-out' of the PQ effect is likely due both to the fact that relapses are thought to activate rapidly in PNG [7] and the replenishment of the hypnozoite 'reservoir' through continued exposure to new infected mosquito bites. The relatively sustained effect of the PQ treatment does however indicate that even in tropical *P. vivax* strains a substantial proportion of hypnozoites remain dormant for 3 or more months.

Children that were not PQ treated were also approximately 4-times more often positive for *P. vivax* gametocytes. Since even low density *P. vivax* infections can infect mosquitoes [49–51], it is thus likely that relapsing infections are the primary source of *P. vivax* transmission.

PNG children acquire immunity to *P. vivax* rapidly [18] and, as shown in earlier studies in the same age group [20], clinical *P. vivax* episodes are rare. Nevertheless, PQ reduced the incidence of clinical *P. vivax* episodes by 69% in the first 3 months after treatment indicating that relapses can cause clinical episodes even in individuals with moderate levels of acquired immunity. Several studies have shown that relapses are often genetically distinct from the initial clinical episode [52,53]. These genetically diverse relapses may either be meiotic siblings [54] or originate from a previous (mosquito) bite and are likely to result in a higher risk of clinical illness in relapsing infection compared to that seen in malaria therapy patients infected twice with the same strain [10].

Primaquine treatment reduced the risk of PCR-detectable *P. ovale* infections by 92% in the first 3 months of follow-up and 69% in the entire follow-up period. This confirms that relapses account for a considerable portion of infections from this less prevalent species of relapsing malaria, and likely also sustain *P. ovale* transmission. This is relevant not only in PNG, but also in Sub-Saharan Africa where *P. ovale* prevalence can reach 4-10% (by LM) in areas of West and Central Africa [25]. We observed no significant association of PQ with risk of PCR-detectable infections from the non-relapsing species of *P. falciparum*. However, a trend towards a reduced risk of *P. malariae* infections in the first 3 months of follow-up was observed in the primaquine arm despite overall low numbers (p=0.055). Although *P. malariae* is not thought to form hypnozoites in the liver, chronic or relapsing infections of *P. malariae* up to 20 years after a person has left an endemic area have been documented [55,56]. Although it is currently not known how and where *P. malariae* infections can remain dormant for such extensive periods of time, our data suggest that such longer-lived *P. malariae* stages may be susceptible to PQ treatment. Larger clinical trials involving both symptomatic and asymptomatic *P. malariae* infections would be required to confirm the prevention of recurrent *P. malariae* infections by PQ treatment.

Given the very large contribution of relapses to the burden of *P. vivax* and *P. ovale* infection, illness and transmission it is essential that all *P. vivax* and *P. ovale*-infected individuals receive both an effective anti-blood-stage and anti-relapse therapy. PNG National Standard Treatment Guidelines recommend treating *P. vivax* or *P. ovale* confirmed cases with 0.25mg/kg primaquine for 14 days, however this is not being consistently implemented due to lack of access to point-of-care tests to screen for G6PD deficiency.

Interestingly, PQ was not only effective in preventing recurrent *P. vivax* infection in children that had PCR-detectable *P. vivax* infections but was equally effective in children with non-*vivax* infections and even those without any *Plasmodium spp.* infections at enrolment. All currently available malaria diagnostic tests only identify active blood-stage infections. They can thus not

identify people who have *P. vivax* hypnozoites in their livers but are free of blood-stage infection. The rapid appearance of *P. vivax* infections and significant reduction in rates of recurrent infections in PQ treated qPCR negative children indicates that there are a comparable number of PNG children without blood-stage infections who carry *P. vivax* hypnozoites as there are children with *P. vivax* infections. The presence of active *P. vivax* blood-stage infection is thus a poor predictor for the risk of *P. vivax* relapses.

The rapid recurrence of *P. vivax* infections after treatment of *P. falciparum* infections has been observed in numerous *P. falciparum* in-vivo drug efficacy trials, both in PNG [44,57] and elsewhere [58]. It has therefore been argued that anti-relapse therapy should be administered for all patients with malaria in regions of *P. vivax* co-endemicity [58]. Our results clearly support this recommendation and also extend it to asymptomatic parasite carriers.

With the renewed drive to eliminate malaria, the role of asymptomatic and/or sub-microscopic infections in sustaining malaria transmission has become a major focus [15,59,60]. An increasing number of studies show that these infections contribute significantly to both *P. falciparum* and *P. vivax* transmission at all levels of endemicity [49–51,61,62]. As first noted by Robert Koch in 1900 during studies in German New Guinea, the control of these infections is essential if elimination is to be achieved rapidly [63].

Mass screening and treatment (MSAT) and mass drug administration (MDA) with Artemisinin-based combination therapies (ACTs) are two interventions aimed at reducing the asymptomatic reservoir [32,64,65]. Although the modelling conducted in the present study indicates that an MSAT programme with a highly sensitive diagnostic test such as qPCR can effectively reduce *P. falciparum* transmission, field trials have shown that MSAT with a less sensitive diagnostic such as an RDT has limited or no effect on transmission [66–68]. As mass-screening by PCR is difficult to implement, focalised MDA may be a more practical approach [69].

Our modelling predicted that MSAT will have only limited effectiveness for *P. vivax* even if conducted with a sensitive molecular diagnostic test and including an anti-liver-stage treatment since it will not target the blood-stage negative population harbouring hypnozoites. MDA, on the other hand, is predicted to be highly effective in reducing the burden of future *P. vivax* infections but only if conducted with anti-blood- and anti-liver-stage treatment. Thus, effective control of *P. vivax* with anti-malarial drugs will require the inclusion of a treatment to attack the hypnozoite reservoir, and mass administration regardless of the presence of blood-stage infections to target the undetectable parasite reservoir.

Currently, PQ is the only licensed drug with activity on the hypnozoite stage capable of preventing relapses [70]. However due to its association with haemolysis in individuals with glucose-6-phosphate dehydrogenase (G6PD) deficiency [70,71] and its long dosing schedule (up to 14 days), this drug is not in widespread use in many endemic areas and WHO currently advises against PQ treatment without prior G6PD deficiency testing. In the absence of a reliable and

affordable point-of-care G6PD test, the routine implementation of PQ for treatment thus remains a challenge in many endemic regions. The challenges of implementing MDA with primaquine are even larger, although not insurmountable [72]. A new generation of G6PD tests are being developed [73,74] and the arrival of tafenoquine, a long acting 8-aminoquinoline that can be given as a single dose [34,74] will not only make MDA logistically simpler, our modeling also predicts that MDA with tafenoquine will be more effective that regimens using primaquine. Nevertheless, the development of alternative anti-hypnozoite treatments remains an important research priority for the elimination of *P. vivax* [16].

In conclusion, this study demonstrates that relapsing infections are the overwhelming source (i.e. ~80%) of not only *P. vivax* blood-stage infections in children, but also clinical episodes and contribute substantially to maintaining transmission. Given the very ambitious timelines set by political leaders of vivax-endemic regions and limited funding, it is essential that scarce resources available for both *P. vivax* research and elimination be optimally allocated. The development of novel anti-hypnozoite drugs and interventions that can specifically target the hypnozoite reservoir are of highest priority. However, by predicting that MSAT programs will not be effective in reducing the burden of *P. vivax* in affected populations, the models presented here also suggest that it is neither worthwhile investigating nor implementing MSAT programs in *P. vivax* endemic countries. Instead the efforts should now be directed towards the development of approaches for MDA programs targeting areas and risk groups with confirmed local transmission.

Acknowledgements

First and foremost, we wish to sincerely thank the children, their parents/guardians, school principals, teachers and communities for their willingness to be involved in this study. We gratefully acknowledge the assistance of staff at Albinama Health Centre and of the network of village-based health workers. We acknowledge the efforts of PNGIMR Maprik field, administration and laboratory staff, in particular Lawrence Rare, Margarina Raymond, Moses Lagog, Lindy Maken, Danga Mark, Heather Huaupe. We acknowledge the efforts of PNGIMR Molecular Parasitology laboratories, in particular Celine Barnadas, Jonah Iga, Lilah Tol and Elmah Nate for overseeing and conducting DNA extractions and Anna Rosanas-Urgell and Alice Ura for RNA preservation. We thank Cristian Koepfli for assistance with qPCR species typing validation and Harin Karunajeewa for advice on modeling DHA-PIP and tafenoquine treatment effects. We sincerely thank Prof. Kevin Baird for assistance in acquiring placebo tablets.

Author contributions

Conceived and designed the study: IM, LS, QB, IF, PS. Enrolled participants and conducted the study: LJR, IB, BK. Sample processing and analysis: LJR, RW, AW, JB, NH, LL, NT. Data management and analysis: CLWS, SK, MS, LS, MW, LJR, IM. Wrote the first draft of the manuscript: LJR, SK, MW, IM. Contributed to the writing of the manuscript: IF, SK, MW, RW, QB,

CLWS, NH. ICMJE criteria for authorship read and met: LJR, RW, IB, MW, SK, CLWS, BK, AW, JB, NH, LL, NT, LS, MS, QB, PS, LS, IF, IM. Agree with manuscript results and conclusions: LJR, RW, IB, MW, SK, CLWS, BK, AW, JB, NH, LL, NT, LS, MS, QB, PS, LS, IF, IM.

Funding

This work was supported by the TransEPI consortium funded by the Bill & Melinda Gates, the NHMRC (#1021544) Foundation Swiss National Science Foundation Grant [grant 310030_134889], the Cellex Foundation and International Centers of Excellence in Malaria Research [grant U19 AI089686). This work was made possible through Victorian State Government Operational Infrastructure Support and Australian Government NHMRC IRIISS. LJ Robinson is supported by an NHMRC Early Career Fellowship #1016443. MW is supported by an MRC Population Health Scientist Fellowship. SK is supported by an NHMRC Early Career Fellowship #1052760. QB has a fellowship from the program Miguel Servet of the ISCIII (Plan Nacional de I+D+I 2008-2011, grant number: CP11/00269). IM is support by an NHMRC Senior Research Fellowship (#1043345). The funders had no role in study design, data collection and analysis, decision to publish, or preparation of the manuscript.

Competing interests

IM has acted as an academic editor for PLoS Medicine. The authors have declared that no competing interests exist.

Abbreviations:

ACTs, Artemisinin-Combination therapies; AL, artemether lumefantrine; CQ, chloroquine; DHA-PIP, dihydroartemisinin-piperaquine; G6PD, glucose-6-phosphate dehydrogenase; HR, hazard ratio; IRR, incidence rate ratio; LM, light microscopy; MDA, mass drug administration; $_{mol}$FOB, molecular force of blood-stage infection; MSAT, mass screening and treatment; PL, placebo; PNG, Papua New Guinea; PQ, primaquine; qPCR, quantitative real-time polymerase chain reaction; qRT-PCR, quantitative reverse transcription PCR; RDT, rapid diagnostic test.

References

1. WHO. World Malaria Report. Geneva; 2014.
2. Cotter C, Sturrock H, Hsiang M, Liu J, Phillips A, Hwang J, et al. The changing epidemiology of malaria elimination: new strategies for new challenges. Lancet. 2013;382: 900–11.
3. PAHO. Central America and Hispaniola seek to eliminate malaria by 2025. 2013.
4. APLMA. East Asia Summit adopts unprecedented regional malaria goal. 2014.
5. Mueller I, Galinski MR, Baird JK, Carlton JM, Kochar DK, Alonso PL, et al. Key gaps in the knowledge of *Plasmodium vivax*, a neglected human malaria parasite. Lancet Infect Dis. 2009;9: 555–566.
6. Baird JK. Eliminating malaria--all of them. Lancet. 2010;376: 1883–5.
7. White NJ. Determinants of relapse periodicity in *Plasmodium vivax* malaria Determinants of relapse periodicity in *Plasmodium vivax* malaria. Malar J. 2011;10: 297.

8. Carson P, Flanagan C, Ickes C, Alving A. Enzymatic Deficiency in Primaquine-Sensitive Erythrocytes. Science. 1956;124: 484–5.
9. White NJ, Imwong M. Relapse. Adv Parasitol. 2012;80: 113–50.
10. Mckenzie FE, Jeffery GM, Collins WE. *Plasmodium vivax* blood-stage dynamics. J Parasitol. 2008;88: 521–535.
11. Barry AE, Waltmann A, Koepfli C, Barnadas C, Mueller I. Uncovering the transmission dynamics of *Plasmodium vivax* using population genetics. Pathog Glob Health. 2015;109: 142–152.
12. Liu Y, Auburn S, Cao J, Trimarsanto H, Zhou H, Gray K-A, et al. Genetic diversity and population structure of *Plasmodium vivax* in Central China. Malar J. 2014;13: 262.
13. Gray K-A, Dowd S, Bain L, Bobogare A, Wini L, Shanks GD, et al. Population genetics of *Plasmodium falciparum* and *Plasmodium vivax* and asymptomatic malaria in Temotu Province, Solomon Islands. Malar J. 2013;12: 429.
14. Gunawardena S, Ferreira M, Kapilananda G, Wirth D, Karunaweera N. The Sri Lankan paradox: high genetic diversity in *Plasmodium vivax* populations despite decreasing levels of malaria transmission. Parasitology. 2014;141: 880–90.
15. Lin JT, Saunders DL, Meshnick SR. The role of submicroscopic parasitemia in malaria transmission : what is the evidence? Trends Parasitol. 2014;30: 183–190.
16. malERA Consultative Group. A research agenda for malaria eradication: drugs. PLoS Med. 2011;8: e1000402.
17. WHO. Plasmodium vivax Control & Elimination : Development of Global Strategy and Investment Case. 2012 pp. 1–5.
18. Lin E, Kiniboro B, Gray L, Dobbie S, Robinson L, Laumaea A, et al. Differential Patterns of Infection and Disease with *P. falciparum* and *P. vivax* in Young Papua New Guinean Children. PLoS One. 2010;5: e9047.
19. Senn N, Rarau P, Stanisic DI, Robinson L, Manong D, Salib M, et al. Intermittent preventive treatment for malaria in Papua New Guinean infants exposed to *Plasmodium falciparum* and *P. vivax*: a randomized controlled trial. PLoS Med. 2012;9: e1001195.
20. Michon P, Cole-Tobian JL, Dabod E, Schoepflin S, Igu J, Susapu M, et al. The risk of malarial infections and disease in Papua New Guinean children. Am J Trop Med Hyg. 2007;76: 997–1008.
21. Kasehagen LJ, Mueller I, McNamara DT, Bockarie MJ, Kiniboro B, Rare L, et al. Changing patterns of *Plasmodium* blood-stage infections in the Wosera region of Papua New Guinea monitored by light microscopy and high throughput PCR diagnosis. Am J Trop Med Hyg. 2006;75: 588–596.
22. Mueller I, Widmer S, Michel D, Maraga S, McNamara DT, Kiniboro B, et al. High sensitivity detection of *Plasmodium* species reveals positive correlations between infections of different species, shifts in age distribution and reduced local variation in Papua New Guinea. Malar J. 2009;8: 41.
23. Arnott A, Barnadas C, Senn N, Siba P, Mueller I, Reeder JC, et al. High genetic diversity of *Plasmodium vivax* on the north coast of Papua New Guinea. Am J Trop Med Hyg. 2013;89: 188–194.
24. Schultz L, Wapling J, Mueller I, Ntsuke PO, Senn N, Nale J, et al. Multilocus haplotypes reveal variable levels of diversity and population structure of *Plasmodium falciparum* in Papua New Guinea, a region of intense perennial transmission. Malar J. 2010;9: 336.
25. Mueller I, Zimmerman PA, Reeder JC. Plasmodium malariae and Plasmodium ovale--the "bashful" malaria parasites. Trends Parasitol. 2007;23: 278–283.
26. Mueller I, Schoepflin S, Smith TA, Benton KL, Bretscher MT, Lin E, et al. Force of infection is key to understanding the epidemiology of *Plasmodium falciparum* malaria in Papua New Guinean children. Proc Natl Acad Sci U S A. 2012;109: 10030–10035.
27. Betuela I, Rosanas-Urgell A, Kiniboro B, Stanisic DI, Samol L, de Lazzari E, et al. Relapses contribute significantly to the risk of *Plasmodium vivax* infection and disease in Papua New Guinean children 1-5 years of age. J Infect Dis. 2012;206: 1771–1780.
28. Hetzel M, Pulford J, Gouda H, Hodge A, Siba P, Mueller I. The Papua New Guinea National Malaria Control Program: Primary Outcome and Impact Indicators, 2009-2014. 2014.
29. Mckenzie FE, Magill AJ, Forney JR, Lucas C, Erhart LM, Meara WPO, et al. Gametocytemia in *Plasmodium vivax* and *Plasmodium falciparum* infections. J Parasitol. 2006;92: 1281–1285.
30. Douglas NM, Simpson J a, Phyo AP, Siswantoro H, Hasugian AR, Kenangalem E, et al. Gametocyte dynamics and the role of drugs in reducing the transmission potential of *Plasmodium vivax*. J Infect Dis. 2013;208: 801–12.
31. Barbosa S, Gozze AB, Lima NF, Batista CL, Bastos MDS, Nicolete VC, et al. Epidemiology of

Disappearing *Plasmodium vivax* Malaria: A Case Study in Rural Amazonia. PLoS Negl Trop Dis. 2014;8: e3109.

32. Okell LC, Griffin JT, Kleinschmidt I, Hollingsworth TD, Churcher TS, White MJ, et al. The potential contribution of mass treatment to the control of *Plasmodium falciparum* malaria. PLoS One. 2011;6: e20179.
33. Grueninger H, Hamed K. Transitioning from malaria control to elimination: the vital role of ACTs. Trends Parasitol. 2013;29: 60–4.
34. Llanos-Cuentas A, Lacerda M V, Rueangweerayut R, Krudsood S, Gupta SK, Kochar SK, et al. Tafenoquine plus chloroquine for the treatment and relapse prevention of *Plasmodium vivax* malaria (DETECTIVE): a multicentre, double-blind, randomised, phase 2b dose-selection study. Lancet. 2014;383: 1049–58.
35. Hanboonkunupakarn B, Ashley EA, Jittamala P, Tarning J, Pukrittayakamee S, Hanpithakpong W, et al. Open-Label Crossover Study of Primaquine and Dihydroartemisinin- Piperaquine Pharmacokinetics in Healthy Adult Thai Subjects. Antimicrob Agents Chemother. 2014;58: 7340–7346.
36. Genton B, D'Acremont VV, Rare L, Baea K, Reeder JC, Alpers MP, et al. *Plasmodium vivax* and Mixed Infections Are Associated with Severe Malaria in Children : A Prospective Cohort Study from Papua New Guinea. PLoS Med. 2008;5: e127.
37. Betuela I, Bassat Q, Kiniboro B, Robinson LJ, Rosanas-Urgell A, Stanisic D, et al. Tolerability and safety of primaquine in Papua New Guinean children 1 to 10 years of age. Antimicrob Agents Chemother. 2012;56: 2146–2149.
38. Wampfler R, Mwingira F, Javati S, Robinson L, Betuela I, Siba P, et al. Strategies for detection of *Plasmodium* species gametocytes. PLoS One. 2013;8: e76316.
39. Rosanas-Urgell A, Mueller D, Betuela I, Barnadas C, Iga J, Zimmerman PA, et al. Comparison of diagnostic methods for the detection and quantification of the four sympatric *Plasmodium* species in field samples from Papua New Guinea. Malar J. 2010;9: 361.
40. Koepfli C, Schoepflin S, Bretscher M, Lin E, Kiniboro B, Zimmerman P a, et al. How much remains undetected? Probability of molecular detection of human *Plasmodia* in the field. PLoS One. 2011;6: e19010.
41. Koepfli C, Colborn KL, Kiniboro B, Lin E, Speed TP, Siba PM, et al. A high force of *Plasmodium vivax* blood-stage infection drives the rapid acquisition of immunity in Papua New Guinean children. PLoS Negl Trop Dis. 2013;7: e2403.
42. R Development Core Team. R: A language and environment for statistical computing. R Found Statistical Computing, Vienna, Austria. 2014; ISBN 3-900051-07-0, URL http://www.R-project.org
43. StataCorp. Stata: Release 12. Stat Software Coll Station TX StataCorp LP. 2011.
44. Karunajeewa HA, Mueller I, Senn M, Lin E, Law I, Gomorrai PS, et al. A trial of combination antimalarial therapies in children from Papua New Guinea. N Engl J Med. 2008;359: 2545–2557.
45. Smith D, McKenzie F. Statics and dynamics of malaria infection in *Anopheles* mosquitoes. Malar J. 2004;3-13.
46. Smith DL, Battle KE, Hay SI, Barker CM, Scott TW, McKenzie FE. Ross, Macdonald, and a Theory for the Dynamics and Control of Mosquito-Transmitted Pathogens. PLoS Pathog. 2012;8: e1002588.
47. White MT, Karl S, Battle KE, Hay SI. Modelling the contribution of the hypnozoite reservoir to *Plasmodium vivax* transmission. Elife. 2014;3: 1–19.
48. Betuela I, Rosanas-Urgell A, Kiniboro B, Stanisic DI, Samol L, de Lazzari E, et al. Relapses contribute significantly to the risk of *Plasmodium vivax* infection and disease in Papua New Guinean children 1-5 years of age. J Infect Dis. 2012;206: 1771–80.
49. Coleman R, Kumpitak C, Ponlawat A, Maneechai N, Phunkitchar V, Rachapaew N, et al. Infectivity of asymptomatic *Plasmodium*-infected human populations to Anopheles dirus mosquitoes in western Thailand. J Med Entomol. 2004;41: 201–8.
50. Sattabongkot J, Maneechai N, Rosenberg R. *Plasmodium vivax*: gametocyte infectivity of naturally infected Thai adults. Parasitology. 1991;102: 27–31.
51. Bharti AR, Chuquiyauri R, Brouwer KC, Stancil J, Lin J, Llanos-cuentas A, et al. Experimental infection of the neotropical malaria vector Anopheles darlingi by human patient-derived *Plasmodium vivax* in the Peruvian Amazon. Am J Trop Med Hyg. 2007;75: 610–616.
52. Imwong M, Boel ME, Pagornrat W, Pimanpanarak M, McGready R, Day NPJ, et al. The first *Plasmodium vivax* relapses of life are usually genetically homologous. J Infect Dis. 2012;205: 680–3.

53. Chen N, Auliff A, Rieckmann K, Gatton M, Cheng Q. Relapses of *Plasmodium vivax* infection result from clonal hypnozoites activated at predetermined intervals. J Infect Dis. 2007;195: 934–41.
54. Bright AT, Manary MJ, Tewhey R, Arango EM, Wang T, Schork NJ, et al. A high resolution case study of a patient with recurrent *Plasmodium vivax* infections shows that relapses were caused by meiotic siblings. PLoS Negl Trop Dis. 2014;8: e2882.
55. White NJ. Malaria. In: Cook, G.C. and Zumla AI, editor. Manson's Tropical Diseases. 21st Editi. W.B. Saunders; 2003. pp. 1205–1296.
56. Siala E, Khalfaoui M, Bouratbine A, Hamdi S, Hili K, Aoun K. Relapse of *Plasmodium malariae* malaria 20 years after living in an endemic area. Press Med. 2005;34: 371–2.
57. Laman M, Moore BR, Benjamin JM, Yadi G, Bona C, Warrel J, et al. Artemisinin-Naphthoquine versus Artemether-Lumefantrine for Uncomplicated Malaria in Papua New Guinean Children : An Open-Label Randomized Trial. PLoS Med. 2014;11.
58. Douglas NM, Nosten F, Ashley E a, Phaiphun L, van Vugt M, Singhasivanon P, et al. *Plasmodium vivax* recurrence following falciparum and mixed species malaria: risk factors and effect of antimalarial kinetics. Clin Infect Dis. 2011;52: 612–20.
59. Karl S, Laman M, Koleala T, Ibam C, Kasian B, Drewei NN, et al. Comparison of three methods for detection of gametocytes in Melanesian children treated for uncomplicated malaria. Malar J. 2014;13: 1–8.
60. Okell LC, Bousema T, Griffin JT, Ouédraogo AL, Ghani AC, Drakeley CJ. Factors determining the occurrence of submicroscopic malaria infections and their relevance for control. Nat Commun. 2012;3: 1237.
61. Schneider P, Bousema J, Gouagna L, Otieno S, van de Vegte-Bolmer M, Omar S, et al. Submicroscopic *Plasmodium falciparum* gametocyte densities frequently result in mosquito infection. Am J Trop Med Hyg. 2007;76: 470–474.
62. Ouédraogo AL, Bousema T, Schneider P, de Vlas SJ, Ilboudo-Sanogo E, Cuzin-Ouattara N, et al. Substantial contribution of submicroscopical *Plasmodium falciparum* gametocyte carriage to the infectious reservoir in an area of seasonal transmission. PLoS One. 2009;4: e8410.
63. Koch R. Professor Koch's Investigations on Malaria. Br Med J. 1900; 1597–1598.
64. Griffin JT, Hollingsworth TD, Okell LC, Churcher TS, White M, Hinsley W, et al. Reducing *Plasmodium falciparum* malaria transmission in Africa: a model-based evaluation of intervention strategies. PLoS Med. 2010;7.
65. Crowell V, Briët OJT, Hardy D, Chitnis N, Maire N, Di Pasquale A, et al. Modelling the cost-effectiveness of mass screening and treatment for reducing *Plasmodium falciparum* malaria burden. Malar J. 2013;12: 4.
66. Tiono AB, Ouédraogo A, Ogutu B, Diarra A, Coulibaly S, Gansané A, et al. A controlled, parallel, cluster-randomized trial of community-wide screening and treatment of asymptomatic carriers of *Plasmodium falciparum* in Burkina Faso. Malar J. 2013;12: 79.
67. Tiono AB, Ouédraogo A, Diarra A, Coulibaly S, Soulama I, Konaté AT, et al. Lessons learned from the use of HRP-2 based rapid diagnostic test in community-wide screening and treatment of asymptomatic carriers of *Plasmodium falciparum* in Burkina Faso. Malar J. 2014;13: 30.
68. Halliday KE, Okello G, Turner EL, Njagi K, Mcharo C, Kengo J, et al. Impact of intermittent screening and treatment for malaria among school children in Kenya: a cluster randomised trial. PLoS Med. 2014;11: e1001594.
69. Mosha JF, Sturrock HJW, Greenhouse B, Greenwood B, Sutherland CJ, Gadalla N, et al. Epidemiology of subpatent *Plasmodium falciparum* infection: implications for detection of hotspots with imperfect diagnostics. Malar J. Malaria Journal; 2013;12: 221.
70. Baird JK, Hoffman SL. Primaquine therapy for malaria. Clin Infect Dis. 2004;39: 1336–45.
71. Beutler E. G6PD deficiency. Blood. 1994;84: 3613–36.
72. Kondrashin A, Baranova AM, Ashley E a, Recht J, White NJ, Sergiev VP. Mass primaquine treatment to eliminate vivax malaria: lessons from the past. Malar J. Malaria Journal; 2014;13: 51.
73. Von Seidlein L, Auburn S, Espino F, Shanks D, Cheng Q, McCarthy J, et al. Review of key knowledge gaps in glucose-6-phosphate dehydrogenase deficiency detection with regard to the safe clinical deployment of 8-aminoquinoline treatment regimens: a workshop report. Malar J. 2013;12: 112.
74. Kim S, Nguon C, Guillard B, Duong S, Chy S, Sum S, et al. Performance of the CareStart™ G6PD deficiency screening test, a point-of-care diagnostic for primaquine therapy screening. PLoS One. 2011;6: e28357.

Supplementary Figures S1 and S2

Figure S1. Drug administration schedule. The drug regimen for the primaquine (PQ) and placebo (PL) treatment arms was administered with direct observation on 20 days (Monday to Friday) over a 4 week (26 day) period.

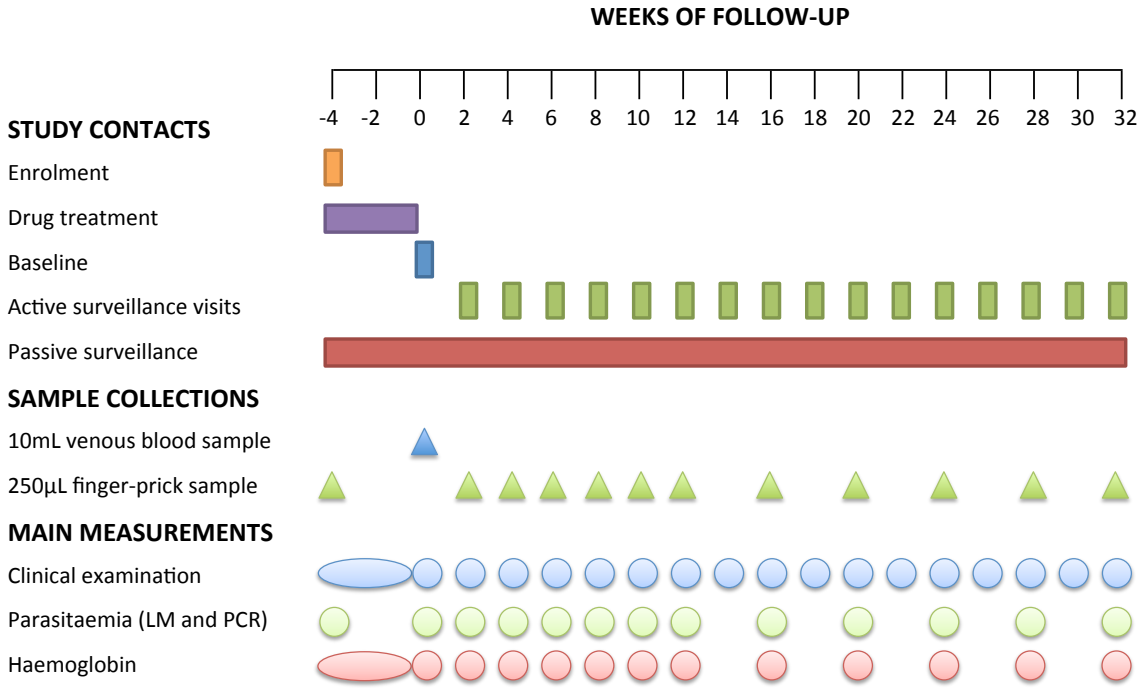

Figure S2. Study design and follow-up schedule.

Supplementary Information Text 1

Detailed description of *P. vivax* transmission model

Malaria control strategies based on the treatment of at-risk populations will not only protect treated individuals, but also the wider community due to the population-level reduction in malaria transmission. Accounting for this community-level protection requires an understanding of malaria transmission dynamics. The dynamics of *P. falciparum* transmission have been well-described using classical Ross-MacDonald compartmental deterministic models [1, 2]. Here, this approach is extended to incorporate relapse infections characteristic of *P. vivax*.

Figure S3 shows a schematic representation of a compartmental model of *P. vivax* transmission and the associated system of differential equations. Humans can be in one of four states: S_0, fully susceptible; I_0, infected with blood-stage parasites; I_L, infected with blood-stage and liver-stage parasites; and S_L, infected with liver-stage parasites. Mosquitoes can be in one of two states: S_M, not infectious (i.e. sporozoite negative); and I_M, infectious (i.e. sporozoite positive). Full definitions of all parameters are given in Table S1. Individuals will be exposed to new infectious bites at a rate $\lambda=mabI_M$ which will cause new blood-stage infections (if not already infected) and new liver-stage infections (if not already carrying hypnozoites). Individuals carrying hypnozoites can relapse at rate f and naturally clear the hypnozoite reservoir at rate γ (e.g. due to the death of hepatocytes).

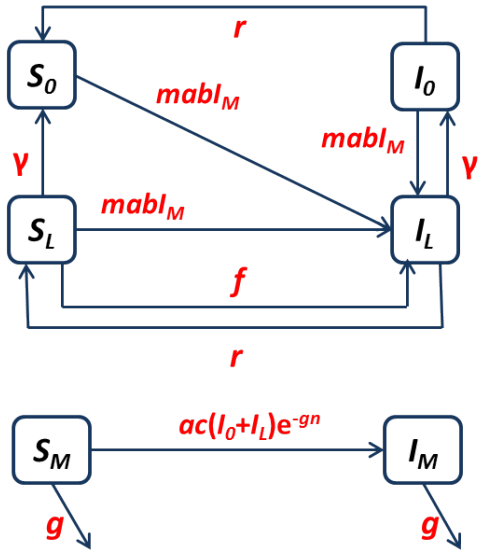

$$\frac{dS_0}{dt} = -mabI_M S_0 + rI_0 + \gamma S_L$$

$$\frac{dI_0}{dt} = -mabI_M I_0 - rI_0 + \gamma I_L$$

$$\frac{dI_L}{dt} = mabI_M \left(S_0 + S_L + I_0\right) + fS_L - \gamma I_L - rI_L$$

$$\frac{dS_L}{dt} = -mabI_M S_L - fS_L + rI_L - \gamma S_L$$

$$\frac{dS_M}{dt} = g - ac\left(I_0 + I_L\right)\left(e^{-gn} - I_M\right) - gS_M$$

$$\frac{dI_M}{dt} = ac\left(I_0 + I_L\right)\left(e^{-gn} - I_M\right) - gI_M$$

Figure S3. Schematic representation of the *P. vivax* transmission model and the associated system of differential equations. S_0 denotes fully susceptible humans, I_0 denotes blood-stage infection, S_L denotes liver-stage infection with hypnozoites, and I_L denotes blood-stage infection and liver-stage infection with hypnozoites.

Although the model described in Figure S3 captures the key drivers of the dynamics of *P. vivax* transmission, it is a simplified representation subject to a number of limiting assumptions. Most notably, there is no heterogeneity or seasonality in transmission, no super-infection, no age

structure and no acquisition of natural immunity. Incorporation of these factors would change the quantitative predictions of the model, but not its qualitative behaviour. The model can be simplified by removing the compartments for infection with liver-stage hypnozoites (S_L and I_L) and hence capture the dynamics of *P. falciparum* transmission [2]. In addition *P. vivax* or *P. falciparum* gametocytes are not explicitly accounted for. It is assumed that individuals infected with either asexual *P. vivax* or *P. falciparum* parasites are capable of transmitting to mosquitoes. Furthermore, we do not account for the effects of primaquine on clearance of gametocytes

Interventions

A potential strategy for malaria control is to administer combinations of anti-malarial drugs to entire populations. Schizonticidal drugs such as chloroquine (CQ), artemether-lumefantrine or dihydroartemisinin-piperaquine (DHA-PIP) can be used to clear *P. falciparum* or *P. vivax* blood-stage infections. *P. vivax* liver-stage infection with hypnozoites can only be cleared with an 8-aminoquinolines such as primaquine or tafenoquine (TQ). In addition to clearing parasites, drugs can provide a period of prophylactic protection where new infections are prevented. Primaquine and tafenoquine cannot be given to G6PD-deficient people[3]. Both are pro-drugs that need to be metabolised by the cytochrome P450 (CYP) 2D6 enzyme to be effective [4, 5]and people with low 2D6 activity will fail primaquine treatment. In PNG ~5% of people expected to be moderately to highly deficient (<40% activity [6]) and <5% low CYP 2D6 metabolisers [7].

Two delivery strategies are considered:

- **Mass drug administration (MDA):** individuals in a population are treated regardless of infection status. The proportion of individuals treated is referred to as the coverage.
- **Mass screen and treat (MSAT):** individuals in a population are tested for the presence of blood-stage parasites with an appropriate diagnostic and treated only if they test positive. The proportion of individuals tested is referred to as the coverage.

For both of these strategies we assume two treatment rounds (each covering 80% of the population) spaced 6 months apart. Importantly, we assume no correlation of coverage between treatment rounds, i.e. the probability of being treated in round 2 is independent of treatment status in round 1. Figure S4 shows the prevalence of blood-stage *P. vivax* and *P. falciparum* parasites following two rounds of either MDA or MSAT predicted by the deterministic transmission model.

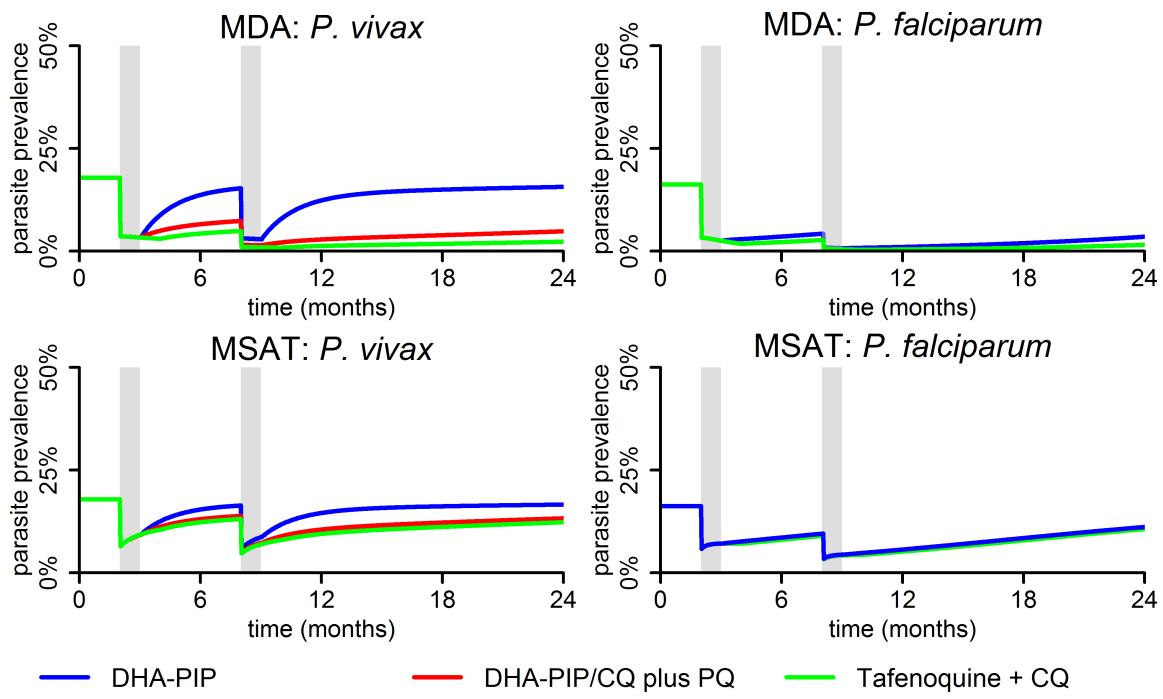

Figure S4. Comparison of two rounds of MDA and MSAT with anti-malarial drugs on P. vivax and P. falciparum blood-stage parasite prevalence, as predicted by the deterministic model. The grey bars denote the time of each treatment round and the duration of prophylactic protection. Dihydroartemisinin-piperaquine (DHA-PIP) or chloroquine (CQ) were assumed to be administered as part of a 3 day regimen providing prophylaxis for one month. Primaquine (PQ) was assumed to be administered as part of a 14 day regimen providing prophylaxis for 15 days. Tafenoquine (TQ) was assumed to be administered via a single dose providing prophylaxis for two months.

Table S2. Description of parameters for malaria transmission model. [a]Estimated numbers of mosquitoes per human predicted to give an equilibrium parasite prevalence of 20% in the deterministic (stochastic) model. [b]Prophylactic prevention of new blood-stage infections. [c]Prophylactic prevention of new blood-stage and liver-stage infections.

parameter	description	value	reference
Mosquitoes			
a	mosquito biting frequency ($a = Q/\delta$)	0.21 day^{-1}	calculated
Q	human blood index (*An. farauti*)	0.64	[8]
δ	length of gonotrophic cycle	3 days	[9]
n	duration of sporogony in mosquito	12 days	[10]
g	mosquito death rate ⇔ 1/mosquito life expectancy	0.1 day^{-1}	[10]
c	transmission probability: human to mosquito (*An. darlingi)*	0.23	[11]
m	number of mosquitoes per human (*P. vivax*)	0.56 (0.511)[a]	calculated
m	number of mosquitoes per human (*P. falciparum)*	1.45 (1.362) [a]	calculated
Humans			
b	transmission probability: mosquito to human	0.5	[12]
r	rate of clearance of blood-stage infections	1/60 day^{-1}	[13]
f	relapse frequency (~ time to first relapse)	1/125 day^{-1}	
h	expected number of relapses	4	
γ	rate of hypnozoite clearance ($\gamma = f/h$)	1/500 day^{-1}	
Treatment			
	coverage (5% pregnant women, 15% missed or refused)	80%	
	diagnostic sensitivity (molecular PCR)	80%	
	diagnostic specificity	95%	
	duration of prophylactic protection (DHA-PIP/chloroquine)[b]	30 days	[14]
	duration of causal prophylactic protection (14 day PQ regimen)[c]	15 days	
	duration of prophylactic protection (tafenoquine)[c]	60 days	[15]
	primaquine effectiveness (5% G6PD deficient, 20% failure including 5% CYP 2D6 low metaboliser)	75%	[15]
	tafenoquine effectiveness (5% G6PD deficient, 5% failure including CYP 2D6 low metaboliser)	90%	[15]

Stochastic implementation

The model described by the equations in Figure S3 can be implemented in a stochastic framework to capture the natural variation that may occur in finite populations due to the chance nature of infectious events., and the possibility of elimination.At time *t* the number of humans and mosquitoes in each compartment is $\left\{S_0^t, I_0^t, I_L^t, S_L^t, S_M^t, I_M^t\right\}$. During time step Δ*t* stochastic transitions of individuals between compartments will result in an updated state of the system at time *t* + Δ*t*: $\left\{S_0^{t+\Delta t}, I_0^{t+\Delta t}, I_L^{t+\Delta t}, S_L^{t+\Delta t}, S_M^{t+\Delta t}, I_M^{t+\Delta t}\right\}$.

Consider individuals moving in and out of the I_0 compartment. Individuals recover from I_0 to S_0 at rate r, and move from I_0 to I_L through infection at rate λ. The total number of individuals leaving compartment I_0 at time t will be given by a Binomial distribution $I_0^- = B\left(I_0^t, (\lambda + \mathrm{r})\Delta t\right)$. The I_0^- individuals moving out of I_0 will move to S_0 or I_L according to competing hazards determined by a Binomial distribution as follows: $\left\{I_0 \to S_0, I_0 \to I_L\right\} = B\left(I_0^-, \left\{\frac{r}{\lambda+r}, \frac{\lambda}{\lambda+r}\right\}\right)$. The number of individuals in compartment I_0 at time t + Δt is then given by $I_0^{t+\Delta t} = I_0^t - I_0^- + \left(I_L \to I_0\right)$. The stochastic transitions between other compartments are similarly defined.

References

Chapter 5: Infection Dynamics of *Plasmodium vivax*

Full title:

Effect of Radical Cure on Dynamics of *Plasmodium vivax* Infections

Rahel Wampfler[1,2], Natalie Hofmann[1,2], Andreea Waltmann[3,4], Mariabeth Silkey[1,2], Leanne J. Robinson[3,4,5], Ivo Mueller[3,4,6], Thomas A. Smith[1,2], Ingrid Felger[1,2]

[1]Molecular Diagnostics Unit, Swiss Tropical & Public Health Institute, Basel, Switzerland
[2]University of Basel, Basel, Switzerland
[3]Divison of Population Health and Immunity, The Walter and Eliza Hall Institute of Medical Research, Parkville, Australia
[4]Department of Medical Biology, University of Melbourne, Victoria, Australia
[5]Vector Borne Diseases Unit, PNG Institute of Medical Research, Madang & Maprik, Papua New Guinea
[6]ISGlobal, Barcelona Ctr. Int. Health Res. (CRESIB), Hospital Clínic - Universitat de Barcelona, Barcelona, Spain

– This manuscript will be submitted after further revisions –

Abstract

Background

Primaquine treatment for radical cure of *Plasmodium vivax* is a key intervention for preventing relapses and reducing transmission. Primaquine treated children were compared with placebo recipients to analyze the infection dynamics and duration of natural *P. vivax* infections and determine the contribution of relapses to parasite clones circulating in the blood.

Methods

A cohort of 504 children aged 5-10 years from Papua New Guinea was randomized into two arms. Treatment at baseline was either blood-stage anti-malarials alone or an additional course of Primaquine. Over 8 months, *P. vivax* positive blood samples were genotyped for marker *msp1*F3. The duration of individual infecting clones and the number of new clones per person and year-at-risk (force of blood-stage infection, $_{mol}$FOB) were compared between treatment arms.

Results

The estimated duration of infection was similar in both arms of the trial (PQ: 60 [95% credible interval: 25, 891] days, placebo: 45 [28, 111] days, p=0.3). Durations increased by age (p= 0.008) with a range of 26 [18, 52] days in the youngest age group to 154 [44, 3458] in the oldest children. Over the 8 months follow up, $_{mol}$FOB was 3.5 [95% CI: 2.7, 4.3] in the PQ-arm compared to 9.9 [8.8, 11.3] in the placebo arm (p<0.001). The mean number of relapses per new infection (estimated from the difference of $_{mol}$FOB between treatment arms over $_{mol}$FOB in PQ arm) was highest in the first 3 months after PQ treatment (2.4 [1.3, 4.0]) and lower thereafter (1.4 [0.6, 2.8]). Children were recruited from five villages differing in transmission intensity. At all of these sites the mean number of relapses per new infection was similar, thus, the higher the prevalence is in a village, the larger the hypnozoite reservoir in that community.

Conclusion

Good agreement in the PQ and Placebo arms for the duration of *P. vivax* infections, parasite densities and detectability suggested that the immune pressure is similar for relapses and new infections in semi-immune children. The relative contribution of relapses and primary infections to force of infection was independent of transmission intensity and age. A lower level of individual exposure of an individual will translate proportionally into a decreased relapse burden.

Introduction

Dormant liver stages, called hypnozoites, contribute significantly to transmission of *Plasmodium vivax* malaria in endemic regions of Southeast Asia and South America (White, 2011; Betuela et al., 2012). Hypnozoites can relapse weeks to months after the initial infection depending on the geographical area (Battle et al., 2014). In Papua New Guinea (PNG), relapses generally appear within 3-5 weeks after antimalarial treatment of the initial infection (Craige and Alving, 1947; Townell et al., 2012). Nevertheless, in some instances long dormancy periods of over one year have been observed with the fast relapsing Papua New Guinean Chesson strain (Jeffery, 1956).

Primaquine (PQ) is the only registered drug to reduce relapse rates by clearing latent hypnozoites. The efficacy of PQ in preventing relapses is depending on the total dose of drug received (Bunnag et al., 1994; Duarte et al., 2001; Galappaththy et al., 2007; Leslie et al., 2008). PQ is given at 0.5 mg/kg daily for 14 days to achieve presumptive radical cure (Hill et al., 2006; Krudsood et al., 2008).

The contribution of *P. vivax* relapses to the infectious reservoir of *P. vivax* in highly endemic areas is difficult to define. In these settings, super-infections are common and the contribution of re-infections, relapses, and persistent blood-stage infections are unclear (Karunajeewa et al., 2008). Prevention of relapses in a subset of children in a longitudinal cohort and subsequent comparison between treatment arms has been proven to be a valuable study design to measure the contribution of relapses to the burden of *P. vivax* malaria (Betuela et al., 2012; Robinson et al., – in preparation). In a previous study conducted in 1-5 years old children from PNG, treatment with Artesunate-Primaquine reduced the risk of *P. vivax* infections by 44% compared to an Artesunate only treatment (Betuela et al., 2012).

Genotyping in cohort studies provide the opportunity to measure the individual exposure by calculating the number of concurrently infecting genotypes (multiplicity of infection, MOI) and the number of newly acquired genotypes per person and time-at-risk (molecular force of infection, $_{mol}$FOI, Box 1) (Smith et al., 1999; Koepfli et al., 2013; Mueller et al., 2012; Robinson et al., – in preparation). Tracking individual genotypes in consecutive blood samples of the same individual permits to estimate the persistence of each parasite clone in a host (Bretscher et al., 2011; Bruce et al., 2000; Smith et al., 1999). The clearance rate can be estimated from the probability at which a genotype persists in consecutive samples.

Parasite densities fluctuate during the course of an infection. This results in imperfect detection of parasite clones in some of the blood samples of a host (Koepfli et al., 2011b; Smith et al., 1999). Both, persistence and clearance rates are thus subject to biases arising from the failure to detect all the genotypes present in the host at any time (Bruce et al., 2000; Smith et al., 1999).

P. vivax poses an additional challenge because genotyping cannot distinguish relapses from new infections (Bright et al., 2014; Bruce et al., 2000). Estimates of force of infection for *P. vivax* therefore comprise two sources of blood-stage infections: newly acquired infections (analogous to *P. falciparum*) and relapses from dormant liver stages. In consideration of relapses, the term molecular force of blood-stage infections ($_{mol}$FOB, Box 1) was introduced for *P. vivax* and corresponds to $_{mol}$FOI for *P. falciparum* (Koepfli et al., 2013).

The present study estimates $_{mol}$FOB and duration of infection for *P. vivax* from repeated blood sampling in a setting with frequent super-infection, using a method that allows for the effects of imperfect detection. This approach makes use of a mathematical model previously designed for calculating clone detectability (probability of detection of a clone in a given sample) and durations of *P. falciparum* infections (Smith et al., 1999). Samples genotyped derived from a recently described randomized treatment to re-infection study in children aged 5-10 years old from PNG (Robinson et al., – in preparation). Children received either antimalarial treatment consisting of PQ-Chloroquine (CQ)- Artemether-Lumefantrine (AL) or of CQ-AL only at baseline. At regular visits blood samples were collected from each participant during 8 months (Robinson et al., – in preparation).

The aim of this study was to assess the infection dynamics of new *P. vivax* infections and relapses by comparing two trial arms that differ by administration of either PQ or Placebo at baseline. The following parameters were estimated: multiplicity of infection, parasite density, duration of naturally clearing infections, detectability of blood-stage clones and the fraction of blood stage infections that can be attributed to relapses.

BOX 1 – DEFINITIONS

New infection	New infections are caused by sporozoite inoculation by a mosquito bite.
Relapse	Reactivated latent hypnozoite causing infection.
MOI	Multiplicity of infection is the number of genotypes concurrently present in a blood sample.
$_{mol}$FOI	Molecular force of infection denotes the number of newly acquired genotypes per person and year-at-risk. It is commonly used for estimation individual exposure in *P. falciparum* endemic settings (Mueller et al., 2012; Smith et al., 1999).
$_{mol}$FOB	Molecular force of blood-stage infections per person and year-at-risk. Blood-stage infections of *P. vivax* derive from two sources: (i) from new infections emerging from the liver several days after an infectious mosquito bite (equivalent to $_{mol}$FOI for *P. falciparum*) and (ii) from relapses emerging from dormant liver stages weeks or months after the infectious bite. To emphasize these two sources of *P. vivax* clones circulating in the blood, the term $_{mol}$FOB was introduced for *P. vivax* and is used instead of $_{mol}$FOI (Koepfli et al., 2013).
PQ-cleared fraction of $_{mol}$FOB	Primaquine-cleared fraction of the force of blood stage infection denotes the number of infections deriving from hypnozoites. In the Primaquine arm this fraction of clones was cleared at baseline. This fraction can serve as an approximation of the contribution of relapses to $_{mol}$FOB (Figure 1).
Mean number of relapses per new infection	The mean number of relapses expected per each new infection observed. In the context of this study, we estimated this number by taking the ratio of the PQ-cleared fraction of $_{mol}$FOB over $_{mol}$FOB of PQ arm.
Detectability	The probability of detection of a clone in a given sample. Imperfect detection of some or all clones in a blood sample is a consequence of fluctuating parasite densities in the course of an infection (Koepfli et al., 2013; Smith et al., 1999).
Clearance rate	The probability that a clone is cleared between two consecutive samples.
Duration of infection	The duration of naturally clearing infection. It is estimated from 1/clearance rate (Smith et al., 1999)

Methods

Study population & ethics

The randomized treatment to re-infection cohort study was carried out in a rural area of Maprik district, East Sepik Province, PNG where *P. falciparum* and *P. vivax* are co-endemic (Hofmann et al., – in preparation; Lin et al., 2010). From August 2009 to July 2010, 524 children aged 5-10 years were randomized to receive 20 days of directly observed treatment (DOT) of either: 3 days CQ, 3 days AL and 20 days PQ (0.5 mg/kg) or 3 days CQ, 3 days AL and 20 days of placebo. Thereafter participants were followed up for 8 months. At initially fortnightly and later monthly visits blood samples and malariological data were collected. Throughout the entire study period, active case detection (ACD) visits were scheduled every two weeks and passive surveillance (PCD) was implemented at the local health centers and aid posts. At each febrile episode, a blood sample was collected from the participants, a rapid diagnostic test (RDT) was performed and a blood slide examined by light microscopy (LM). Each thick film was examined for up to 200-500 fields by two independent microscopists. AL treatment was administered upon a positive RDT or LM result. Details of the study are published elsewhere (Hofmann et al., – in preparation; Robinson et al., – in preparation). Each participant contributed up to 13 regular samples, one at enrolment and 12 during follow up. Ethical clearance for molecular analyses was obtained from the PNG IMR Institutional Review Board (no.0908), the PNG Medical Advisory Committee (no. 09.11), the Ethikkomission beider Basel (no. 237/11) and was registered on ClinicalTrial.gov (NCT02143934).

DNA extraction, qPCR and genotyping

DNA was extracted using a FavorPrep™ 96-well genomic DNA extraction kit (Favorgen, Ping-Tung, Taiwan) according to the manufacturer's instructions. All samples were run on a generic *Plasmodium spp.* qPCR assay prior to *P. falciparum* and *P. vivax* species-specific *18S rRNA* qPCR assays for molecular species detection and quantification. qPCR assays were previously published and validated (Rosanas-Urgell et al., 2010; Wampfler et al., 2013). All samples positive for *P. vivax* by qPCR were genotyped for marker *msp1*F3. PCR fragments were sized by capillary electrophoresis (CE) for precise longitudinal tracking of individual clones. Genotyping assay conditions were identical to those described elsewhere (Koepfli et al., 2011a) except for a higher number of PCR cycles (30 in primary and 35 in nested PCR). For CE-sizing, products were diluted in water according to their agarose gel band intensity. Samples were analyzed by ABI3130*xl* using GS500LIZ as size standard (Applied Biosystems, Germany). Electropherograms were analyzed using GeneMapper Software version 3.7 (Applied Biosystems). A cut-off set at 500 fluorescence units (FU) defined the minimal required peak height. Stutter peaks (defined by accompanying peaks with a regular pattern of <6 bp or a height of <20% of the main peak) were censored. Further stutter peaks nor matching these requirements but repeatedly observed to accompany strong peaks of over 5000 FU were defined as artifact peaks and censored. A bin width of 3 bp was defined for each allele to accommodate small variations in fragment sizing.

Statistical analysis of the study cohort

Difference of prevalence by treatment arm was tested by Pearson X^2 and by Kruskal-Wallis X^2 for prevalence by villages and age categories. Geometric mean of *pv18S rRNA* copies/µl and *pvs25* transcripts/µl and were used as surrogate for asexual densities. Differences of geometric mean of parasite densities by treatment arm were tested by Welch's Two-sample t-test. Correlation of parasite densities with continuous age was tested by Pearson's correlation r^2. ANOVA was used to test differences of parasite densities between villages or age categories. Association of MOI and asexual density at baseline and during follow up was tested by log-transformed regression using a Poisson distribution. The statistical tests were calculated by R version 3.1.1.

Estimation of force of infection, duration and detectability

$_{mol}$FOI was estimated separately for each arm of the trial, for each age category, and for each village, by counting of all newly acquired genotypes over the time at risk (Koepfli et al., 2013; Mueller et al., 2012; Smith et al., 1999). Detectability of clones in consecutive samples from a host and duration of infections were based on the "triplet" model (Smith et al., 1999), which represents a sliding window over the follow up period of each individual and counts the different patterns of appearance and disappearance of clones in three successive samples, starting with each positive sample, assuming a Markov process for clearance and independent detection of an infecting genotype in successive samples (Smith et al., 1999). This approach naturally addresses missing data, in contrast to alternative methods that depend on complete data (Sama et al., 2005; Smith and Vounatsou, 2003), and provides an algorithm for adjusting the $_{mol}$FOI estimates to allow for imperfect detection bias. The original implementation of the model (Smith et al., 1999) was adapted i) for the unequal spacing of our regular bleed intervals (6 time two-weekly and 5 times monthly intervals), and ii) for allowing for many missed visits. Detailed description of the extended triplet model can be found in the Supplementary Methods S1.

The model was first run on a data set comprising only regular bleeds of children who didn't experience any antimalarial treatment during follow up, to assess the clearance rate per interval (M) and the detectability (S) by Bayesian inference. Subsequently, overall M and S values were estimated for an enhanced dataset containing data from active and passive case detection samples in addition to routine visits. In this dataset, following each AL treatment a period of 14 days was considered as interval-censored and removed from the days-at-risk to capture the post-treatment protective effect of AL (Salman et al., 2011). A bootstrap approach was used for assessing confidence intervals of $_{mol}$FOB. The PQ-cleared fraction of $_{mol}$FOB is the difference of $FOB_{Placebo}$ minus FOB_{PQ} and is used as surrogate for the contribution of relapses to infection (Figure 1A). The mean number of relapses per new infection is the ratio between PQ-cleared fraction of $_{mol}$FOB over FOB_{PQ}. The correlation of prevalence and FOB_{PQ} by villages was calculated with Spearman's rank correlation ρ.

Results

During the follow up period of 8 months 2526 blood samples were collected from 247 children in the PQ arm and 2588 blood samples from 257 children in the placebo arm. 4928 of these samples were collected during regular follow up visits, 57 samples derived from passive case detection at the local health facility and 129 samples from active case detection. On average 12 [IQR: 10, 13] blood samples per child were obtained in both arms. By qPCR 962 samples were positive for *P. vivax*.

The study participants originated from five villages, which differed substantially in their *P. vivax* prevalence at enrolment (Table 1). Highest *P. vivax* prevalence was found in Bolumita (66%), lowest prevalence in Amahup (38%). This significant difference among the five villages persisted during follow up ($p<0.001$). No significant difference of *P. vivax* prevalence was observed among age categories (Table 1). Owing to the PQ effect against relapses, major differences in *P. vivax* prevalence were evident between treatment arms during follow up (Table 2). The effect of PQ was greater in the first 3 months than in later months (Table 2) suggesting that the drug effect of PQ vanished during the follow up period.

Table 1. Mean prevalence, mean MOI and geometric mean *pv18S rRNA* copies/µl WB at enrolment

At enrolment	Prevalence [95 CI][a]	Mean MOI [95 CI][b]	Geometric mean of *pv18S rRNA* copies/µl WB [95 CI][c]
Treatment			
PQ	0.48 [0.39, 0.51]	2.18 [1.91, 2.44]	4.79 [2.88, 8.51]
Placebo	0.51 [0.44, 0.57]	2.01 [1.72, 2.30]	1.66 [0.95, 2.95]
p-value	*0.3*	*0.4*	*0.006**
Villages			
Albinama	0.53 [0.44, 0.62]	1.82 [1.52, 2.12]	3.80 [1.86, 7.76]
Amahup	0.38 [0.30, 0.47]	2.12 [1.75, 2.49]	3.09 [1.41, 6.61]
Balanga	0.43 [0.30, 0.57]	1.96 [1.37, 2.55]	1.78 [0.34, 9.12]
Balif	0.43 [0.34, 0.52]	1.74 [1.38, 2.09]	2.14 [0.95, 4.79]
Bolumita	0.66 [0.54, 0.77]	2.94 [2.32, 3.55]	3.31 [1.32, 8.51]
p-value	*<0.001**	*0.003**	*0.8*
Ages			
4-6.67 years	0.52 [0.44, 0.60]	2.18 [1.87, 2.50]	6.03 [3.39, 10.72]
6.67-8.5 years	0.48 [0.41, 0.56]	1.91 [1.63, 2.20]	2.57 [1.35, 5.01]
8.5-11 years	0.42 [0.34, 0.50]	2.20 [1.77, 2.63]	1.32 [0.63, 2.69]
p-value	*0.15*	*0.6*	*0.006**

[a] Differences in proportions were tested by Pearson X^2.

[b] Differences in mean MOI were assessed by Wilcoxon rank sum tests (by treatment arms) and Kruskal-Wallis rank sum tests (villages and age categories).

[c] Differences in mean $\log_{10}$ transformed *pv18S rRNA* copies were calculated by Welch two sample T-test (by treatment arms) and ANOVA (villages and age categories).

**p-values* <0.05

Parasite densities were measured by qPCR and expressed in *pv18S rRNA* copies/µl whole blood (WB). Geometric mean density was similar between villages and correlated negatively with age (Table 1; r^2=0.038 at enrolment, p=0.001; r^2=0.008 during follow up, p<0.001). The geometric mean density at enrolment dropped by 17.6% [-28.3, -6.9] per one year of age, as expected for children acquiring immunity as a consequence of exposure. At enrolment density was significantly lower in the placebo arm (Table 1), but during follow up no difference between treatment arms was observed (Table 2). Thus we concluded that parasitaemia at enrolment did not determine parasitaemia during follow up.

Table 2. Mean prevalence, mean MOI, geometric mean *pv18S rRNA* copies/µl WB, detectability and duration of infection by treatment arms over the entire follow up period or separately over the first 3 months and the last 5 months

Over study period	PQ	Placebo	*p-value*[a]
Mean Prevalence [95 CI][b]			
Entire follow up period	0.05 [0.05, 0.06]	0.16 [0.15, 0.18]	<0.001
First 3 months	0.05 [0.04, 0.06]	0.20 [0.18, 0.22]	<0.001
Last 5 months	0.06 [0.05, 0.07]	0.13 [0.12, 0.15]	<0.001
Mean MOI [95 CI][c]			
Entire follow up period	1.66 [1.49, 1.83]	1.78 [1.68, 1.87]	0.08
First 3 months	1.82 [1.54, 2.11]	1.88 [1.74, 2.01]	0.6
Last 5 months	1.55 [1.32, 1.78]	1.64 [1.50, 1.77]	0.2
Geometric mean of *pv18S rRNA* copies/µl WB [95 CI][d]			
Entire follow up period	12.9 [10.2, 16.2]	12.6 [11.0, 14.5]	0.9
First 3 months	17.4 [12.3, 24.0]	19.1 [15.8, 22.9]	0.6
Last 5 months	9.8 [7.1, 13.2]	7.1 [5.9, 8.7]	0.1
Detectability [95 CI][e]			
Entire follow up period	0.27 [0.15, 0.50]	0.30 [0.20, 0.42]	0.4
First 3 months	0.25 [0.10, 0.64]	0.27 [0.19, 0.42]	0.4
Last 5 months	0.30 [0.14, 0.65]	0.50 [0.22, 0.83]	0.2
Median duration of infection [95 CI][e]			
Entire follow up period	60 days [25, 891]	45 days [28, 111]	0.3
First 3 months	32 days [11, 630]	67 days [27, 933]	0.3
Last 5 months	68 days [26, 1129]	29 days [19, 73]	0.1

[a]Prevalence differences between treatment arms were tested by Pearson X^2 tests. MOI differences between treatment arms were tested by Wilcoxon rank sum test. Mean $\log_{10}$ *pv18S rRNA* copies differences between treatment arms were tested by Welch's Two-sample t-tests. Detectability and 1/duration difference between treatment arms were tested by Welch's Two-sample t-tests.

[b] Confidence intervals of prevalence come from X^2 distribution.

[c] Confidence intervals of MOI come from T distribution.

[d] Confidence intervals of log10 *pv18S* copies/µl come from T distribution.

[e] Credible intervals of detectability and of median duration of infection come from Bayesian 2.5 and 97.5 quantiles.

890 of the 962 (92.5%) *P. vivax* positive samples by qPCR were also positive by nested PCR for genotyping marker *P. vivax msp1*F3. A total of 50 *msp1*F3 genotypes were observed, of these three genotypes were detected only at enrolment and 12 only during follow up. The most frequent *msp1*F3 genotype represented 21.6% (105/485) of all fragments at enrolment, and 19.7% (150/761) of fragments during follow up (genotypes were counted only once per child).

PQ treatment failures were suspected in 19/115 *P. vivax* positive children because the same genotype was observed at enrolment and in a follow up sample. The majority of these were of the most frequent genotype M262.9. Therefore these 19 samples were typed for two additional markers, *MS2* and *pv3.27*. The identical genotypes by all three markers was observed for 4/115 (3.5%) children. These must be considered treatment failures as all these children adhered to the treatment schedule. This finding of a residual PQ failure despite direct observed treatment is in line with previous reports (Bennett et al., 2013) and may reflect the poor quality of Primaquine in PNG (Hetzel et al., 2014).

MOI is the number of genotypes detected simultaneously in a sample. MOI differed significantly by villages at enrolment (Table 1) and during follow up (p=0.008). No significant association was observed between MOI and prevalence (Spearman r^2=0.04, p=0.7). MOI was similar between treatment arms and age categories at enrolment (Table 1; Table 2) and during follow up (p=0.6). Geometric mean of parasite density increased by 31% with every additional infecting clone at enrolment (coefficient: 0.31 [95 CI: 0.21, 0.41], r^2=0.13, p<0.001). Thus it seems that *P. vivax* MOI in 4-11 years old children in PNG is not determined by the substantial differences in transmission level between home villages of the children, nor by the age of a child nor PQ treatment.

Detectability of *P. vivax* clones

Fluctuations in *P. vivax* parasite densities frequently result in genotypes falling below the detection limit of PCR. Detectability of individual genotypes was estimated from the records in the longitudinal genotyping data set by applying the triplet model (Supplementary methods S1). The data set used for estimating detectability included only regular follow up bleeds. 130 children who received antimalarial treatment during follow up were excluded, because any treatment, even if caused by *P. falciparum*, shortens the duration of an infection.

Detectability of *P. vivax* genotypes in the PQ and placebo arm showed similar trends in the effects of age, village and follow up interval (Table 2). Detectability in both arms was highest in the youngest children <6.67 years and dropped with older age (<6.67y=0.48 [95% credible interval: 0.28, 0.71], 6.67-8.5y=0.34 [0.20, 0.53] and >8.5y=0.18 [0.13, 0.29]); this corresponded well to the observed trend in densities and confirms that genotypes more frequently remain undetected in samples of lower parasite density. Detectability was highest in Albinama and Amahup village, but differences were not statistically significant (Albinama=0.42 [95% credible interval: 0.22, 0.68], Amahup=0.37 [0.12, 0.78], Balanga=0.23 [0.14, 0.43], Balif=0.27 [0.16, 0.46] and Bolumita=0.30

[0.15, 0.53]). Because differences between villages and age groups were not statistically significant, all further analyses of infection dynamics used a summary measurement of detectability of 0.29 [95% credible interval: 0.20, 0.39].

Duration of infection

The duration, defined as 1/daily clearance rate, was estimated by the triplet model. The average duration of infection was 60 [95% credible interval: 25, 891] days in the PQ arm and 45 [28, 111] days in the placebo arm (Table 2). Durations in older children >8.5 years were longer with 154 [44, 3458] days compared to 40 [24, 144] days in children 6.67-8.5 years and 26 [18, 52] days in the youngest children <6.67 years (p=0.008). Older children also carried lower parasite densities than younger children, suggesting that acquired immunity in older children controls densities to lower levels and at the same time tolerates longer duration. The duration of infection did not differ by village, suggesting that age is a major determinant, not transmission intensity (as measured by prevalence).

PQ-cleared fraction of relapses and mean number of relapses per new infection

The number of new *P. vivax* blood-stage clones per child per year ($_{mol}$FOB) (Koepfli et al., 2013) was assessed on all samples collected from the cohort including regular bleeds plus the samples from active and passive case detection (ACD and PCD). The latter two sources contributed 22/1137 clones. For estimating $_{mol}$FOB by treatment arm, the overall detectability of 0.29 was used. This value and the clearance rate were both obtained from genotyping data including only samples from regular follow up bleeds (see sections above). $_{mol}$FOB was significantly different between treatment arms in most age categories and villages (Table 3).

We assumed that the difference in $_{mol}$FOB between PQ and placebo arms represents an approximation of the contribution of relapses to the number of new clones detected in a blood sample. However, an added complication derives from the fact that new infections from mosquitoes also give rise to hypnozoites in PQ treated individuals after waning of the drug effect. These additional relapses in PQ arm are not captured when determining the fraction of relapses among all clones. Therefore the fraction of relapse-derived genotypes and the estimated mean number of relapses per new infection will be underestimated by our approach. "PQ-cleared fraction of $_{mol}$FOB" can be viewed as the difference in force of infection between treatment arms. The ratio between the PQ-cleared fraction of $_{mol}$FOB over $_{mol}$FOB of PQ arm (FOB_{PQ}) estimates the mean number of relapses per new infection in our cohort (Figure 2A).

The PQ-cleared fraction of $_{mol}$FOB was significantly larger in the first three months compared to the period thereafter (Figure 2A, p=0.04). The mean number of relapses per new infection was 2.4 [1.3, 4.0] in the first three months and 1.4 [0.6, 2.8] in the later 5 months (Figure 2A). The PQ-cleared fraction of $_{mol}$FOB differed significantly between villages (Figure 2C). No significant difference by age category was observed (Figure 2B). The mean number of relapses per new

infection was similar over all villages and age categories. This suggests that the number of hypnozoites cleared by PQ is proportional to the number of new infections observed in the corresponding village or age category.

We hypothesize that $_{mol}$FOB in the PQ arm may represent an approximation of a child's individual exposure to infected mosquito bites. Support for this assumption derives from a good correlation between FOB_{PQ} and the parasite prevalence in all 5 villages (Figure 2D, p=0.09). Children from Bolumita, the village with the highest prevalence, were most exposed, as measured by FOB_{PQ}. As predicted, Bolumita also showed the largest difference between $_{mol}$FOB in the two treatment arms. In contrast, $_{mol}$FOB and prevalence in Amahup indicated low exposure and indeed showed a smaller difference between treatment arms. This is in line with the intuitive expectation that higher transmission intensity corresponds to a larger hypnozoite reservoir in the liver. These observations also highlight the substantial heterogeneity in malaria transmission among neighboring villages in PNG.

Discussion

The contribution of relapses to the dynamics of *P. vivax* infections and the duration of infections in semi-immune hosts are key elements of *P. vivax* epidemiology. Here we demonstrated for the first time that the appearance and clearance of *P. vivax* clones can be described, despite the major complication caused by relapses, by applying a mathematical model to cope with imperfect detectability of clones and by radical cure in one of two compared arms of a trial. Methods to estimate theses parameters might prove very useful for evaluating the effect of interventions against malaria in clinical trials, e.g. in trials of experimental vaccines or new drugs.

Applying the triplet approach to *P. vivax* data demonstrated that clone detectability, mean parasite densities and the estimated duration of infection were all similar in both treatment arms. These findings were surprising, because antigens of relapsing clones likely gave rise to a very recent immune response, thus relapses should persist for a shorter period of time. We speculate that the age of our study participants accounts for these findings. This study was conducted in schoolchildren of a mean age of 7.6 years. It is probable that semi-immunity against *P. vivax* malaria may have been fully established in our participants as suggested by the low number of their clinical *P. vivax* episodes (Hofmann et al., – in preparation). Immunity against *P. vivax* developing early in life could explain why no strong age effects on detectability, duration of infection and MOI were observed. Indeed, our earlier work also suggested that the high number of *P. vivax* infections acquired in the first four years of life is a significant contributor to the rapid acquisition of immunity (Koepfli et al., 2013). On the other hand, the longest duration of infection in our study was observed in the oldest children. This age trend corresponds well to our earlier

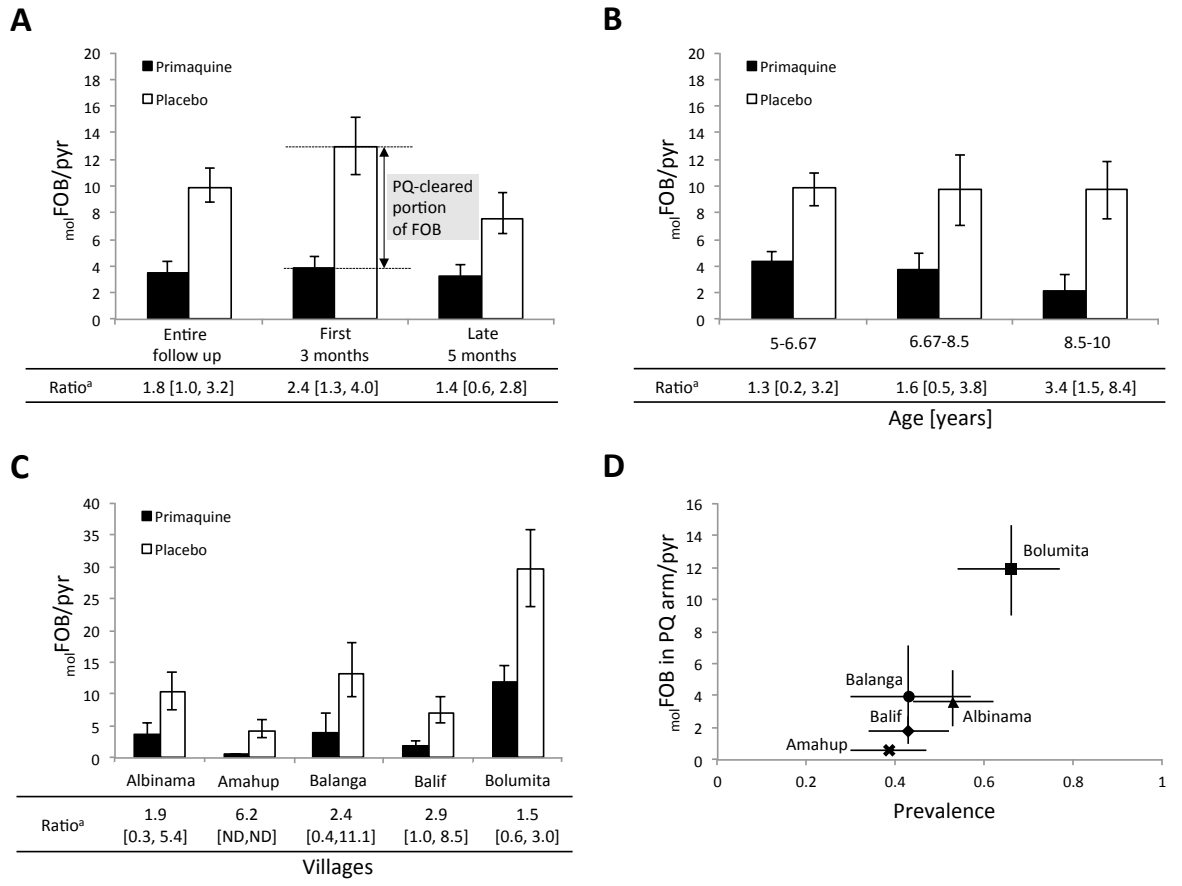

Figure 2. Force of blood-stage infection by treatment arm and mean number of relapses per new infection. $_{mol}$FOB per person and year-at-risk (pyr) was calculated from a data set including regular bleeds, ACD and PCD with 14 days censored after antimalarial treatment during follow up. [a]Ratio is expressing the mean number of relapses per new infection. It was calculated by dividing the PQ-cleared portion of $_{mol}$FOB over $_{mol}$FOB in PQ arm. **A**. $_{mol}$FOB by treatment arms and mean number of relapses per new infection calculated over entire follow up, over the first three months or the last 5 months. **B**. $_{mol}$FOB by treatment arms and mean number of relapses per new infection by age categories. **C**. $_{mol}$FOB by treatment arms and mean number of relapses per new infection by villages. **D**. $_{mol}$FOB of PQ arm and prevalence at enrolment for each village. Error bars of $_{mol}$FOB values indicate empirical 95% confidence interval of 100 runs of Bootstrap of infection counts. Error bars of prevalence indicate 95% confidence interval of X^2-distribution. Bootstrap of Amahup of PQ arm failed because there were too few infections in this subset.

findings in *P. falciparum* showing a peak in duration of infections in 5-9 years old Ghanaean children. Our data gained from a small age range only is consistent with an in increasing tolerability for low density *P. vivax* infections leading to longer durations as children grow older and immunity increases. Further studies on duration of infection in adults and younger children would be important to better understand the role of immunity in *P. vivax* malaria.

The estimated average persistence of *P. vivax* clones in both treatment arms was shorter than the durations of relapses observed of historical *P. vivax* infection experiments, which gave estimates of about 80 days of relapse duration (Ross *et al.* – personal communication). Durations of untreated relapses in human volunteers became shorter as more attacks were experienced (Coatney et al., 1950). Our data suggested that on average all untreated *P. vivax* infections, irrespective of the source from hypnozoite or primary infection, persist equally long in a host. This broad consistency of our estimated durations with the persistence of relapses in experimental human infection implies that our study participant from PNG aged 5-10 years had acquired a level of semi-immunity against new infections and relapses, which was similar to that raised against multiple homologous relapses in the historical artificial infections. This raises the interesting question whether relapses detected in PNG children were homologous or heterologous with respect to the preceding infection. We indeed observed that not only the duration of infection in both treatment arms was very similar, but also the mean parasite densities were concordant in both arms.

Two scenarios could explain the similar durations and densities of relapses and new infections in our cohort: (i) most of the relapses observed in our study cohort were heterologous. Then relapses would be antigenically different and experience a similar immune pressure, just like new infections. (ii) The acquired semi-immunity against multiple strains experienced by our study participants in the past confers some protection against new infections. Then new infections and relapse are alike in being controlled by acquired immunity. In this scenario homologous or heterologous relapses would be equally well controlled. Most likely both scenarios are represented in our cohort. Studies on relapses observed in newborns and their mother showed that the first relapses experienced by the newborns were homologous to their first infection (Imwong et al., 2012). Relapses experienced later in life might rise from activation of latent hypnozoites from previous inoculations (Imwong et al., 2012; Kim et al., 2012). A recently published case report revealed that relapses were meiotic siblings (Bright et al., 2014). Meiotic siblings are heterologous in some genetic traits only if hybridization of two genetically distinct gametes in the mosquito proceeded. Genetic diversity of *P. vivax* is high in PNG (Koepfli et al., 2011a), arguing for concurrent transmission of multiple clones to mosquitoes, but no evidence from epidemiological data is yet available. In historical experimental data partial immunity against heterologous strains was observed (Whorton and Pullman, 1947). We argue that the similar duration of infection observed in relapses and new infections in our cohort might be accounted for by the infection history of these older children leading to semi-immunity against heterologous or homologous

relapses and new infections, and by a large number of antigenically diverse hypnozoites, the relapses of which stimulate cross-reactive immune responses.

The overall short duration of infection in *P. vivax* compared to *P. falciparum* is a remarkable feature of *P. vivax* infection dynamics already observed in an earlier study in PNG (Bruce et al., 2000). Short duration of *P. vivax* infections is expected because antigenic variation, the major factor contributing to immune evasion and very long durations in *P. falciparum*, is developed only rudimentary in *P. vivax* (Jemmely et al., 2010). We observed in both treatment arms an equally high number of infections that occurred only at one time point, suggesting a rapid turnover of clones in *P. vivax*. Indeed, the observed lack of difference in mean MOI between treatment arms, despite an over twice as high $_{mol}$FOB in placebo arm, is also arguing for infections of short durations with little overlap.

Overall the mathematical methods applied here provided valid estimates of the duration of both, relapses and primary blood stage infections. Owing to the wide intervals between blood sampling in our study, short lasting relapses would have escaped detection and we cannot exclude selection bias towards longer persisting relapses. This also implies that the $_{mol}$FOB in both arms may be widely underestimated. An alternative simpler estimation of $_{mol}$FOB for this cohort had shown 1.35 new infections per person-year-at-risk in the PQ arm and over three times as much, 4.43 new infections, in placebo recipients (Robinson et al. – in preparation). The triplet model estimates for $_{mol}$FOB were more than twice as high for each of the treatment arms. This difference between $_{mol}$FOB estimates obtained by the two approaches derived from the correction for detectability in the triplet model. Detectability of *P. vivax* genotypes generally was low, presumably owing to a 10 times lower parasite density in *P. vivax* compared to *P. falciparum*. The triplet approach-derived detectability indicated that 71% of the genotypes present in the participants were missed by our genotyping method. Thus the earlier analysis of Robinson and colleagues (– in preparation) has likely underestimated the true number of clones coming in or being cleared.

On average 1.8 relapses were observed per newly acquired genotype. As expected from the waning PQ drug effect, this number was larger in the first 3 months of follow up (2.4 relapses/new infection) compared to the later 5 months (1.4 relapses/new infection). Data from 15 experimental sporozoite-induced human infections with *P. vivax* Chesson strain (one mosquito bite per man) of the late 1940s suggested that 3 [IQR 3-5] relapses per individual occurred after the single mosquito bite (Coatney et al., 1950). Later re-exposure of these volunteers to an infectious bite showed a drop in the number of (microscopic) relapses experienced. The authors suggested that the number of relapses per new infection decreased with acquired immunity (Coatney et al., 1950). However, no age effect on the number of relapses per new infection was observed in our cohort. Analysis of molecular data of similar cohorts conducted in younger children, e.g. from Betuela *et al* (Betuela et al., 2012), will reveal valuable information on a possible age trend and as consequence on the role of acquired immunity.

Ross *et al.* analyzed genotyping data from an earlier cohort of children aged <4.5 years from the same study area (Ross et al., – in preparation). They found that the seasonality of primary infections and relapses differs, and so the ratio of relapses to primary infections changes throughout the year. Our study began in August 2009. Assuming the same seasonal pattern as the study reported by Ross *et al.*, our study would have started at the time with the highest ratio of relapses to primary infections (Ross et al., – in preparation).

Under the assumption that $_{mol}$FOB of the PQ arm represents the exposure of study participants, we were able to describe the transmission intensity in 5 study villages. The contribution of relapses relative to primary infections seemed to be independent of transmission intensity, i.e. highly exposed children experienced proportionally more relapses than less exposed children. Allelic diversity and heterozygosity were observed to be similar in all villages (Supplementary figure S2), and are therefore unlikely contributing to inter-village differences in transmission intensity.

Conclusion

The triplet approach, previously developed for *P. falciparum*, was applied to estimate for the first time the duration of *P. vivax* infections in naturally exposed individuals. Our study design with two treatment arms made it possible to estimate the natural force of infection and to estimate the mean number of relapses per new infection in semi-immune children from a highly endemic area. We observed that increasing individual exposure of participants translated proportionally into an increased relapse burden. Approaches to monitor efficacies of interventions in the field should therefore stratify for transmission intensity.

A key finding of our investigation of *P. vivax* infection dynamics was that relapses and new infections are presumably under the same immune pressure in semi-immune children as indicated by a similar duration, parasite density and detectability in both treatment arms. This result points to the basic research question on genetic similarity of relapses and may provide a rationale for a future investigation of the genetic variability of relapses compared to their preceding blood-stage genotypes, i.e. relapses being meiotic siblings (Bright et al., 2014) in order to survive the acquired immune response triggered by the initial inoculation.

The mathematical model applied to genotyping data from the two treatment arms proved very useful to evaluate the infection dynamics of *P. vivax* in semi-immune children. This was achieved despite a major complication of *P. vivax* molecular epidemiology, namely the unknown history of infections in our participants before baseline, but still giving rise to relapses in our participants. This study design and the analytical approach presented here might be valuable for evaluating the effect of interventions in drug or vaccine trials against *P. vivax* malaria.

Acknowledgments

We thank Amanda Ross, Michael White, Stephan Karl, Cristian Koepfli and Ian Hastings for helpful exchanges. We also thank the study participants and their parents or guardians, and the field teams in PNG.

Author contributions

RW and IF designed and performed research and wrote the article; MS and TS contributed to statistical analysis and mathematical modeling. NH, AW, LJR, PS and IM contributed to study design, field surveys and experimental work.

Financial support

This work was supported by the Swiss National Science Foundation (grant no. 310030_134889) and the International Centers of Excellence in Malaria Research (grant no. U19 AI089686-03). LJR was supported by an Australian National Health and Medical Research Council (NHMRC) Early Career Fellowship (grant no. 1016443). IM is supported by an NHMRC Senior Research Fellowship (grant no. 1043345). TS was supported by an UK MRC grant (grant no. MR/K014676/1). The funders had no role in study design, data collection and analysis, decision to publish, or preparation of the manuscript.

Potential conflicts of interest.

All authors: No reported conflicts.

References

Battle, K.E., Karhunen, M.S., Bhatt, S., Gething, P.W., Howes, R.E., Golding, N., Van Boeckel, T.P., Messina, J.P., Shanks, G.D., Smith, D.L., Baird, J.K., Hay, S.I., 2014. Geographical variation in Plasmodium vivax relapse. Malar. J. 13, 144. doi:10.1186/1475-2875-13-144

Bekessy, A., Molineaux, L., Storey, J., 1976. Estimation of incidence and recovery rates of Plasmodium falciparum parasitaemia from longitudinal data. Bull. World Health Organ. 54, 685–693.

Bennett, J.W., Pybus, B.S., Yadava, A., Tosh, D., Sousa, J.C., McCarthy, W.F., Deye, G., Melendez, V., Ockenhouse, C.F., 2013. Primaquine failure and cytochrome P-450 2D6 in Plasmodium vivax malaria. N. Engl. J. Med. 369, 1381–1382. doi:10.1056/NEJMc1301936

Betuela, I., Rosanas-Urgell, A., Kiniboro, B., Stanisic, D.I., Samol, L., de Lazzari, E., Del Portillo, H.A., Siba, P., Alonso, P.L., Bassat, Q., Mueller, I., 2012. Relapses contribute significantly to the risk of Plasmodium vivax infection and disease in Papua New Guinean children 1-5 years of age. J. Infect. Dis. 206, 1771–1780. doi:10.1093/infdis/jis580

Bretscher, M.T., Maire, N., Chitnis, N., Felger, I., Owusu-Agyei, S., Smith, T., 2011. The distribution of Plasmodium falciparum infection durations. Epidemics 3, 109–118. doi:10.1016/j.epidem.2011.03.002

Bretscher, M.T., Valsangiacomo, F., Owusu-Agyei, S., Penny, M.A., Felger, I., Smith, T., 2010. Detectability of Plasmodium falciparum clones. Malar. J. 9, 234. doi:10.1186/1475-2875-9-234

Bright, A.T., Manary, M.J., Tewhey, R., Arango, E.M., Wang, T., Schork, N.J., Yanow, S.K., Winzeler, E.A., 2014. A high resolution case study of a patient with recurrent Plasmodium vivax infections shows that relapses were caused by meiotic siblings. PLoS Negl. Trop. Dis. 8, e2882. doi:10.1371/journal.pntd.0002882

Bruce, M.C., Galinski, M.R., Barnwell, J.W., Donnelly, C.A., Walmsley, M., Alpers, M.P., Walliker, D., Day, K.P., 2000. Genetic diversity and dynamics of plasmodium falciparum and P. vivax populations in multiply infected children with asymptomatic malaria infections in Papua New Guinea. Parasitology 121 (Pt 3), 257–272.

Bunnag, D., Karbwang, J., Thanavibul, A., Chittamas, S., Ratanapongse, Y., Chalermrut, K., Bangchang, K.N., Harinasuta, T., 1994. High dose of primaquine in primaquine resistant vivax malaria. Trans. R. Soc. Trop. Med. Hyg. 88, 218–219.

Coatney, G.R., Cooper, W.C., Young, M.D., 1950. Studies in human malaria. XXX. A summary of 204 sporozoite-induced infections with the Chesson strain of Plasmodium vivax. J. Natl. Malar. Soc. US 9, 381–396.

Craige, B., Alving, A.S., 1947. The Chesson strain of Plasmodium vivax malaria; relationship between prepatent period, latent period and relapse rate. J. Infect. Dis. 80, 228–236.

Duarte, E.C., Pang, L.W., Ribeiro, L.C., Fontes, C.J., 2001. Association of subtherapeutic dosages of a standard drug regimen with failures in preventing relapses of vivax malaria. Am. J. Trop. Med. Hyg. 65, 471–476.

Galappaththy, G.N.L., Omari, A.A.A., Tharyan, P., 2007. Primaquine for preventing relapses in people with Plasmodium vivax malaria. Cochrane Database Syst. Rev. Online CD004389. doi:10.1002/14651858.CD004389.pub2

Hetzel, M.W., Page-Sharp, M., Bala, N., Pulford, J., Betuela, I., Davis, T.M.E., Lavu, E.K., 2014. Quality of antimalarial drugs and antibiotics in Papua New Guinea: a survey of the health facility supply chain. PloS One 9, e96810. doi:10.1371/journal.pone.0096810

Hill, D.R., Baird, J.K., Parise, M.E., Lewis, L.S., Ryan, E.T., Magill, A.J., 2006. Primaquine: report from CDC expert meeting on malaria chemoprophylaxis I. Am. J. Trop. Med. Hyg. 75, 402–415.

Hofmann, N., Robinson, L.J., Wampfler, R., Betuela, I., Waltmann, A., Mueller, I., Felger, I., – in preparation. Changing patterns of malarial infection and disease after intensified control efforts in Papua New Guinean children.

Imwong, M., Boel, M.E., Pagornrat, W., Pimanpanarak, M., McGready, R., Day, N.P.J., Nosten, F., White, N.J., 2012. The first Plasmodium vivax relapses of life are usually genetically homologous. J. Infect. Dis. 205, 680–683. doi:10.1093/infdis/jir806

Jeffery, G.M., 1956. Relapses with Chesson strain Plasmodium vivax following treatment with chloroquine. Am. J. Trop. Med. Hyg. 5, 1–13.

Jemmely, N.Y., Niang, M., Preiser, P.R., 2010. Small variant surface antigens and Plasmodium evasion of

immunity. Future Microbiol. 5, 663–682. doi:10.2217/fmb.10.21

Karunajeewa, H.A., Mueller, I., Senn, M., Lin, E., Law, I., Gomorrai, P.S., Oa, O., Griffin, S., Kotab, K., Suano, P., Tarongka, N., Ura, A., Lautu, D., Page-Sharp, M., Wong, R., Salman, S., Siba, P., Ilett, K.F., Davis, T.M.E., 2008. A trial of combination antimalarial therapies in children from Papua New Guinea. N. Engl. J. Med. 359, 2545–2557. doi:10.1056/NEJMoa0804915

Kim, J.-R., Nandy, A., Maji, A.K., Addy, M., Dondorp, A.M., Day, N.P.J., Pukrittayakamee, S., White, N.J., Imwong, M., 2012. Genotyping of Plasmodium vivax reveals both short and long latency relapse patterns in Kolkata. PloS One 7, e39645. doi:10.1371/journal.pone.0039645

Koepfli, C., Colborn, K.L., Kiniboro, B., Lin, E., Speed, T.P., Siba, P.M., Felger, I., Mueller, I., 2013. A high force of plasmodium vivax blood-stage infection drives the rapid acquisition of immunity in papua new guinean children. PLoS Negl. Trop. Dis. 7, e2403. doi:10.1371/journal.pntd.0002403

Koepfli, C., Ross, A., Kiniboro, B., Smith, T.A., Zimmerman, P.A., Siba, P., Mueller, I., Felger, I., 2011a. Multiplicity and diversity of Plasmodium vivax infections in a highly endemic region in Papua New Guinea. PLoS Negl. Trop. Dis. 5, e1424. doi:10.1371/journal.pntd.0001424

Koepfli, C., Schoepflin, S., Bretscher, M., Lin, E., Kiniboro, B., Zimmerman, P.A., Siba, P., Smith, T.A., Mueller, I., Felger, I., 2011b. How Much Remains Undetected? Probability of Molecular Detection of Human Plasmodia in the Field. PLoS ONE 6. doi:10.1371/journal.pone.0019010

Krudsood, S., Tangpukdee, N., Wilairatana, P., Phophak, N., Baird, J.K., Brittenham, G.M., Looareesuwan, S., 2008. High-dose primaquine regimens against relapse of Plasmodium vivax malaria. Am. J. Trop. Med. Hyg. 78, 736–740.

Leslie, T., Mayan, I., Mohammed, N., Erasmus, P., Kolaczinski, J., Whitty, C.J.M., Rowland, M., 2008. A randomised trial of an eight-week, once weekly primaquine regimen to prevent relapse of plasmodium vivax in Northwest Frontier Province, Pakistan. PloS One 3, e2861. doi:10.1371/journal.pone.0002861

Lin, E., Kiniboro, B., Gray, L., Dobbie, S., Robinson, L., Laumaea, A., Schöpflin, S., Stanisic, D., Betuela, I., Blood-Zikursh, M., Siba, P., Felger, I., Schofield, L., Zimmerman, P., Mueller, I., 2010. Differential patterns of infection and disease with P. falciparum and P. vivax in young Papua New Guinean children. PloS One 5, e9047. doi:10.1371/journal.pone.0009047

Mueller, I., Schoepflin, S., Smith, T.A., Benton, K.L., Bretscher, M.T., Lin, E., Kiniboro, B., Zimmerman, P.A., Speed, T.P., Siba, P., Felger, I., 2012. Force of infection is key to understanding the epidemiology of Plasmodium falciparum malaria in Papua New Guinean children. Proc. Natl. Acad. Sci. U. S. A. 109, 10030–10035. doi:10.1073/pnas.1200841109

Muench, H., 1959. Catalytic Models in Epidemiology. Camb. Mass Harv. Univ. Press.

Robinson, L.J., Wampfler, R., Betuela, I., White, M., Karl, S., Kiniboro, B., Waltmann, A., Hofmann, N., Lorry, L., Tarongka, N., Silkey, M., Bassat, Q., Schofield, L., Felger, I., Mueller, I., – in preparation. Strategies for understanding and reducing the Plasmodium vivax hypnozoite reservoir in Papua New Guinean children: A randomised placebo-controlled trial and mathematical model.

Rosanas-Urgell, A., Mueller, D., Betuela, I., Barnadas, C., Iga, J., Zimmerman, P.A., del Portillo, H.A., Siba, P., Mueller, I., Felger, I., 2010. Comparison of diagnostic methods for the detection and quantification of the four sympatric Plasmodium species in field samples from Papua New Guinea. Malar. J. 9, 361. doi:10.1186/1475-2875-9-361

Ross, A., Koepfli, C., Schoepflin, S., Timinao, L., Siba, P., Tanner, M., Mueller, I., Felger, I., Smith, T.A., – in preparation. The dynamics of Plasmodium vivax primary infections and relapses in a cohort of children in Papua New Guinea.

Salman, S., Page-Sharp, M., Griffin, S., Kose, K., Siba, P.M., Ilett, K.F., Mueller, I., Davis, T.M.E., 2011. Population pharmacokinetics of artemether, lumefantrine, and their respective metabolites in Papua New Guinean children with uncomplicated malaria. Antimicrob. Agents Chemother. 55, 5306–5313. doi:10.1128/AAC.05136-11

Sama, W., Owusu-Agyei, S., Felger, I., Vounatsou, P., Smith, T., 2005. An immigration-death model to estimate the duration of malaria infection when detectability of the parasite is imperfect. Stat. Med. 24, 3269–3288. doi:10.1002/sim.2189

Smith, T., Felger, I., Fraser-Hurt, N., Beck, H.P., 1999. Effect of insecticide-treated bed nets on the dynamics of multiple Plasmodium falciparum infections. Trans. R. Soc. Trop. Med. Hyg. 93 Suppl 1, 53–57.

Smith, T., Vounatsou, P., 2003. Estimation of infection and recovery rates for highly polymorphic parasites when detectability is imperfect, using hidden Markov models. Stat. Med. 22, 1709–1724. doi:10.1002/sim.1274

Townell, N., Looke, D., McDougall, D., McCarthy, J.S., 2012. Relapse of imported Plasmodium vivax malaria is related to primaquine dose: a retrospective study. Malar. J. 11, 214. doi:10.1186/1475-2875-11-214

Wampfler, R., Mwingira, F., Javati, S., Robinson, L., Betuela, I., Siba, P., Beck, H.-P., Mueller, I., Felger, I., 2013. Strategies for detection of Plasmodium species gametocytes. PloS One 8, e76316. doi:10.1371/journal.pone.0076316

White, N.J., 2011. Determinants of relapse periodicity in Plasmodium vivax malaria. Malar. J. 10, 297. doi:10.1186/1475-2875-10-297

Whorton, C.M., Pullman, T.N., 1947. The Chesson strain of Plasmodium vivax malaria; immunity. J. Infect. Dis. 81, 1–6.

Supplementary Methods S1

Estimation of force of infection and clearance rates allowing for detectability

Analysis of the genotypes of malaria parasites in sequential blood samples collected several weeks apart from the same infected hosts, can be used to estimate the force of infection of the parasite. Such data can also be used to estimate how long parasites persist if they are not treated. A significant complication is that even PCR does not detect all infections (Bretscher et al., 2010). This means that, when serial samples from the same host are considered, disappearance of a specific genotype in the second sample of a pair (a "loss" corresponding to a (+ −) pattern) can be either the result of imperfect detection of a persisting clone, or of clearance. Similarly, a "gain" (− +) can be the result of acquisition of parasites of the specific genotype, or of imperfect detection in the first sample of the pair.

The mathematics is best illustrated by the case of exchangeable genotypes, i.e. the rates of clearance of each genotype are the same and each genotype is equally detectible. In applications where this assumption does not hold, analyses can be carried out stratified by genotype or host characteristics. To estimate the rates of clearance allowing for the proportion of clones that are detected, sequences of at least three samples need to be considered. The following text is an expanded version of the original exposition of this method (Smith et al., 1999).

Clearance and detectability

To estimate the clearance rates and the detectability, a simple analytical approach is to group the data into "triplets" comprising sequences of three samples starting with each one that typed positive for each specific genotype, so that the total number of triplets is equal to the sum over all genotypes of the positive typings. These are then categorized according to the typing result and the presence of data for the second and third samples into categories (Figure S1 and Table S1).

The analysis estimates both the detectability and the probability that an infection existing at the start is cleared during the interval between the first sample (t=1) and the second sample (t=2).

Assuming a Markov process for clearance (Smith et al., 1999), and assuming the probability of reinfection within the same interval to be close to zero. The typing results at t=2 depend on probability, (M) , of clearance of an infection during any single interval and on the proportion of true infections detected in any given sample (S), as indicated in Table S1. In the case that the sample at t=2 is negative, the samples at t=3 are informative about whether a negative sample at t=2 was a true, or false negative. This method classifies pairs or triplets commencing with a positive sample into four categories (numbered 1-4 in Table S1 and Figure S1a), depending on the existence of data from samples at time t=2 and t=3. The likelihood of each of these 4 patterns, equivalent to the probability that it will be observed, conditional on the availability of the required

typing data, is given in Table S1.

The original method (Smith et al., 1999) (Figure S1a) analyses only the minimal dataset required to make the problem identifiable, counting only the pairs or triplets where samples are available at t=2, and distinguishing between cases where only pairs of samples (t=1 and t=2) are available from those where full triplets are available (t=1, t=2 and t=3). When the second sample is positive, the status at t=3 is not considered. The approach can be extended to incorporate information from all triplets with data from t=3, or from more complicated sample sets, including sequences of 4 or more samples and sequences with missing data. One such example is the case when the data at t=2 is missing (Figure S1b), but a sample at t=3 has been typed. Positivity at t=3 is then also indicative of persistence, and thus the t=3 provides some additional information about M and S. In the case that complete data are available from longer sample sets, the method is equivalent to that of Sama (Sama et al., 2005). The challenge of extending the methodology to analysis of longer series with complex patterns of missing data remains to be addressed.

Table S1. Patterns of infection detected by genotyping in sequences starting with positive samples, and their likelihoods

K	First sample	Second sample	Third sample	Likelihood
1	+	+	-, +, or missing	$L_1 = (1-M)S$
2	+	-	+	$L_2 = (1-M)^2(1-S)S$
3	+	-	-	$L_3 = 1 - L_2 - L_1$
4	+	-	Missing	$L_4 = 1 - L_1$
5	+	Missing	+	$L_5 = (1-M)^2S$
6	+	Missing	-	$L_6 = 1 - L_5$

The values of *M* and *S* can be estimated by maximum likelihood from the overall likelihood constructed by multiplying the likelihoods for all the observed triplets, or equivalently from the log likelihood:

$$lnL = \sum_{k=1}^{4} n_k lnL_k$$

where n_k is the frequency of triplet pattern *k* (Table S1) . Alternatively, a Bayesian Markov chain Monte Carlo (MCMC) algorithm can be employed using WinBugs or JAGS software assigning uniform priors to both *M* and *S* (see Appendix below). The decision points in Figure S1, then correspond to stochastic nodes with the probabilities for each branch proportional to the likelihoods from Table S1. The MCMC approach has the advantage of providing interval estimates for the parameters, and also allows the uncertainty in the estimation of M and S to be propagated in further calculations (e.g. bias-adjustments in estimates of the force of infection, see below).

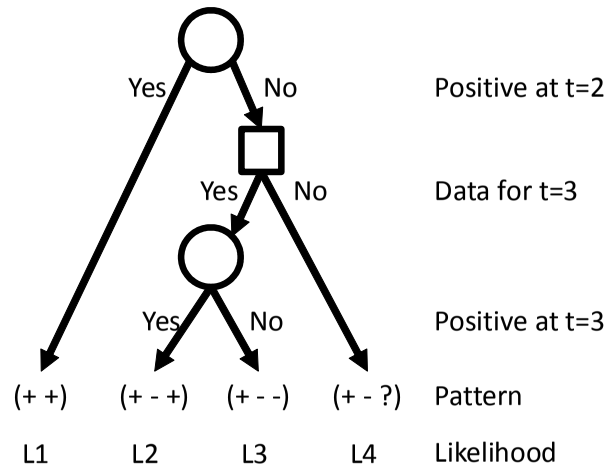

A: Analysis including only pairs and triplets with data at t=2

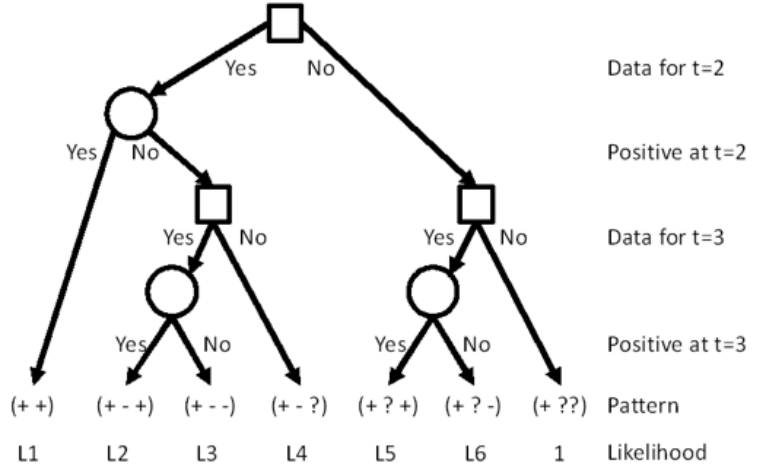

B: Analysis including triplets with missing data at t=2

Figure S1. Classification of triplets, illustrated as a branching process. The circles represent stochastic nodes; the squares represent branching where the frequencies depend on whether samples are available, and thus do not provide information about infection dynamics.

Table S2. Patterns of infection in sequences starting with samples testing negative for a specific genotype (i), and their probabilities of occurrence

K	True pattern (T)	Probability that this pattern occurs	Probability that the first sample tests negative	Probability that this pattern occurs and the first sample tests negative (*Pr*(T))	Probability (- -) is observed $Pr(--\,|\mathrm{T}=\mathrm{k})$ if the first sample tests negative	Probability (- +) is observed $Pr(-+\,|\mathrm{T}=\mathrm{k})$ if the first sample tests negative
1	-	$(1-p_i)(1-\Lambda_i)$	*1*	$(1-p_i)(1-\Lambda_i)$	*1*	0
2	+	$(1-p_i)\Lambda_i$	1	$(1-p_i)\Lambda_i$	$1-S$	S
3	+ -	p_iM	$1-S$	$p_iM(1-S)$	1	0
4	+ +	$p_i(1-M)$	$1-S$	$p_i(1-M)(1-S)$	$1-S$	S

Infection/Acquisition probability

The acquisition probability for each genotype is estimated from the data of sequential pairs of samples, where the sequence starts with a sample that typed negative. The naïve estimate of the average number of infections acquired in each interval for genotype, *i*, is then:

$$\Lambda'_i = \frac{n_{-+}}{n_{--} + n_{-+}}$$

where n_{-+} is the total number of "gains" (− +) divided by the total intervals at risk, which is computed from sum of the number of "gains", n_{-+} , and n_{--} , the number of (− −) pairs for the genotype. This is a biased estimate of the true probability that there is a new infection during the interval, Λ_i, because of imperfect detection, which might affect either the first or second sample of the pair. The bias depends on *M*, *S*, and also on p_i , the true point prevalence of the genotype (i.e. the proportion of hosts infected by it on average at a single time point) (Table S2).

The overall probability that the observed pattern for genotype *i* in any sequential pair of samples is (- -) is obtained as:

$$Pr(- \ -) = \sum Pr(\mathrm{T})Pr(- \ - \,|\mathrm{T} = \mathrm{k})$$

i.e.

$$Pr(- \ -) = (1-p_i)(1-\Lambda_i) + (1-S)(1-p_i)\Lambda_i + (1-S)p_iM + p_i(1-M)(1-S)^2,$$

and the overall probability that the observed pattern is (- +) is:

$$Pr(- \ +) = \sum Pr(\mathrm{T})Pr(- \ + \,|\mathrm{T} = \mathrm{k})$$

i.e.

$$Pr(- \ +) = S(1-p_i)\Lambda_i + p_i(1-M)(1-S)S.$$

In the large sample case, the observed proportion of intervals during which an infection appears to be acquired is then the ratio:

$$\Lambda'_i = \frac{Pr(- \ +)}{Pr(- \ -) + Pr(- \ +)}$$

which is therefore equivalent to:

$$\Lambda'_i = \frac{S\Lambda_i - Sp_i\big(\Lambda_i - (1-S)(1-M)\big)}{1 - Sp_i}$$

and,

$$\Lambda'_i = \frac{S\Lambda_i - p'_i\big(\Lambda_i - (1-S)(1-M)\big)}{1 - p'_i}$$

where: $p'_i = Sp_i$, is the point prediction of the observed prevalence which is estimated by:

$$\hat{p}'_i = \frac{n_+}{n_- + n_+}$$

n_- is the total number of samples testing negative for the genotype, and n_+ is the total testing positive.

Solving for Λ_i and substituting the field-based estimates, provides a formula for the bias adjusted estimate of Λ_i as a function of $\hat{p}'_i$ and of the estimated detectability, $\hat{S}$, and clearance probability, $\widehat{M}$.

$$\hat{\Lambda}_i = \frac{\Lambda'_i - \hat{p}'_i\left(\Lambda'_i + \left(1-\hat{S}\right)\left(1-\widehat{M}\right)\right)}{\hat{S} - \hat{p}'_i}$$

This is a correction to the formula originally published in 1999 (Smith et al., 1999).

The ratio, $\hat{\Lambda}_i/\Lambda'_i$ which measures the bias in the crude estimate of the number of new infections, is highly sensitive to $\hat{S}$. If detection is perfect, it has a value of 1.0, corresponding to no bias. At low values of $\hat{S}$, $\hat{\Lambda}_i$ can be substantially higher than Λ'_i especially if $\widehat{M}$ is high, corresponding to long survey intervals or rapid turnover of infections (Figure S2). Figure S2 At values of $\widehat{M}$ < 0.2 (within the ranges observed in field studies in Tanzania and Ghana (Sama et al., 2005; Smith et al., 1999) the ratio of $\hat{\Lambda}_i/\Lambda'_i$ is a non-monotonic function of $\hat{S}$ but remains fairly close to unity (implying only modest levels of bias). The bias is very insensitive to $\hat{p}'_i$ over a wide range of prevalence values. In general, since the analysis is applied to genotype specific data, $\hat{p}'_i$ is expected to be low.

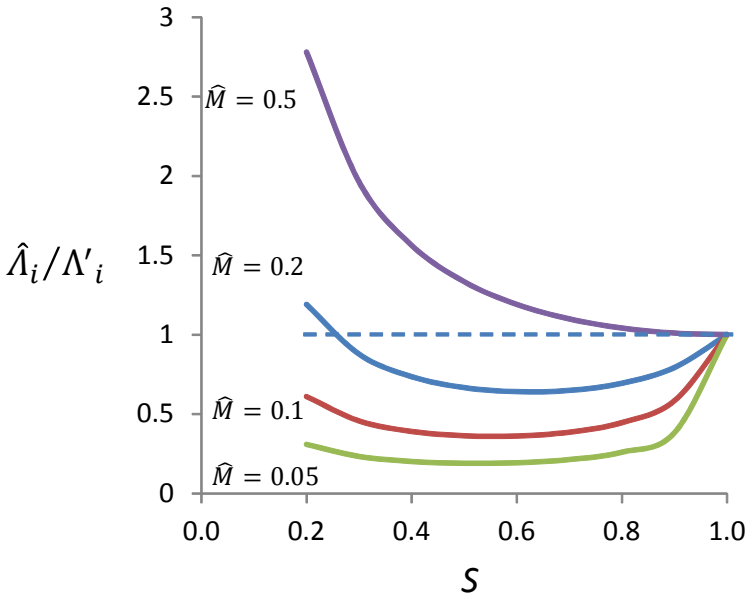

Figure S2. Bias in estimated force of infection. The quantity plotted is the ratio of the true value to the unadjusted estimate in each case for $\hat{p}'_i = 0.002$. The horizontal dashed line corresponds to the case of no bias.

Conversion to rates

$\widehat{M}$ and $\hat{\Lambda}_i$ are estimates of transition probabilities, and are therefore specific for the interval length used in any specific study. These must be converted to rates in continuous time if they are to be compared across studies with different interval durations. The continuous time analogues correspond to the reversible catalytic model (Bekessy et al., 1976; Muench, 1959). This provides expressions for transition probabilities as functions of the rates:

$$\hat{\Lambda}_i = \frac{\hat{\lambda}_i}{\hat{\lambda}_i + \widehat{\mu_\iota}}\left[1 - exp\left(-\left(\hat{\lambda}_i + \widehat{\mu_\iota}\right)t\right)\right]$$

and:

$$\widehat{M} = \frac{\widehat{\mu_\iota}}{\hat{\lambda}_i + \widehat{\mu_\iota}}\left[1 - exp\left(-\left(\hat{\lambda}_i + \widehat{\mu_\iota}\right)t\right)\right]$$

where t is the duration of the inter-survey interval, $\hat{\mu}$ is the estimate of the clearance rate, and $\hat{\lambda}_i$is the estimate of the genotype specific force of infection. Rearrangement of these formulae and solving for $\widehat{\mu_\iota}$ and $\hat{\lambda}_i$ gives:

$$\widehat{\mu_\iota} = \frac{-\widehat{M} ln\left(1 - \left(\hat{\Lambda}_i + \widehat{M}\right)\right)}{\left(\hat{\Lambda}_i + \widehat{M}\right)t}$$

and:

$$\hat{\lambda}_i = \frac{\hat{\Lambda}_i}{\widehat{M}}\widehat{\mu_\iota}$$

The overall force of infection is estimated as the sum of the individual $\hat{\lambda}_i$ values. Although we use a common value of $\widehat{M}$ across all genotypes, this analysis leads to slightly different values of $\widehat{\mu_\iota}$. The mean of these calculated allele-specific values is reported as the clearance rate, $\bar{\mu}$. The reported average duration of infection in days is then proportional to the reciprocal of this value, $1/\bar{\mu}$.

Interval estimation

Estimation of force of infection, clearance rates, and detectability can be carried out by Maximum Likelihood, or alternatively by Bayesian MCMC. The latter has the advantage that it provides sampling-based interval estimates for all the parameters, potentially allowing for the uncertainties at each stage of the algorithm. Code for MCMC estimation is appended.

Discussion and application of this approach to the study cohort

Adaptation of the triplet approach to *P. vivax* was a major challenge in part because our study design included initially two-weekly and later monthly intervals, but mainly because the approach takes into account a window of 3 consecutive samples independent of the exact time interval between sampling. This is a shortfall of the triplet approach, because a genotype that appeared once, remained undetectable for the next 2 time points and reappeared thereafter would be considered as two new infections. This scenario was observed 52 times, 10 times in PQ arm and 42 times in placebo arm. As a consequence the durations in the placebo arm might have been underestimated. Therefore the PQ-cleared portion of $_{mol}$FOB may have been overrated by underestimating the duration of infection in placebo arm. However, also the opposite trend could be true: the duration of infection in the placebo arm may be composed of several short-term relapses of identical genotype. Thus, the real duration of relapsing infections would be shorter, but owing to short intervals between relapsing infections, the model regards relapses as a continuous infection. Relapses are only taken as new infections if relapses of identical genotype have a latency period as long as at least 28 days in early phase of cohort (corresponding to two intervals of 14 days) and 60 days in last five months of the follow up period (2 monthly intervals). If the latency period of relapses were shorter, they would be considered as continuous infection with a missed detection in one follow up sample. This possibility poses a threat for the triplet approach, as short lasting relapses may be common in tropical areas and were reported to have a latency period of three weeks if short-eliminating antimalarials were given (Battle et al., 2014; White, 2011).

WinBugs/JAGS code for estimating $\widehat{M}$, S, $\hat{\lambda}_i$, $\widehat{\mu_i}$.

 # IMPLEMENTATION OF THE MODEL OF FIGURE S1A WITH DETERMINISTIC ESTIMATION OF THE FORCE OF INFECTION

```
model {
#ESTIMATION OF M AND S
  L1<- (1-M)*S
  L2<- (1-M)*(1-M)*(1-S)*S
  L3<- 1 - L1- L2
  L4<- 1 - L1

#
  pr2<- L2/(L2+L3)
  s1total <- n11+n101+n100+n10
  s2total <- n101+n100

# binomial sampling of stochastic nodes 1, 2
  n11  ~ dbin(L1,s1total)
  n101 ~ dbin(pr2,s2total)

# uniform prior for M and S
  M ~ dunif(0,1)
  S ~ dunif(0,1)

#ESTIMATION OF FORCE OF INFECTION AND BIAS ADJUSTMENT
 for (i in 1:NumberOfGenotypes)
   {
   L[i] <- (lambdaPrime[i] - p[i]*(lambdaPrime[i] + (1-M)*(1-S)))/(S - p[i])
   p[i] <- n1[i]/n[i]
   lambdaPrime[i] <- n01[i]/n0[i]

# transform to continuous time
   muDaily[i]<- -M*log(1-(L[i]+ M))/((L[i]+M)*t)
   lambdaDaily[i]<- -L[i]*log(1 - (L[i]+M))/((L[i]+M)*t)
 }

#summaries over all genotypes
ClearanceDaily<-mean(muDaily[])
FOIDaily<-sum(lambdaDaily[])
}


# TEST DATA

list(NumberOfGenotypes=7, n11=211, n101=61, n100=209,n10=71,t=14)

n0[]  n01[]  n[]     n1[]
560 11      3000    53
560 18      3000    57
560 10      3000    43
560 9       3000    23
560 11      3000    56
560 15      3000    72
560 5       3000    15
END

# EXAMPLE INITIAL VALUES (1 CHAIN)
list(
M = 0.1440881879701678,
S = 0.4112187770372916,
logitlambdaPrime = c(
-4.207892579282936,-4.168605593430168,-3.965568672495186,-4.388163834738868,-3.892549139358283,
```

```
-3.908037902822194,-5.066532048318275),
logitlambdaPrimebar = -3.823480945836294,
logitp = c(
-4.086307570550217,-4.004132629521775,-4.390522771059175,-4.994397880509394,-3.750283683731104,
-3.892052972624451,-5.191441694450187),
logitpbar = -4.172449215059147,
tau = 2.818547930754359,
taup = 2.08985431148514)
```

 # IMPLEMENTATION OF THE MODEL OF FIGURE S1B WITH STOCHASTIC ESTIMATION OF THE FORCE OF INFECTION

```
model {
#ESTIMATION OF M AND S
  L1<- (1-M)*S
  L2<- (1-M)*(1-M)*(1-S)*S
  L3<- 1 - L1- L2
  L4<- 1 - L1
  L5<- (1-M)*(1-M)*S
  L6<- 1 - L5
#
  pr2<- L2/(L2+L3)
  pr3<- L5/(L5+L6)
  s1total <- n11+n101+n100+n10
  s2total <- n101+n100
  s3total <- n1_1+n1_0

# binomial sampling of stochastic nodes 1, 2 and 3
  n11  ~ dbin(L1,s1total)
  n101 ~ dbin(pr2,s2total)
  n1_1 ~ dbin(pr3,s3total)

# uniform prior for M and S
  M ~ dunif(0,1)
  S ~ dunif(0,1)

#ESTIMATION OF FORCE OF INFECTION AND BIAS ADJUSTMENT
 for (i in 1:NumberOfGenotypes)
   {
   L[i]<- (lambdaPrime[i] - p[i]*(lambdaPrime[i] + (1-M)*(1-S)))/(S - p[i])
   n1[i]~dbin(p[i],n[i])
   n01[i]~dbin(lambdaPrime[i],n0[i])

# random effects for genotype specific prevalence and incidence
   lambdaPrime[i]<- 1/(1+exp(-logitlambdaPrime[i]))
   logitlambdaPrime[i]~dnorm(logitlambdaPrimebar,tau)
   p[i]<- 1/(1+exp(-logitp[i]))
   logitp[i]~dnorm(logitpbar,taup)

# transform to continuous time
   muDaily[i]<- -M*log(1-(L[i]+ M))/((L[i]+M)*t)
   lambdaDaily[i]<- -L[i]*log(1 - (L[i]+M))/((L[i]+M)*t)
 }

#priors for metaparameters of random effects
logitlambdaPrimebar~dnorm(0,1.0E-2)
tau~dunif(0,10)
logitpbar~dnorm(0,1.0E-2)
taup~dunif(0,10)

#summaries over all genotypes
ClearanceDaily<-mean(muDaily[])
FOIDaily<-sum(lambdaDaily[])
}
```

```
# TEST DATA

list(NumberOfGenotypes=7, n11=211, n101=61, n100=209,n10=71,n1_0=30,n1_1=10,t=14)

n0[]  n01[] n[]     n1[]
560 11      3000    53
560 18      3000    57
560 10      3000    43
560 9       3000    23
560 11      3000    56
560 15      3000    72
560 5       3000    15
END

# EXAMPLE INITIAL VALUES (1 CHAIN)

list(
M = 0.2938271930359447,
S = 0.5093814682038473,
logitlambdaPrime = c(
-3.562748062328747,-3.678312884623953,-3.841609547868719,-4.561559522968858,-3.54204822963872,
-3.543603660614651,-4.123941440039693),
logitlambdaPrimebar = -3.637727825838637,
logitp = c(
-4.164460955662759,-4.017057261011612,-4.191668882209104,-4.558031283327824,-3.778424732596439,
-3.785125363187561,-4.934854572547822),
logitpbar = -4.653282454126015,
tau = 2.097024953285597,
taup = 2.599193884837493)


# M,S, ClearanceDaily and FOIDaily are the main parameters of interest.
```

Supplementary Figure S2

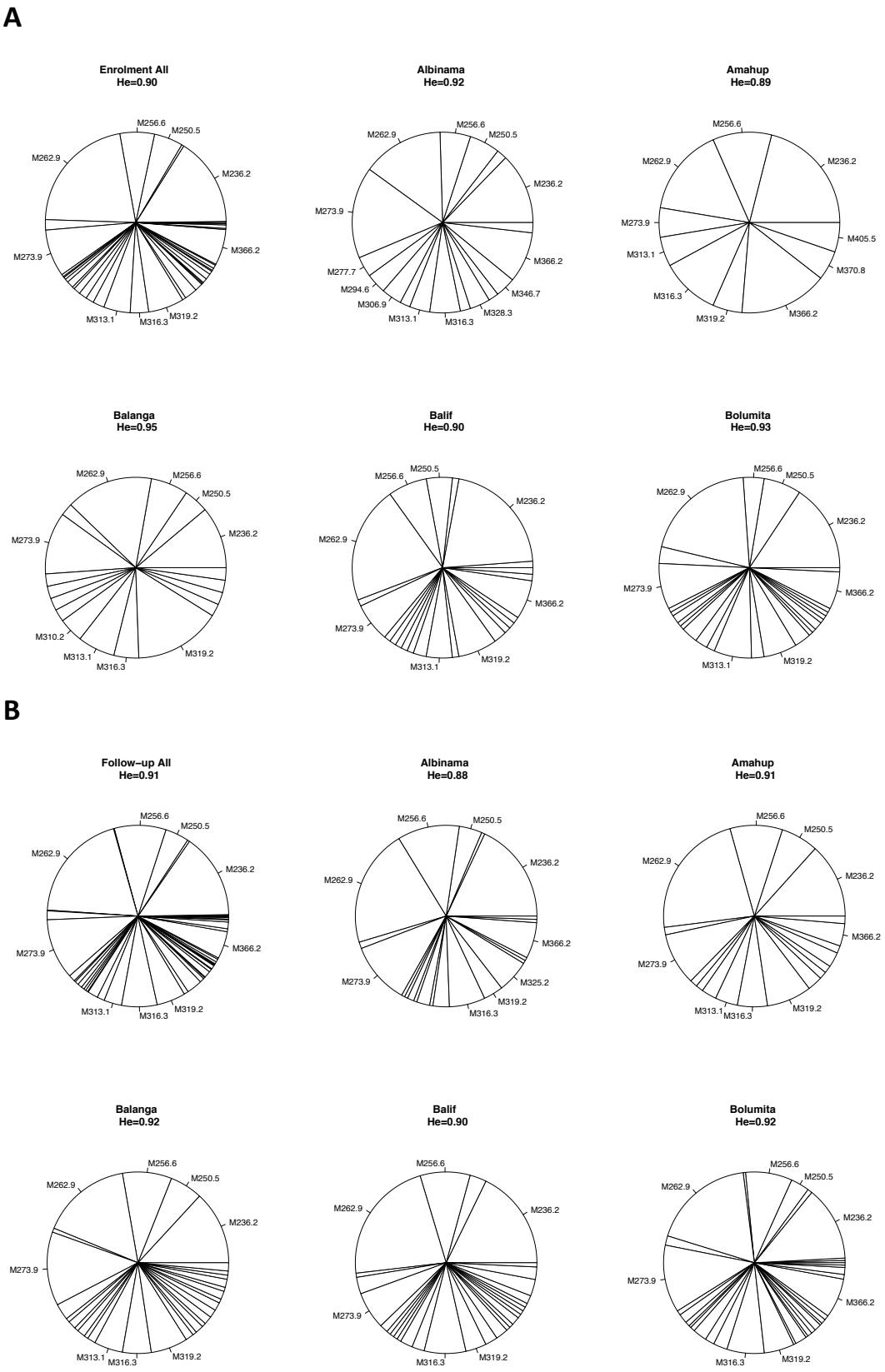

Figure S1. Allelic diversity and heterozygosity by village. **A**. At enrolment. Alleles with prevalence above 0.03 were labeled. Expected heterozygosity (H_E) was calculated according to Koepfli and co-workers (Koeplfi 2011). **B**. During follow up. Each allele was counted only once per child.

Chapter 6: *Plasmodium vivax* and *P. falciparum* Transmission-stage Dynamics

Full title:

Effects of Liver-Stage Clearance by Primaquine on Gametocyte Carriage of *Plasmodium vivax* and *P. falciparum*

Rahel Wampfler[1,2], Natalie E. Hofmann[1,2], Stephan Karl[3,4], Inoni Betuela[5], Benson Kinboro[5], Mariabeth Silkey[1,2], Leanne J. Robinson[3,4,5], Ivo Mueller[3,4,6,7], Ingrid Felger[1,2]

[1]Swiss Tropical and Public Health Institute, Basel, Switzerland
[2]University of Basel, Basel, Switzerland
[3]Divison of Population Health and Immunity, The Walter and Eliza Hall Institute of Medical Research, Parkville, Australia
[4]Department of Medical Biology, University of Melbourne, Victoria, Australia
[5]Vector Borne Diseases Unit, PNG Institute of Medical Research, Madang & Maprik, Papua New Guinea
[6]Malaria Parasites & Hosts Unit, Institut Pasteur, Paris, France.
[7]ISGlobal, Barcelona Ctr. Int. Health Res. (CRESIB), Hospital Clínic - Universitat de Barcelona, Barcelona, Spain

– This manuscript will be submitted to PLOS NTD after further revisions –

Abstract

Background

Primaquine (PQ) is the only currently licensed antimalarial that eliminates *Plasmodium vivax* (*Pv*) hypnozoites. It also clears mature *P. falciparum* (*Pf*) gametocytes, thereby reducing post-treatment transmission. Randomized PQ treatment in a treatment-to-reinfection cohort in Papua New Guinean children permitted to study *Pv* and *Pf* gametocyte carriage after radical cure and to investigate the contribution of *Pv* relapses.

Methods

Children received radical cure with Chloroquine, Artemether-Lumefantrine plus either PQ or placebo. Blood samples were subsequently collected in 2-to 4-weekly intervals over 8 months. Gametocytes were detected by quantitative reverse transcription-PCR targeting *pvs25* and *pfs25*.

Results

PQ treatment reduced the incidence of *Pv* gametocytes by 73%, which was comparable to the effect of PQ on incidence of blood-stage infections. 92% of *Pv* and 79% of *Pf* gametocyte-positive infections were asymptomatic. *Pv* and to a lesser extent *Pf* gametocyte positivity and density were associated with high blood-stage parasite densities. Multivariate analysis revealed that the odds of gametocytes were significantly reduced in mixed-species infections compared to single-species infections for both species (OR_{Pv}=0.39 [95% CI 0.25-0.62], OR_{Pf}=0.33 [95% CI 0.18-0.60], p<0.001). No difference between the PQ and placebo treatment arms was observed in density of *Pv* gametocytes or in the proportion of *Pv* infections that carried gametocytes. First infections after blood-stage and placebo treatment, likely caused by a relapsing hypnozoite, were equally likely to carry gametocytes than first infections after PQ treatment, likely caused by an infective mosquito bite.

Conclusion

Pv relapses and new infections are associated with similar levels of gametocytaemia. Relapses thus contribute considerably to the *P. vivax* transmission reservoir highlighting the importance of effective anti-hypnozoite treatment for efficient control of *Pv*.

Key words: Plasmodium vivax, Plasmodium falciparum, gametocytes, relapses, hypnozoites, pvs25, pfs25, Primaquine, Artemether-Lumefantrine, Chloroquine, mixed-species infection

Introduction

Primaquine (PQ) is the only currently licensed drug for clearance of *Plasmodium vivax* (*Pv*) hypnozoites in the liver (John et al., 2012), and also the only effective drug against mature gametocytes of *P. falciparum* (*Pf*) (Eziefula et al., 2014; Shekalaghe et al., 2007). Since 2012, the World Health Organization recommends a single dose of PQ for treatment of *Pf* infections with the aim to reduce post-treatment *Pf* gametocyte carriage and thus the potential for onward malaria transmission (WHO, 2012).

Gametocyte development as well as morphology differs considerably between *Pv* and *Pf* (Bousema and Drakeley, 2011). *Pv* gametocytes mature rapidly and are detectable in the peripheral blood as early as two or three days following detection of blood-stage parasites by qPCR or light microscopy (LM), respectively (McCarthy et al., 2013; McKenzie et al., 2007). In contrast, *Pf* gametocytes sequester for 7-10 days in the bone marrow before being released into the blood circulation (Aguilar et al., 2014), where they are observed by LM 10-15 days after the first detection of asexual parasites (Eichner et al., 2001). Gametocytes were observed in symptomatic *Pv* episodes at higher frequency compared to *Pf* episodes, despite 10-fold lower blood-stage *Pv* densities compared to *Pf* (Mckenzie et al., 2006). After drug treatment, *Pv* gametocytes are cleared within days after clearance of blood-stage infections in contrast to *Pf* gametocytes, which circulate over 3 weeks following successful blood-stage clearance (Bousema et al., 2010; Eichner et al., 2001; McCarthy et al., 2013; Pukrittayakamee et al., 2008). Altogether the published data suggests that *Pv* infections produce proportionally higher gametocyte densities than *Pf* infections (at the same levels of asexual parasitaemia), and that *Pv* gametocytes mature more rapidly (Eichner et al., 2001; Nacher et al., 2004; Pukrittayakamee et al., 2008; Taylor and Read, 1997).

Not much is known on gametocyte production in primary *Pv* infections versus relapses from activated hypnozoites, mainly because in endemic settings it is impossible to distinguish both sources of infection. Our previous work in Papua New Guinea (PNG) showed that relapsing *Pv* infections contributed 73% of the gametocyte carriage (Robinson et al., 2015). A study in Thailand and Indonesia reported that densities by LM of *Pv* blood-stage parasites and gametocytes were similar in new infections and relapses (Douglas et al., 2013). Both studies indicated the need for efficient treatment of the hypnozoite reservoir for reducing *Pv* transmission (Douglas et al., 2013; Robinson et al., 2015).

A challenge in studying the investment of *Pv* infections in gametocytogenesis is the generally low and often submicroscopic density of asexual parasites and gametocytes. In addition, scarce *Pv* gametocytes can easily be misclassified by LM due to their resemblance to late trophozoites (WHO, 2010). Investigating gametocyte production of *Pv* infections hence requires sensitive molecular methods. For *Pf,* studying gametocytes by LM is more feasible because of the distinct crescent-shaped morphology of gametocytes and generally higher parasite densities; however also

for *Pf*, molecular methods are crucial for studying gametocytes in low-density *Pf* infections. Molecular detection of gametocytes usually targets transcripts of the *Pf* or *Pv* 25 kDa ookinete surface antigen precursor (*pfs25* or *pvs25*, respectively) (Schneider et al., 2004; Wampfler et al., 2013), which are highly expressed in mature gametocytes (Bozdech et al., 2008; Young et al., 2005). Both *pfs25* and *pvs25* quantitative reverse transcription PCR (qRT-PCR) or nucleic acid sequence-based amplification (NASBA) can detect as few as 1 *Pf* gametocyte or 10 *Pv* gametocytes per 50 µl blood and are therefore up to 50x more sensitive than LM (Koepfli et al., 2015; Schneider et al., 2004; Wampfler et al., 2013).

This study investigated gametocyte dynamics of *Pf* and *Pv* infections in school-aged PNG children after randomized treatment with blood-stage antimalarials plus PQ or placebo. This trial design permitted to quantify the contribution of hypnozoites to parasitological parameters assessed during follow-up by comparing treatment arms (Robinson et al., 2015). The present study aimed to extend in greater detail our previous analysis of gametocyte carriage in these children by addressing the following questions: (i), what are risk factors for *Pf* and *Pv* gametocyte carriage? (ii), does gametocytaemia differ between *Pv* new infections and relapses? And (iii), does PQ treatment exert a long-term effect on *Pf* and *Pv* gametocytaemia?

Methods

Study design

The study was conducted in 2009 to 2010 in the Albinama area, East Sepik province, in PNG. A detailed study protocol has been published previously (Robinson et al., 2015). 504 children aged 5 to 10 years were randomized to two treatment arms and completed directly observed treatment (DOT) with a 3-day dose of Chloroquine (CQ), a 3-day dose of Artemether-Lumefantrine (AL) and either 20 doses of PQ (per day: 0.5 mg/kg) or placebo over four weeks. Venous blood samples were collected at enrolment (prior to treatment) and 3 days after the final dose of DOT. The latter date represented day 0 of follow-up. Finger-prick samples were taken every two weeks for the first 3 months and monthly for the remaining 5 months of follow-up. Symptomatic children detected during follow-up were treated with a 3-day course of AL after confirming *Plasmodium* infection by rapid diagnostic test (RDT, CareStart^{TM}Malaria pLDH/HRP2 Combo, AccessBio, USA). The study received ethical clearance by the PNG Institute of Medical Research (IMR) Institutional Review Board (0908), the PNG Medical Advisory Committee (09.11), the Ethikkommission beider Basel (237/11) and was registered on ClinicalTrial.gov (NCT02143934).

Detection of blood-stage parasites and gametocytes

All blood samples collected were examined by LM and quantitative PCR (qPCR). Blood slides were examined by at least two independent microscopists and declared parasite negative only after examination of 200 thick-film fields (Robinson et al., 2015). Parasite DNA was extracted from

100-150 µl blood cell pellet using the FavorPrep™ 96-well genomic DNA extraction kit (Favorgen, Taiwan) and analyzed for *Pf* and *Pv* positivity by *18S rRNA* qPCR (Wampfler et al., 2013). All *Pv* and *Pf* qPCR positive samples were genotyped using markers *Pv-msp1*F3 and *Pf-msp2*, respectively, following previously published protocols (Koepfli et al., 2011; Schoepflin et al., 2009).

RNA was extracted from all samples positive in *Pf* or *Pv* qPCR. RNA was extracted using the RNEasy 96 kit (Qiagen, Switzerland) as described previously (Wampfler et al., 2013) from 50µl whole blood spotted on filter papers that had been air-dried and stored in TRIzol reagent (Life Technologies, Switzerland). Gametocyte-specific transcripts were detected by *pfs25* or *pvs25* qRT-PCR (Wampfler et al., 2013) in all RNA samples for which the corresponding DNA sample had been positive by species-specific qPCR.

Statistical analysis

Children were censored on the last visit before two consecutively missed scheduled follow-up visits (Robinson et al., 2015). Comparison of LM-positive versus submicroscopic infections, and symptomatic versus asymptomatic infections was performed with 5019 samples from the follow-up period for which LM data was available. A symptomatic malaria episode was defined as fever (axillary temperature >37.5°C and/or fever reported in previous 2 days) and the presence of *Plasmodium spp*. parasites by LM.

Differences in proportions were tested for statistical significance using X^2 test with continuity correction. To achieve normal distribution, qPCR densities were expressed as $\log_{10}$-transformed *18S rRNA* genomic copies/µl blood for asexual parasites, and $\log_{10}$-transformed *pfs25* or *pvs25* transcripts/µl blood for gametocytes. Geometric means of densities were calculated. Differences in densities of asexual or sexual-stage parasites were tested for statistical significance using Welch's Two-sample t-test.

Negative binomial regression models were used to calculate the incidence rate of *Pv* and *Pf* gametocyte positivity as previously described (Robinson et al., 2015). Gametocyte positivity during follow-up was modeled using binomial generalized estimating equations (GEE) with logit link using an exchangeable correlation matrix. Log_{10}-transformed blood-stage parasite density and gametocyte density during follow-up were modeled using Gaussian GEEs with log link using an exchangeable correlation matrix. Linear fit for $\log_{10}$-transformed blood-stage parasite density was previously analyzed and considered adequate for both species (Supplementary Document S1). All Models were back selected. Statistical analyses were conducted using R version 3.1.1 (R Core Team, 2014) or STATA version 14.

Results

Gametocyte positivity and density in submicroscopic infections

Molecular methods were superior to LM especially for detection of gametocytes but also for blood-stage parasites (Figure 1). By LM *Pv* gametocytes were detected in only 44 out of 366 *Pv* positive samples (12%), whereas by molecular detection 265 out of 705 *Pv* samples (38%, p<0.001) were gametocyte-positive. *Pf* gametocyte rates by LM were 21% (52/237) and by qRT-PCR 25% (107/426). 84% [CI_{95}: 79-88%] and 53% [CI_{95}: 43-63%] gametocytaemia was submicroscopic, for *Pv* and *Pf* respectively (Figure 1A and 1D). In three samples gametocytes were detected by LM but not by qRT-PCR, indicating RNA degradation. Due to the low sensitivity of LM in gametocyte detection, all further results presented here derive from molecular gametocyte detection.

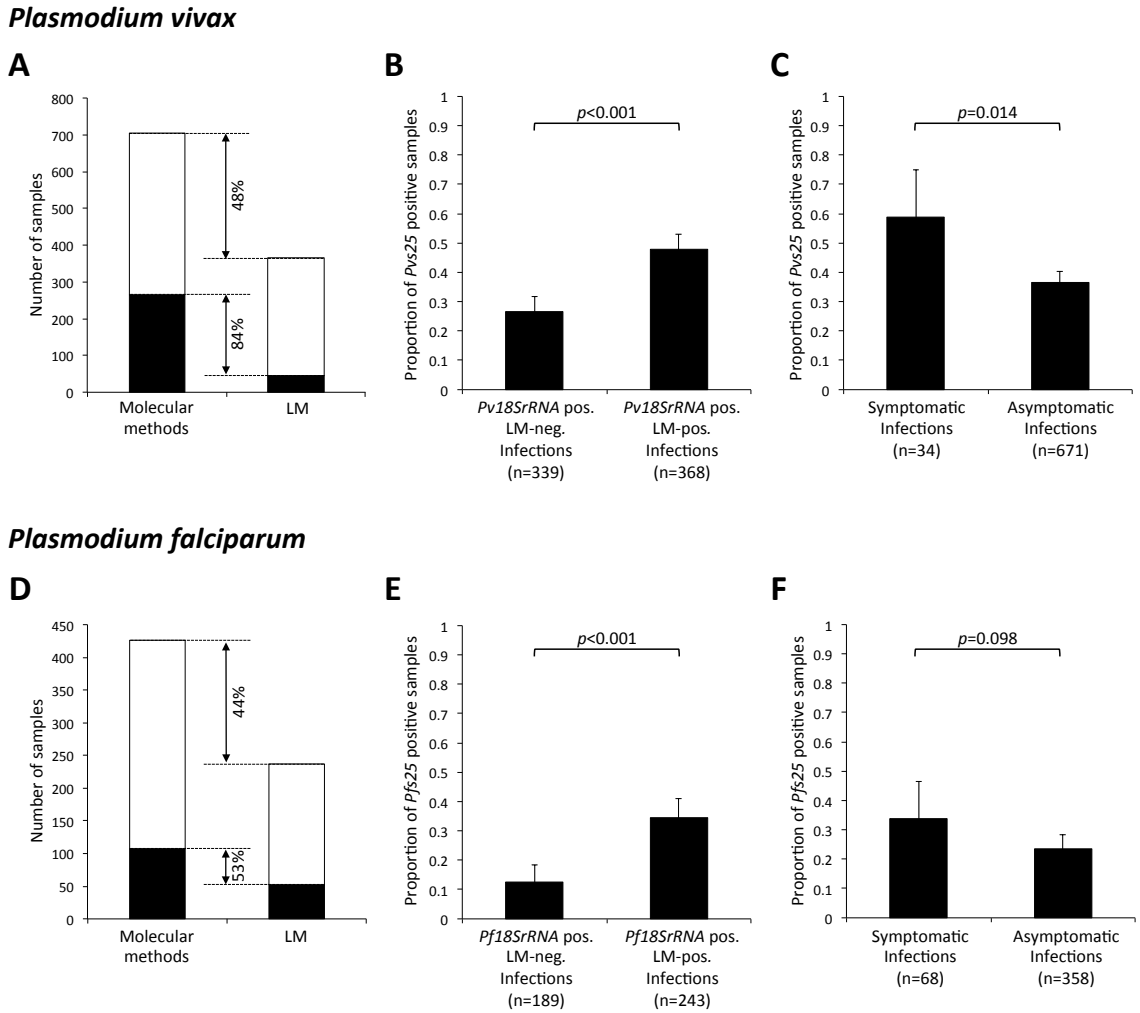

Figure 1. *Pv* (top) and *Pf* (bottom) gametocyte positivity among 5019 follow-up samples. (**A, D**) Detection of blood stage parasites and gametocytes by LM and molecular methods, using *pv18S* or *pf18S rRNA* qPCR for detection of blood-stage parasites and *pvs25* or *pfs25* qRT-PCR for detection of gametocytes. Black: gametocyte positive samples. White: parasite positive samples without gametocytes. (**B**, **E**) Proportion of gametocytes positives (by molecular methods) in submicroscopic and LM-positive samples. (**C**, **F**) Proportion of gametocyte positives (by molecular methods) in symptomatic and asymptomatic infections. Error bars indicate 95% confidence intervals by X^2 distribution.

Significantly more *Pv* infections carried qRT-PCR detectable gametocytes compared to *Pf* (38% vs. 25%, $p<0.001$). Microscopically patent infections of both species carried gametocytes more often than submicroscopic infections (*Pv*: 48% vs. 27%, *Pf*: 35% vs. 13%, $p<0.001$, Figure 1B and 1E). Similarly, gametocyte-specific transcript numbers were significantly higher in LM-positive than LM-negative samples for both species (Supplementary Document S2).

Gametocyte positivity and density in symptomatic versus asymptomatic infections

During the follow-up period, 34 *Pv* episodes and 68 *Pf* clinical episodes were observed. The proportion of gametocyte carriers was 22% higher in symptomatic infections compared to asymptomatic *P. vivax* infections (59% vs. 37%, $p=0.014$, Figure 1C). For *P. falciparum*, a similar trend was observed but did not reach statistical significance (34% vs. 23%, $p=0.098$, Figure 1F). However, due to a much higher number of asymptomatic than symptomatic infections, the overwhelming majority of *Pv* and *Pf* gametocyte carriage (92% [CI_{95}: 88-95%] and 79% [CI_{95}: 69-86%]) occurred in asymptomatic children. *Pv* gametocyte densities mirrored asexual densities well in both symptomatic and asymptomatic infections, but this was not the case for *Pf* (Supplementary Document S3).

The effect of PQ treatment on gametocytaemia during follow-up

Pv gametocyte prevalence increased steadily throughout the follow-up period and was on average almost 3-fold higher in the placebo arm than in the PQ arm, similar to patterns observed in *Pv* blood-stage parasite prevalence (*Pv* gametocytes median fold difference PL>PQ: 2.9 [IQR: 2.0-3.8], *Pv* blood-stages median fold difference PL>PQ: 2.8 [IQR: 2.2-4.2], Figure 2A). No difference in *Pf* gametocyte prevalence was observed between study arms (*Pf* gametocytes median fold difference PL>PQ 1.0 [IQR: 0.7-1.4], *Pf* blood-stages median fold difference PL>PQ: 1.1 [IQR: 0.9-1.3], Figure 2B).

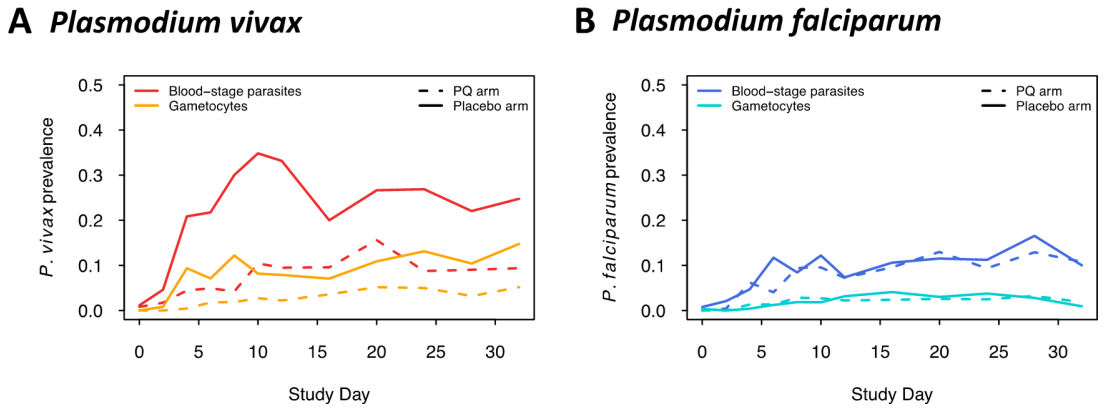

Figure 2. Prevalence of blood-stage parasites and gametocytes of *Pv* (**A**) and *Pf* (**B**) during follow-up by treatment arm.

To assess in detail *Pv* gametocyte production in primary infections versus relapses, we compared gametocyte positivity and density in first infections after blood-stage plus placebo (first *Pv* infection either from relapse (80%) or infective bite (20%) or blood-stage plus PQ treatment (first *Pv* infection always from infective bite) (Robinson et al., 2015). We also assessed subsequent *Pv* infections, i.e. all but the first parasite-positive sample per child, which in both arms can result from an ongoing infection, a relapsing hypnozoite or a new infection from a mosquito. First *Pv* re-infections after baseline treatment were equally likely to carry gametocytes in both treatment arms (PQ: 29% vs. Placebo: 31%, Figure 3A), and the same was observed for subsequent infections (PQ: 42% [CI_{95}: 32-52%] vs. Placebo: 41% [CI_{95}: 36-47%], p=1). To investigate whether gametocyte densities were simply following the asexual densities or if other factors play a role, we compared absolute as well as normalized gametocyte densities. Gametocyte densities were normalized by

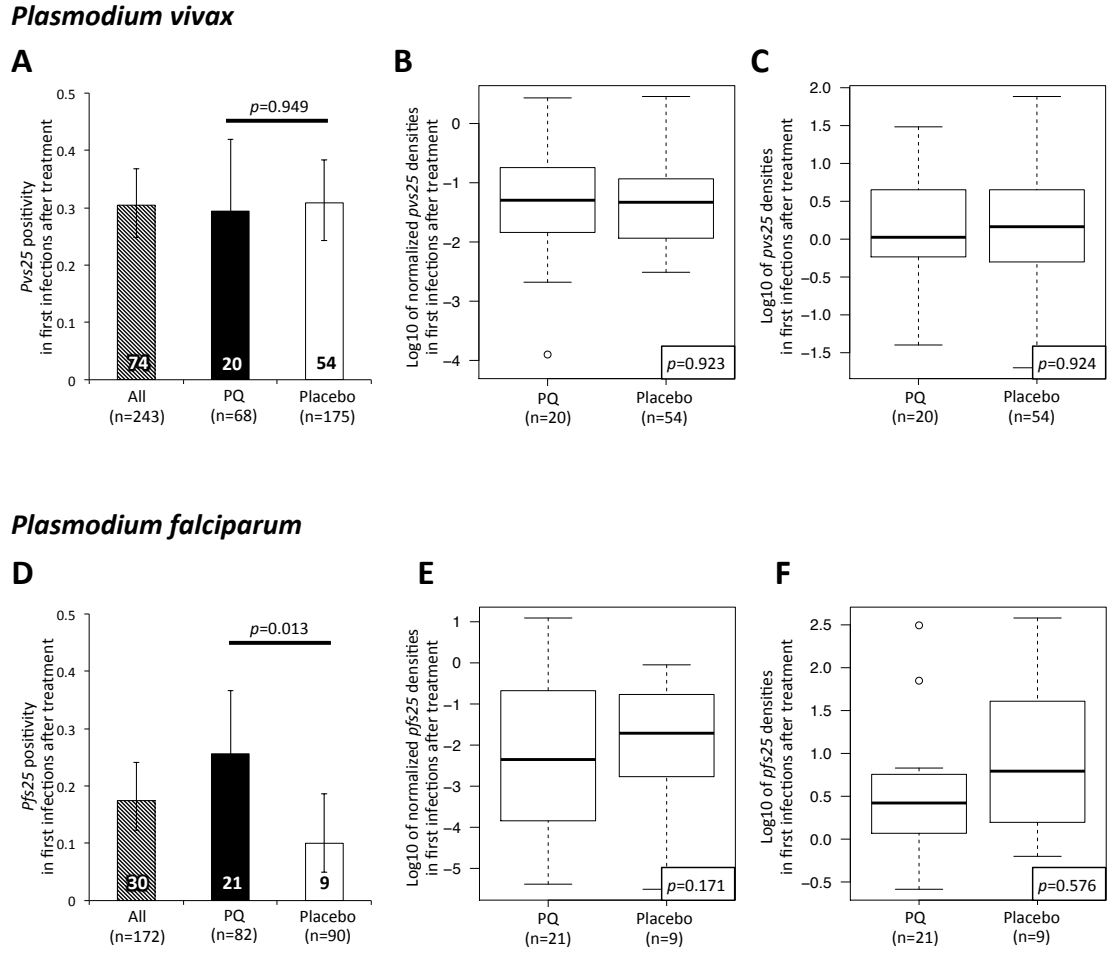

Figure 3. Gametocyte positivity and density in first *Pv* (top) and *Pf* (bottom) infections after treatment with blood-stage antimalarials alone (placebo) or blood-stage antimalarials plus PQ (PQ). **A**. and **D**. Proportion of *Pv* and *Pf* gametocyte carriers among first infections by treatment arm. Figures within the bars indicate absolute numbers of gametocyte-positive first infections following treatment. Error bars indicate 95% confidence intervals by X^2 distribution. **B**. and **E**. Normalized *Pv* and *Pf* gametocyte densities in first infections by treatment arm. Densities were normalized by dividing *pvs25* or *pfs25* transcript numbers/µl by *Pv-* or *Pf-18S rRNA* copy numbers/µl. **C**. and **F**. Absolute *Pv* and *Pf* gametocyte densities in first infections by treatment arm. Densities are expressed as log_{10} of *pvs25* and *pfs25* transcripts/µl.

dividing *pvs25* or *pfs25* transcript numbers/µl by *Pv-* or *Pf-18S rRNA* copy numbers/µl. Absolute and normalized *Pv* gametocyte densities did not differ between treatment arms in first infections (Figure 3B and 3C) nor in subsequent infections (Supplementary Document S4).

We also investigated *Pf* gametocyte carriage by comparing *Pf* gametocyte positivity and density in first *Pf* infections after treatment. Significantly more *Pf* gametocyte carriers were observed among first infections in the PQ-arm compared to the placebo arm (PQ: 26% vs. Placebo: 10%, Figure 3D). No significant difference between trial arms was observed in subsequent samples (PQ: 30% [CI_{95} 22-39%] vs. Placebo: 31% [CI_{95} 23-40%], p=0.961). *Pf* absolute and normalized gametocyte densities did not differ significantly between the treatment arms (Figure 3E and 3F, Supplementary Document S4).

Risk factors for gametocytes positivity and density

Pv gametocytes were detected more frequently (Table 1, OR for 1-log increase of density=1.95, $p<0.001$) and in higher densities (Table 2, $p<0.001$) with increasing blood-stage parasite density. Apart from reducing the number of *Pv* positive samples during follow-up (Supplementary Document S5), PQ treatment had no further effect on *Pv* gametocyte positivity (Table 1).

In *Pv* positive samples, the odds of *Pv* gametocytes were 60% reduced and gametocyte densities were 30% lower in mixed *Pf*/*Pv* infections compared to single-species *Pv* infections (Table 1, $p<0.001$; Table 2 $p=0.003$). The odds for *Pv* gametocyte carriage increased significantly over the whole follow-up period (Table 1 and Figure 2, $p<0.001$), and a 36% reduction on the odds of being gametocyte positive was observed in first *Pv* infections compared to subsequent infections (Table 1, $p=0.040$). No other factors were associated with the odds for *Pv* gametocyte carriage during follow-up (Table 1). *Pv* gametocyte density, but not positivity, decreased with age (Table 2, $p=0.017$) following the age trend in asexual parasites (Table 3, (Hofmann et al., in preparation)).

As for *Pv* gametocytes, the odds for *Pf* gametocytes were 70% reduced in mixed *Pf*/*Pv* infections compared to single-species *Pf* infections (Table 1, $p<0.001$). As an effect of delayed *Pf* gametocyte maturation, gametocyte positivity was 55% lower in first *Pf* infections compared to subsequent infections (Table 1, $p=0.007$). Other risk factors for *Pf* gametocytes were investigated, but none of the parameters tested was significant. The *Pf* gametocyte positivity was slightly higher in samples with high asexual densities, yet this association did not reach the 5% significance level (Table 1, OR for 1-log increase of density=1.23, $p=0.059$). In contrast to *Pv, Pf* gametocyte densities were not associated with any of the factors assessed (Supplementary Document S1). Fever was strongly associated with increasing blood-stage *Pf* parasitaemia (Table 3, OR=2.41, $p<0.001$), but had no effect on gametocyte density.

Analysis of only subsequent infections showed similar results to the analysis of the entire follow-up period (Supplementary Document S6). Considering subsequent infections only, *Pv*

gametocytes were reduced by 47% [13-68%] and *Pf* gametocytes were reduced by 63% [26-82%] in mixed-species infections compared to single-species infections (*Pv* *p*-value: 0.013, *Pf* *p*-value: 0.006, Supplementary Document S6). The effect of mixed-species co-infection on gametocyte carriage in first positive samples following treatment was not possible to be analyzed because of too small sample size for either species.

Table 1. Multivariable predictors of *Pv* and *Pf* gametocyte positivity during follow-up.

	Pv gametocyte positive				*Pf* gametocyte positive			
	OR	95% CI		*p*-value	OR	95% CI		*p*-value
Blood-stage density (by qPCR), per 10x increase	1.95	1.47	2.58	<0.001	1.23	0.99	1.51	0.059
PQ treatment	1.03	0.68	1.58	0.878	1.21	0.78	1.90	0.395
Mixed *Pf*/*Pv* (by qPCR)	0.39	0.25	0.62	<0.001	0.33	0.18	0.60	<0.001
First infection	0.64	0.42	0.98	0.040	0.45	0.25	0.81	0.007
Days after DOT (ref:0-60)								
61-120	0.59	0.39	0.89		1.31	0.62	2.76	
121-180	1.48	0.91	2.42	<0.001	1.32	0.63	2.75	0.266
>180	2.54	1.47	4.39		0.73	0.32	1.67	
Constant	0.36	0.22	0.59	<0.001	0.29	0.11	0.77	<0.013

OR, odds ratio, DOT, directly observed treatment. ORs were obtained using binomial generalized estimating equations with logit-link allowing for repeated visits by back-selection from the full model. The full model included fever, infection status at enrolment by qPCR (*Pf* or *Pv* positive), LLIN use (less than 100%), sex, village of residence, hemoglobin at baseline (>9 g/dl), age. No significant interaction of PQ treatment with days post DOT was detected.

Table 2. Multivariable predictors of *Pv* and *Pf* gametocyte density during follow-up.

	Pv gametocyte density			
	exp(β)	95% CI		*p*-value
Blood-stage density (by qPCR) per 10x increase	1.37	1.20	1.56	<0.001
PQ treatment	0.97	0.80	1.18	0.765
Mixed *Pf*/*Pv* (by qPCR)	0.73	0.59	0.90	0.003
Age	0.94	0.89	0.99	0.017
Days after DOT (ref: 0-60)				
61-120	1.08	0.86	1.35	
121-180	1.15	0.90	1.47	0.163
>180	1.30	1.03	1.64	
Constant	1.11	0.69	1.81	0.661

β, regression coefficient. Coefficients were obtained using Gaussian generalized estimating equations with log-link by allowing for repeated visits and by back-selection from the full model. The full model included fever, infection status at enrolment by qPCR (*Pf* or *Pv* positive), LLIN use (less than 100%), sex, village of residence, hemoglobin at baseline (>9 g/dl), first infection. No predictors were associated with *Pf* gametocyte densities (Supplementary Document S1). No significant interaction of PQ treatment with days post DOT was detected.

Table 3. Multivariate predictors *Pv* and *Pf* blood-stage parasite density during follow-up.

	Pv blood-stage density				*Pf* blood-stage density			
	exp(β)	95% CI		*p*-value	exp(β)	95% CI		*p*-value
PQ treatment	1.04	0.93	1.15	0.505	0.85	0.68	1.06	0.143
Mixed *Pf*/*Pv* (by qPCR)	-	-	-	-	0.79	0.63	1.00	0.048
Fever	-	-	-	-	2.41	1.82	3.19	<0.001
Age	0.96	0.92	0.99	0.014	-	-	-	-
Days after DOT (ref: 0-60)								
61-120	0.94	0.83	1.07		0.93	0.69	1.25	
121-180	0.72	0.62	0.83	<0.001	0.89	0.62	1.25	<0.001
>180	0.51	0.44	0.59		0.59	0.43	0.80	
Constant	5.13	3.83	6.87	<0.001	16.37	12.37	21.66	<0.001

β, regression coefficient. Coefficients were obtained using Gaussian generalized estimating equations with log-link by allowing for repeated visits and by back-selection from the full model. The full model included fever, infection status at enrolment by qPCR (*f.* or *v.* positive), LLIN use (less than 100%), sex, village of residence, hemoglobin at baseline (>9 g/dl), first infection. Non-associated predictors were shown by "-" in the respective line. No significant interaction of PQ treatment with days post DOT was detected.

Discussion

This study represents a first detailed investigation of the contribution of *Pv* relapses to the infectious reservoir. The transmission potential attributable to relapses was estimated by comparing gametocyte positivity and density in children that had received either PQ or placebo treatment. A major finding was that *Pv* gametocytes were detected in equal proportions and equal density in *Pv* positive samples of both trial arms. In the PQ arm, the majority of *Pv* infections derived from new mosquito bites, while in the placebo arm 80% of infections were caused by relapsing hypnozoites (Robinson et al., 2015). Gametocyte densities as well as the proportion of gametocyte carriers concurred in both arms, thus indicating that new and relapsing infections produce gametocytes at equal rates. Similar conclusions were drawn from a study in south-east Asia, where *Pv* gametocyte densities and positivity had closely mirrored parasitaemia in both, clinical primary and recurrent infections (Douglas et al., 2013). Gametocyte production in relapses thus seems indistinguishable from that in new infections. This finding highlights the importance of hypnocidal drugs to prevent relapses for an effective interruption of *Pv* transmission.

Sample storage in this cohort was not optimal for RNA preservation. Blood was spotted onto Whatman 3MM filter paper in the field, and stored at room temperature for up to 5 weeks until transferred into TRIzol reagent. This procedure was suboptimal compared to sampling in RNA-stabilizing reagents (Wampfler et al., 2013). A more recent cross-sectional study in PNG employed sampling in RNAprotect Cell Reagent (Qiagen, Switzerland) and found gametocytes in 78% and 60% of *Pf* and *Pv* qPCR-positive samples in children aged 6-9 years (Koepfli et al., 2015). Almost universal *Pv* gametocyte prevalence (95%) was found in Brazilian samples stored in liquid nitrogen

(Lima et al., 2012). The relatively low gametocyte positivity in this cohort was indicative of poor RNA quality, which likely resulted in a substantial underestimation of gametocyte rates. The gametocyte rate in the present study thus reflects a minimum prevalence. Because RNA quality and sample volume did not vary within the study, the comparative analyses of treatment arms and risk factors remain unaffected, even if these results need to be regarded as referring to infections with moderately high gametocyte densities.

The vast majority (>80%) of gametocyte carriers were asymptomatic for both species, and over 20% of *Pv* and over 30% of *Pf* gametocyte positive samples were submicroscopic. Although gametocyte densities were lower in submicroscopic infections compared to LM-positive infections for both species, they may nonetheless be potentially infective to mosquitoes. Mosquito feeding experiments have demonstrated that submicroscopic infections can infect mosquitoes, albeit at lower rates than microscopically patent infections, and thus contribute to onward transmission (Alves et al., 2005; Bousema et al., 2012; Churcher et al., 2013; Ouédraogo et al., 2009; Vallejo et al., 2016). Our results highlight the importance of treating all malaria infections in the community, as asymptomatic individuals will not report themselves to health facilities and thus generally remain untreated.

Co-infections with both species are common in PNG (Mehlotra et al., 2000; Mueller et al., 2009) including in this cohort. A negative correlation between *Pf* and *Pv* infections and a cross-protection of asymptomatic *Pv* infections against *Pf* episodes have been proposed (Bruce et al., 2000; Smith et al., 2001; Hofmann et al., in preparation). It seems plausible that also competition for transmission success, i.e. gametocyte densities, may occur between co-infecting species. Our results suggest that *Pf* and *Pv* infections may suppress gametocytes of the opposite species when occurring in mixed infections. Yet these findings are only first indications that require confirmation in a similar cohort study with sympatric parasite species.

In the first post-treatment *Pf* infections gametocytes were more frequently detected in the PQ arm than in the placebo arm. This is likely explained by the slower acquisition of new *Pv* infections in hypnozoite-cleared individuals, compared to a fast relapse rate in individuals retaining hypnozoites in the liver. Indeed, in the placebo arm 52% of first *Pf* infections carried a *Pv* co-infection as opposed to only 21% in the PQ arm. Accordingly, the multivariate analysis showed reduced odds of *Pf* as well as *Pv* gametocytes in mixed-species infections compared to single-species infections. In addition, a *Pf* co-infection reduced *Pv* gametocyte densities by half. A study in 0.5 to 5 year old PNG children with uncomplicated malaria confirmed that *Pv* gametocytaemia in *Pf*/*Pv* mixed infections was reduced compared to *Pv* single infections (Karl et al., 2016). Moreover, a community study in PNG showed a lower proportion of *Pf* gametocyte carriers in *Pf*/*Pv* mixed infections compared to *Pf* single-species infections (Koepfli et al., 2015). Similar findings had been reported from Thailand (Price et al., 1999). More longitudinal studies designed specifically to

address gametocyte dynamics in mono- and mixed-species infections are needed to confirm potential cross-species interaction and its effect on sexual stage development.

Conclusion

Onset and rate of *Pv* gametocyte production did not differ between relapses and primary infections. This is a strong argument for treatment policies and elimination strategies that support PQ treatment of all *Pv* infections. The vast majority of gametocyte carriers in this study were detected in asymptomatic infections, which suggests that sensitive detection and early treatment of asymptomatic and submicroscopic Plasmodium *spp.* infections may be crucial for an effective control of transmission. PQ treatment cleared hypnozoites and thus reduced *Pv* gametocyte carriage by 73%. These and other *Plasmodium* species interactions that can substantially affect gametocyte production warrant further investigation.

Acknowledgments

We gratefully acknowledge the study participants and their parents or guardians, and the field team in PNG. We specially thank Anna Rosanas-Urgell and Alice Ura from the PNGIMR Molecular Parasitology laboratory for RNA preservation of the samples.

Author contributions

R. W., N. H. and I. F. wrote the article; R.W. and N.H. performed the experiments; R. W., N. H., M. S. and S. K. contributed to statistical analysis. L.J. R., and I. M. contributed to study design and collection of field samples.

Financial support

This work was supported by the Swiss National Science Foundation (grant no. 310030_134889) and the International Centers of Excellence in Malaria Research (grant no. U19 AI089686-03) and National Health and Medical Research Council (NHMRC grant no 1021544). S.K. is currently supported by a NHMRC Early Career Fellowship (grant no. 1052760). L.J.R was supported by an Australian NHMRC Early Career Fellowship (grant no. 1016443). I.M. is supported by an NHMRC Senior Research Fellowship (grant no. 1043345). The funders had no role in study design, data collection and analysis, decision to publish, or preparation of the manuscript.

Potential conflict of interest

All authors: No reported conflicts.

References

Aguilar, R., Magallon-Tejada, A., Achtman, A.H., Moraleda, C., Joice, R., Cisteró, P., Li Wai Suen, C.S.N., Nhabomba, A., Macete, E., Mueller, I., Marti, M., Alonso, P.L., Menéndez, C., Schofield, L., Mayor, A., 2014. Molecular evidence for the localization of Plasmodium falciparum immature gametocytes in bone marrow. Blood 123, 959–966.

Alves, F.P., Gil, L.H.S., Marrelli, M.T., Ribolla, P.E.M., Camargo, E.P., Da Silva, L.H.P., 2005. Asymptomatic carriers of Plasmodium spp. as infection source for malaria vector mosquitoes in the Brazilian Amazon. J. Med. Entomol. 42, 777–779.

Bousema, T., Dinglasan, R.R., Morlais, I., Gouagna, L.C., van Warmerdam, T., Awono-Ambene, P.H., Bonnet, S., Diallo, M., Coulibaly, M., Tchuinkam, T., Mulder, B., Targett, G., Drakeley, C., Sutherland, C., Robert, V., Doumbo, O., Touré, Y., Graves, P.M., Roeffen, W., Sauerwein, R., Birkett, A., Locke, E., Morin, M., Wu, Y., Churcher, T.S., 2012. Mosquito feeding assays to determine the infectiousness of naturally infected Plasmodium falciparum gametocyte carriers. PloS One 7, e42821.

Bousema, T., Drakeley, C., 2011. Epidemiology and infectivity of Plasmodium falciparum and Plasmodium vivax gametocytes in relation to malaria control and elimination. Clin. Microbiol. Rev. 24, 377–410.

Bousema, T., Okell, L., Shekalaghe, S., Griffin, J.T., Omar, S., Sawa, P., Sutherland, C., Sauerwein, R., Ghani, A.C., Drakeley, C., 2010. Revisiting the circulation time of Plasmodium falciparum gametocytes: molecular detection methods to estimate the duration of gametocyte carriage and the effect of gametocytocidal drugs. Malar. J. 9, 136.

Bozdech, Z., Mok, S., Hu, G., Imwong, M., Jaidee, A., Russell, B., Ginsburg, H., Nosten, F., Day, N.P.J., White, N.J., Carlton, J.M., Preiser, P.R., 2008. The transcriptome of Plasmodium vivax reveals divergence and diversity of transcriptional regulation in malaria parasites. Proc. Natl. Acad. Sci. U. S. A. 105, 16290–16295.

Churcher, T.S., Bousema, T., Walker, M., Drakeley, C., Schneider, P., Ouédraogo, A.L., Basáñez, M.-G., 2013. Predicting mosquito infection from Plasmodium falciparum gametocyte density and estimating the reservoir of infection. eLife 2, e00626.

Douglas, N.M., Simpson, J.A., Phyo, A.P., Siswantoro, H., Hasugian, A.R., Kenangalem, E., Poespoprodjo, J.R., Singhasivanon, P., Anstey, N.M., White, N.J., Tjitra, E., Nosten, F., Price, R.N., 2013. Gametocyte dynamics and the role of drugs in reducing the transmission potential of Plasmodium vivax. J. Infect. Dis. 208, 801–812.

Eichner, M., Diebner, H.H., Molineaux, L., Collins, W.E., Jeffery, G.M., Dietz, K., 2001. Genesis, sequestration and survival of Plasmodium falciparum gametocytes: parameter estimates from fitting a model to malariatherapy data. Trans. R. Soc. Trop. Med. Hyg. 95, 497–501.

Eziefula, A.C., Bousema, T., Yeung, S., Kamya, M., Owaraganise, A., Gabagaya, G., Bradley, J., Grignard, L., Lanke, K.H.W., Wanzira, H., Mpimbaza, A., Nsobya, S., White, N.J., Webb, E.L., Staedke, S.G., Drakeley, C., 2014. Single dose primaquine for clearance of Plasmodium falciparum gametocytes in children with uncomplicated malaria in Uganda: a randomised, controlled, double-blind, dose-ranging trial. Lancet Infect. Dis. 14, 130–139.

Hofmann, N.E., Karl, S., Wampfler, R., Betuela, I., Felger, I., Mueller, I., Robinson, L.J., submitted. Heterogeneity in malaria transmission: defining the relationship between molecular force of infection and incidence of P. falciparum and P. vivax episodes. Submitt. Parasite Epidemiol. Control.

John, G.K., Douglas, N.M., von Seidlein, L., Nosten, F., Baird, J.K., White, N.J., Price, R.N., 2012. Primaquine radical cure of Plasmodium vivax: a critical review of the literature. Malar. J. 11, 280.

Karl, S., Laman, M., Moore, B.R., Benjamin, J.M., Salib, M., Lorry, L., Maripal, S., Siba, P., Robinson, L.J., Mueller, I., Davis, T.M.E., 2016. Risk factors for Plasmodium falciparum and Plasmodium vivax gametocyte carriage in Papua New Guinean children with uncomplicated malaria. Acta Trop. 160, 1–8.

Koepfli, C., Robinson, L.J., Rarau, P., Salib, M., Sambale, N., Wampfler, R., Betuela, I., Nuitragool, W., Barry, A.E., Siba, P., Felger, I., Mueller, I., 2015. Blood-Stage Parasitaemia and Age Determine Plasmodium falciparum and P. vivax Gametocytaemia in Papua New Guinea. PloS One 10, e0126747.

Koepfli, C., Ross, A., Kiniboro, B., Smith, T.A., Zimmerman, P.A., Siba, P., Mueller, I., Felger, I., 2011. Multiplicity and diversity of Plasmodium vivax infections in a highly endemic region in Papua New Guinea. PLoS Negl. Trop. Dis. 5, e1424.

Lima, N.F., Bastos, M.S., Ferreira, M.U., 2012. Plasmodium vivax: reverse transcriptase real-time PCR for

gametocyte detection and quantitation in clinical samples. Exp. Parasitol. 132, 348–354.

McCarthy, J.S., Griffin, P.M., Sekuloski, S., Bright, A.T., Rockett, R., Looke, D., Elliott, S., Whiley, D., Sloots, T., Winzeler, E.A., Trenholme, K.R., 2013. Experimentally induced blood-stage Plasmodium vivax infection in healthy volunteers. J. Infect. Dis. 208, 1688–1694.

McKenzie, F.E., Jeffery, G.M., Collins, W.E., 2007. Gametocytemia and fever in human malaria infections. J. Parasitol. 93, 627–633.

Mckenzie, F.E., Wongsrichanalai, C., Magill, A.J., Forney, J.R., Permpanich, B., Lucas, C., Erhart, L.M., O'Meara, W.P., Smith, D.L., Sirichaisinthop, J., Gasser, R.A., Jr, 2006. Gametocytemia in Plasmodium vivax and Plasmodium falciparum infections. J. Parasitol. 92, 1281–1285.

Mehlotra, R.K., Lorry, K., Kastens, W., Miller, S.M., Alpers, M.P., Bockarie, M., Kazura, J.W., Zimmerman, P.A., 2000. Random distribution of mixed species malaria infections in Papua New Guinea. Am. J. Trop. Med. Hyg. 62, 225–231.

Mueller, I., Widmer, S., Michel, D., Maraga, S., McNamara, D.T., Kiniboro, B., Sie, A., Smith, T.A., Zimmerman, P.A., 2009. High sensitivity detection of Plasmodium species reveals positive correlations between infections of different species, shifts in age distribution and reduced local variation in Papua New Guinea. Malar. J. 8, 41.

Nacher, M., Silachamroon, U., Singhasivanon, P., Wilairatana, P., Phumratanaprapin, W., Fontanet, A., Looareesuwan, S., 2004. Risk factors for Plasmodium vivax gametocyte carriage in Thailand. Am. J. Trop. Med. Hyg. 71, 693–695.

Ouédraogo, A.L., Bousema, T., Schneider, P., de Vlas, S.J., Ilboudo-Sanogo, E., Cuzin-Ouattara, N., Nébié, I., Roeffen, W., Verhave, J.P., Luty, A.J.F., Sauerwein, R., 2009. Substantial contribution of submicroscopical Plasmodium falciparum gametocyte carriage to the infectious reservoir in an area of seasonal transmission. PloS One 4, e8410.

Price, R., Nosten, F., Simpson, J.A., Luxemburger, C., Phaipun, L., ter Kuile, F., van Vugt, M., Chongsuphajaisiddhi, T., White, N.J., 1999. Risk factors for gametocyte carriage in uncomplicated falciparum malaria. Am. J. Trop. Med. Hyg. 60, 1019–1023.

Pukrittayakamee, S., Imwong, M., Singhasivanon, P., Stepniewska, K., Day, N.J., White, N.J., 2008. Effects of Different Antimalarial Drugs on Gametocyte Carriage in P. Vivax Malaria. Am. J. Trop. Med. Hyg. 79, 378–384.

R Core Team, 2014. R: A language and environment for statistical computing. R Foundation for Statistical Computing, Vienna, Austria.

Robinson, L.J., Wampfler, R., Betuela, I., Karl, S., White, M.T., Li Wai Suen, C.S.N., Hofmann, N.E., Kinboro, B., Waltmann, A., Brewster, J., Lorry, L., Tarongka, N., Samol, L., Silkey, M., Bassat, Q., Siba, P.M., Schofield, L., Felger, I., Mueller, I., 2015. Strategies for Understanding and Reducing the Plasmodium vivax and Plasmodium ovale Hypnozoite Reservoir in Papua New Guinean Children: A Randomised Placebo-Controlled Trial and Mathematical Model. PLoS Med. 12, e1001891.

Schneider, P., Schoone, G., Schallig, H., Verhage, D., Telgt, D., Eling, W., Sauerwein, R., 2004. Quantification of Plasmodium falciparum gametocytes in differential stages of development by quantitative nucleic acid sequence-based amplification. Mol. Biochem. Parasitol. 137, 35–41.

Schoepflin, S., Valsangiacomo, F., Lin, E., Kiniboro, B., Mueller, I., Felger, I., 2009. Comparison of Plasmodium falciparum allelic frequency distribution in different endemic settings by high-resolution genotyping. Malar. J. 8, 250.

Shekalaghe, S.A., Drakeley, C., Gosling, R., Ndaro, A., van Meegeren, M., Enevold, A., Alifrangis, M., Mosha, F., Sauerwein, R., Bousema, T., 2007. Primaquine clears submicroscopic Plasmodium falciparum gametocytes that persist after treatment with sulphadoxine-pyrimethamine and artesunate. PloS One 2, e1023.

Taylor, L.H., Read, A.F., 1997. Why so few transmission stages? Reproductive restraint by malaria parasites. Parasitol. Today Pers. Ed 13, 135–140.

Vallejo, A.F., García, J., Amado-Garavito, A.B., Arévalo-Herrera, M., Herrera, S., 2016. Plasmodium vivax gametocyte infectivity in sub-microscopic infections. Malar. J. 15, 48.

Wampfler, R., Mwingira, F., Javati, S., Robinson, L., Betuela, I., Siba, P., Beck, H.-P., Mueller, I., Felger, I., 2013. Strategies for detection of Plasmodium species gametocytes. PloS One 8, e76316.

WHO, 2010. Basic Malaria Microscopy - Part I. Learner's guide.

WHO, 2012. Malaria Policy Advisory Committee to the WHO: conclusions and recommendations of September 2012 meeting. Malar. J. 11, 424.

Young, J.A., Fivelman, Q.L., Blair, P.L., de la Vega, P., Le Roch, K.G., Zhou, Y., Carucci, D.J., Baker, D.A.,

Winzeler, E.A., 2005. The Plasmodium falciparum sexual development transcriptome: A microarray analysis using ontology-based pattern identification. Mol. Biochem. Parasitol. 143, 67–79.

Supplementary Document S1

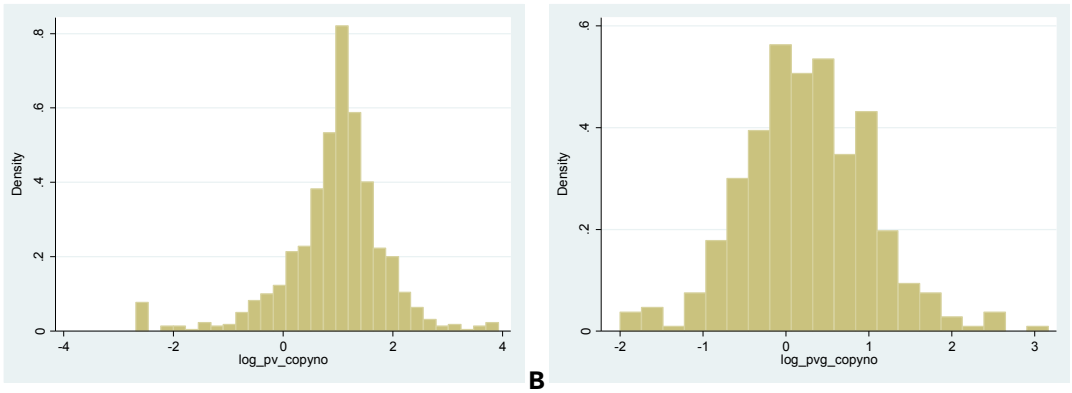

A B

Figure S1.1 Density distribution of *P. vivax*. (A) *Pv* blood-stage densities by genomic 18S rRNA copies/µl (log_{10}). (B) *Pv* gametocytes densities by *pvs25* transcript copies/µl (log_{10}). Log_{10} transformations of copies/µl show normal distribution.

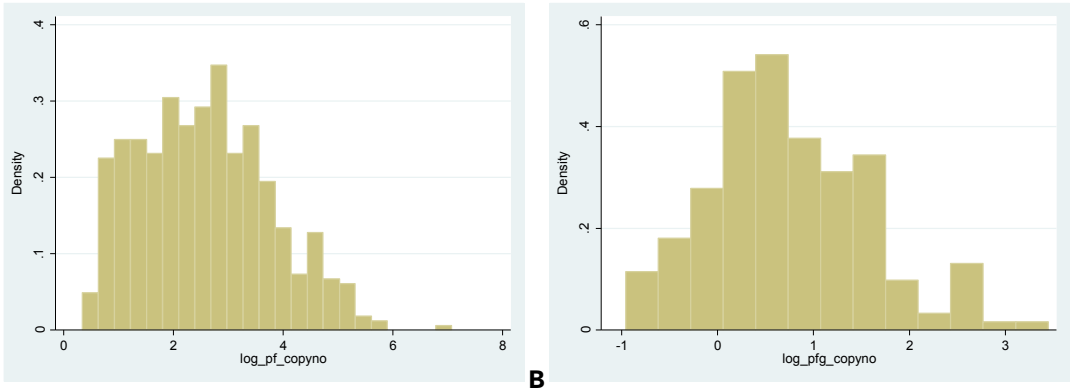

A B

Figure S1.2 Density distribution of *P. facliparum*. (A) *Pf* blood-stage densities by genomic 18S rRNA copies/µl (log_{10}). (B) *Pf* gametocytes densities by *pfs25* transcript copies/µl (log_{10}). Log_{10} transformations of copies/µl show almost normal distribution.

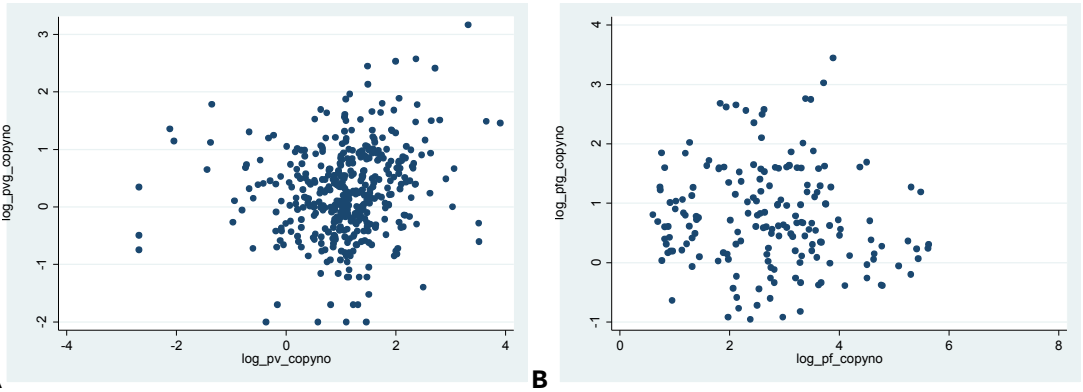

A B

Figure S1.3 Scatterplot of *Pv* (A) and *Pf* (B) blood-stage vs. gametocyte density (log_{10}).

Table S1.1 GEE Models for *P. vivax* gametocyte positivity with categorical (red) *Pv* blood-stage densities (genomic 18S rRNA copies/µl). NOTE: Association of categorical *Pv* densities with *Pv* gametocyte positivity is almost linear.

***Pv* gametocyte positivity – categorical *Pv* density**	**OR**	**95% CI**		**p-value**
Pv density (ref: log10 density <0)				
0-0.5	2.12	0.90	4.98	<0.001
0.5-1	2.73	1.25	5.93	
1-1.5	3.01	1.43	6.34	
1.5-2	4.09	1.83	9.15	
>2	10.48	4.22	26.06	
PQ treatment	1.03	0.67	1.57	0.905
Mixed Pf/Pv	0.40	0.25	0.63	<0.001
First Pv infection	0.63	0.41	0.96	0.031
Days post treatment (ref: 0-60)				
61-120	0.58	0.39	0.87	<0.001
121-180	1.46	0.89	2.38	
>180	2.42	1.38	4.23	
Constant	0.25	0.11	0.57	0.001

Table S1.2 Category counts of the GEE Models for *P. vivax* gametocyte positivity with categorical *Pv* blood-stage densities (genomic 18S rRNA copies/µl). NOTE: The increase of *Pv* gametocyte positivity with increasing *Pv* asexual density is almost linear.

Category counts	***Pv* gametocyte positivity**		
Pv density category $\log_{10}$(18S rRNA copyno)	0	1	Total
<0	74	36	110
0-0.5	59	38	97
0.5-1	140	95	235
1-1.5	183	134	317
1.5-2	58	61	119
>2	28	52	80
Total	542	416	958

Table S1.3 GEE Models for *P. vivax* gametocyte density (pvs25 transcripts/µl) with categorical (red) *Pv* blood-stage densities (genomic 18S rRNA copies/µl). NOTE: Association of categorical *Pv* densities with *Pv* gametocyte densities is almost linear.

***Pv* gametocyte density – categorical *Pv* density**	**OR**	**95% CI**		**p-value**
Pv density (ref: log10 density <0)				
0-0.5	1.56	1.01	2.41	<0.001
0.5-1	1.49	0.92	2.40	
1-1.5	1.43	0.93	2.19	
1.5-2	2.35	1.43	3.86	
>2	2.50	1.54	4.04	
PQ treatment	0.95	0.79	1.16	0.648
Mixed Pf/Pv	0.72	0.58	0.90	0.003
Age	0.94	0.90	0.99	0.031

Days post treatment (ref: 0-60)				
61-120	1.05	0.84	1.31	0.272
121-180	1.12	0.89	1.40	
>180	1.24	0.99	1.54	
Constant	0.97	0.54	1.73	0.909

Table S1.4 GEE Models for *P. falciparum* gametocyte positivity with categorical (red) *Pf* blood-stage densities (genomic 18S rRNA copies/µl). NOTE: Association of categorical *Pf* densities with *Pf* gametocyte positivity is not very linear, but *Pf* density is anyways not significant neither as linear nor categorical. For simplicity, linear was chosen.

***Pf* gametocyte positivity – categorical *Pf* density**	**OR**	**95% CI**		**p-value**
Pf density (ref: log10 density <1)				
1-2	0.35	0.13	0.94	0.089
2-3	0.88	0.37	2.08	
3-4	0.90	0.39	2.12	
>4	1.09	0.42	2.87	
PQ treatment	1.16	0.73	1.83	0.526
Mixed Pf/Pv	0.32	0.17	0.58	<0.001
First Pf infection	0.45	0.25	0.81	0.007
Days post treatment (ref: 0-60)				
61-120	1.33	0.63	2.81	0.299
121-180	1.40	0.67	2.94	
>180	0.79	0.35	1.78	
Constant	0.65	0.23	1.83	0.417

Table S1.5 Category counts of the GEE Models for *P. falciparum* gametocyte positivity with categorical *Pf* blood-stage densities (genomic 18S rRNA copies/µl). NOTE: The increase of *Pf* gametocyte positivity with increasing *Pf* asexual density is not very linear because of the initial decrease from the reference category to categories 1-2, 3-4 and >4.

Category counts	***Pf* gametocyte positivity**		
Pf density category $\log_{10}$(copyno)	0	1	Total
<1	40	17	57
1-2	114	32	146
2-3	106	55	161
3-4	69	51	120
>4	47	24	71
Total	376	179	555

Table S1.6 GEE Models for *P. falciparum* gametocyte density (*pfs25* transcripts/µl) with categorical (red) *Pf* blood-stage densities (genomic 18S rRNA copies/µl). NOTE: Association of categorical *Pf* densities with *Pf* gametocyte densities is not very linear, but *Pf* density is anyways not at all significant neither as linear nor categorical. For simplicity, linear was chosen.

Pf* gametocyte density – categorical *Pf density	**OR**	**95% CI**		**p-value**
Pf density (ref: log10 density <1)				
1-2	0.77	0.48	1.24	0.145
2-3	0.65	0.41	1.04	
3-4	0.88	0.56	1.39	
>4	0.58	0.34	1.01	
PQ treatment	0.84	0.66	1.08	0.176
First Pf infection	0.96	0.68	1.36	0.825
Mixed Pf/Pv	0.76	0.53	1.08	0.13
Fever	0.76	0.49	1.17	0.211
Days post treatment (ref: 0-60)				
61-120	0.78	0.48	1.28	0.597
121-180	0.74	0.44	1.24	
>180	0.74	0.47	1.16	
Constant	4.13	2.60	6.58	<0.001

Supplementary Figure S2

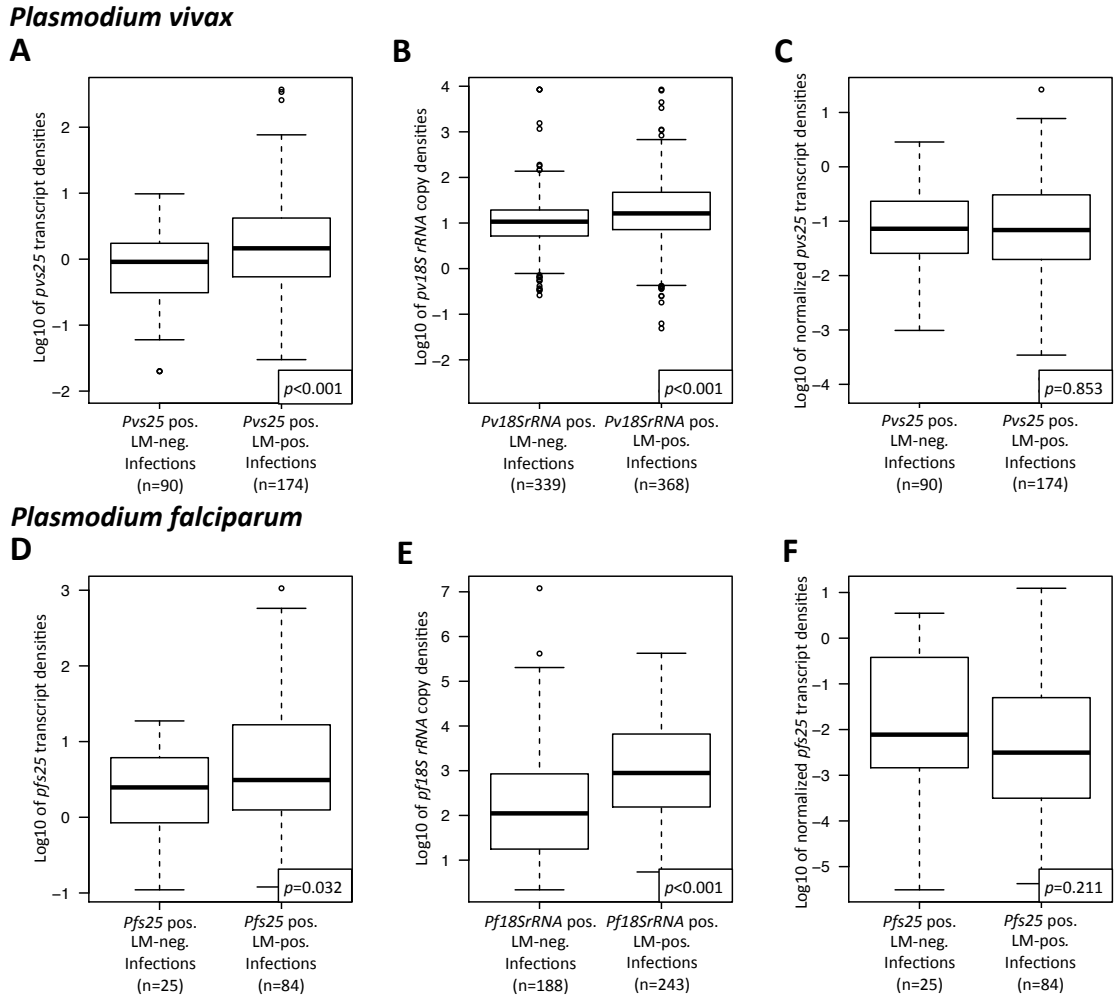

Figure S2. Gametocyte and overall parasite density in submicroscopic and LM-positive *Pv* (top) and *Pf* (bottom) infections. **A**. and **D**. *Pv* and *Pf* gametocyte densities were expressed as log10 of *pvs25* and *pfs25* transcripts/µl. **B**. and **C**. *Pv* and *Pf* parasite densities were expressed as log10 of *pv18S rRNA* and *pf18S rRNA* gene copies/µl . **D**. and **F**. *Pv* and *Pf* normalized gametocyte densities. Densities were normalized by division of *pvs25* and *pfs25* transcripts/µl by *pv18S rRNA* or *Pf18S rRNA* genomic copies/µl, respectively.

Supplementary Document S3

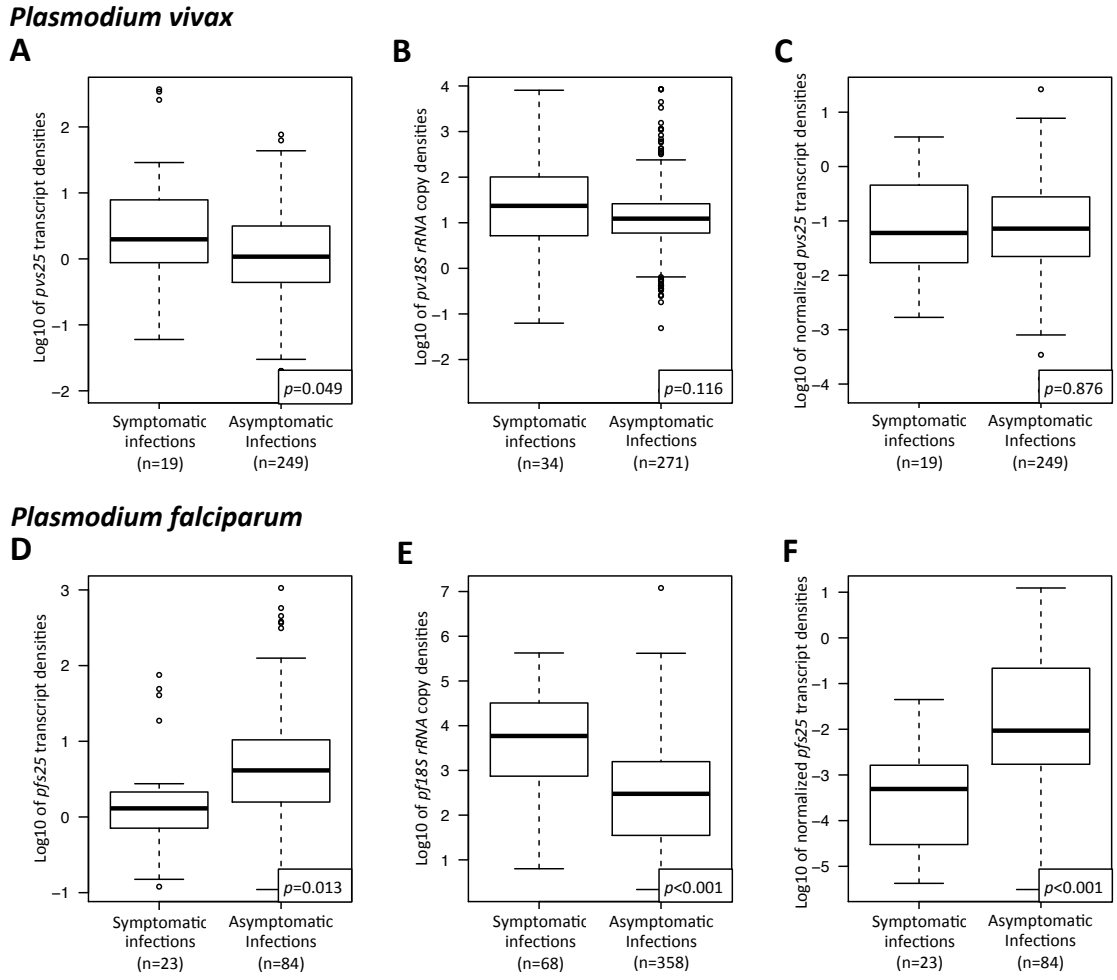

Figure S3. Gametocyte and parasite density in symptomatic and asymptomatic *Pv* (top) and *Pf* (bottom) infections. **A**. and **D**. *Pv* and *Pf* gametocyte densities were expressed as log10 of *pvs25* and *pfs25* transcripts/µl. **B**. and **E**. *Pv* and *Pf* parasite densities were expressed as log10 of *pv18S rRNA* and *pf18S rRNA* gene copies/µl . **E**. and **F**. *Pv* and *Pf* normalized gametocyte densities. Densities were normalized by division of *pvs25* and *pfs25* transcripts/µl by *pv18S rRNA* or *Pf18S rRNA* genomic copies/µl, respectively.

Supplementary Document S4

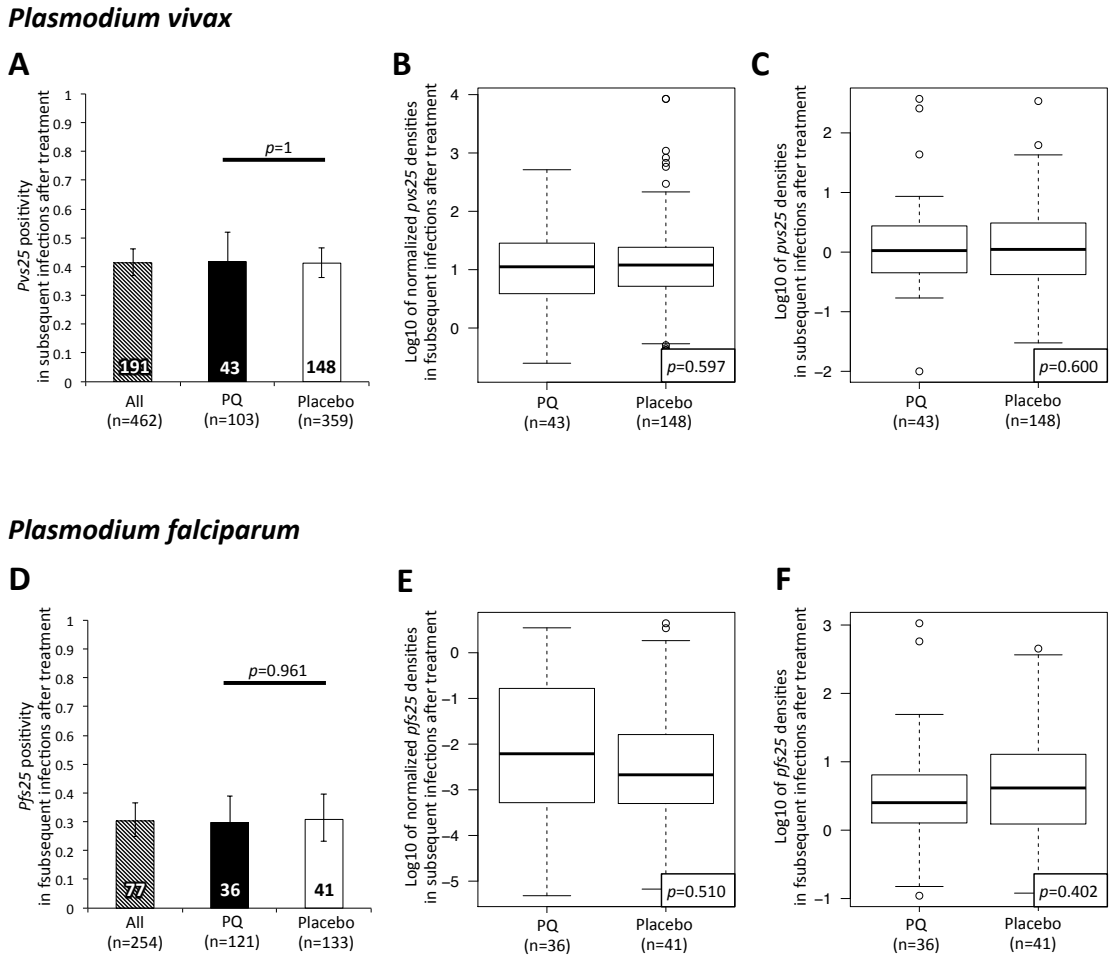

Figure S4. Gametocyte positivity and density in subsequent (i.e. not first) *P. vivax* (top) and *P. falciparum* (bottom) infections after treatment with blood-stage antimalarials alone (Placebo) or blood-stage antimalarials plus Primaquine (PQ). **A**. and **D**. Proportion of *P. vivax* and *P. falciparum* gametocyte carriers among subsequent infections by treatment arm. Figures within the bars indicate absolute numbers of gametocyte-positive subsequent infections following treatment. Error bars indicate 95% confidence intervals by X^2 distribution. **B**. and **E**. Normalized *P. vivax* and *P. falciparum* gametocyte densities in subsequent infections by treatment arm. Normalization was done by dividing *pvs25* or *pfs25* transcript numbers/µl by *Pv-* or *Pf-18S rRNA* copy numbers/µl. **C**. and **F**. Absolute *P. vivax* and *P. falciparum* gametocyte densities in subsequent infections by treatment arm. Densities are expressed as $\log_{10}$ of *pvs25* and *pfs25* transcripts/µl.

Supplementary Document S5

Table S5. Multivariate risk factors of *P. vivax* and *P. falciparum* asexual parasite positivity during follow-up. Positivity was assessed by *Pv-* or *Pf-18S rRNA* qPCR.

	***P. vivax* parasite positive**				***P. falciparum* parasite positive**			
	OR	**95% CI**		**p-value**	**OR**	**95% CI**		**p-value**
PQ treatment	0.14	0.09	0.22	<0.001	0.90	0.61	1.32	0.591
Mixed P.f./P.v. (by qPCR)	1.82	1.33	2.49	<0.001	1.83	1.38	2.42	<0.001
Fever	0.69	0.51	0.93	0.016	3.69	2.63	5.17	<0.001
Infection at enrolment (same species, qPCR)	1.38	1.05	1.81	0.023	1.93	1.25	3.00	0.003
Village								
Albinama	1				1			
Amahup	0.29	0.18	0.47		0.65	0.31	1.34	
Balanga	1.43	0.91	2.24	<0.001	2.05	1.03	4.05	<0.001
Balif	0.72	0.47	1.11		0.89	0.46	1.73	
Bolumita	2.30	1.53	3.48		9.40	4.97	17.80	
Numangu	0.56	0.30	1.04		3.44	1.81	6.55	
Age								
<6y	1				1			
6-7.5y	1.07	0.72	1.58	0.246	1.46	0.85	2.51	0.018
7.6-9y	0.91	0.60	1.38		1.97	1.15	3.40	
>9y	0.73	0.47	1.14		2.18	1.28	3.72	
Days after DOT								
0-60	1				1			
61-120	1.89	1.46	2.44	<0.001	1.91	1.37	2.67	<0.001
121-180	1.48	1.09	2.01		2.39	1.66	3.44	
>180	1.20	0.89	1.62		2.43	1.70	3.48	
Interaction Days after DOT x PQ treatment								
0-60 x PQ	1							
61-120 x PQ	1.47	0.84	2.55	0.175				
121-180 x PQ	2.61	1.44	4.75	0.002	not significant			
>180 x PQ	2.04	1.07	3.91	0.031				

OR, odds ratio, DOT, directly observed treatment. ORs were obtained using binomial generalized estimating equations with logit-link allowing for repeated visits by backselection from the full model. The full model included fever, infection status at enrolment by qPCR (*P.f.* or *P.v.* positive), LLIN use (less than 100%), sex, village of residence, hemoglobin at baseline (>9 g/dl). No significant interaction of PQ treatment with days post DOT was detected for *P. falciparum*.

Supplementary Document S6

Table S6.1 Multivariate risk factors of *P. vivax* gametocyte carriage in subsequent infections during follow-up. Positivity was assessed by *pvs25 rRNA* qPCR.

***Pv* gametocyte positivity**	**OR**	**95% CI**		**p-value**
Pv density (10x increase)	1.88	1.32	2.68	<0.001
PQ treatment	0.94	0.56	1.56	0.797
Mixed Pf/Pv	0.53	0.32	0.87	0.013
Days post treatment (ref: 0-60)				
61-120	0.65	0.38	1.14	<0.001
121-180	1.51	0.82	2.80	
>180	2.58	1.40	4.76	
Constant	0.35	0.19	0.62	<0.001

β, regression coefficient. Coefficients were obtained using Gaussian generalized estimating equations with log-link allowing for repeated visits by back-selection from the full model. The full model included fever, infection status at enrolment by qPCR (*Pf* or *Pv* positive), LLIN use (less than 100%), sex, village of residence, hemoglobin at baseline (>9 g/dl), fever, age. No significant interaction of PQ treatment with days post DOT was detected.

Table S6.2 Multivariate risk factors of *P. falciparum* gametocyte carriage in subsequent infections during follow-up. Positivity was assessed by *pfs25 rRNA* qPCR.

***Pf* gametocyte positivity**	**OR**	**95% CI**		**p-value**
Pf density (10x increase)	1.40	1.07	1.84	0.016
PQ treatment	0.90	0.49	1.63	0.721
Mixed Pf/Pv	0.37	0.18	0.74	0.006
Days post treatment (ref: 0-60)				
61-120	1.25	0.42	3.74	0.031
121-180	1.06	0.37	3.05	
>180	0.42	0.14	1.30	
Constant	0.28	0.08	1.03	0.056

β, regression coefficient. Coefficients were obtained using Gaussian generalized estimating equations with log-link allowing for repeated visits by back-selection from the full model. The full model included fever, infection status at enrolment by qPCR (*Pf* or *Pv* positive), LLIN use (less than 100%), sex, village of residence, hemoglobin at baseline (>9 g/dl), fever, age. No significant interaction of PQ treatment with days post DOT was detected.

Chapter 7: General Discussion

Strategies for malaria control and elimination require novel tools to identify reservoirs of malaria transmission in endemic settings. Data on the infectious reservoir of *P. vivax* are scarce, first and foremost because of the most striking difference to *P. falciparum*: the *P. vivax* hypnozoite reservoir in the liver. These dormant stages may be reactivated weeks or months after the first infection and contribute subsequently to onwards transmission. Studies on submicroscopic *P. vivax* gametocytes and their infectiveness are urgently needed to gain knowledge about the frequency and epidemiology of *P. vivax* gametocyte carriage in different transmission settings, to identify possible risk factors and to evaluate transmission blocking interventions.

This chapter discusses the relevance of transmission-stages and the complex biology of *P. vivax* relapses, summarizes results and contributions, examines the challenges of mass drug administration (MDA) aimed to reduce transmission of *P. vivax*, and provides direction for future work.

This thesis was nested in a major treatment-to-reinfection cohort study conducted in PNG by members of the PNG Institute of Medical Research in Madang in 2009 and 2010. At one of the follow-up bleeds alternative sampling methods were tested and were summarized in a cross-sectional study.

The importance of transmission-stages in malaria elimination

Gametocytes are the sexual parasite stage transmitted from human to mosquito. Different strategies for sample collection and subsequent detection of gametocytes in field settings were validated during the course of this thesis (chapter 2). In the 315 samples analyzed in the cross-sectional study, light microscopy (LM) missed 73% of *P. falciparum* gametocyte carriers and 100% of *P. vivax* gametocyte carriers in comparison to qPCR (chapter 2). Similarly, among the 6607 longitudinal samples, 72% *P. falciparum* gametocyte positive samples and 95% *P.* vivax

gametocyte positive samples were missed by light microscopy (chapter 6). Significantly more *P. vivax* gametocyte-positive samples were missed compared to *P. falciparum*. Two reasons can explain the poor *P. vivax* gametocyte detection by light microscopy in these samples: (i) due to the very similar morphology of *P. vivax* gametocytes and *P. vivax* trophozoites, gametocytes might be misclassified as trophozoites and therefore missed during routine microscopy (Karl et al., 2014), and (ii) owing to the preference of *P. vivax* to infect reticulocytes, overall parasite densities are 10 times lower for *P. vivax* than for *P. falciparum* (Triglia et al., 2001) and often fall below the limit of detection of light microscopy, leading to many missed infections.

In view of the superior sensitivity of molecular methods over light microscopy, should molecular methods be applied in all epidemiological studies to screen for gametocyte carriers? Molecular detection and genotyping of gametocytes, as presented in this thesis, are imperfect surrogate markers for transmission potential, although commonly used in studies aiming to evaluate the effects of transmission-reducing interventions such as specific drugs and vaccines (Churcher et al., 2013; Ouédraogo et al., 2009). Direct assessment of the human-to-mosquito infection potential is only possible by laborious experimental direct skin feeding or membrane feeding of mosquitos (White et al., 2014), but studies on infectivity of gametocytes to mosquitoes are scarce.

While individuals with higher gametocyte density are generally more infectious to mosquitoes than those with lower *P. falciparum* and *P. vivax* gametocyte density (Bousema et al., 2012; Carter and Graves, 1988; Sattabongkot et al., 1991), asexual parasite density, sex ratio of gametocytes, fever and naturally acquired immunity were also suggested to play a role in the infectivity to mosquitoes (Bousema et al., 2012; Carter and Graves, 1988; Churcher et al., 2013; Sattabongkot et al., 2003). Submicroscopic *P. falciparum* gametocyte carriers successfully infected mosquitoes in several African countries mosquito (Bousema et al., 2012; Ouédraogo et al., 2009; Schneider et al., 2007). Although twofold lower proportion of mosquitoes are infected by submicroscopic *P. falciparum* gametocyte densities (Schneider et al., 2007), this low infection rate is counterbalanced by the abundance of submicroscopic infections in the population. Because submicroscopic gametocyte densities in PNG are 2 to 9 times more prevalent than microscopic-positive gametocyte densities, these infections are likely to be the major source of *Plasmodium spp.* mosquito infections in PNG.

What is thus the best strategy to target the submicroscopic gametocyte reservoir and reduce transmission? In this thesis, two thirds of submicroscopic gametocyte densities harbored microscopic-positive blood-stage densities for both species and overall 49% *P. vivax* and 47% *P. falciparum* submicroscopic blood-stage infections were detected (chapter 6). The non-negligible contribution of submicroscopic blood-stage infections to *P. falciparum* transmission has been shown by failure of Mass Screen and Treatment interventions in Burkina Faso and Zanzibar, in which diagnosis was based on rapid diagnostic tests (RDT) or LM alone (Cook et al., 2014; Tiono et al., 2013). Authors agreed that more sensitive point-of-care diagnostic tools, such as Loop-

Mediated-Isothermal-Amplification (LAMP) or highly sensitive RDTs are desired for the detection of asexual *P. falciparum* parasites in the context of MSAT (Cook et al., 2014; Tiono et al., 2013). The use of low-dose PQ for clearing *P. falciparum* gametocytes and thus blocking transmission of *P. falciparum* an additional valuable tool to stop *P. falciparum* transmission in all endemic settings (Eziefula et al., 2014; Lubell et al., 2014; White et al., 2014). In this survey, more sensitive point-of-care diagnostic tools were beneficial in the context of MSAT to reduce the infectious reservoir of *P. falciparum* (chapter 4), however these tools would miss an important infectious reservoir in *P. vivax* infections: the hypnozoites.

No diagnostic method that can discriminate hypnozoite carriers from individuals without liver-stage parasites has been discovered so far. Gametocyte positivity data generated during the course of this thesis were used to highlight that hypnozoites were the largest contributor to *P. vivax* transmission in PNG, as suggested by a >70% reduced risk for gametocyte carriage after PQ treatment (chapter 4). Remarkably, PQ treatment had the same effect in children with or without PCR-detectable *P. vivax* infection at enrolment. This argues for a massive reservoir of undetectable dormant liver stages in these children.

Molecular analysis of gametocyte positivity, conversion rates and densities in both trial arms pointed out that relapses and new infections are undistinguishable in their contribution to transmission in semi-immune individuals (chapter 6). Similar findings, although based on light microscopy, were found in semi-immune individuals from Thailand and Indonesia (Douglas et al., 2013), supporting the conclusion that relapses contribute equally to transmission as new infections. Prevention of relapses is thus the most efficient strategy to reduce the infectious reservoir of *P. vivax* malaria in semi-immune children in PNG.

The complex molecular epidemiology of relapsing infections

The ability of *P. vivax* to produce latent hypnozoites with varying periods of dormancy is a major challenge for malaria control and elimination strategies. Most knowledge on *P. vivax* infection and relapse was gained from experimental human infection trials in US penitentiaries in the late 1940s to 1950s (Coatney et al., 1950), treatment of neurosyphilis patients by infection with *P. vivax* (reviewed in (McKenzie et al., 2002)) and from soldiers and travelers returning from *P. vivax* endemic countries (Sutanto et al., 2013). This thesis aimed at filling the gap in the understanding of *P. vivax* infection dynamics in semi-immune individuals with a long history of infections.

For this, a mathematical approach – the triplet model – that allows for correction for detectability (probability of a clone to be detected in a given sample) was applied for the first time to investigate the infection dynamics of relapses and new infections (Smith et al., 1999). This model was previously designed for *P. falciparum* infections and was now successfully applied to study *P. vivax* duration of infections and molecular force of blood-stage infections ($_{mol}$FOB).

Although this model is a powerful tool to study infection dynamics in *Plasmodium spp.* infections, differences apply for the fast-relapsing tropical *P. vivax* strains, the most important one probably being the assumption of the model that the probability of reinfection within the interval of three consecutive samples is close to zero. If the latency period of relapses is shorter than the time span between these three bleeds (i.e. 28 days in the first 3 months and 60 days in the last 5 months of the present survey), homologous relapses are regarded as a continuous infection with a missed detection between these bleeds. This is a possible limitation of the presented results, because *P. vivax* strains in PNG are known to have latency periods as short as three weeks if short-eliminating antimalarials were given (Battle et al., 2014; White, 2011). As a consequence, duration of infection could be overestimated and detectability could be underestimated in the placebo arm of the trial, where the most relapses were observed. Nevertheless, good association of parasite density and detectability in both trial arms is suggesting that there is no major bias of the results due to this assumption.

In the past the fast-relapsing *P. vivax* Chesson strain isolated from Papua New Guinea was well-studied (Ehrman et al., 1945). Key observations gained from the available data on *P. vivax* relapses are:

- Relapses were observed earlier and more frequently when higher sporozoite loads were inoculated (Craige and Alving, 1947)
- Overall parasite density decreased with each relapse (Coatney et al., 1950).
- The duration of blood-stage infection decreased with each relapse (Coatney et al., 1950)
- Reinfection with the same strain resulted in fewer fever episodes accompanied with lower temperatures (Whorton and Pullman, 1947)
- Parasite densities and symptoms of reinfection with a parasite strain different from the first infection resembled the primary infection in some cases, while symptoms were markedly reduced in other cases (Whorton and Pullman, 1947).
- Long dormancy periods of over 200 days were observed for the Chesson strain despite the fact that it is generally characterized as fast-relapsing (Jeffery, 1956).

These findings highlight the complexity of relapse biology especially of tropical-zone strains such as found in PNG, as well as the central role of acquired immunity in the control of *P. vivax* relapses.

In PNG, previous studies in children showed that clinical immunity against *P. vivax* is acquired in early childhood due to the high number of infections experienced in these young children (Koepfli et al., 2013; Lin et al., 2010). On average, a child was infected with over 14 *P. vivax* clones per year (Koepfli et al., 2013). The number of infections acquired per time (FOI, force of infection) did not change with age in 1-5 years old children, suggesting that the decrease in *P. vivax* clinical incidence is a result of acquired immunity (Koepfli et al., 2013). FOI in this present study was lower with estimated 10 infections per year in semi-immune children treated with blood-stage antimalarials only, owing most probably to reduced parasite prevalence observed in PNG between

these two surveys (Hofmann et al., – in preparation; Lin et al., 2010). In line with the earlier survey, no age trend in the number of infections experienced was observed in these semi-immune children. However, durations of infection increased with age when densities and detectability decreased. Although the age-range analyzed was tide, acquired immunity in this cohort appeared to increase the tolerability for longer durations of low-density infections (chapter 5). Future investigations on infection dynamics in adults and younger children are thus desired to elucidate these findings.

The design of the present survey permitted the comparison of infection dynamics between relapses and new infections. On average two relapses were observed per each new infection experienced by these semi-immune children (chapter 5). Comparisons between trial arms revealed that relapses and new infections are presumably under the same immune pressure as demonstrated by similar parasite density, duration of infection and clone detectability in both trial arms (chapter 5). Also no apparent difference in investment in gametocytogenesis between relapses and new infections was observed. Therefore in semi-immune children of an endemic area, transmission dynamics of relapses are related to the history of infections as much as are those from newly incoming infections.

The similar infection dynamics between relapses and new infections argue for the hypothesis that relapses found in these semi-immune children were heterologous to the first infection. A possible explanation for the heterologous relapses was recently published by Bright *et al.*, who sequenced consecutive relapses of a single patient and they found that these were likely meiotic siblings (Bright et al., 2014). Meiotic siblings are heterologous in some genetic traits if hybridization of two genetically distinct gametes occurred in the mosquito. Genetic diversity and multiplicity of *P. vivax* infections was high in our cohort and most probably promoted multiple-clone infections and hence recombination in the mosquito, although direct entomological evidence is missing. Imwong *et al.* studied mixed *P. falciparum* and *P. vivax* infections in PNG mosquitoes, revealing that mixed-species infections were significantly more common than expected (Imwong et al., 2011). This argues also for a high proportion of multiple-clone infections in PNG mosquitoes, suggesting high rates of hybridization. The resulting partly related relapses would have a better chance to escape the immune system, and, as consequence, "behave" like new infections as observed in our cohort.

Overall, evidence gained from these findings on infection dynamics of relapses and new infections urges the implementation of interventions targeting the hypnozoite reservoir. One of the possible interventions is mass drug administration of PQ as discussed in the following paragraph.

Mass drug administration to control *P. vivax*

Genotyping and gametocytes data generated during the course of this thesis was used to highlight the large contribution of hypnozoites to the infectious reservoir. The lack of a biomarker for predicting the dormant parasite reservoir in an individual's liver argues for MDA in endemic settings. Although Mass screen and treatment (MSAT) with molecular methods would target also submicroscopic infections, individuals with dormant hypnozoites but no apparent blood-stage parasitaemia would remain undetected. This is a major difference to *P. falciparum*, where the implementation of MSAT and MDA into control programs are highly debated (Griffin et al., 2010; Halliday et al., 2014; Okell et al., 2011; Tiono et al., 2013).

However, recent reports from areas where *vivax* malaria burden was successfully reduced or even eliminated by MDA with PQ (Hsiang et al., 2013; Kondrashin et al., 2014) support the implementation of MDA with PQ to combat *P. vivax* malaria, at least in temperate zones with seasonal transmission. In one study, MDA with PQ significantly reduced and subsequently eliminated *P. vivax* malaria in China despite low coverage (Hsiang et al., 2013), while other reports highlight the necessity of a high coverage (85-95%) to achieve a sustained effect (Kondrashin et al., 2014).

In the present survey, PQ was not only effective in reducing the risk of infection with *P. vivax* in children that were PCR-positive for *P. vivax* at enrolment, but equally reduced the risk in children with non-*vivax* infections (either *P. falciparum, P. ovale* or *P. malariae*) and even in those negative for any *Plasmodium spp*. Although children parasite-free at enrolment were less likely to be re-infected during follow-up compared to those positive for any *Plasmodium spp*. irrespective of treatment arm. These results indicate that more than half of these children harboured hypnozoites. Analysis of infection dynamics confirms that at higher transmission intensity, contribution of *P. vivax* relapses to the infectious reservoir increased (chapter 4).

Data of this thesis was also used for mathematical modelling of the long-term impact of MSAT and MDA. Findings showed that MSAT using a molecular detection method and including a hypnocidal drug would have only limited effect owing to this undetected hypnozoite reservoir. Instead, the model predicted that a MDA including a hypnocidal drug is highly effective to reduce *P. vivax* malaria infections.

Mathematical modelling is highly useful for predicting the effect of malaria interventions on the burden of disease. Ishikawa *et al.* proposed a mathematical model for studying the impact of MDA and various vector control measures on the burden of *P. vivax* infections in the Solomon Islands (Ishikawa et al., 2003). They highlighted that 1-2 rounds of MDA, accompanied by effective mosquito control thereafter, are needed for reducing *P. vivax* prevalence below 1% in the long term. The mathematical model used for this present survey did not include any vector control measures but also highlighted the striking effect of 2 rounds of MDA with PQ and 80% coverage

on *P. vivax* transmission. Once malaria endemicity is reduced to few hotspots, selective or focal MDA targeting households or villages around an indicator case might suffice to fully eliminate *P. vivax* malaria, like done in China (Hsiang et al., 2013).

However, following limitations in the use of PQ in MDA shall be considered:

First, PQ causes acute hemolysis in Glucose-6-Phosphate-Dehydrogenase deficient individuals. Currently, G6PD deficiency testing is often impracticable for routine care and as consequence PQ is frequently not administered in many endemic countries such as in PNG (Howes et al., 2012). New generation of G6PD rapid tests is presently being tested (Kim et al., 2011), but their specificity and sensitivity need further improvement before they can safely be used to assess the risk of PQ treatment in large interventions (Howes et al., 2012).

Second, poor compliance with the long course of PQ treatment – e.g. 14 days in East Asia and Oceania - is a major challenge. The arrival of Tafenoquine (TQ), a long acting 8-aminoquinoline that can be given as a single dose (Kim et al., 2011; Llanos-Cuentas et al., 2014) will make hyponozoite-targeting MDA more feasible.

Third, 8-aminoquinolines are the only available drug category to efficiently eliminate hypnozoites. Resistance to this class would be a striking drawback in the elimination of *P. vivax*. Numerous PQ treatment failures were reported, most of them due to lack of compliance, host genetic factors and/or parasite geographic origin (Townell et al., 2012). Host genetic factors that influence PQ activity generally affect one of two Cytochrome P450 enzymes (2D6 and MAO-A) that play a major role in the breakdown of PQ into its active metabolites (Pybus et al., 2012).

Overall, evidence for the success of MDA in the context of *P. vivax* control and elimination was shown in temperate zones with seasonal transmission, yet, more evidence from MDA in tropical zones is needed. Data from this thesis was used to clearly demonstrate that MDA with PQ is a valuable tool in the fight against *P. vivax* malaria in PNG, but also highlighted the possible drawbacks and concerns about G6PD deficiency testing and compliance.

Open questions and directions for future work

- The comparison of LM, DNA and RNA-based detection methods and the low detectability observed in the trial suggest that numerous *P. vivax* infections are missed even by molecular methods. However, even the most sensitive detection method will miss the infectious reservoir of blood-stage negative individuals carrying *P. vivax* hypnozoites. A biomarker for latent liver stages would be promising, especially in regions where MSAT against *P. vivax* is considered.

- For the first time, the triplet model approach was applied to assess *P. vivax* infection dynamics parameters. The application of a mathematical method previously designed for *P. falciparum* on *P. vivax* was a major challenge. Although the correction of duration and force of blood-stage infection for detectability is a smart strategy to cope with missed infectious clones due to low parasite density, shorter spacing between bleeds in our cohort might have been of great advantage. The duration of a *P. vivax* infection, despite being considerably shorter than reported for *P. falciparum*, might be overestimated in our cohort because of misinterpretation of short-lasting homologous relapses as a continuous infection. Computationally more intensive models for calculating infection dynamics were designed for *P. falciparum* (Felger et al., 2012), e.g. the immigration-death model. This model might prove more appropriate once applied on the genotyping data of this cohort.

- The RNA sampling strategy applied in the longitudinal cohort did not benefit from the results obtained from the analysis of the cross-sectional survey presented in the first chapter of this thesis. RNAprotect proved to be the most sensitive and reliable strategy for detecting gametocytes in field surveys, yet blood in this trial was sampled on filter paper and stored in TRIzol for RNA extraction. Albeit samples from both trial arms were subject to the same suboptimal sampling strategy and thus remain comparable with each other, comparison of gametocyte data from this study to results from future cohort studies using better RNA sampling methods should be done with great caution. Numerous recent surveys have already used RNAprotect-based sampling strategy (Mwingira et al., 2014; Tiono et al., 2013). Quantification of *P. vivax* gametocytes based on *pvs25* transcripts in RNAprotect was also recently assessed (Koepfli et al., – in press). Results from this thesis highly recommend the use of RNAprotect for all future surveys with the aim of monitoring gametocytes.

Conclusion

This thesis has for the first time assessed infection and transmission dynamics of *P. vivax* relapses and new infections in a cohort of semi-immune children living in an endemic area in PNG. This was possible by detecting gametocytes and genotyping asexual parasites in blood samples collected in a cohort study, in which relapses were prevented in a subset of children. The high contribution of relapses to the burden of *P. vivax* clinical malaria and blood-stage infections emphasized the importance of relapses for sustaining *P. vivax* transmission. Effective control of *P. vivax* with anti-malarial drugs will thus require the inclusion of a treatment that attacks the hypnozoite reservoir. The data generated in the course of this thesis demonstrates that MDA with PQ might be a valuable tool to target this undetectable parasite reservoir.

Comparison of infection dynamics between the treatment arms revealed that relapses and new infections are presumably under the same immune pressure in semi-immune children. We observed similar duration, parasite density, detectability and investment in gametocytogenesis in both treatment arms. *P. vivax* molecular force of blood-stage infections in the placebo arm was 2-3 times higher than in the PQ arm. The increased individual exposure of participants translated proportionally into an increased relapse burden and contribution to transmission. Approaches to monitor efficacies of interventions in the field should therefore stratify for transmission intensity.

During the course of this thesis, we also investigated the best strategy for RNA sampling in field surveys, validated molecular detection of *P. vivax* gametocytes by targeting *pvs25* transcripts, and established *P. falciparum* gametocyte genotyping assays. Although it was not possible to apply all of these in our longitudinal cohort, these tools have shown great potential for future investigations of transmission dynamics.

References

Battle, K.E., Karhunen, M.S., Bhatt, S., Gething, P.W., Howes, R.E., Golding, N., Van Boeckel, T.P., Messina, J.P., Shanks, G.D., Smith, D.L., Baird, J.K., Hay, S.I., 2014. Geographical variation in Plasmodium vivax relapse. Malar. J. 13, 144.

Bousema, T., Dinglasan, R.R., Morlais, I., Gouagna, L.C., van Warmerdam, T., Awono-Ambene, P.H., Bonnet, S., Diallo, M., Coulibaly, M., Tchuinkam, T., Mulder, B., Targett, G., Drakeley, C., Sutherland, C., Robert, V., Doumbo, O., Touré, Y., Graves, P.M., Roeffen, W., Sauerwein, R., Birkett, A., Locke, E., Morin, M., Wu, Y., Churcher, T.S., 2012. Mosquito feeding assays to determine the infectiousness of naturally infected Plasmodium falciparum gametocyte carriers. PloS One 7, e42821.

Bright, A.T., Manary, M.J., Tewhey, R., Arango, E.M., Wang, T., Schork, N.J., Yanow, S.K., Winzeler, E.A., 2014. A high resolution case study of a patient with recurrent Plasmodium vivax infections shows that relapses were caused by meiotic siblings. PLoS Negl. Trop. Dis. 8, e2882.

Carter, R., Graves, P.M., 1988. Gametocytes Carter R, Graves PM. Gametocytes. In: Wernsdorfer WH, McGregor I, editors. Malaria. Churchill Livingstone; Edinburgh, U.K.: 1988. pp. 253–306. In: Malaria. Churchill Livingstone; Edinburgh, U.K., pp. pp. 253–306.

Churcher, T.S., Bousema, T., Walker, M., Drakeley, C., Schneider, P., Ouédraogo, A.L., Basáñez, M.-G., 2013. Predicting mosquito infection from Plasmodium falciparum gametocyte density and estimating the reservoir of infection. eLife 2, e00626.

Coatney, G.R., Cooper, W.C., Young, M.D., 1950. Studies in human malaria. XXX. A summary of 204 sporozoite-induced infections with the Chesson strain of Plasmodium vivax. J. Natl. Malar. Soc. US 9, 381–396.

Cook, J., Xu, W., Msellem, M., Vonk, M., Bergström, B., Gosling, R., Al-Mafazy, A.-W., McElroy, P., Molteni, F., Abass, A.K., Garimo, I., Ramsan, M., Ali, A., Mårtensson, A., Björkman, A., 2014. Mass Screening and Treatment on the Basis of Results of a Plasmodium falciparum-Specific Rapid Diagnostic Test Did Not Reduce Malaria Incidence in Zanzibar. J. Infect. Dis.

Craige, B., Alving, A.S., 1947. The Chesson strain of Plasmodium vivax malaria; relationship between prepatent period, latent period and relapse rate. J. Infect. Dis. 80, 228–236.

Douglas, N.M., Simpson, J.A., Phyo, A.P., Siswantoro, H., Hasugian, A.R., Kenangalem, E., Poespoprodjo, J.R., Singhasivanon, P., Anstey, N.M., White, N.J., Tjitra, E., Nosten, F., Price, R.N., 2013. Gametocyte dynamics and the role of drugs in reducing the transmission potential of Plasmodium vivax. J. Infect. Dis. 208, 801–812.

Ehrman, F.C., Ellis, J.M., Young, M.D., 1945. PLASMODIUM VIVAX CHESSON STRAIN. Science 101, 377.

Eziefula, A.C., Bousema, T., Yeung, S., Kamya, M., Owaraganise, A., Gabagaya, G., Bradley, J., Grignard, L., Lanke, K.H.W., Wanzira, H., Mpimbaza, A., Nsobya, S., White, N.J., Webb, E.L., Staedke, S.G., Drakeley, C., 2014. Single dose primaquine for clearance of Plasmodium falciparum gametocytes in children with uncomplicated malaria in Uganda: a randomised, controlled, double-blind, dose-ranging trial. Lancet Infect. Dis. 14, 130–139.

Felger, I., Maire, M., Bretscher, M.T., Falk, N., Tiaden, A., Sama, W., Beck, H.-P., Owusu-Agyei, S., Smith, T.A., 2012. The dynamics of natural Plasmodium falciparum infections. PloS One 7, e45542.

Griffin, J.T., Hollingsworth, T.D., Okell, L.C., Churcher, T.S., White, M., Hinsley, W., Bousema, T., Drakeley, C.J., Ferguson, N.M., Basáñez, M.-G., Ghani, A.C., 2010. Reducing Plasmodium falciparum malaria transmission in Africa: a model-based evaluation of intervention strategies. PLoS Med. 7.

Halliday, K.E., Okello, G., Turner, E.L., Njagi, K., Mcharo, C., Kengo, J., Allen, E., Dubeck, M.M., Jukes, M.C.H., Brooker, S.J., 2014. Impact of intermittent screening and treatment for malaria among school children in Kenya: a cluster randomised trial. PLoS Med. 11, e1001594.

Hofmann, N., Robinson, L.J., Wampfler, R., Betuela, I., Waltmann, A., Mueller, I., Felger, I., – in preparation. Changing patterns of malarial infection and disease after intensified control efforts in Papua New Guinean children.

Howes, R.E., Piel, F.B., Patil, A.P., Nyangiri, O.A., Gething, P.W., Dewi, M., Hogg, M.M., Battle, K.E., Padilla, C.D., Baird, J.K., Hay, S.I., 2012. G6PD deficiency prevalence and estimates of affected populations in malaria endemic countries: a geostatistical model-based map. PLoS Med. 9, e1001339.

Hsiang, M.S., Hwang, J., Tao, A.R., Liu, Y., Bennett, A., Shanks, G.D., Cao, J., Kachur, S.P., Feachem, R.G., Gosling, R.D., Gao, Q., 2013. Mass drug administration for the control and elimination of Plasmodium vivax malaria: an ecological study from Jiangsu province, China. Malar. J. 12, 383.

Imwong, M., Nakeesathit, S., Day, N.P., White, N.J., 2011. A review of mixed malaria species infections in anopheline mosquitoes. Malar. J. 10, 253.

Ishikawa, H., Ishii, A., Nagai, N., Ohmae, H., Harada, M., Suguri, S., Leafasia, J., 2003. A mathematical model for the transmission of Plasmodium vivax malaria. Parasitol. Int. 52, 81–93.

Jeffery, G.M., 1956. Relapses with Chesson strain Plasmodium vivax following treatment with chloroquine. Am. J. Trop. Med. Hyg. 5, 1–13.

Karl, S., Laman, M., Koleala, T., Ibam, C., Kasian, B., N'Drewei, N., Rosanas-Urgell, A., Moore, B.R., Waltmann, A., Koepfli, C., Siba, P.M., Betuela, I., Woodward, R.C., St Pierre, T.G., Mueller, I., Davis, T.M.E., 2014. Comparison of three methods for detection of gametocytes in Melanesian children treated for uncomplicated malaria. Malar. J. 13, 319.

Kim, S., Nguon, C., Guillard, B., Duong, S., Chy, S., Sum, S., Nhem, S., Bouchier, C., Tichit, M., Christophel, E., Taylor, W.R.J., Baird, J.K., Menard, D., 2011. Performance of the CareStart™ G6PD deficiency screening test, a point-of-care diagnostic for primaquine therapy screening. PloS One 6, e28357.

Koepfli, C., Colborn, K.L., Kiniboro, B., Lin, E., Speed, T.P., Siba, P.M., Felger, I., Mueller, I., 2013. A high force of plasmodium vivax blood-stage infection drives the rapid acquisition of immunity in papua new guinean children. PLoS Negl. Trop. Dis. 7, e2403.

Koepfli, C., Robinson, L., Rarau, P., Salib, M., Sambale, N., Betuela, I., Nuitragool, W., Barry, A.E., Siba, P., Felger, I., Mueller, I., – in press. Blood-stage parasitaemia and age determine Plasmodium falciparum and P. vivax gametocytaemia in Papua New Guinea. PLoS One.

Kondrashin, A., Baranova, A.M., Ashley, E.A., Recht, J., White, N.J., Sergiev, V.P., 2014. Mass primaquine treatment to eliminate vivax malaria: lessons from the past. Malar. J. 13, 51.

Lin, E., Kiniboro, B., Gray, L., Dobbie, S., Robinson, L., Laumaea, A., Schöpflin, S., Stanisic, D., Betuela, I., Blood-Zikursh, M., Siba, P., Felger, I., Schofield, L., Zimmerman, P., Mueller, I., 2010. Differential patterns of infection and disease with P. falciparum and P. vivax in young Papua New Guinean children. PloS One 5, e9047.

Llanos-Cuentas, A., Lacerda, M.V., Rueangweerayut, R., Krudsood, S., Gupta, S.K., Kochar, S.K., Arthur, P., Chuenchom, N., Möhrle, J.J., Duparc, S., Ugwuegbulam, C., Kleim, J.-P., Carter, N., Green, J.A., Kellam, L., 2014. Tafenoquine plus chloroquine for the treatment and relapse prevention of Plasmodium vivax malaria (DETECTIVE): a multicentre, double-blind, randomised, phase 2b dose-selection study. Lancet 383, 1049–1058.

Lubell, Y., White, L., Varadan, S., Drake, T., Yeung, S., Cheah, P.Y., Maude, R.J., Dondorp, A., Day, N.P.J., White, N.J., Parker, M., 2014. Ethics, economics, and the use of primaquine to reduce falciparum malaria transmission in asymptomatic populations. PLoS Med. 11, e1001704.

McKenzie, F.E., Jeffery, G.M., Collins, W.E., 2002. Plasmodium vivax blood-stage dynamics. J. Parasitol. 88, 521–535.

Mwingira, F., Genton, B., Kabanywanyi, A.-N.M., Felger, I., 2014. Comparison of detection methods to estimate asexual Plasmodium falciparum parasite prevalence and gametocyte carriage in a community survey in Tanzania. Malar. J. 13, 433.

Okell, L.C., Griffin, J.T., Kleinschmidt, I., Hollingsworth, T.D., Churcher, T.S., White, M.J., Bousema, T., Drakeley, C.J., Ghani, A.C., 2011. The potential contribution of mass treatment to the control of Plasmodium falciparum malaria. PloS One 6, e20179.

Ouédraogo, A.L., Bousema, T., Schneider, P., de Vlas, S.J., Ilboudo-Sanogo, E., Cuzin-Ouattara, N., Nébié, I., Roeffen, W., Verhave, J.P., Luty, A.J.F., Sauerwein, R., 2009. Substantial contribution of submicroscopical Plasmodium falciparum gametocyte carriage to the infectious reservoir in an area of seasonal transmission. PloS One 4, e8410.

Pybus, B.S., Sousa, J.C., Jin, X., Ferguson, J.A., Christian, R.E., Barnhart, R., Vuong, C., Sciotti, R.J., Reichard, G.A., Kozar, M.P., Walker, L.A., Ohrt, C., Melendez, V., 2012. CYP450 phenotyping and accurate mass identification of metabolites of the 8-aminoquinoline, anti-malarial drug primaquine. Malar. J. 11, 259.

Sattabongkot, J., Maneechai, N., Rosenberg, R., 1991. Plasmodium vivax: gametocyte infectivity of naturally infected Thai adults. Parasitology 102 Pt 1, 27–31.

Sattabongkot, J., Tsuboi, T., Hisaeda, H., Tachibana, M., Suwanabun, N., Rungruang, T., Cao, Y.-M., Stowers, A.W., Sirichaisinthop, J., Coleman, R.E., Torii, M., 2003. Blocking of transmission to mosquitoes by antibody to Plasmodium vivax malaria vaccine candidates Pvs25 and Pvs28 despite antigenic polymorphism in field isolates. Am. J. Trop. Med. Hyg. 69, 536–541.

Schneider, P., Bousema, J.T., Gouagna, L.C., Otieno, S., van de Vegte-Bolmer, M., Omar, S.A., Sauerwein,

R.W., 2007. Submicroscopic Plasmodium falciparum gametocyte densities frequently result in mosquito infection. Am. J. Trop. Med. Hyg. 76, 470–474.

Smith, T., Felger, I., Fraser-Hurt, N., Beck, H.P., 1999. Effect of insecticide-treated bed nets on the dynamics of multiple Plasmodium falciparum infections. Trans. R. Soc. Trop. Med. Hyg. 93 Suppl 1, 53–57.

Sutanto, I., Tjahjono, B., Basri, H., Taylor, W.R., Putri, F.A., Meilia, R.A., Setiabudy, R., Nurleila, S., Ekawati, L.L., Elyazar, I., Farrar, J., Sudoyo, H., Baird, J.K., 2013. Randomized, open-label trial of primaquine against vivax malaria relapse in Indonesia. Antimicrob. Agents Chemother. 57, 1128–1135.

Tiono, A.B., Ouédraogo, A., Ogutu, B., Diarra, A., Coulibaly, S., Gansané, A., Sirima, S.B., O'Neil, G., Mukhopadhyay, A., Hamed, K., 2013. A controlled, parallel, cluster-randomized trial of community-wide screening and treatment of asymptomatic carriers of Plasmodium falciparum in Burkina Faso. Malar. J. 12, 79.

Townell, N., Looke, D., McDougall, D., McCarthy, J.S., 2012. Relapse of imported Plasmodium vivax malaria is related to primaquine dose: a retrospective study. Malar. J. 11, 214.

Triglia, T., Thompson, J., Caruana, S.R., Delorenzi, M., Speed, T., Cowman, A.F., 2001. Identification of proteins from Plasmodium falciparum that are homologous to reticulocyte binding proteins in Plasmodium vivax. Infect. Immun. 69, 1084–1092.

White, N.J., 2011. Determinants of relapse periodicity in Plasmodium vivax malaria. Malar. J. 10, 297.

White, N.J., Ashley, E.A., Recht, J., Delves, M.J., Ruecker, A., Smithuis, F.M., Eziefula, A.C., Bousema, T., Drakeley, C., Chotivanich, K., Imwong, M., Pukrittayakamee, S., Prachumsri, J., Chu, C., Andolina, C., Bancone, G., Hien, T.T., Mayxay, M., Taylor, W.R., von Seidlein, L., Price, R.N., Barnes, K.I., Djimdé, A., Ter Kuile, F., Gosling, R., Chen, I., Dhorda, M.J., Stepniewska, K., Guérin, P., Woodrow, C.J., Dondorp, A.M., Day, N.P., Nosten, F.H., 2014. Assessment of therapeutic responses to gametocytocidal drugs in Plasmodium falciparum malaria. Malar. J. 13, 483.

Whorton, C.M., Pullman, T.N., 1947. The Chesson strain of Plasmodium vivax malaria; immunity. J. Infect. Dis. 81, 1–6.

Appendix

During the course of this PhD thesis contributions were made to the following project entitled: "Heterochromatin protein 1 secures survival and transmission of malaria parasites" published in Cell Host Microbe. It exhibits the key role of the Heterochromatin Protein 1 (HP1) in silencing the ApAP2-G locus, a transcription factor required for gametocyte conversion.

This publication is not directly linked to this thesis, however the contributed work consisted in RNA extraction of *in vitro* reared gametocytes, design and analysis of multiple real-time assays.

Cell Host & Microbe
Article

Heterochromatin Protein 1 Secures Survival and Transmission of Malaria Parasites

Nicolas M.B. Brancucci,[1,2,4] Nicole L. Bertschi,[1,2,4] Lei Zhu,[3] Igor Niederwieser,[1,2] Wai Hoe Chin,[3] Rahel Wampfler,[1,2] Céline Freymond,[1,2] Matthias Rottmann,[1,2] Ingrid Felger,[1,2] Zbynek Bozdech,[3] and Till S. Voss[1,2,*]
[1]Department of Medical Parasitology and Infection Biology, Swiss Tropical and Public Health Institute, Socinstrasse 57, Basel 4051, Switzerland
[2]University of Basel, Petersplatz 1, Basel 4003, Switzerland
[3]School of Biological Sciences, Nanyang Technological University, 50 Nanyang Avenue, Singapore 639798, Singapore
[4]Co-first author
*Correspondence: till.voss@unibas.ch
http://dx.doi.org/10.1016/j.chom.2014.07.004

SUMMARY

Clonally variant expression of surface antigens allows the malaria parasite *Plasmodium falciparum* to evade immune recognition during blood stage infection and secure malaria transmission. We demonstrate that heterochromatin protein 1 (HP1), an evolutionary conserved regulator of heritable gene silencing, controls expression of numerous *P. falciparum* virulence genes as well as differentiation into the sexual forms that transmit to mosquitoes. Conditional depletion of *P. falciparum* HP1 (PfHP1) prevents mitotic proliferation of blood stage parasites and disrupts mutually exclusive expression and antigenic variation of the major virulence factor PfEMP1. Additionally, PfHP1-dependent regulation of PfAP2-G, a transcription factor required for gametocyte conversion, controls the switch from asexual proliferation to sexual differentiation, providing insight into the epigenetic mechanisms underlying gametocyte commitment. These findings show that PfHP1 is centrally involved in clonally variant gene expression and sexual differentiation *in P. falciparum* and have major implications for developing antidisease and transmission-blocking interventions against malaria.

INTRODUCTION

The protozoan parasite *Plasmodium falciparum* elicits the most severe form of malaria in humans and causes several hundred million clinical cases and 700,000 deaths annually (World Health Organisation, 2013). Malaria morbidity and mortality occur due to the massive expansion of the parasite population during blood-stage infection. Here, parasites mature intracellularly through the ring and trophozoite stages, before successive S/M-phases produce a multinucleated schizont that releases up human host, in particular those imposed by the immune system (Rovira-Graells et al., 2012; Cortés et al., 2012).

The most striking example of CVGE is erythrocyte membrane protein 1 (PfEMP1), the major antigen and prime immune target on the surface of infected RBCs (iRBCs) (Scherf et al., 2008). PfEMP1 is encoded by the 60-member *var* gene family (Su et al., 1995; Baruch et al., 1995) and mediates cytoadherence of iRBCs to microvascular endothelium, which prevents parasite clearance in the spleen and causes pathology that contributes substantially to severe malaria outcomes (Kyes et al., 2001). *var* transcription conforms to the concept of singular gene choice (or mutual exclusion); in each parasite only a single *var* gene is active, while all other members remain silenced (Scherf et al., 1998). Transcriptional switches in *var* gene expression result in CVGE and consequently antigenic variation of PfEMP1 and immune evasion (Smith et al., 1995; Scherf et al., 1998). Importantly, this survival strategy is directly linked to malaria transmission; during each replicative cycle a small number of parasites commit to sexual development and differentiate into mature stage V gametocytes, the only stage capable of transmitting the infection to the mosquito vector (Baker, 2010).

Singular *var* gene choice is regulated by a poorly understood interplay between transcriptional and epigenetic control mechanisms (Guizetti and Scherf, 2013). Particularly striking is the observation that *var* genes are associated with histone 3 lysine 9 trimethylation (H3K9me3) and heterochromatin protein 1 (HP1) (Salcedo-Amaya et al., 2009; Lopez-Rubio et al., 2009; Flueck et al., 2009; Pérez-Toledo et al., 2009; Chookajorn et al., 2007; Lopez-Rubio et al., 2007). HP1 is an evolutionarily conserved regulator of heterochromatin formation and heritable gene silencing and was originally described in *Drosophila melanogaster* as a suppressor of position effect variegation (Eissenberg et al., 1990). HP1 binds to H3K9me2/H3K9me3, the hallmark histone modification of heterochromatin, and recruits H3K9-specific methyltransferases (HKMTs) that modify adjacent nucleosomes (Lomberk et al., 2006). As a result, HP1 sustains a self-perpetuating mechanism for heterochromatin spreading and heritable gene silencing. In addition, HP1 also regulates euchromatic genes and is involved in other chromatin-related

diverse proteins (Lomberk et al., 2006; Kwon and Workman, 2008).

P. falciparum contains only a single HP1 protein that localizes primarily to H3K9me3-enriched heterochromatic regions. These chromosomal domains incorporate all *var* genes and hundreds of other clonally variant genes (such as *rif*, *stevor*, and *pfmc-2tm*) encoding species-specific blood-stage antigens. At the same time, PfHP1 is also found at a small number of euchromatic loci (Flueck et al., 2009; Pérez-Toledo et al., 2009). PfHP1 overexpression leads to increased silencing of some heterochromatic genes (Flueck et al., 2009), and the presence or absence of PfHP1 is linked to the silenced or active state of *var* genes, respectively (Pérez-Toledo et al., 2009). Together, these observations suggest key functions for PfHP1 in heritable silencing and phenotypic variation of a large set of factors implicated in host-parasite interactions and immune evasion. However, if and to what extent PfHP1 is indeed required for mutually exclusive *var* expression and/or for CVGE in general is unknown. Moreover, since the *pfhp1* locus is refractory to genetic deletion (Flueck et al., 2009; Pérez-Toledo et al., 2009), additional unknown HP1-dependent pathways essential for parasite proliferation are likely to exist in *P. falciparum*.

Here, we conducted a comprehensive functional analysis of PfHP1 by generating a conditional PfHP1 loss-of-function mutant. We show that PfHP1 is indispensable for the heritable silencing of heterochromatic genes in general and in particular for the maintenance of singular *var* gene choice and antigenic variation of PfEMP1. In addition, PfHP1 is required at the G1/S transition phase for mitotic proliferation of blood-stage parasites. Intriguingly, we also discovered that PfHP1 controls sexual commitment by regulating the bistable expression of single euchromatic locus encoding an ApiAP2 transcription factor.

RESULTS

PfHP1 Is Indispensable for Mitotic Proliferation of Blood-Stage Parasites

We applied the FKBP destabilization domain (DD) technique that allows modulating expression levels through the stabilizing compound Shield-1 (Banaszynski et al., 2006; Armstrong and Goldberg, 2007) and generated a clonal parasite line expressing endogenous PfHP1 as a C-terminally tagged GFP-DD fusion (3D7/HP1^{ON}) (Figure S1, available online). In the presence of Shield-1, 3D7/HP1^{ON} parasites exhibited no growth phenotype (Figure 1A) and multiplied at a rate within a single asexual replication cycle (3.8-fold ± 0.6 SD) similar to that of 3D7/HP1^{ctrl} parasites in which PfHP1 is tagged with GFP only (4.4-fold ± 0.4 SD). When Shield-1 was withdrawn at 4–12 hr postinvasion (hpi), 3D7/HP1^{OFF} parasites completed the current intraerythrocytic developmental cycle (IDC) and subsequent ring-stage development with normal kinetics. Strikingly, however, these parasites arrested prior to schizogony in generation 2 (Figure 1A), and all efforts to select for proliferating subpopulations were unsuccessful.

Live-cell imaging revealed the expected perinuclear localization of tagged PfHP1 in 3D7/HP1^{ON} and 3D7/HP1^{ctrl} parasites throughout the IDC, whereas in 3D7/HP1^{OFF} parasites PfHP1 was undetectable 12 hr after Shield-1 withdrawal (Figure 1B). A more direct assessment by parallel western blot and immunofluorescence assays (IFA) showed that after Shield-1 removal at 4–12 hpi, PfHP1 was still detectable but reduced in late ring stages (16–24 hpi) and early schizonts (32–40 hpi) and localized diffusely to the nucleoplasm and cytoplasm (Figure 1C). After reinvasion, PfHP1 was undetectable in 3D7/HP1^{OFF} parasites by both methods. Similarly, targeted chromatin immunoprecipitation (ChIP-qPCR) showed that PfHP1 occupancy at subtelomeric (PF3D7_0426000) and chromosome-internal (PF3D7_0412400) *var* loci was unchanged in late ring stages but substantially reduced in schizonts and subsequent generation 2 ring stages (Figure 1D).

We next analyzed parasite viability using isothermal microcalorimetry (Wenzler et al., 2012). In generation 1, 3D7/HP1^{ON} and 3D7/HP1^{OFF} populations both displayed a typical heat emission profile marked by increased heat flow in trophozoites and schizonts (Figure 1E). In generation 2, however, the metabolic activity in PfHP1-depleted parasites changed dramatically, and heat emission remained low over the entire 48 hr period of measurement. Importantly, these parasites were still viable since they emitted heat at a rate significantly higher than that of uninfected RBCs.

PfHP1 Controls Sexual Differentiation

Intriguingly, prolonged microscopic observation revealed that PfHP1-depleted parasites consisted of a mixture of growth-arrested trophozoites and sexual forms undergoing gametocyte development (Figure 2A). Note that sexual conversion occurs through an unknown mechanism during the cell cycle prior to gametocyte development and that all daughter parasites released from a committed schizont undergo sexual differentiation (Bruce et al., 1990). To discriminate quantitatively between growth-arrested and sexual forms, we visualized the gametocyte-specific marker Pfs16 (Bruce et al., 1994) and knob-associated histidine-rich protein (KAHRP) (a marker for iRBCs) (Taylor et al., 1987) by indirect IFA. Remarkably, 52.7% (±3.1 SD) of 3D7/HP1^{OFF} parasites expressed Pfs16 in generation 2, compared to only 2.3% (±1.2 SD) of background conversion in the 3D7/HP1^{ON} population (Figure 2B). Overview images of a Giemsa-stained blood smear (6 days postinvasion) and an α-Pfs16 IFA experiment (32–40 hpi) provide visual confirmation of this phenotype showing a high proportion of stage II/III and stage I gametocytes, respectively, in 3D7/HP1^{OFF} parasites (Figures 2C and 2D). Notably, PfHP1-depleted gametocytes completed sexual development within 8–10 days, similar to control gametocytes (Figure S2). Hence, PfHP1 depletion triggers the synchronous hyperinduction of viable gametocytes, which demonstrates that sexual commitment in malaria parasites is epigenetically regulated.

PfHP1-Depleted Asexual Parasites Enter a Reversible Cell-Cycle Arrest

To investigate at which stage of the cell cycle the nongametocyte subpopulation of 3D7/HP1^{OFF} parasites arrested, we performed single-cell DNA content analysis by flow cytometry. This revealed that in contrast to 3D7/HP1^{ON} parasites, virtually all parasites in the 3D7/HP1^{OFF} population failed to replicate their genome in generation 2 (Figure 3A). While this is expected for nonproliferative gametocytes, this result demonstrates that the population of asexual parasites arrested prior to or during the

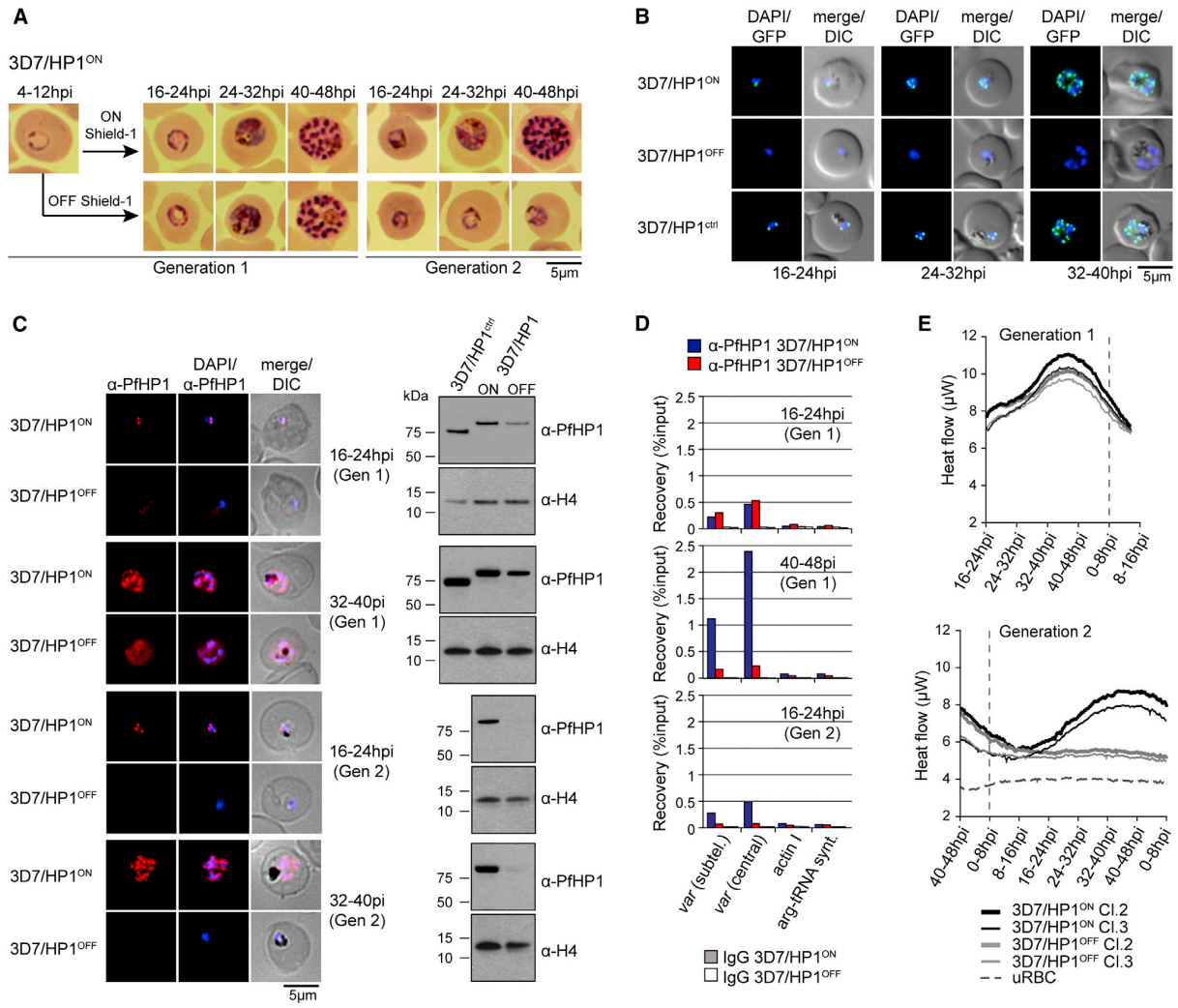

Figure 1. Growth Phenotype of a Conditional PfHP1 Loss-of-Function Mutant and Kinetics of PfHP1 Depletion

(A) Giemsa-stained blood smears showing development of 3D7/HP1^{ON} and 3D7/HP1^{OFF} parasites over two generations (96 hr). See also Figure S1.

(B) Expression and localization of PfHP1 in 3D7/HP1^{ON}, 3D7/HP1^{OFF}, and 3D7/HP1^{ctrl} parasites by live fluorescence microscopy (images taken 12 hr after removal of Shield-1).

(C) Expression and localization of PfHP1 in 3D7/HP1^{ON} and 3D7/HP1^{OFF} parasites by IFA and western blot (Shield-1 removal at 4–12 hpi). The production and specificity of affinity-purified polyclonal α-PfHP1 antibodies is described in Figure S1 and the Supplemental Experimental Procedures.

(D) PfHP1 occupancy at two heterochromatic *var* and two euchromatic control loci in 3D7/HP1^{ON} and 3D7/HP1^{OFF} parasites was determined by ChIP-qPCR (Shield-1 removal at 4–12 hpi). See also Figure S6.

(E) Heat emission as determined by isothermal microcalorimetry in two 3D7/HP1 clones (Cl.2 and Cl.3) grown in the presence or absence of Shield-1. uRBC, uninfected RBCs.

first S phase of schizogony. Interestingly, this cell-cycle defect was reversible since PfHP1-depleted trophozoites reentered S phase and mitotic proliferation when Shield-1 was added back to the culture medium (Figure 3B). Even after 12 days in the absence of Shield-1, rescued trophozoites reaccumulated perinuclear PfHP1 and progressed through schizogony (Figure 3C). This was not due to a genetic reversion, as rescued parasites entered developmental arrest and gametocyte hyperconversion when Shield-1 was withdrawn for a second time (data not shown). With prolonged time in the absence of Shield-1, however, the parasitemia decreased, and the time required for growth resumption after Shield-1 replenishment increased, showing that a subset of PfHP1-depleted parasites died over time (Figures 3B and 3D). Together, these data corroborate the essential function of PfHP1 in mitotic proliferation and show that a subset of PfHP1-depleted trophozoites remained in a state of dormancy capable of reentering the cell cycle if PfHP1 expression was restored.

Cell Host & Microbe
HP1-Dependent Gene Regulation in Malaria Parasites

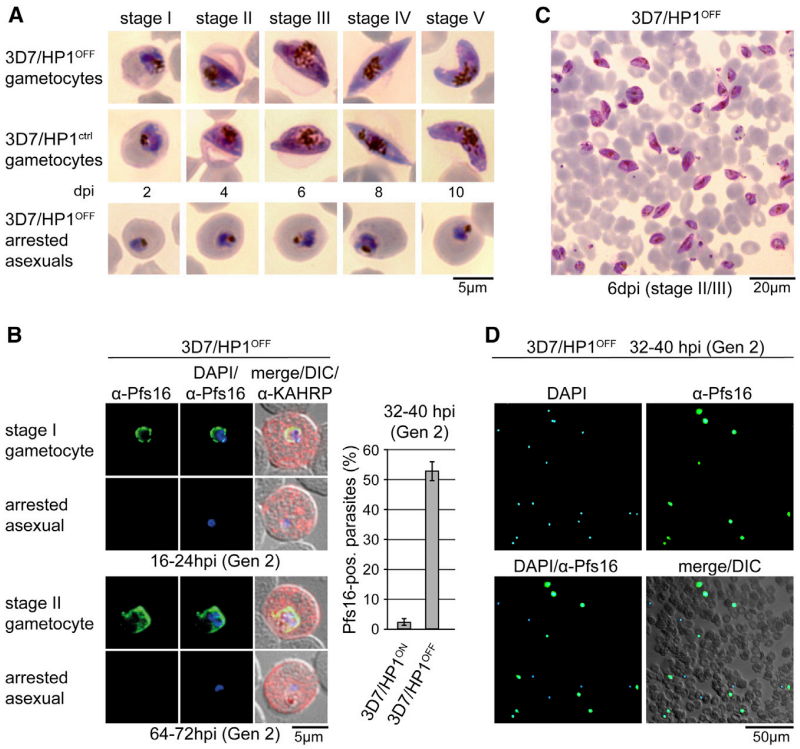

Figure 2. PfHP1 Depletion Induces Gametocyte Conversion

(A) 3D7/HP1^{OFF} and 3D7/HP1^{ctrl} gametocytes and cell-cycle-arrested 3D7/HP1^{OFF} trophozoites. dpi, days postreinvasion.

(B) Distinction between 3D7/HP1^{OFF} early gametocytes and arrested trophozoites by IFA (left) and proportion of Pfs16/KAHRP-positive parasites in 3D7/HP1^{ON} and 3D7/HP1^{OFF} (right). Values show the mean ± SD of three biological replicates (100 KAHRP-pos. iRBCs were scored per experiment).

(C) Giemsa-stained blood smear of a 3D7/HP1^{OFF} parasite culture (Shield-1 removal at 4–12 hpi) at 6 days postreinvasion (dpi) (image taken at 60× magnification). The gametocyte hyperinduction phenotype is highlighted by the high proportion of stage II/III gametocytes among all iRBCs.

(D) α-Pfs16 IFA of a 3D7/HP1^{OFF} parasite culture (Shield-1 removal at 4–12 hpi) at 32–40 hr postreinvasion (image taken at 40× magnification). The gametocyte hyperinduction phenotype is highlighted by the high proportion of Pfs16-positive stage I gametocytes among all DAPI-positive iRBCs. See also Figure S2.

Lack of S/M Phase Entry Correlates with Decelerated Transcriptome Progression in G1 Phase

We next conducted genome-wide transcriptional profiling of paired synchronous 3D7/HP1^{ON} and 3D7/HP1^{OFF} cultures at 11 consecutive time points (TPs) spanning generations 1 and 2 to (i) study the effect of PfHP1 on heritable gene silencing and (ii) identify the PfHP1-dependent pathway responsible for gametocyte conversion (Figure 4A and Table S1). Until 16–24 hpi in generation 2, the corresponding transcriptomes were highly comparable between both populations (Figure 4A) and progressed with similar kinetics through the first IDC and second-generation ring-stage development (TPs 2–9) (Figures 4B and 4C). In contrast, at 24–48 hr after reinvasion (TPs 10–12), when 3D7/HP1^{ON} parasites went through schizogony and the 3D7/HP1^{OFF} population consisted of a mixture of early gametocytes and arrested trophozoites, the transcriptomes correlated poorly (Figure 4A), and parasites failed to launch a schizont-specific transcription profile (Figures 4B and 4C). This slowdown in transcriptome development reflects a substantial deceleration in G1 progression and failure to enter S phase in generation 2, which is consistent with the growth phenotype observed for 3D7/HP1^{OFF} parasites.

PfHP1 Silences Heterochromatic Genes and Is Essential for the Maintenance of Singular *Var* Gene Choice

To identify genes differentially expressed in direct response to PfHP1 depletion, we focused our analysis on the comparable growth phase ranging from generation 1 trophozoites to late ring stages in generation 2 (TPs 4–9). Consistent with the conserved role for HP1 in heritable gene silencing, we observed a general derepression of heterochromatic genes in 3D7/HP1^{OFF} parasites, and 113 PfHP1-associated genes (31.2%) displayed a significant increase in mean expression (>1.5-fold, false discovery rate [FDR] < 0.1) compared to 3D7/HP1^{ON} parasites (Figure 5A and Table S1). In contrast, only 16 euchromatic genes (0.34%) were differentially expressed, of which four upregulated genes had previously been associated with early gametocyte development: PF3D7_1102500 (*phistb*; GEXP02), PF3D7_1335000 (*msrp1*), PF3D7_1472200 (class II histone deacetylase [HDAC]), and PF3D7_1473700 (*nup116*) (Silvestrini et al., 2010; Eksi et al., 2012) (Figure 5B and Table S1). Strikingly, the strongest derepression was observed for the *var* gene family; 52 out of 60 members were significantly and highly upregulated in PfHP1-depleted parasites. In addition, many *rif* and *pfmc-2tm* genes and several members of other subtelomeric gene families were significantly induced, and even among the nonsignificantly deregulated heterochromatic genes, the majority was still upregulated in the absence of PfHP1 (Figures 5A and S3).

We next investigated the prevailing role of PfHP1 in *var* gene silencing in more detail. Removal of Shield-1 at 4–12 hpi had no immediate effect on *var* transcription in generation 1 (Figure 6A), which is explained by the persistent binding of PfHP1 to chromatin shortly after Shield-1 withdrawal (Figure 1D). *var* transcription was also unchanged in schizonts, demonstrating that *var* promoters retain their ring-stage-specific activation profile even in the absence of PfHP1. By contrast, almost all *var* genes were massively upregulated after reinvasion, and individual genes showed expression levels up to 30-fold higher (Figure 6A). Importantly, however, the few *var* genes already dominantly expressed in 3D7/HP1^{ON} parasites, most notably *var2csa* (PF3D7_1200600) (Salanti et al., 2003), were not or

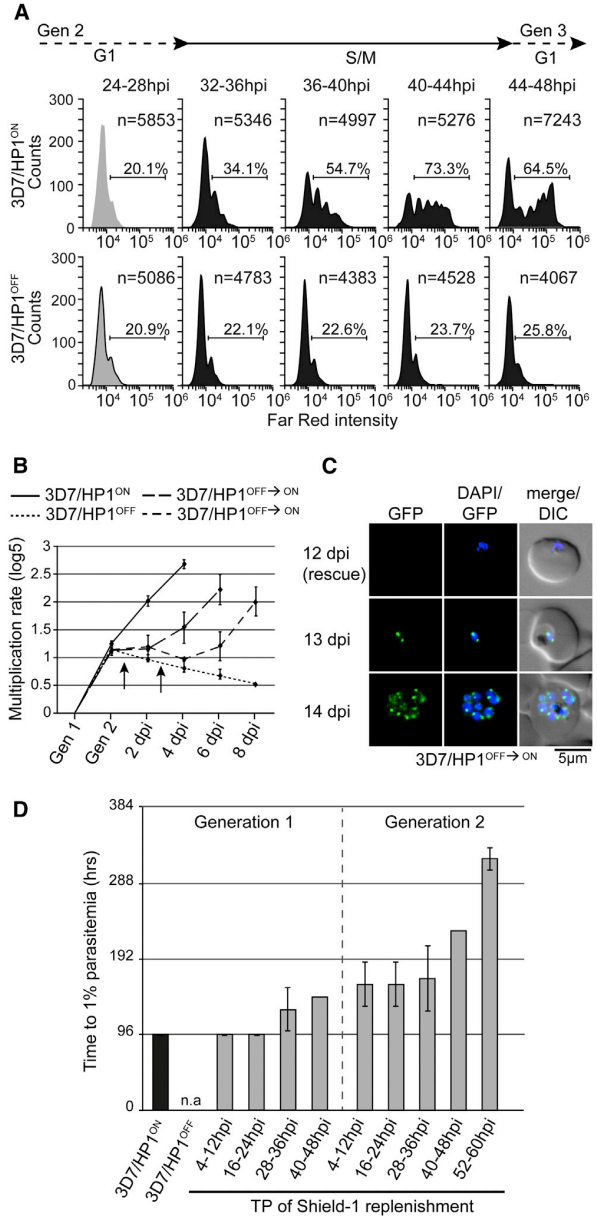

Figure 3. PfHP1 Depletion Causes Reversible Cell-Cycle Arrest at the G1/S Transition Phase

(A) Flow cytometry analysis of genomic DNA content in 3D7/HP1^{ON} and 3D7/HP1^{OFF} parasites at five consecutive time points in generation 2. The percentage of iRBCs with ≥2 genomes is indicated. Prior to S phase (gray), this value corresponds to RBCs infected with ≥2 parasites (confirmed by microscopy). *n*, number of gated iRBCs.

(B) Cell-cycle-arrested 3D7/HP1^{OFF} parasites reestablish asexual growth after adding back Shield-1 at 24 or 72 hr postreinvasion (arrows). Values show the mean of three biological replicates ± SD.

(C) Growth-arrested 3D7/HP1^{OFF} parasites reenter mitotic proliferation after Shield-1 replenishment. dpi, days postreinvasion.

(D) Synchronous 3D7/HP1^{ON} cultures (~0.1% parasitemia) were split at 0–8 hpi and cultured in either the presence or absence of Shield-1. Shield-1 was added back to 3D7/HP1^{OFF} cultures at nine consecutive TPs. Cultures were smeared daily and analyzed by Giemsa staining until they reached a parasitemia of >1%. Values show the mean of three biological replicates ± SD.

only slightly induced (Figures 6A and S4). This proves that *var* activation was not due to transcriptional switches but that all *var* genes were active simultaneously in 3D7/HP1^{OFF} parasites. Consistent with these findings, PfHP1-depleted parasites coexpressed several PfEMP1 variants of different sizes, whereas 3D7/HP1^{ON} parasites predominantly expressed a single protein consistent with the size of VAR2CSA (Figure 6B). IFAs further corroborated hyperexpression of PfEMP1 in 3D7/HP1^{OFF} parasites at the single-cell level and indicated correct trafficking of PfEMP1 to the iRBC surface (Figure 6C).

Sexual Differentiation Is Linked to the PfHP1-Dependent Derepression of the ApiAP2 Transcription Factor PfAP2-G

Interestingly, a single member of the *apiap2* family of genes encoding phylum-specific transcription factors (TFs) (Balaji et al., 2005) was also significantly derepressed in 3D7/HP1^{OFF} parasites (Figure 5A). This *apiap2* gene (PF3D7_1222600) represents the only PfHP1-associated member of the family (Flueck et al., 2009) and encodes the TF AP2-G that is essential for gametocyte conversion in *P. falciparum* and *P. berghei* (Kafsack et al., 2014; Sinha et al., 2014). Moreover, among all deregulated PfHP1-associated loci, *pfap2-g* was the only gene that does not encode a surface antigen or exported protein (Table S1). We observed that *pfap2-g* derepression was already initiated in 3D7/HP1^{OFF} generation 1 schizonts (32–40 hpi), coincident with the dissociation of PfHP1 from the *pfap2-g* locus (Figure 7A). Importantly, when 3D7/HP1^{OFF} parasites were allowed to reaccumulate PfHP1 prior to schizogony (28–36 hpi), gametocyte hyperconversion was prevented (Figures 7B and S5). Restoring PfHP1 expression at 34–42 hpi was only moderately effective in preventing sexual commitment, and parasites rescued at 40–48 hpi or after reinvasion showed a hyperconversion phenotype similar to that of nonrescued parasites. The temporal correlation between derepression of *pfap2-g* and gametocyte commitment during schizogony, together with the fact that both processes are strictly PfHP1 dependent, identifies the targeted activation of PfAP2-G as the key mechanism responsible for sexual conversion.

PfHP1 Depletion Results in Reduced H3K9me3 Levels at Heterochromatic Loci

HP1-dependent recruitment of SU(VAR)3-9-type HKMTs is essential for the spreading and inheritance of H3K9me3 marks in model eukaryotes (Grewal and Jia, 2007). We therefore tested if the local depletion of PfHP1 caused a reduction of H3K9me3 levels. Indeed, ChIP-qPCR experiments demonstrated that H3K9me3 occupancy was substantially reduced at *var* genes and the *pfap2-g* locus in 3D7/HP1^{OFF} parasites, in both generation 1 schizonts and generation 2 ring stages (Figure S6). Notably, the drop in H3K9me3 enrichment at individual loci was pronounced to a degree equal to that of the depletion of PfHP1 itself. As expected, PfHP1 and H3K9me3 were not associated with the early gametocyte marker *pfs16* in both cultures at both TPs, which confirms that upregulation of *pfs16* in early gametocytes is PfHP1 independent and rather occurs as a result of

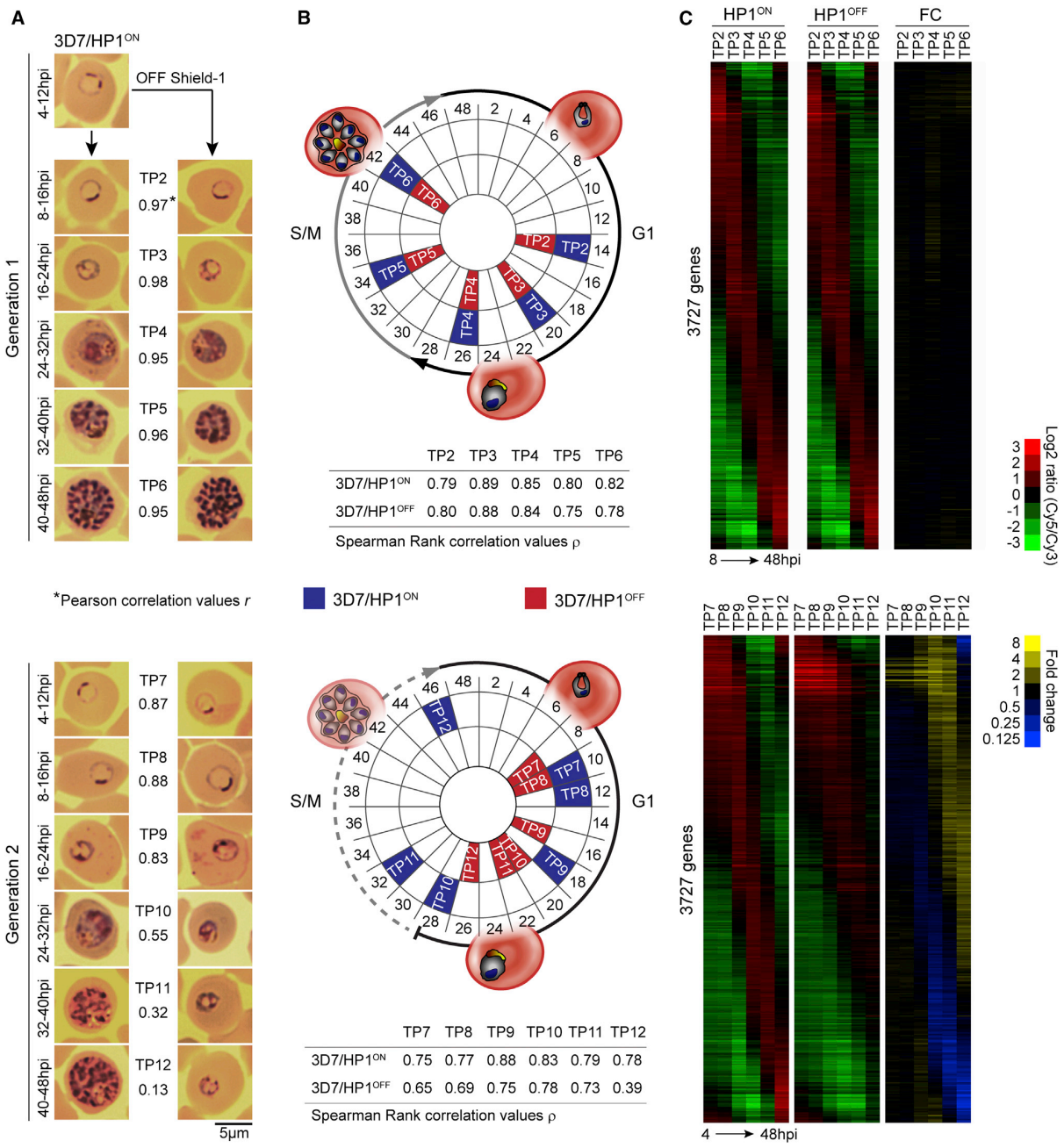

Figure 4. *Pf*HP1 Depletion Leads to a Marked Slowdown in Transcriptome Progression

(A) 3D7/HP1^{ON} and 3D7/HP1^{OFF} parasites were sampled for comparative transcriptome analysis. Pairwise correlation between transcriptomes of corresponding TPs is indicated by Pearson correlation coefficient *r* (asterisk).

(B) Mapping of experimental transcriptomes to a high-resolution reference data set (Mok et al., 2011). Blue and red boxes identify the best-fit TP (hpi) in a high-resolution reference data set for each 3D7/HP1^{ON} and 3D7/HP1^{OFF} transcriptome, respectively. Spearman rank coefficients (ρ) are provided. See also Supplemental Experimental Procedures.

(C) Comparison of global temporal expression profiles in generations 1 and 2. Heatmaps are ordered according to the phase calculated for 3D7/HP1^{ON} parasites (TPs 7–12, starting at $-\pi/2$) and display relative gene expression levels (red/green) and fold changes (FCs) in gene expression (yellow/blue). See also Table S1 and Supplemental Experimental Procedures.

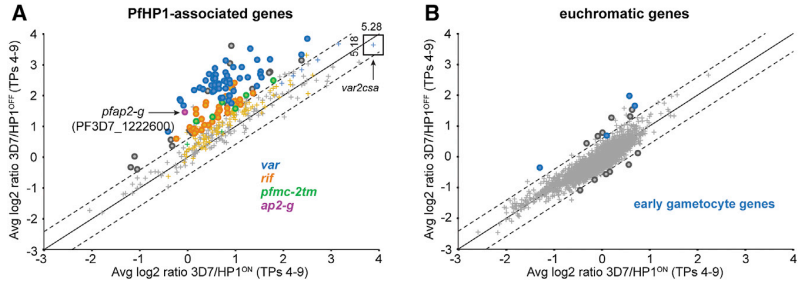

Figure 5. PfHP1 Depletion Leads to Derepression of PfHP1-Associated Genes

(A) Scatter plot comparing mean relative expression values of all 362 PfHP1-associated genes. Significantly deregulated genes are indicated by circles (>1.5-fold; FDR < 0.1). See also Figure S3 and Table S1.

(B) Scatter plot comparing mean relative expression values of all 4,771 euchromatic genes. Significantly deregulated genes are indicated by circles (>1.5-fold; FDR < 0.1). See also Table S1.

a gametocyte-specific transcriptional program. Together, these findings show that, in analogy to other eukaryotes, PfHP1 is required for the local deposition and inheritance of H3K9me3 marks on newly replicated chromatin. This is likely mediated by the PfHP1-dependent recruitment of a H3K9-specific HKMT (probably PfSET3; Volz et al., 2010; Lopez-Rubio et al., 2009). However, confirmation of PfSET3 as a functional SU(VAR)3-9 homolog as well as a possible physical interaction of this factor with PfHP1 remains to be determined.

Identification of Genes Associated With Early Gametocyte Development

Our experimental setup combined with the high rate of synchronous gametocyte induction in PfHP1-depleted parasites allowed us to identify transcriptional events linked to gametocyte conversion in real time and based on comparison of two isogenic clones. Following derepression of *pfap2-g* in generation 1, known markers of early sexual development were upregulated only after reinvasion (Table S1), and this was confirmed by quantitative RT-PCR (qRT-PCR) (Figure 7C). We therefore queried our data set to identify genes induced upon gametocyte conversion and identified 29 additional early gametocyte candidate genes (Figure 7D and Table S1). Notably, 17 (58.6%) of these genes have been linked to early sexual development in previous high-throughput studies (Silvestrini et al., 2005, 2010; Eksi et al., 2012; Young et al., 2005), which underpins the high accuracy and stringency of our search. qRT-PCR confirmed upregulation of these genes in 3D7/HP1^{OFF} parasites and showed that apart from *pfap2-g*, only one additional gene (PF3D7_0832300; *phista*-like) was upregulated already during the commitment phase. In contrast, induction of all other genes was delayed until the sexual ring stage and increased further during stage I gametocyte development (24–40 hpi) (Figures 7D and S7). Finally, we tested if these candidate genes are also upregulated in naturally induced gametocytes by comparing their transcription between 3D7 wild-type parasites and a gametocyte-deficient clone of 3D7 (F12) (Alano et al., 1995). Indeed, all predicted genes showed consistently higher transcription levels in 3D7 compared to F12, which ultimately confirms that their activation is related to early gametocyte differentiation (Figure S7).

DISCUSSION

Our study shows that PfHP1 is strictly required to propagate nonpermissive heterochromatin to daughter cells in order to silence a vast antigenic repertoire and, in particular, to perpetuate mutually exclusive *var* transcription. Since the landmark discovery of the *var* gene family (Su et al., 1995; Baruch et al., 1995; Smith et al., 1995), a large number of studies firmly established that antigenic variation in *P. falciparum* is controlled by a complex epigenetic strategy involving reversible histone modifications, chromatin remodeling, and locus repositioning (Lopez-Rubio et al., 2007, 2009; Jiang et al., 2013; Freitas-Junior et al., 2005; Tonkin et al., 2009; Duraisingh et al., 2005; Petter et al., 2011; Voss et al., 2006; Ralph et al., 2005). Together, these findings support a model in which singular *var* gene choice is achieved by restricting transcription of a single locus to an elusive perinuclear *var* expression site (VES) and where switching occurs through competitive replacement of the active gene with a previously silenced member. How these different processes and layers of regulation are interconnected to control antigenic variation, however, is only poorly understood.

Here, we demonstrate that depletion of PfHP1 during schizogony leads to the simultaneous activation of all *var* genes and concomitant hyperexpression of PfEMP1 in daughter parasites. This shows that PfHP1 is required to protect *var* genes from activation outside the VES, which is further supported by the fact that *var* promoter fragments activate stage-specific transcription by default when placed upstream of the transcriptional start site of a euchromatic gene (Brancucci et al., 2012). Hence, unlike in African trypanosomes (Navarro and Gull, 2001), the functional principle of the VES is not based on the sequestration of exclusive transcription machinery but rather depends on histone modifying and remodeling activities capable of disassembling heterochromatin at a single locus. This concept is consistent with the recent description of the H3K4me-specific methyltransferase (HKMT) PfSET10 that localizes exclusively to the VES (Volz et al., 2012). Note that mutually exclusive *var* transcription is also disrupted in parasites lacking expression of the H3K36-specific HKMT PfSET2 (also known as PfSETvs) (Jiang et al., 2013). Interestingly, Jiang et al. (2013) observed a reduction in H3K36me3 as well as H3K9me3 occupancy at active *var* loci in ΔPfSET2 parasites, suggesting functional interdependence of different epigenetic control processes in regulating antigenic variation. Taken together, these results fill an important gap in our understanding of the regulatory mechanisms underlying mutually exclusive *var* gene transcription and antigenic variation of PfEMP1 and will be instrumental for the further functional dissection of this important immune evasion strategy. Moreover, the PfEMP1 hyperexpression phenotype reported here will serve as a useful tool to study PfEMP1-based pathogenesis and immunity and may provide opportunities for the development of a

Cell Host & Microbe
HP1-Dependent Gene Regulation in Malaria Parasites

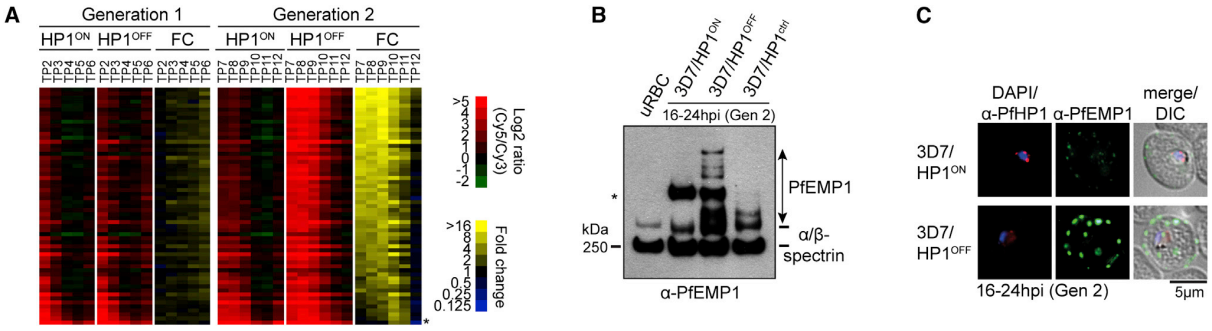

Figure 6. PfHP1 Is Required for Heritable *var* Gene Silencing and Maintenance of Singular *var* Gene Choice

(A) Temporal progression of relative abundance (red/green) and fold change (FC) in expression (yellow/blue) for all *var* genes in 3D7/HP1^{ON} and 3D7/HP1^{OFF} parasites across all 11 TPs analyzed. Asterisk, *var2csa*. See also Figure S4 and Table S1.

(B) PfEMP1 expression in 3D7/HP1^{ON}, 3D7/HP1^{OFF}, and 3D7/HP1^{ctrl} parasites at 16–24 hpi in generation 2. Equal cell numbers were analyzed in each lane. The pan-specific α-PfEMP1 antibody (mAb 6H1) was raised against a part of the C-terminal acidic terminal segment (ATS) domain that is conserved among PfEMP1 variants (Duffy et al., 2002). uRBC, uninfected RBCs (note that α-PfEMP1 antibodies cross-react with human spectrin).

(C) α-PfHP1/α-PfEMP1 (mAb 6H1) IFAs of 3D7/HP1^{ON} and 3D7/HP1^{OFF} parasites at 16–24 hpi in generation 2.

malaria vaccine. Notably, in an analogous system, immunization with mutant *Giardia lamblia* parasites coexpressing many variant-specific surface proteins has successfully been applied to induce strain-transcendent protective immunity in an experimental infection model (Rivero et al., 2010).

In addition to virulence gene silencing, we also identified an essential role for PfHP1 in mitotic proliferation. In the absence of PfHP1, asexual trophozoites fail to proliferate and enter a state of cell-cycle arrest that is reversible in a PfHP1-dependent manner. Although the exact pathway in which PfHP1 is required for cell-cycle progression remains unknown, the lack of significant levels of DNA synthesis in PfHP1-depleted trophozoites is indicative of defects in S phase entry or progression. Indeed, HP1 directly interacts with several factors involved in prereplicative complex assembly and replication initiation or elongation (e.g., CDC18/CDC6, ORCs, MCMs, CAF1) in model eukaryotes (Kwon and Workman, 2008; Christensen and Tye, 2003; Li et al., 2011). Moreover, loss of HP1 function causes delayed replication timing and/or S phase progression defects in *S. pombe*, *D. melanogaster*, and mouse cells (Hayashi et al., 2009; Schwaiger et al., 2010; Quivy et al., 2008). Hence, it is conceivable that PfHP1 may be essential for DNA replication in *P. falciparum*, and further experiments are now required to test this intriguing hypothesis in more detail.

Remarkably, we demonstrate that PfHP1's capacity to regulate the bistable transcription of a single euchromatic gene balances mitotic proliferation and sexual differentiation of malaria blood-stage parasites. In this context, it is notable that silencing of heterochromatic genes in *P. falciparum* is functionally dependent on the sirtuin HDACs PfSIR2A/PfSIR2B (Tonkin et al., 2009; Duraisingh et al., 2005), PfSET2 (Jiang et al., 2013), and the class II HDAC PfHDA2 (Coleman et al., 2014). Of these histone-modifying enzymes, however, only PfHDA2 also controls *pfap2-g* expression, suggesting that PfHP1 and PfHDA2 cooperate in a distinct silencing pathway to also regulate euchromatic genes. It will therefore be interesting to test if PfHP1 and PfHDA2 occur together in a specific silencing complex. Indeed, several class II HDACs interact directly with HP1 and are important for HP1-dependent gene silencing in model eukaryotes (Yamada et al., 2005; Zhang et al., 2002). We propose that epigenetic silencing of *pfap2-g* promotes continuous mitotic proliferation and antagonizes sexual conversion, while local dissociation of PfHP1 from the *pfap2-g* locus activates PfAP2-G expression and triggers sexual conversion and gametocyte differentiation. In analogy to the essential role of ApiAP2 TFs in stage-specific gene expression and parasite development in other life cycle stages (Yuda et al., 2009, 2010; Iwanaga et al., 2012), PfAP2-G likely regulates a transcriptional response effecting gametocyte development and cell-cycle exit. In both *P. falciparum* and *P. berghei*, PfAP2-G binding motifs were indeed found enriched in the upstream region of genes associated with sexual differentiation, and the occurrence of the respective target sites upstream of *pfap2-g* itself further indicates that PfAP2-G may establish an autoregulatory feedback loop (Kafsack et al., 2014; Sinha et al., 2014). Interestingly, we demonstrate that transcriptional changes associated with the early phase of differentiation are limited to a small number of genes but become more pronounced once gametocytes enter stage I development. We explain this by the fact that both asexual and sexually committed schizonts need to produce invasive merozoites capable of establishing RBC infection. In fact, many of the early gametocyte genes predicted here and elsewhere (Eksi et al., 2005; Silvestrini et al., 2010) code for proteins implicated in host cell remodeling, which is indicative for the requirement of gametocyte-specific host cell modifications. While it is possible that PfAP2-G regulates some or all of these genes directly, genome-wide ChIP approaches will be necessary for a comprehensive identification of PfAP2-G target genes and understanding of PfAP2-G function.

Our results reveal important mechanistic insight into the pathway underlying sexual commitment and identify PfHP1 as a crucial factor in controlling cell-fate decision in *P. falciparum*. Interestingly, the blood stage of infection is the only phase of the entire life cycle where parasites have a choice to enter either one of two developmental pathways. It thus appears likely that the epigenetic basis for this switch evolved to adapt sexual

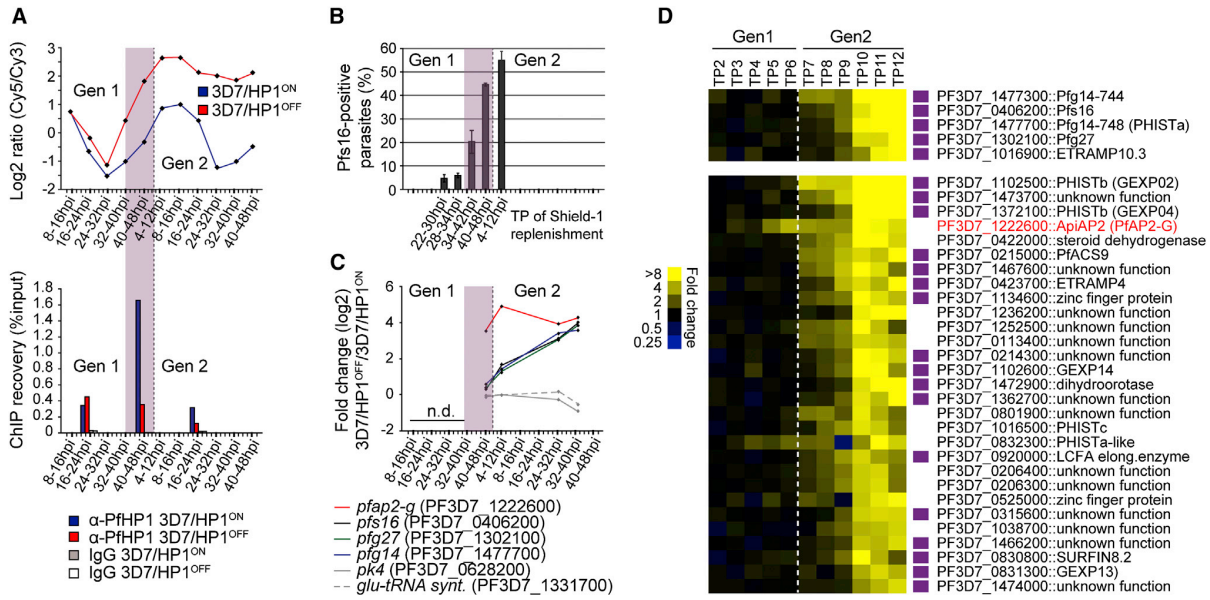

Figure 7. Gametocyte Differentiation Is Linked to the PfHP1-Dependent Activation of *pfap2-g*

(A) Temporal expression profile (Cy5/Cy3 log2 ratios) of *pfap2-g* (top) and ChIP-qPCR results showing PfHP1 occupancy at the *pfap2-g* locus (bottom). The sexual commitment phase is highlighted in purple. See also Figure S6 and Table S1.

(B) Proportion of Pfs16/KAHRP-positive parasites in 3D7/HP1^{OFF} populations rescued at different TPs in generation 1 (x axis) as determined by IFA at 32–40 hr post reinvasion in generation 2. Values show the mean ± SD of three biological replicates. See also Figure S5.

(C) Induction of *pfap2-g* and the three early gametocyte markers *pfs16* (PF3D7_0406200) (Bruce et al., 1994), *pfg27* (PF3D7_1302100) (Alano et al., 1991), and *pfg14_748* (PF3D7_1477700) (Eksi et al., 2005) in 3D7/HP1^{OFF} compared to 3D7/HP1^{ON} parasites as determined by qRT-PCR on biological replicate samples. Negative control genes are in gray. n.d., not determined.

(D) Temporal progression of fold changes in expression of known (upper heatmap) and predicted (lower heatmap) early gametocyte genes in 3D7/HP1^{OFF} compared to 3D7/HP1^{ON} parasites. Early gametocyte genes identified in previous studies are highlighted in purple. See also Figure S7, Table S1, and Supplemental Experimental Procedures.

conversion rates for optimal transmission during the course of infection. Indeed, gametocyte conversion rates are highly variable between different isolates and clones and influenced by a broad spectrum of environmental conditions (Baker, 2010; Alano and Carter, 1990). Although the molecular factor(s) triggering gametocyte conversion have not been identified, two recent studies reported that cell-cell communication via exosomes/microvesicles causes a dramatic increase in gametocyte conversion (Regev-Rudzki et al., 2013; Mantel et al., 2013). It is therefore tempting to speculate that cargo delivered by these vesicles may trigger a signaling cascade that ultimately evicts PfHP1 from the *pfap2-g* locus.

In conclusion, we identified PfHP1 as an essential factor in mitotic proliferation and as a key mediator of two systems of CVGE that secure the survival and transmission of malaria blood-stage parasites, respectively. Our data provide important mechanistic insight into the regulatory processes underlying antigenic variation and sexual conversion and generate knowledge relevant for investigating conceptually similar systems in other eukaryotes. Importantly, we established that gametocyte commitment is epigenetically regulated. This significant discovery will facilitate the targeted dissection of the molecular pathway triggering sexual conversion and has major implications for the identification of approaches to prevent malaria transmission.

EXPERIMENTAL PROCEDURES

Parasite Culture and Transfection

P. falciparum 3D7 cell culture and transfection was performed as described (Trager and Jenson, 1978; Lambros and Vanderberg, 1979; Voss et al., 2006). Transfection constructs are described in the Supplemental Experimental Procedures and in Figure S1. Parasites were grown in the presence of the indicated combinations of 4 nM WR99210 (WR) and 625 nM Shield-1. 3D7/HP1^{ON} clones were obtained by limiting dilution.

Western Blot Analysis

Nuclei were isolated as described (Voss et al., 2003) and lysed in 2% SDS, 10 mM Tris, 1 mM dithiothreitol (pH 8.0). Proteins were detected using rabbit α-PfHP1 1:5,000 (Figure S1 and Supplemental Experimental Procedures) and α-H4 1:10,000 (Abcam ab10158). PfEMP1 was extracted as described (Van Schravendijk et al., 1993) and detected using the pan-specific α-PfEMP1 mouse monoclonal antibody (mAb) 1B/6H-1 (1:500) (Duffy et al., 2002).

Fluorescence Microscopy

Live-cell fluorescence microscopy and IFAs were performed as described (Witmer et al., 2012). IFAs were performed on methanol-fixed cells using mouse immunoglobulin G2a (IgG2a) mAb α-HRP1 (α-KAHRP) (kind gift from D. Taylor), 1:500; mouse IgG1 mAb α-Pfs16 (kind gift from Robert W. Sauerwein), 1:250; mouse IgG1 mAb α-PfEMP1 (1B/6H-1) (Duffy et al., 2002), 1:150; and rabbit α-PfHP1, 1:100. Secondary antibody dilutions were as follows: Alexa Fluor 568-conjugated α-rabbit IgG (Molecular Probes), 1:250; Alexa Fluor 568-conjugated α-mouse IgG2a (Molecular Probes), 1:250; Alexa Fluor 488-conjugated α-mouse IgG1 (Molecular Probes),

1:250; and FITC-conjugated α-mouse IgG (Kirkegaard Perry Laboratories), 1:250. Images were taken at 96-fold magnification on a Leica DM 5000B microscope with a Leica DFC 300 FX camera, acquired via the Leica IM 1000 software, and processed using Adobe Photoshop CS6. For each experiment, images were acquired and processed with identical settings.

Isothermal Microcalorimetry

Isothermal microcalorimetry measures the heat flow produced by a biological sample over time. Isothermal microcalorimetry experiments and data analysis were performed as described using a Thermal Activity Monitor (Model 3102 TAM III, TA Instruments) with minor modifications (Wenzler et al., 2012) (see Supplemental Experimental Procedures).

qRT-PCR

3D7/HP1^{ON} parasites were synchronized twice 16 hr apart to obtain an 8 hr growth window and then split into two populations at 4–12 hpi and cultured in either the presence or absence of Shield-1. 3D7/HP1^{ON} and 3D7/HP1^{OFF} parasites were harvested at 40–48 hpi in generation 1 and at three consecutive time points in generation 2 (4–12 hpi, 24–32 hpi, and 32–40 hpi). 3D7 and F12 populations were synchronized identically, and time points were harvested at 4–12 hpi, 24–32 hpi, and 40–48 hpi. Isolation and processing of total RNA and qRT-PCR were conducted as described with minor modifications (Witmer et al., 2012) (see Supplemental Experimental Procedures). Primer sequences are listed in Table S2.

Targeted Chromatin Immunoprecipitation

3D7/HP1^{ON} parasites were synchronized twice 16 hr apart to obtain an 8 hr growth window and then split into two populations, one of which was taken off Shield-1 at 4–12 hpi. Sample pairs were harvested at 16–24 hpi and 40–48 hpi in generation 1 and at 16–24 hpi in generation 2. Isolation of formaldehyde-crosslinked chromatin and ChIP-qPCR analysis were performed as described with minor modifications (Flueck et al., 2009) using 0.6 μg affinity-purified α-PfHP1, 5 μg α-H3K9me3 (Millipore 07_442), or 5 μg rabbit IgG negative control antibodies (Millipore 12–370) (see Supplemental Experimental Procedures). Primer sequences are listed in Table S2.

Flow Cytometry

Tightly synchronized 3D7/HP1^{ON} parasites were split at 0–4 hpi and cultured in either the presence or absence of Shield-1. At 20–24 hpi after reinvasion, the 3D7/HP1^{ON} and 3D7/HP1^{OFF} populations were synchronized again to obtain a 4 hr growth window. DNA content analysis was carried out on five consecutive TPs in generation 2, starting at 24–28 hpi. Packed RBCs (100 μl) were fixed in 4% formaldehyde/0.015% glutaraldehyde; washed three times in RPMI-HEPES; incubated in 1 ml RPMI-HEPES, 0.1%Triton X-100, 0.1 μg/ml RNase A, and 20 μM FxCycle Far Red stain (Molecular Probes) for 30 min in the dark; and analyzed using an AccuriC6 instrument (BD Biosciences). A minimum of 4,000 gated iRBCs were measured (excitation 640 nm; 30 mW diode; emission detection FL4 675 nm ± 12.5 nm). Acquired data were processed using FlowJo software (Version 10.0.5).

Microarray Experiments and Data Analysis

RNA extraction and cDNA synthesis were carried out as described (Bozdech et al., 2003). Cy5-labeled test cDNAs were hybridized against a Cy3-labeled 3D7 cDNA reference pool that was made by combining total RNA isolated from five consecutive time points across the IDC. Equal amounts of Cy5- and Cy3-labeled samples were hybridized on a *P. falciparum* glass slide microarray containing 10,416 70-mer open reading frame probes (Hu et al., 2007). Hybridization was carried out at 65°C in a MAUI automated hybridization station for at least 12 hr (Bozdech et al., 2003). Slides were washed twice in 0.5× saline-sodium citrate (SSC)/0.02% SDS, once in 0.05× SSC, spun dry, and scanned using the GenePix scanner 4000B and GenePix pro 6.0 software (Axon Laboratory). Detailed protocols describing microarray reannotation, data processing, and analysis are provided in the Supplemental Experimental Procedures section.

ACCESSION NUMBERS

The Gene Expression Omnibus accession number for the microarray data reported in this paper is GSE53176.

SUPPLEMENTAL INFORMATION

Supplemental Information includes Supplemental Experimental Procedures, seven figures, and two tables and can be found with this article online at http://dx.doi.org/10.1016/j.chom.2014.07.004.

AUTHOR CONTRIBUTIONS

N.M.B.B. and N.L.B. designed and performed experiments, analyzed data, prepared illustrations, and wrote the paper. W.H.C. performed microarray hybridizations. I.N. expressed recombinant PfHP1 and produced affinity-purified α-PfHP1 antibodies. L.Z. analyzed microarray data. R.W. designed and performed qRT-PCR experiments. C.F. performed isothermal microcalorimetry experiments. M.R., I.F., and Z.B. designed experiments and interpreted data. T.S.V. supervised the study, designed experiments, analyzed data, prepared illustrations, and wrote the manuscript.

ACKNOWLEDGMENTS

We thank M. Filarsky for critically reading the manuscript. We are grateful to R. Sauerwein and D. Taylor for providing antibodies, to M. Jud and M. Tamborrini for help in IgG subclass typing, and to C. Gysel and T.N.H. Bui for technical assistance. This work was supported by the Swiss National Science Foundation (grant numbers PP00P3_130203, 31003A_143916, 310030_134889), the Singaporean National Medical Research Council (grant number NMRC/CBRG/0001/2012), the OPO Foundation, and the Rudolf Geigy Foundation. N.M.B.B. received a Boehringer Ingelheim PhD scholarship. The authors declare no conflict of interest.

Received: January 26, 2014
Revised: April 28, 2014
Accepted: June 6, 2014
Published: August 13, 2014

REFERENCES

Alano, P., and Carter, R. (1990). Sexual differentiation in malaria parasites. Annu. Rev. Microbiol. *44*, 429–449.

Alano, P., Premawansa, S., Bruce, M.C., and Carter, R. (1991). A stage specific gene expressed at the onset of gametocytogenesis in Plasmodium falciparum. Mol. Biochem. Parasitol. *46*, 81–88.

Alano, P., Roca, L., Smith, D., Read, D., Carter, R., and Day, K. (1995). Plasmodium falciparum: parasites defective in early stages of gametocytogenesis. Exp. Parasitol. *81*, 227–235.

Armstrong, C.M., and Goldberg, D.E. (2007). An FKBP destabilization domain modulates protein levels in Plasmodium falciparum. Nat. Methods *4*, 1007–1009.

Baker, D.A. (2010). Malaria gametocytogenesis. Mol. Biochem. Parasitol. *172*, 57–65.

Balaji, S., Babu, M.M., Iyer, L.M., and Aravind, L. (2005). Discovery of the principal specific transcription factors of Apicomplexa and their implication for the evolution of the AP2-integrase DNA binding domains. Nucleic Acids Res. *33*, 3994–4006.

Banaszynski, L.A., Chen, L.C., Maynard-Smith, L.A., Ooi, A.G., and Wandless, T.J. (2006). A rapid, reversible, and tunable method to regulate protein function in living cells using synthetic small molecules. Cell *126*, 995–1004.

Baruch, D.I., Pasloske, B.L., Singh, H.B., Bi, X., Ma, X.C., Feldman, M., Taraschi, T.F., and Howard, R.J. (1995). Cloning the P. falciparum gene encoding PfEMP1, a malarial variant antigen and adherence receptor on the surface of parasitized human erythrocytes. Cell *82*, 77–87.

Bozdech, Z., Llinás, M., Pulliam, B.L., Wong, E.D., Zhu, J., and DeRisi, J.L. (2003). The transcriptome of the intraerythrocytic developmental cycle of Plasmodium falciparum. PLoS Biol. *1*, E5.

Brancucci, N.M., Witmer, K., Schmid, C.D., Flueck, C., and Voss, T.S. (2012). Identification of acis-acting DNA-protein interaction implicated in singular var gene choice in Plasmodium falciparum. Cell. Microbiol. *14*, 1836–1848.

Bruce, M.C., Alano, P., Duthie, S., and Carter, R. (1990). Commitment of the malaria parasite Plasmodium falciparum to sexual and asexual development. Parasitology *100*, 191–200.

Bruce, M.C., Carter, R.N., Nakamura, K., Aikawa, M., and Carter, R. (1994). Cellular location and temporal expression of the Plasmodium falciparum sexual stage antigen Pfs16. Mol. Biochem. Parasitol. *65*, 11–22.

Chookajorn, T., Dzikowski, R., Frank, M., Li, F., Jiwani, A.Z., Hartl, D.L., and Deitsch, K.W. (2007). Epigenetic memory at malaria virulence genes. Proc. Natl. Acad. Sci. USA *104*, 899–902.

Christensen, T.W., and Tye, B.K. (2003). Drosophila MCM10 interacts with members of the prereplication complex and is required for proper chromosome condensation. Mol. Biol. Cell *14*, 2206–2215.

Coleman, B.I., Skillman, K.M., Jiang, R.H.Y., Childs, L.M., Altenhofen, L.M., Ganter, M., Leung, Y., Goldowitz, I., Kafsack, B.F.C., Marti, M., et al. (2014). A Plasmodium falciparum histone deacetylase regulates antigenic variation and gametocyte conversion. Cell Host Microbe *16*, this issue, 177–186.

Cortés, A., Crowley, V.M., Vaquero, A., and Voss, T.S. (2012). A view on the role of epigenetics in the biology of malaria parasites. PLoS Pathog. *8*, e1002943.

Duffy, M.F., Brown, G.V., Basuki, W., Krejany, E.O., Noviyanti, R., Cowman, A.F., and Reeder, J.C. (2002). Transcription of multiple var genes by individual, trophozoite-stage Plasmodium falciparum cells expressing a chondroitin sulphate A binding phenotype. Mol. Microbiol. *43*, 1285–1293.

Duraisingh, M.T., Voss, T.S., Marty, A.J., Duffy, M.F., Good, R.T., Thompson, J.K., Freitas-Junior, L.H., Scherf, A., Crabb, B.S., and Cowman, A.F. (2005). Heterochromatin silencing and locus repositioning linked to regulation of virulence genes in Plasmodium falciparum. Cell *121*, 13–24.

Eissenberg, J.C., James, T.C., Foster-Hartnett, D.M., Hartnett, T., Ngan, V., and Elgin, S.C. (1990). Mutation in a heterochromatin-specific chromosomal protein is associated with suppression of position-effect variegation in Drosophila melanogaster. Proc. Natl. Acad. Sci. USA *87*, 9923–9927.

Eksi, S., Haile, Y., Furuya, T., Ma, L., Su, X., and Williamson, K.C. (2005). Identification of a subtelomeric gene family expressed during the asexual-sexual stage transition in Plasmodium falciparum. Mol. Biochem. Parasitol. *143*, 90–99.

Eksi, S., Morahan, B.J., Haile, Y., Furuya, T., Jiang, H., Ali, O., Xu, H., Kiattibutr, K., Suri, A., Czesny, B., et al. (2012). Plasmodium falciparum gametocyte development 1 (Pfgdv1) and gametocytogenesis early gene identification and commitment to sexual development. PLoS Pathog. *8*, e1002964.

Flueck, C., Bartfai, R., Volz, J., Niederwieser, I., Salcedo-Amaya, A.M., Alako, B.T., Ehlgen, F., Ralph, S.A., Cowman, A.F., Bozdech, Z., et al. (2009). Plasmodium falciparum heterochromatin protein 1 marks genomic loci linked to phenotypic variation of exported virulence factors. PLoS Pathog. *5*, e1000569.

Freitas-Junior, L.H., Hernandez-Rivas, R., Ralph, S.A., Montiel-Condado, D., Ruvalcaba-Salazar, O.K., Rojas-Meza, A.P., Mâncio-Silva, L., Leal-Silvestre, R.J., Gontijo, A.M., Shorte, S., and Scherf, A. (2005). Telomeric heterochromatin propagation and histone acetylation control mutually exclusive expression of antigenic variation genes in malaria parasites. Cell *121*, 25–36.

Grewal, S.I., and Jia, S. (2007). Heterochromatin revisited. Nat. Rev. Genet. *8*, 35–46.

Guizetti, J., and Scherf, A. (2013). Silence, activate, poise and switch! Mechanisms of antigenic variation in Plasmodium falciparum. Cell. Microbiol. *15*, 718–726.

Hayashi, M.T., Takahashi, T.S., Nakagawa, T., Nakayama, J., and Masukata, H. (2009). The heterochromatin protein Swi6/HP1 activates replication origins at the pericentromeric region and silent mating-type locus. Nat. Cell Biol. *11*, 357–362.

Hu, G., Llinás, M., Li, J., Preiser, P.R., and Bozdech, Z. (2007). Selection of long oligonucleotides for gene expression microarrays using weighted rank-sum strategy. BMC Bioinformatics *8*, 350.

Iwanaga, S., Kaneko, I., Kato, T., and Yuda, M. (2012). Identification of an AP2-family protein that is critical for malaria liver stage development. PLoS ONE *7*, e47557.

Jiang, L., Mu, J., Zhang, Q., Ni, T., Srinivasan, P., Rayavara, K., Yang, W., Turner, L., Lavstsen, T., Theander, T.G., et al. (2013). PfSETvs methylation of histone H3K36 represses virulence genes in Plasmodium falciparum. Nature *499*, 223–227.

Kafsack, B.F., Rovira-Graells, N., Clark, T.G., Bancells, C., Crowley, V.M., Campino, S.G., Williams, A.E., Drought, L.G., Kwiatkowski, D.P., Baker, D.A., et al. (2014). A transcriptional switch underlies commitment to sexual development in malaria parasites. Nature *507*, 248–252.

Kwon, S.H., and Workman, J.L. (2008). The heterochromatin protein 1 (HP1) family: put away a bias toward HP1. Mol. Cells *26*, 217–227.

Kyes, S., Horrocks, P., and Newbold, C. (2001). Antigenic variation at the infected red cell surface in malaria. Annu. Rev. Microbiol. *55*, 673–707.

Lambros, C., and Vanderberg, J.P. (1979). Synchronization of Plasmodium falciparum erythrocytic stages in culture. J. Parasitol. *65*, 418–420.

Li, P.C., Chretien, L., Côté, J., Kelly, T.J., and Forsburg, S.L. (2011). S. pombe replication protein Cdc18 (Cdc6) interacts with Swi6 (HP1) heterochromatin protein: region specific effects and replication timing in the centromere. Cell Cycle *10*, 323–336.

Lomberk, G., Wallrath, L., and Urrutia, R. (2006). The Heterochromatin Protein 1 family. Genome Biol. *7*, 228.

Lopez-Rubio, J.J., Gontijo, A.M., Nunes, M.C., Issar, N., Hernandez Rivas, R., and Scherf, A. (2007). 5′ flanking region of var genes nucleate histone modification patterns linked to phenotypic inheritance of virulence traits in malaria parasites. Mol. Microbiol. *66*, 1296–1305.

Lopez-Rubio, J.J., Mancio-Silva, L., and Scherf, A. (2009). Genome-wide analysis of heterochromatin associates clonally variant gene regulation with perinuclear repressive centers in malaria parasites. Cell Host Microbe *5*, 179–190.

Mantel, P.Y., Hoang, A.N., Goldowitz, I., Potashnikova, D., Hamza, B., Vorobjev, I., Ghiran, I., Toner, M., Irimia, D., Ivanov, A.R., et al. (2013). Malaria-infected erythrocyte-derived microvesicles mediate cellular communication within the parasite population and with the host immune system. Cell Host Microbe *13*, 521–534.

Mok, S., Imwong, M., Mackinnon, M.J., Sim, J., Ramadoss, R., Yi, P., Mayxay, M., Chotivanich, K., Liong, K.Y., Russell, B., et al. (2011). Artemisinin resistance in Plasmodium falciparum is associated with an altered temporal pattern of transcription. BMC Genomics *12*, 391.

Navarro, M., and Gull, K. (2001). A pol I transcriptional body associated with VSG mono-allelic expression in Trypanosoma brucei. Nature *414*, 759–763.

Pérez-Toledo, K., Rojas-Meza, A.P., Mancio-Silva, L., Hernández-Cuevas, N.A., Delgadillo, D.M., Vargas, M., Martínez-Calvillo, S., Scherf, A., and Hernandez-Rivas, R. (2009). Plasmodium falciparum heterochromatin protein 1 binds to tri-methylated histone 3 lysine 9 and is linked to mutually exclusive expression of var genes. Nucleic Acids Res. *37*, 2596–2606.

Petter, M., Lee, C.C., Byrne, T.J., Boysen, K.E., Volz, J., Ralph, S.A., Cowman, A.F., Brown, G.V., and Duffy, M.F. (2011). Expression of P. falciparum var genes involves exchange of the histone variant H2A.Z at the promoter. PLoS Pathog. *7*, e1001292.

Quivy, J.P., Gérard, A., Cook, A.J., Roche, D., and Almouzni, G. (2008). The HP1-p150/CAF-1 interaction is required for pericentric heterochromatin replication and S-phase progression in mouse cells. Nat. Struct. Mol. Biol. *15*, 972–979.

Ralph, S.A., Scheidig-Benatar, C., and Scherf, A. (2005). Antigenic variation in Plasmodium falciparum is associated with movement of var loci between subnuclear locations. Proc. Natl. Acad. Sci. USA *102*, 5414–5419.

Regev-Rudzki, N., Wilson, D.W., Carvalho, T.G., Sisquella, X., Coleman, B.M., Rug, M., Bursac, D., Angrisano, F., Gee, M., Hill, A.F., et al. (2013). Cell-cell communication between malaria-infected red blood cells via exosome-like vesicles. Cell *153*, 1120–1133.

Rivero, F.D., Saura, A., Prucca, C.G., Carranza, P.G., Torri, A., and Lujan, H.D. (2010). Disruption of antigenic variation is crucial for effective parasite vaccine. Nat. Med. *16*, 551–557, 1p, 557.

Rovira-Graells, N., Gupta, A.P., Planet, E., Crowley, V.M., Mok, S., Ribas de Pouplana, L., Preiser, P.R., Bozdech, Z., and Cortés, A. (2012).

Transcriptional variation in the malaria parasite Plasmodium falciparum. Genome Res. *22*, 925–938.

Salanti, A., Staalsoe, T., Lavstsen, T., Jensen, A.T., Sowa, M.P., Arnot, D.E., Hviid, L., and Theander, T.G. (2003). Selective upregulation of a single distinctly structured var gene in chondroitin sulphate A-adhering Plasmodium falciparum involved in pregnancy-associated malaria. Mol. Microbiol. *49*, 179–191.

Salcedo-Amaya, A.M., van Driel, M.A., Alako, B.T., Trelle, M.B., van den Elzen, A.M., Cohen, A.M., Janssen-Megens, E.M., van de Vegte-Bolmer, M., Selzer, R.R., Iniguez, A.L., et al. (2009). Dynamic histone H3 epigenome marking during the intraerythrocytic cycle of Plasmodium falciparum. Proc. Natl. Acad. Sci. USA *106*, 9655–9660.

Scherf, A., Hernandez-Rivas, R., Buffet, P., Bottius, E., Benatar, C., Pouvelle, B., Gysin, J., and Lanzer, M. (1998). Antigenic variation in malaria: in situ switching, relaxed and mutually exclusive transcription of var genes during intra-erythrocytic development in Plasmodium falciparum. EMBO J. *17*, 5418–5426.

Scherf, A., Lopez-Rubio, J.J., and Riviere, L. (2008). Antigenic variation in Plasmodium falciparum. Annu. Rev. Microbiol. *62*, 445–470.

Schwaiger, M., Kohler, H., Oakeley, E.J., Stadler, M.B., and Schübeler, D. (2010). Heterochromatin protein 1 (HP1) modulates replication timing of the Drosophila genome. Genome Res. *20*, 771–780.

Silvestrini, F., Bozdech, Z., Lanfrancotti, A., Di Giulio, E., Bultrini, E., Picci, L., Derisi, J.L., Pizzi, E., and Alano, P. (2005). Genome-wide identification of genes upregulated at the onset of gametocytogenesis in Plasmodium falciparum. Mol. Biochem. Parasitol. *143*, 100–110.

Silvestrini, F., Lasonder, E., Olivieri, A., Camarda, G., van Schaijk, B., Sanchez, M., Younis Younis, S., Sauerwein, R., and Alano, P. (2010). Protein export marks the early phase of gametocytogenesis of the human malaria parasite Plasmodium falciparum. Mol. Cell. Proteomics *9*, 1437–1448.

Sinha, A., Hughes, K.R., Modrzynska, K.K., Otto, T.D., Pfander, C., Dickens, N.J., Religa, A.A., Bushell, E., Graham, A.L., Cameron, R., et al. (2014). A cascade of DNA-binding proteins for sexual commitment and development in Plasmodium. Nature *507*, 253–257.

Smith, J.D., Chitnis, C.E., Craig, A.G., Roberts, D.J., Hudson-Taylor, D.E., Peterson, D.S., Pinches, R., Newbold, C.I., and Miller, L.H. (1995). Switches in expression of Plasmodium falciparum var genes correlate with changes in antigenic and cytoadherent phenotypes of infected erythrocytes. Cell *82*, 101–110.

Su, X.Z., Heatwole, V.M., Wertheimer, S.P., Guinet, F., Herrfeldt, J.A., Peterson, D.S., Ravetch, J.A., and Wellems, T.E. (1995). The large diverse gene family var encodes proteins involved in cytoadherence and antigenic variation of Plasmodium falciparum-infected erythrocytes. Cell *82*, 89–100.

Taylor, D.W., Parra, M., Chapman, G.B., Stearns, M.E., Rener, J., Aikawa, M., Uni, S., Aley, S.B., Panton, L.J., and Howard, R.J. (1987). Localization of Plasmodium falciparum histidine-rich protein 1 in the erythrocyte skeleton under knobs. Mol. Biochem. Parasitol. *25*, 165–174.

Tonkin, C.J., Carret, C.K., Duraisingh, M.T., Voss, T.S., Ralph, S.A., Hommel, M., Duffy, M.F., Silva, L.M., Scherf, A., Ivens, A., et al. (2009). Sir2 paralogues cooperate to regulate virulence genes and antigenic variation in Plasmodium falciparum. PLoS Biol. *7*, e84.

Trager, W., and Jenson, J.B. (1978). Cultivation of malarial parasites. Nature *273*, 621–622.

Van Schravendijk, M.R., Pasloske, B.L., Baruch, D.I., Handunnetti, S.M., and Howard, R.J. (1993). Immunochemical characterization and differentiation of two approximately 300-kD erythrocyte membrane-associated proteins of Plasmodium falciparum, PfEMP1 and PfEMP3. Am. J. Trop. Med. Hyg. *49*, 552–565.

Volz, J., Carvalho, T.G., Ralph, S.A., Gilson, P., Thompson, J., Tonkin, C.J., Langer, C., Crabb, B.S., and Cowman, A.F. (2010). Potential epigenetic regulatory proteins localise to distinct nuclear sub-compartments in Plasmodium falciparum. Int. J. Parasitol. *40*, 109–121.

Volz, J.C., Bártfai, R., Petter, M., Langer, C., Josling, G.A., Tsuboi, T., Schwach, F., Baum, J., Rayner, J.C., Stunnenberg, H.G., et al. (2012). PfSET10, a Plasmodium falciparum methyltransferase, maintains the active var gene in a poised state during parasite division. Cell Host Microbe *11*, 7–18.

Voss, T.S., Kaestli, M., Vogel, D., Bopp, S., and Beck, H.P. (2003). Identification of nuclear proteins that interact differentially with Plasmodium falciparum var gene promoters. Mol. Microbiol. *48*, 1593–1607.

Voss, T.S., Healer, J., Marty, A.J., Duffy, M.F., Thompson, J.K., Beeson, J.G., Reeder, J.C., Crabb, B.S., and Cowman, A.F. (2006). A var gene promoter controls allelic exclusion of virulence genes in Plasmodium falciparum malaria. Nature *439*, 1004–1008.

Wenzler, T., Steinhuber, A., Wittlin, S., Scheurer, C., Brun, R., and Trampuz, A. (2012). Isothermal microcalorimetry, a new tool to monitor drug action against Trypanosoma brucei and Plasmodium falciparum. PLoS Negl. Trop. Dis. *6*, e1668.

Witmer, K., Schmid, C.D., Brancucci, N.M., Luah, Y.H., Preiser, P.R., Bozdech, Z., and Voss, T.S. (2012). Analysis of subtelomeric virulence gene families in Plasmodium falciparum by comparative transcriptional profiling. Mol. Microbiol. *84*, 243–259.

World Health Organisation (2013). World Malaria Report 2013. (Geneva: WHO Press).

Yamada, T., Fischle, W., Sugiyama, T., Allis, C.D., and Grewal, S.I. (2005). The nucleation and maintenance of heterochromatin by a histone deacetylase in fission yeast. Mol. Cell *20*, 173–185.

Young, J.A., Fivelman, Q.L., Blair, P.L., de la Vega, P., Le Roch, K.G., Zhou, Y., Carucci, D.J., Baker, D.A., and Winzeler, E.A. (2005). The Plasmodium falciparum sexual development transcriptome: a microarray analysis using ontology-based pattern identification. Mol. Biochem. Parasitol. *143*, 67–79.

Yuda, M., Iwanaga, S., Shigenobu, S., Mair, G.R., Janse, C.J., Waters, A.P., Kato, T., and Kaneko, I. (2009). Identification of a transcription factor in the mosquito-invasive stage of malaria parasites. Mol. Microbiol. *71*, 1402–1414.

Yuda, M., Iwanaga, S., Shigenobu, S., Kato, T., and Kaneko, I. (2010). Transcription factor AP2-Sp and its target genes in malarial sporozoites. Mol. Microbiol. *75*, 854–863.

Zhang, C.L., McKinsey, T.A., and Olson, E.N. (2002). Association of class II histone deacetylases with heterochromatin protein 1: potential role for histone methylation in control of muscle differentiation. Mol. Cell. Biol. *22*, 7302–7312.